

A Planning Scheme for Penetrating Embedded Generation in  
Power Distribution Grids

by

Jiankang Wang

E.B., Zhejiang University (2007)

M.S., Massachusetts Institute of Technology (2009)

Submitted to the Department of Electrical Engineering and Computer Science  
in Partial Fulfillment of the Requirements for the Degree of

Doctor of Philosophy

at the

MASSACHUSETTS INSTITUTE OF TECHNOLOGY

September, 2013

© 2013 Massachusetts Institute of Technology. All rights reserved

Signature of Author .....

Department of Electrical Engineering and Computer Science

August 27, 2013

Certified by .....

James L. Kirtley

Professor of Electrical Engineering and Computer Science

Thesis Supervisor

Accepted by.....

Leslie A. Kolodziejski

Chairman, Committee on Graduate Students of

Department Electrical Engineering and Computer Science



A Planning Scheme for Penetrating Embedded Generation  
in Power Distribution Grids

by

Jiankang Wang

Submitted to the Department of Electrical Engineering and Computer Science  
on August 30, 2013 in Partial Fulfillment of the Requirement for the Degree of  
Doctor of Philosophy

ABSTRACT

Penetrating Embedded Generation, or Distributed Generation (DG), in power distribution grids presents great benefits and substantial positive social impacts to utilities, system operators and electricity consumers. Existing research and practices on DG penetration planning have a few deficiencies: (1) limited to specific system configurations and capacities; (2) inaccurate and tending to lose its optimality in application to specific scenario; (3) computationally expensive in time and space; and (4) in need of considerable investment in sensors, communication assets, and retrofitting equipment with control functionalities.

This thesis proposes a planning scheme for DG penetration in distribution systems that maximizes DG penetration's benefit, in terms of power delivery loss reduction, and restricts its adverse impact of steady-state voltage rise. A unique approach is taken to simplify the DG penetration problem with two sets of rules that describes the interaction of DG penetration and power delivery loss and voltage profiles in distribution systems.

The proposed planning scheme is generally applicable to any distribution system regardless of its configuration and load capacity. More importantly, it is a theoretical toolkit that can provide users an intuition how DG penetration affects the performance of a distribution system. The policy makers, regulators, industries and utilities will be able to use this toolkit, without going through complicated computations, as guidelines to make policies, standards and decisions in DG penetration and related business.

# Acknowledgements

---

Although I was told acknowledgements is the easiest chapter to write in a Ph.D. dissertation, until started this part, I found this was never true. There are many people have contributed to the production of this dissertation, and I could hardly find words to express my gratefulness to them.

I want to thank my committee: David Perreault (MIT), Pedro Carvalho (Technical University of Lisbon), Marija Ilic (CMU). I've enjoyed working with and learning from you individually and especially seeing how in combination a range of thoughtful perspectives can greatly strengthen the research process.

My deepest gratitude is to my advisor, Prof. James Kirtley. I have been so fortunate to have an advisor who gave me the freedom to explore on my own, and at the same time the guidance to recover when my steps faltered. His patience and support helped me overcome many crisis situations and finish this dissertation. I learned from him not just the specialized knowledge in power engineering, but also an attitude toward research. I hope that one day I would become as good a scientist, an engineer and an advisor as James has been.

I am grateful for being a part of Laboratory of Electromagnetic and Electronic Systems (LEES). Thanks to John Kassakian, Steven Leeb, Leslie Norford and other faculty in LEES for making it such an inspiring and supportive place for research, learning and self-discovery. Thanks to Makiko Wada, Vivian Mizuno, Donna Gale, Dimonika Bizi, and other staff. They offered me much more than what their jobs were and made my graduate life very joyful experience. Thanks to all my friends and colleagues in LEES: Matthew D'Asaro, Becky Asher, Olivia Leitermann, Richard Zhang, Lisa Pawlowicz, Yiou He, Dave Giuliano, Jackie Hu, George Hwang, Seungbum Lim, Riccardo Signorelli, Samantha Gunter, Samuel Chang, Huan Santiago, David Jenicek, Jouya Jadidian, Minjie Chen, Nelson Xuntuo Wang, Jorge Elizondo Martinez, Youngjin Kim, and Wardah Inam.

This research was funded by the MIT Martin Family Sustainability Fellowship, and the Cooperative Agreement between the Masdar Institute of Science and Technology (Masdar Institute), Abu Dhabi, UAE and MIT. Thanks to Instituto de Optimização Aplicada (IOA), Lisbon, Portugal for its support of providing the DPlan software package. Thanks to Chiang Chen Industrial Charity Foundation for support my first year of study at MIT.

Special thanks to Wei Li and his wife, Nicole Hung, Jillaine Hadfield, and Hueihan Jhuang. They helped me stay sane (if not cool) through these difficult days (if not years). Their support and care helped me overcome setbacks and stay focused on my graduate study. I greatly value their friendship and I deeply appreciate their belief in me.

Most importantly, none of this would have been possible without the love and patience of my family. My parents and my passed grandfather, to whom this dissertation is dedicated to, have been a constant source of love, concern, support and strength all these years. I would like to express my heart-felt gratitude to my family.

# Contents

---

Forward .....	11
Logic and Structure .....	12
Chapter 1: Background, Basic Concepts and Models .....	15
1.1 Distributed Generation .....	16
1.1.1 What is DG? .....	16
1.1.2 Why to connect DG to the grid? .....	18
1.1.3 Current Status of DG Penetration in the Grid .....	20
1.1.4 Challenges to increased penetration of DG .....	21
1.1.5 Existing Approach to Planning DG Penetration .....	26
1.2 In Scope of Distribution Systems .....	30
1.2.1 Distribution Systems .....	30
1.2.2 Feeder Systems .....	34
1.3 Models and Concepts .....	41
1.3.1 Voltage Effective Power .....	41
1.3.2 Induced Power Flow Model .....	46
2.1 Visualizing Feeder's Voltage Profile .....	51
2.1.1 Zero Point on Feeder .....	51
2.1.2 A Graphical Method .....	54
2.1.3 Area Criterion .....	56
2.2 Penetrating DG with Voltage Reliability .....	58
2.2.1 How Much DG can be Penetrated? .....	58
2.2.2 An Accurate Definition for Permissible DG Penetration Level .....	64
2.3 Six Factors Influencing Feeder Voltage Profile .....	66
2.3.1 Principles of Feeder Voltage Variation .....	67
2.3.2 Practical Methods to Voltage Control .....	76
2.4 Two Innovative Approaches for Voltage Mitigation .....	82
2.4.1 Demand Response for Voltage Rise Mitigation .....	85
2.4.2 Reconfiguration in Voltage Regulation .....	95

Chapter 3: Minimizing Power Delivery Loss in DG Penetration .....	103
3.1 Optimal DG Location.....	104
3.1.1 Half Capacity Rule .....	104
3.1.2 Examples and Implications .....	106
3.2 Optimal DG Capacity.....	111
3.2.1 Equal Voltage Rule .....	111
3.2.2 Examples and Implications .....	113
3.3 Penetration of Multiple DG Units .....	117
3.3.1 Superposition Rule .....	117
3.3.2 Numerical Examples and Computational Complexity .....	122
3.4 Optimal Location of Variable Energy Resources (VERs) .....	133
3.4.1 DG Variance Rule .....	133
3.4.2 Examples and Implications .....	138
Chapter 4: the Overall Planning Scheme .....	141
4.1 Estimating optimal DG capacity and location.....	142
4.2 Refining optimal DG location .....	148
4.3 Determining optimal DG operational point.....	151
Chapter 5: Conclusion.....	156
Appendix A .....	162
Appendix B .....	167
B.1 Proof of Half Capacity Rule .....	167
B.2 Proof of Equal Voltage Rule .....	171
B.3 Proof of Superposition Rule .....	175
B.4 Proof of DG Variance Rule .....	181
Appendix C .....	191
Appendix D .....	196
Bibliography.....	229

# List of Figures

---

Figure 1. Technical blueprint of the thesis. ....	12
Figure 2. 20 MIT power plants (building 42) shots from the side and front. ....	17
Figure 3. Renewable Portfolio Standards of 29 States. ....	20
Figure 4. Effect of connecting a DG unit on the voltage profile along an 11 kV overhead feeder...	25
Figure 5. Algorithm chart of using repetitive power flow to site DG for minimum loss. ....	28
Figure 6. Hierarchy of a power system. ....	31
Figure 7. Topologies of feeder systems. ....	36
Figure 8. Voltage constrained DG penetration is simplified onto basis of feeder systems. ....	38
Figure 9. A 50MW distribution system in São Miguel Island is decomposed into eight feeder systems in voltage-constrained analysis. ....	39
Figure 10. A 10 kV two-feeder system extracted from a 50 MW distribution system in Figure 9. .	40
Figure 11. Line diagram for a two-bus system. ....	45
Figure 12. Two ways of routing a radial feeder to 108 service transformers. ....	46
Figure 13. A practical feeder system penetrated with DG and its voltage-effective power flow. ....	47
Figure 14. A screen shot from DPlan. ....	49
Figure 15. Zero point created by DG penetration. ....	51
Figure 16. Voltage-effective power flow and voltage profile on a DG-integrated feeder. ....	55
Figure 17. Relation between areas under the voltate-effective power curve and the feeder's voltage profile. ....	57
Figure 18. DG penetration chart. ....	60
Figure 19. Voltage profiles after penetrating a single DG unit at three locations of Feeder 1 in Figure 9. ....	63
Figure 20. Voltage profile under 20% penetration rate of four types of definitions. ....	65
Figure 21. Voltage profiles of Feeder 1 under three setups of DG output. ....	68
Figure 22. Voltage-effective power flow (top) and voltage profile (bottom) varying with DG location. ....	69
Figure 23. Voltage-effective power flow and voltage profiles varying with DG dispersion level. ..	71
Figure 24. Voltage profiles of Feeder 1 under three levels of DG dispersion. ....	72
Figure 25. Voltage-effective power flow (Top) and voltage profile (Bottom) varying with the ratio of reactance to resistance $x/r$ or load profile of a feeder. ....	74

Figure 26. Voltage-effective power flow (Top) and voltage profile (Bottom) varying with load profile. ....	75
Figure 27. DR's priority regions defined by its cost-effectiveness on voltage rise mitigation. ....	87
Figure 28. DR cost varying with depth on feeder. ....	89
Figure 29. Linear cost function of DR. ....	90
Figure 30. A two-branch feeder circuit. ....	92
Figure 31. DR's priority regions when DG is inserted at a branch of a feeder. ....	93
Figure 32. Schematic diagram of partial distribution system at primary level.....	96
Figure 33. Voltage-effective power flow in reconfiguration on a circuit loop.....	97
Figure 34. Priority zones on DG connected feeder for closers to trip on. ....	99
Figure 35. Voltage-effective power change after DG reconnected to a different substation. ....	101
Figure 36. Optimal DG location that induces minimum power delivery loss.....	105
Figure 37. Equal Voltage Rule for choosing DG output/ capacity at a given location. ....	112
Figure 38. Voltage constraint can be implied by the Equal Voltage Rule in the DG optimization problem. ....	115
Figure 39. Optimal locations for placing multiple DG units on a feeder system. ....	119
Figure 40. Optimal capacity/output of multiple-DG-unit sizing on a feeder system. ....	121
Figure 41. Possible sequences of DG placement on the test system in Figure 10 and DG groups in Table 12.....	124
Figure 42. DG placement and induced power loss on the test system in Figure 10 with the DG groups in Table 12.....	126
Figure 43. Apparent power flow on the feeder system in Figure 10 after the placement of every DG unit at their optimal locations.....	127
Figure 44. Optimal DG capacities and their induced power deliver loss. ....	130
Figure 45. Optimal DG capacities/output and their induced voltage profile. ....	131
Figure 46. Optimal DG placement and sizing of multiple DG units is simplified into the same problem of a single DG unit under the Superposition Rule. ....	132
Figure 47. The Modified Half Capacity Rule for optimal Variable Energy Resources (VERs). ....	135
Figure 48. Optimal Variable Energy Resources (VERs) locations tested on the feeder system in Figure 10. ....	139
Figure 49. With the DG Variance Rule, the DG placement and sizing problem of VERs is equalized into the one of static output. ....	140



Figure 50. Overall planning scheme for DG penetration in distribution systems. ....	142
Figure 51. Step one: estimating optimal DG capacity and location for each feeder systems. ....	143
Figure 52. Optimal DG placement and sizing for the test system in Figure 10. ....	146
Figure 53. Algorithm of the first planning step.....	147
Figure 54. Step two: with the obtained optimal DG capacity and predicted DG variation, recalibrating optimal DG location.....	148
Figure 55. Recalibration of optimal VER location automatically satisfies the voltage constraint..	150
Figure 56. Step three: Determining optimal VER operational point.....	151
Figure 57. Optimal DG operational point for a given voltage profile.....	153
Figure 58. Optimal DG power factor when DG operates at its full capacity. ....	154
Figure 59. Approximation of voltage drop over a conductor section.....	162
Figure 60. Actual voltage profiles measured the test system (Figure 9). ....	164
Figure 61. Errors induced by voltage approximation of Equation 1. ....	165
Figure 62. Errors of approximating scattered loads to continuous loads. ....	166

# List of Tables

---

Table 1. Theoretical Benefits of Distributed Generation. ....	18
Table 2. Physical and Equipment Level Statistics for a Medium-Sized Power System. ....	32
Table 3. Statistics of the two-feeder system in Figure 10. ....	41
Table 4. $S$ versus $S^V$ : Duality between regular and voltage-effective apparent power. ....	45
Table 5. Means to mitigate voltage rise in DG penetrated distribution systems. ....	83
Table 6. Reconfiguration applications and their benefits. ....	98
Table 7. Optimal DG location for three typical load distributions. ....	107
Table 8. Power loss varying with DG location on feeders of three load distributions. ....	109
Table 9. Optimal DG location for three DG capacities penetrated on the feeder system in Figure 10. ....	110
Table 10. Power delivery loss and voltage profiles under varying DG capacity/output. ....	114
Table 11. Computational complexity comparison of the proposed DG placement process and repetitive power flow. ....	123
Table 12. Parameters of DG units by their capacity and number per group. ....	123
Table 13. Computational complexity comparison between the proposed DG sizing method and repetitive power flow. ....	129
Table 14. Parameters of the test system in Figure 9. ....	164
Table 15. Number of Components ....	191
Table 16. System Capacity. ....	191
Table 17. Transformers. ....	191
Table 18. Feeders ....	192
Table 19. Power Balance. ....	192
Table 20. Power Delivery Loss. ....	192
Table 21. Operation Status Measured at Feeders' Substations. ....	192
Table 22. Load Capacity. ....	193
Table 23. Feeder Power Delivery Status. ....	195

# Forward

---

Distributed Generation (DG), or embedded generation, is often defined as small-scale generators that produce several kilowatts to tens of megawatts of electricity. Given today's majority electricity are generated by power plants that are connected to high voltage transmission networks, DG provides the option for utilities and network owners at low voltage distribution levels. In the past ten years, a number of utilities have started to offer backup generation as a service. In 2009, 16 MW DG units were connected to utility systems in the U.S., occupying 20% of the newly installed generation [1].

One primary reason for the popularity of DG penetration is its potential to reduce power delivery loss and therefore to defer investments in transmission or distribution infrastructure. It is estimated that replacing 30% of today's generation can reduce power loss up to 15%, which can be translated in the U.S. every year as six billion kilo-watt-hour (*kwh*) energy savings or \$250 million in dollars. In addition, DG presents great potential benefits to power system security, economic, reliability and emission [1-3].

To realize these benefits, utilities and network owners are facing challenges at the same brought by DG penetration in distribution systems which are not conventionally designed for connection of generators. A technical bottleneck widely considered for DG penetration is the steady-state voltage rise effect. Voltage exceeding these limits may cause damage to equipment on both system and user sides, and lead to malfunction of protection devices and excessive loss [4-9].

This thesis proposes a planning scheme for DG penetration in distribution systems that maximizes DG penetration's benefits, in terms of power delivery loss reduction, and restricts its adverse impact of steady-state voltage rise. Understanding many more constraints existing in practical DG penetration, technical, economic and policy-wise, this thesis poses such a planning scheme to provide the base line of DG penetration, on which the other constraints can be imposed in need of adjusting to a comprehensive system configuration and wider timeframe.

Distinguished from previous studies, which plans optimal DG penetration for specific distribution systems, the proposed planning scheme is generally applicable to any distribution system regardless of its configuration and load capacity. More importantly, this planning scheme is not "a black box,"

from which only the final DG plan is visible to its users, but it is a theoretical toolkit that aims at providing the users an intuition how DG penetration affects the performance of a distribution system. The policy makers, regulators, industries and utilities will be able to use this toolkit, without going through complicated computations, as guidelines to make policies, standards and decisions in DG penetration and related business.

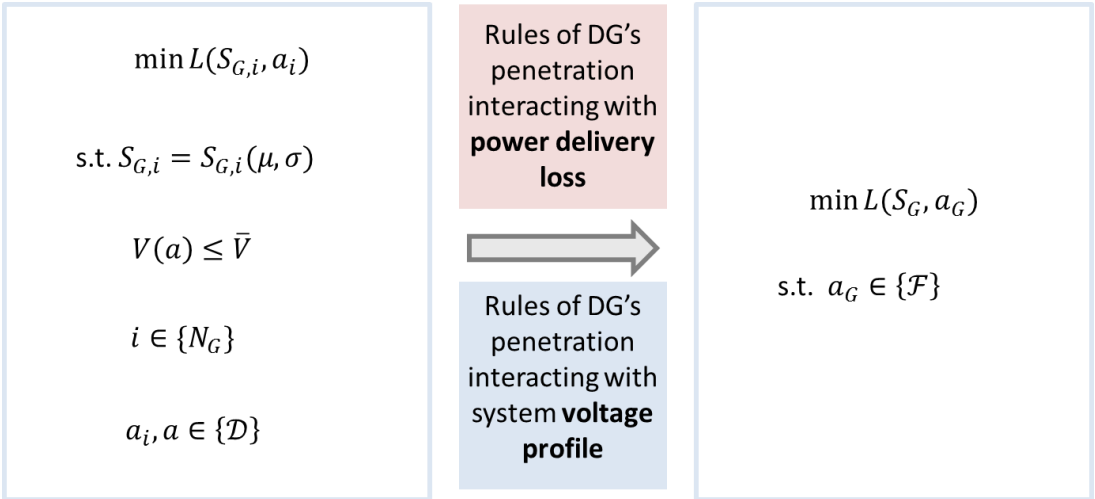


Figure 1. Technical blueprint of the thesis.

The optimization problem of DG penetration on the left is simplified to the one on left with two sets of rules of DG penetration interacting with system power delivery loss and voltage profiles. These two sets of rules and their application in the problem simplification together makes the planning scheme sought for.

### Logic and Structure

Finding the planning scheme for DG penetration in distribution systems can be poised as an optimization problem, which is formed on the left of Figure 1. The objective of DG penetration is to

minimize the power delivery loss induced. To realize this objective, the DG penetration must ensure its induced voltage is within the predetermined upper limit (the second constraint). This optimization could cost substantial computational effort when DG is carried out by renewable technologies of time-varying output (the first constraint), with many units spread out on a distribution system covering wide geographic area (the third and fourth constraint). On the contrary, it would be much easier to solve a DG penetration problem on the right of Figure 1, which searches for location and capacity of a single DG unit on a feeder system<sup>1</sup>.

In this thesis, two sets of rules are proposed to transform the complicated problem of DG penetration to the simple problem, as illustrated in Figure 1. These rules together with the transformation process compose the planning scheme for DG penetration in distribution systems.

Chapter 1 introduces the major concepts and models for the development of the two sets of rules. Voltage-effective power, with which voltage can be fast estimated and modeled in real domain (comparing to conventional voltage calculation in complex domain), is originally proposed in this chapter. The power flow model built on this concept and test systems for simulations in this thesis are also introduced in this chapter.

Chapter 2 presents the rules of DG penetration interacting with voltage profiles in distribution system. It proposes a *graphical method* that visualizes the voltage profile change during DG penetration. It also derives an *Area Criterion* as a revision of the zero-point analysis, which has been conventionally used in determining the possibility of overvoltage occurrence. Based on the proposed method and criterion, this chapter further revises the definition of permissible DG penetration in a distribution grid, as well as proposes a handy DG penetration chart for distribution planners to examine DG penetration feasibility. It then identifies six factors that causes voltage rise in DG penetration, followed by mitigation methods, among which demand response and reconfiguration are highlighted.

Chapter 3 proposes rules of DG penetration interacting with power delivery loss in distribution systems. Starting with single DG unit sizing and placement, this chapter proposes the *Half Capacity Rule* and the *Equal Voltage Rule*. These rules are then extended to multiple DG unit penetration with the *Superposition Rule*, which significantly reduce the computational efforts of DG penetration

---

<sup>1</sup> Definition of distribution system and feeder system are given in Chapter 1.

planning. Effects of time-varying output of DG units that are driven by Variable Energy Resources (VERs) are included by the *DG Variance Rule*.

The rules derived in Chapter 2 and 3 are not limited to certain distribution system configuration or capacity. They are generally applicable and can be used separately to suit any specific DG penetration situation. With these rules, Chapter 4 presents the overall planning scheme for DG penetration in distribution systems, which completes the transformation shown in Figure 1. The proposed planning scheme covers DG penetration in the planning stage that determines optimal DG locations, capacities, and operational points, and in the post-planning/ operation stage that decides optimal DG output power and power factor.

Chapter 5 serves as the conclusion of this thesis. First, the thesis motivation and approach are briefly reviewed. Then the assumptions and study scopes defined in all chapters are then summarized. In addition, the two sets of rules and the final planning scheme for DG penetration are concluded in this chapter, followed by recommendations for policy and industry decision makers.

This thesis also includes four appendices for interest in further reading. Appendix A examines the approximations made in this thesis and their induced errors. Appendix B includes the mathematical development of all the rules derived in this thesis for DG penetration. The proofs in this appendix ensure the general applicability of the rules proposed. Appendix C presents the data of the test systems. Finally, Appendix D includes the MATLAB code used in all the simulations of this thesis.

# Chapter 1: Background, Basic Concepts and Models

---

This chapter introduces the major concepts and models of this thesis.

Section 1.1 provides a brief description of *Distributed Generation's* (DG) definition, benefits, and increasing penetration trend, which motivates the study in this thesis. It outlines the two major criteria considered in DG penetration: energy efficiency, measured by power delivery loss; and reliability, epitomized by steady-state voltage rise, of a power system. It further surveys the existing research on DG penetration of four categories: qualitative approach, engineering approach, repetitive power flow, and Jacobian matrix.

Section 1.2 then provides the basic concepts and power engineering background of this study in two subsections: distribution systems, and feeder systems, where primary distribution system is often regarded as DG connection level and is defined as the physical level of our study scope in power systems. An important statement made in this section is: feeder systems are independent in (steady-state) voltage analysis.

Section 1.3 presents the fundamental mathematical concepts and models in this thesis: voltage-effective power, which is proposed in this thesis, and its associated power flow model of feeder systems. With voltage-effective power, voltage can be fast estimated and modeled in real domain (comparing to conventional voltage calculation that runs power flow in complex domain). It is also demonstrated as a dual concept in pair with apparent power that is associated with current and used in power loss estimation. These models and concepts are the fundamentals on which the findings are built in the rest of the thesis.

The test system and software tools used to verify the proposed results are introduced in Section 1.2.2 and Section 1.3.2 respectively.

## 1.1 Distributed Generation

### 1.1.1 What is DG?

*Distributed Generation* (DG), or embedded generation, is a concept relative to the traditional centralized generation from power plants, in terms of generators' size and its connection location in power systems. Generators carry on this concept is referred to as Distributed Generators. They generally refer to the relatively small-scale generators that produce several kilowatts (*kW*) to tens of megawatts (*MW*) of power and are generally connected to the grid at the distribution or substation levels [10-12].

DG is available in sizes from less than 5 *kW* to 25,000 *kVA* (even larger turbine and diesel units are available, but 25,000 *kW* is generally considered the top of the "DG range") [3, 13]. Generally, large reciprocating and combustion turbine generators are designed for heavy, long-term use, and are available in sizes from 1,000 *kW* on upwards. Large fuel cell systems are available in capacities from 1,000 *kW* up to 10,000 *kVA*. **DG of these larger sizes are usually installed at the primary distribution voltage<sup>2</sup>**, e.g., on portions of the electric system between 2 and 25 kV phase to ground, and are restricted to applications at large industrial sites, or on the electric utility system itself. Some are applied as base load, used 8,760 hours per year, while others serve as peak-reduction units used only during periods of high power demand [10, 14, 15].

Smaller DG units are available in sizes from 1,500 *kW* down to as small as 5 *kW*. These units are intended for heavily dispersed applications, as generators for individual homes and small businesses or as portable power units for construction sites, etc. Reciprocating piston, fuel cell, and a type of turbine (micro-turbine) are all available in this range [2, 16]. Such "mini" and "micro" generators are almost always installed on utilization voltage level ( $120\text{ V}/240\text{ V}$ , 480 *V*, or 600 *V*) circuits, often on the customer side of the electric utility meter. Applications for these types of units can include providing power for all of the electrical demand at a residence or small commercial site, or just providing power for peak shaving. They can also be devoted solely to improving availability of power, including usage in UPS (uninterruptible power supply) and standby or emergency power systems [12, 17, 18].

---

<sup>2</sup> Wind farms and solar farms that aggregate DG output and are connected to the transmission networks are not really "distributed" in power systems. These forms of generation, despite of composed of DG units, are not discussed in this thesis.



**Because it has the greatest penetration capacity and put forward most challenges in power systems, this thesis restricts its discussion on DG of the larger sizes connecting to the primary distribution voltage [12, 19-23].** To DG of more fractional sizes, the methods proposed in the later chapters can be applied by aggregating the small sizes into one big sized unit and their installed locations into a geographical range at a primary distribution grid.

A wide range of generation technologies are deployed in DG applications, including gas turbines, diesel engines, solar photovoltaic (PV), wind turbines, fuel cells, biomass, and small hydroelectric generators [3, 24]. Conventional fossil fuel driven DG is the most often used form, like gasoline, diesel or fuel oil, natural gas, propane, methane, or gasified coal, to produce electric power. In every case, regardless of fuel, through very careful design and often intricate timing of events, measured amounts of the fossil fuel are oxidized - purposely combined with oxygen - to produce heat, and perhaps pressure, and, ultimately, electricity. Some DG units that use conventional fuel-burning engines are designed to operate as combined heat and power (CHP) systems that are capable of providing heat for buildings or industrial processes using the “waste” energy from electricity generation [10, 20, 25, 26]. Results proposed in this thesis are not limited to a certain type of DG technology, and can be generally applied.



Figure 2. 20 MIT power plants (building 42) shots from the side and front.

When connected to power grids, DG can be a single unit, multiple units of the same or a mixture of technologies. Figure 2 shows an example of DG owned by MIT. It has a combined heating, cooling, and power plant based on a gas turbine engine rated at about 20 MW, connected to our local utility at distribution primary voltage (13.8 kV).

**1.1.2 Why to connect DG to the grid?**

Distributed generation can be owned and operated by utilities or their customers and can provide a variety of theoretical benefits to their owners and the broader power system. In 2007, Department of Energy published a report listing a litany of good things DG can do (see Table 1). Distributed generation installations theoretically can improve reliability, reduce costs, reduce emissions, and improve power quality [2, 13, 27].

Table 1. Theoretical Benefits of Distributed Generation.  
[2, 13, 27]

Reliability and Security Benefits	Economic Benefits	Emission Benefits	Power Quality Benefits
<ul style="list-style-type: none"> <li>• Increased security for critical loads</li> <li>• Relieved transmission and distribution congestion</li> <li>• Reduced impacts from physical or cyber-attacks</li> <li>• Increased generation diversity</li> </ul>	<ul style="list-style-type: none"> <li>• Reduced costs associated with power loss</li> <li>• Deferred investments for generation, transmission, or distribution upgrades</li> <li>• Lower operation costs due to peak shaving</li> <li>• Reduced fuel costs due to increased overall efficiency</li> <li>• Reduced land use for generation</li> </ul>	<ul style="list-style-type: none"> <li>• Reduced line loss</li> <li>• Reduced pollutant emissions</li> </ul>	<ul style="list-style-type: none"> <li>• Voltage profile improvement</li> <li>• Reduced flicker</li> <li>Reduced harmonic distortion</li> </ul>

Improved system reliability results from the ability of DG units to maintain supply to local loads in the event of a broader system outage. This could be done by creating “islands” in which a section of a distribution feeder is disconnected from a faulted area. Such an action is called “islanding.” Successful islanded operation requires sufficient generation to serve local loads and also the necessary distributed system control capabilities [16]. The potential reliability benefits of generators based on variable energy resources, generators with limited fuel reserves, or generators with low individual reliability are limited even if islanded operation is possible [28, 29].

Economic benefits can be realized when utilities deploy DG to defer investments in transmission or distribution infrastructure. Since DG is typically located closer to load relative to central plants, it can reduce congestion and system loss in some instances [27]. It is estimated that replacing 30% of today's generation can reduce power loss up to 15%, which can be translated in the U.S. every year as six billion kilowatt-hour (*kwh*) energy savings or \$250 million in dollars. Customer-sited DG, on the other hand, often reduces utility revenue but can offer customers long-term electricity cost stability and, in some cases, savings. This savings can come in different forms. First, current rules allow customers with DG to avoid paying their share of fixed network costs. Second, because electricity generated by DG is typically more expensive than electricity generated in central power plants, customers subject to increasing block electricity tariffs (in which customers who use more than some amount of electric energy pay a high rate) or who are offered sufficient subsidies can realize energy cost savings with DG. Combined heat and power (CHP) systems also can reduce total energy costs for their owners [13, 15].

Emission benefits can be realized by renewable generators, such as solar photovoltaic (PV), which have no marginal emissions, or CHP systems whose use of waste heat can result in higher efficiencies than central generation units [3, 13, 30]. The magnitudes of emissions benefits associated with DG depend on both the characteristics of individual DG units and the characteristics of the power system to which they are connected.

Distributed generation capable of providing constant, uninterrupted power can improve power quality by mitigating flicker and other voltage regulation problems. With properly designed and implemented power electronics interface, connection of DG to the grid could theoretically cancel grid distortions and help regulate voltage [31-33]. Many inverters on the market today are capable

of these advanced functions, but such features add cost, and today DG owners rarely have incentives to invest in this added functionality [10, 34-36].

### 1.1.3 Current Status of DG Penetration in the Grid

Though gaining more attention recently, DG is not a new concept in power systems and has been widely used in the industry for decades, but almost exclusively as backup generation aimed at providing a type of improved reliability [2, 37]. Energy consumers, mostly commercial and industrial users with high costs of sustained interruptions, have created a very large and healthy market for backup generation systems [38].

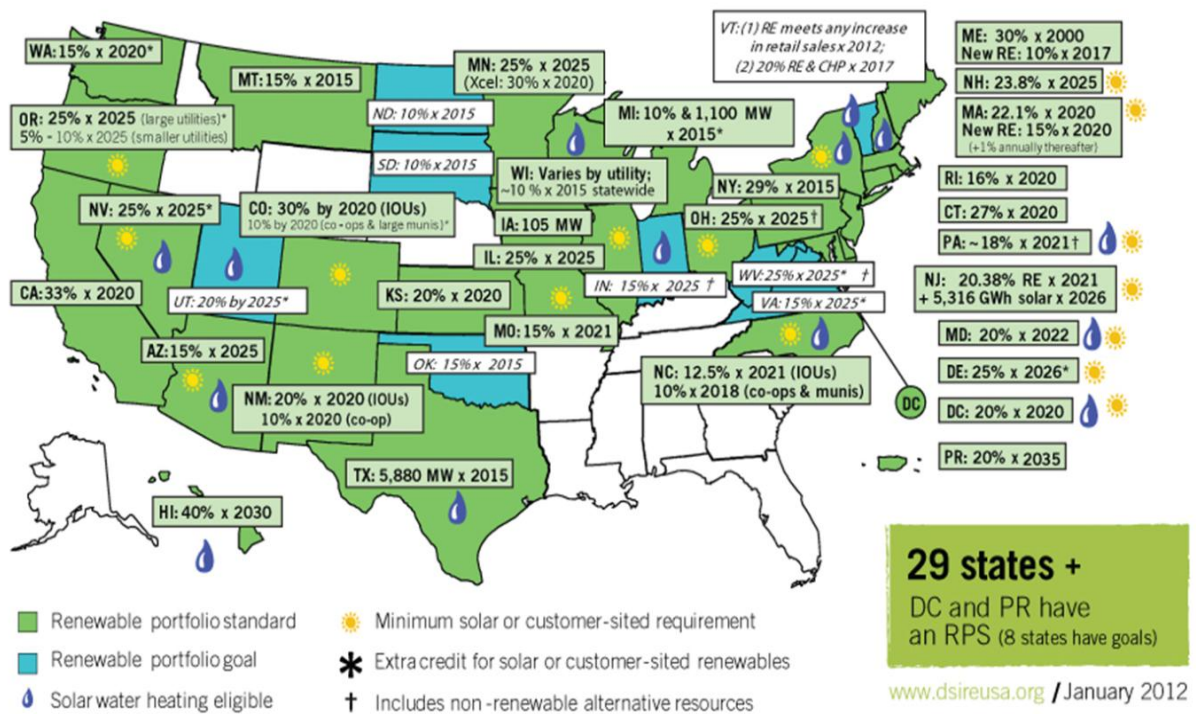


Figure 3. Renewable Portfolio Standards of 29 States.

However, in the past ten years, a number of utilities have started to offer backup generation as a service, which largely promotes the penetration of DG, in particular, among small industrial, commercial and residential users [39, 40]. In 2009, 16 MW DG units were connected to utility systems in the U.S., occupying 20% of the newly installed generation [1]. Federal and state policies are expected to drive growth in DG in the coming decades. Twenty nine states and District of Columbia had set renewable portfolio standards, in which sixteen states and the District of Columbia currently have renewable portfolio standards with specific DG provisions (see Figure 3). For example, some states have provisions in their renewable portfolio standards that require some fraction of retail electricity sales to come from renewable DG by 2020 [3, 13].

At present installed costs, many renewable DG installations remain dependent on these mandates or subsidies. The durability of such government policies will largely determine the rate of growth of installations over the next several years. In the long term, cost reductions also may drive DG growth. The average installed cost of residential and commercial solar PV installations dropped from about \$10.50 per WDC in 1998 to about \$7.60 per WDC in 2007 (both figures are in 2007 USD before incentives or tax credits) [3]. As of September 2011, residential, commercial, and industrial PV installed system costs had fallen to \$7.10, \$5.10, and \$3.70 per WDC, respectively [30]. Although these costs are not competitive with conventional generating sources in most locations, if they continue to fall, solar PV systems will ultimately become competitive [2, 41]. In addition, net metering policies that favor renewable DG could accelerate the adoption of residential rooftop solar PV generation even before this type of generation becomes otherwise economically viable [42].

#### **1.1.4 Challenges to increased penetration of DG**

Despite of the tremendous benefits of DG connection to the grid and therefore its increased penetration, challenges comes from commercial, regulatory, and most essentially, technical, to which much of the first two challenges can be attributed. That is, the benefits of DG are highly dependent on the characteristics of each installation and the characteristics of the local power system. Furthermore, many benefits accrue to specific stakeholders and may not benefit the distribution system operator or the other customers of the system. Finally, existing DG interconnection standards prevent owners from realizing some of these hypothetical benefits.

### *Commercial Challenges*

Large DG units are typically dispatchable and communicate with system operators like central station generation facilities do. However, neither utilities nor system operators typically monitor or control the operation of small DG units, especially those in residential applications [43, 44]. Renewable DG from wind and solar power also typically is not dispatchable or easily controllable [45, 46]. In 2009, about 13,000 commercial and industrial DG units with a combined capacity of about 16 *GW* were connected to utility systems in the U.S. Of these units, 10,800 (83%) were smaller than 1 *MW*, averaging 100 *kW* each [1, 47]. Internal combustion engines, combustion turbines, and steam turbines comprised more than 4 *GW* each of installed capacity, while hydroelectric, wind, and other generator technologies totaled 3 *GW*. In the same year, 93,000 residential PV installations totaled about 450 *MW* of capacity [1]. While 90% of solar PV installations between 1998 and 2007 were smaller than 10 *kW*, the largest installations generated more than 14 *MW* [2, 15].

**Due to the great challenges these units present to the grid in operation, utilities and system planners should pay attention and take actions as possible at the stage of their connection to the grid.**

### *Regulatory Challenges*

In the absence of a clear policy and associated regulatory instruments on the treatment of DG, it is very unlikely that this type of generation will thrive. The reasons for this are partly historical and related to the way distribution grids have not been developed and operated for DG connection. **In order to foster the required changes, there is a clear need to develop and articulate appropriate policies that support the integration of DG into distribution grids** [10, 38, 48].

### *Technical Challenges*

The introduction of DG can significantly impact the efficiency and reliability of its connected distribution grids. In fact, power system operations may be adversely impacted by the introduction of DG if certain minimum standards for control, installation and placement are not maintained. There are many technical issues that must be considered when connecting DG to the distribution system, such as:

- power quality (such as flicker, harmonics)
- protection
- stability
- steady-state voltage rise
- loss

Apart from loss, all the other technical issues can be classified as system reliability problems.

### Power quality

Two aspects of power quality are usually considered to be important: (1) transient voltage variations and (2) harmonic distortion of the network voltage. DG connected to the grid via power electronic inverters (e.g., solar PV, fuel cells, and most wind turbines) are widely understood to be sources of voltage waveform distortion [18, 48, 49]. Depending on the particular circumstance, DG plant can either decrease or increase the quality of the voltage received by other users of the distribution network. An adverse example is that a single large DG, e.g. a wind turbine, on a weak network may lead to power quality problems particularly during starting and stopping [45].

### Protection

A number of different aspects of DG protection can be identified: Protection of the generation equipment from internal faults; protection of the faulted distribution network from fault currents supplied by the DG; anti-islanding or loss-of-mains protection (islanded operation of DG will be possible in future as penetration of DG increases) and impact of DG on existing distribution system protection [8, 50-52]. All these aspects are important and need to be carefully addressed in connecting DG to distribution networks.

### Stability

Traditionally, distribution network design did not need to consider issues of stability as the network was passive and remained stable under most circumstances provided the transmission network was itself stable. Even at present stability is hardly considered when assessing renewable distributed generation schemes [39, 53, 54]. However, this is likely to change as the DG penetration increases and its contribution to network security becomes greater. The areas that need to be considered

include transient (first swing stability) as well as long term dynamic stability and voltage collapse [55, 56].

### Voltage Regulation

**The voltage rise effect is a key factor that limits the amount of additional DG capacity that can be connected to distribution grids.** This subject has recently called considerable attention of the technological community and many works have been devoted to deal with this important subject [4, 12, 57, 58]. Connecting a generator to the distribution system will affect the flow of power and raise the voltage profiles. In the U.S., distribution system voltage is regulated by ANSI C84.1<sup>3</sup> (which full title is American National Standard for Electric Power Systems and Equipment Voltage Ratings (60 Hz)). This standard requires, for each nominal system voltage, two ranges for service voltage and utilization voltage should be met, designated as Range A and Range B.

Basically, the Range A voltage range is plus or minus 5% of nominal. It is required for distribution grid operated under normal conditions. The Range B voltage range is plus 6% to 13% of nominal. Range B includes voltages above and below Range A limits that necessarily result from practical design and operating conditions on supply or user systems, or both [59]. Although such conditions are a part of practical operations, they shall be limited in extent, frequency, and very short duration.

Voltage exceeding these limits may cause damage to equipment on both system and user sides, cause malfunction of protection devices and excessive loss [60-62]. This thesis restricts its study scope to steady-state performance of DG connected power grids. Therefore, Range A is used to define the voltage limits in the numerical examples in the later chapters.

While the physical principle of voltage raised by DG connection is explained in Chapter 2, Figure 4 illustrates this by an example: connecting a DG unit (operating at unity power factor) at 12 km from the primary substation (controlled at 103% of nominal voltage). When the unit's size is

---

<sup>3</sup> Standards for steady-state voltage vary by countries. For example, in U.K., the Electricity Safety, Quality and Continuity Regulations stipulate that, unless otherwise agreed, the steady-state voltage of systems between 1000 V and 132 kV should be maintained within +6% of the nominal voltage. It is the Distribution Network Operator's (DNO's) responsibility to ensure that its systems are operated within the voltage limits. However, at the planning stage, the 11 kV system is often designed to maintain voltages within  $\pm 3\%$  of nominal, so that the voltage variations seen by the LV connected customers remain within the permitted +10% and -6% limits.



300 kW, the resultant voltage falls as the distance from the primary substation increases, as before DG connection, but the voltage drop is less profound. Increasing the generation to 1 MW reverses the flow of power along the line, from the generator towards the primary substation [4]. The voltage at the generator rises above that elsewhere, thus allowing the power to be exported in both directions. In this example, the voltage in some parts of the system rises above the permitted +6% voltage limit.

The voltage rise is more onerous when there is no demand on the system, as all the generation is exported back to the primary substation. With 1 MW of generation connected, the voltage rises to 112% of nominal. This suggests that it is the voltage rise during periods of no/minimum demand that limits how much generation can be connected.

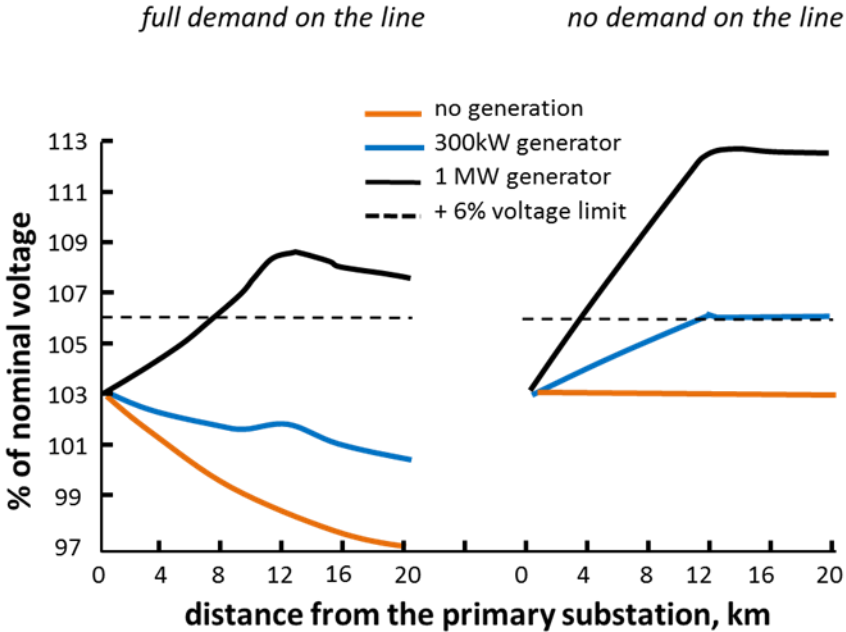


Figure 4. Effect of connecting a DG unit on the voltage profile along an 11 kV overhead feeder.

The feeder is 20 km long measured from the primary substation, comprising 16 mm<sup>2</sup> copper conductors. Every 4 km along the line is a three-phase load of 100 kW and 20 kvar. The DG unit is connected at 12 km away from the feeder’s primary side [4].

### Loss

Distributed generation will also impact loss on the feeder. DG units can be placed at optimal locations where they provide the best reduction in feeder loss. Siting of DG units to minimize loss is like siting capacitor banks for loss reduction [63-66]. **The only difference is that the DG units will impact both the real and reactive power flow. Capacitors only impact the reactive power flow.** Most generators will be operated between 0.85 lagging and 1.0 power factor, but some inverter technologies can provide reactive compensation (leading current). On feeders where loss are high, a small amount of strategically placed DG with an output of just 10% to 20% of the feeder demand can have a significant loss reduction benefit for the system [27, 67, 68].

Larger DG units must be sited with consideration of feeder capacity limits. In some cases overhead lines and cables may be thermally limited meaning that the DG can inject power that exceeds the line's thermal limit without causing a voltage problem on the feeder [69-71]. The power flow analysis should "flag" the locations where capacity constraints will be an issue from a perspective of thermal as well as voltage. In general, a DG at a location that is thermally limited is naturally neither optimal point from a "power loss" perspective [37, 72].

#### **1.1.5 Existing Approach to Planning DG Penetration**

A successful case of DG penetration can be interpreted as satisfying three conditions: (1) fulfilling the designated political goals and environmental requirements; (2) realizing DG benefits to the greatest extent in the penetrated distribution system; and (3) mitigating, and if it were to happen, to the greatest extent restricting DG potential adverse impact on the penetrated distribution system. The three conditions represent social satisfaction, efficiency and reliability of DG penetrated systems. While social satisfaction depends on specific cases, or can be simplified as maximizing DG penetration (to reach the upper bar set by the political and environmental requirements), power system efficiency is primarily represented as power delivery loss; and voltage rise is the major reliability issue induced by DG penetration.

Due to their paramount importance, minimizing power delivery loss and mitigating voltage rise in DG penetrated systems have been gaining increasing attention in research and practices. Although the two problems are treated separately by some studies, they are more often considered as a whole, if represented in optimization formula, with the objective of power loss minimization and constraint of voltage limits. There are four major existing approaches to the problem: power flow, engineering

approach, scenario analysis, and active network planning. The rest of this subsection introduces their principles and deficiencies in turn. In addition, an approach gaining popularity, active network planning, is reviewed.

### *Scenario approach*

In a few studies, specific scenarios are investigated to find a DG siting plan that ensures system efficiency and voltage reliability. For example, Dinic et al. [73] consider voltage limitations and installed DG capacity, relative to the system fault level, in 33 kV networks and conclude that capacitive compensation can allow capacity maximization within operational limits. Quezada et al. [74] examine the impact of increased DG penetration on electrical loss within the IEEE 34-node test network and conclude that loss follow a U-shaped trajectory when plotted as a function of DG penetration. Jupe et al. [75] make the analysis of predicting how loss will vary when connecting a specific photovoltaic plant to a specific feeder, based on a feeder section-by-section analysis.

Except for very rare cases, the results of these studies are only limited to their investigated scenarios. Extending the results derived from specific scenarios, or even a number of scenarios, to more general cases may lead to extra power delivery loss and risk the penetrated grids' voltage reliability. This is because power distribution systems differ much in configuration. Important information, such as, location of a certain DG type, is hard to be conveyed by a general penetration guideline, for example, the ratio of total DG capacity to demand in the penetrated grid [4, 47, 76-78].

### *Power flow*

A very often used way to analyze the power loss and voltage behavior of a system with DG is to run a power flow simulation using software capable of analyzing multiple sources on the distribution system and under varying penetrated grid conditions [72, 79-81]. Figure 5 illustrates the principle of this approach: in order to obtain the optimal location and size of DG, successive power flow studies based on the try-and-error method. **A major limit of this approach is the great computational effort and time due to the repetitive implementation of a Security Constrained Optimal Power Flow (SCOPF).** The optimization method aims to find the optimal locations and capacities of DG so that the penetrated network loss is minimized. Such an objective is subject to a number of technical constraints imposed by regulations, including thermal limits of line and transformer, and

bus voltage limits. By fulfilling these constraints, an optimal DG penetration plan (or dispatch schedule of DG output and control scheme of voltage regulation devices) is generated.

To reduce the computational effort, some studies propose to use only the Jacobian sensitivities in estimation of the maximum DG output that will not voltage limit violation [68, 82-84]. This method is based on only one matrix operation and one power flow solution and assuming no substantial changes in the system structure. However, this method is only valid for small DG penetration variations. And the results' accuracy heavily depends on the initial condition at which the power flow Jacobian matrix is established.

**Engineering approach**

After DG has been penetrated, power delivery loss can be minimized and voltage rise can be mitigated through deployment of online devices, such as capacitor, control of DG, and reconfiguration the penetrated network. Many studies take these engineering approaches to assist DG penetration in distribution grids.

For example, Senjyu et al. [85] propose a genetic algorithm to coordinate the reactive power compensators and distributed generators in the presence of a widespread communication system. Carvalho et al. [57] and Salomonsson et al. [86] calculates DG power factor to avoid voltage rises of a simple distribution network. Kiparkis [87] uses an intelligent method using DG for voltage control in a distribution network was proposed. Madureira et al. [88] not only presents a voltage

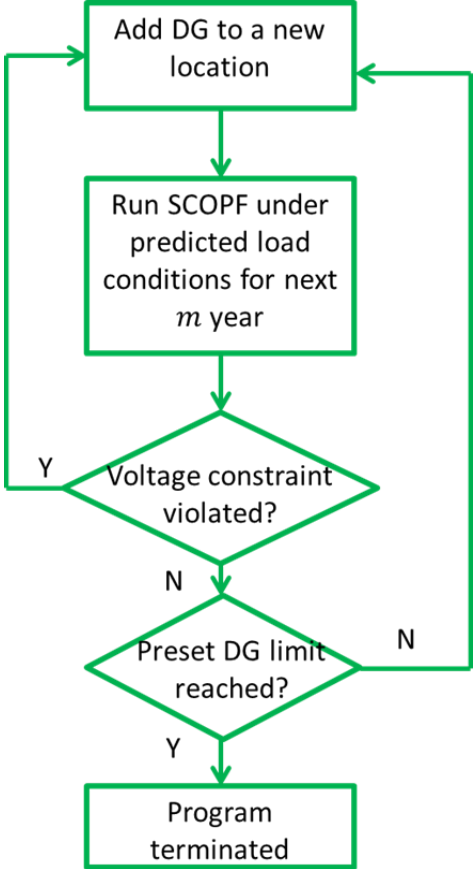


Figure 5. Algorithm chart of using repetitive power flow to site DG for minimum loss.

SCOPT stands for Security Constrained Optimal Power Flow.

control method with a single DG was presented, but also offers a method for coordinating DG and traditional voltage control devices using a centralized system to minimize loss. More complex distributed approaches have been proposed to control the target voltage of automatic voltage control relays at primary substations [78], and to combine fixed power factor with automatic voltage control [89].

There have been a few publications proposing coordinated or distributed voltage regulation and loss minimization in a centralized manner, through wide area voltage control and reactive power management [35, 90-92]. For example, Turitsyn et al. [92] uses the surplus reactive capacity of PV type DG to manage the line voltage via cooperative control. This specific method is sometimes referred as Active Network Management (ANM).

A strong limitation of engineering approach is that its results depend on the deployment of specific types of devices and therefore is hard to be realized in more general cases. In order to apply these results and realize the benefits induced, it requires significant investment in the devices, in particular for the centralized methods, which need sensors, communications, and control systems, which makes their application to massive DG situations difficult to implement [38, 93-95].

### ***Active network planning approach***

Considering the centralized engineering approach (or ANM) at the planning stage of DG penetration is regarded as active network planning. DG penetration capacity is enhanced through this method [2, 23]. Taking a similar approach to that used in transmission systems, a distribution management system controller would be used for wide area voltage control and reactive power management [96]. It would employ state estimation to assess voltage profile and dispatch DG and other network elements accordingly to minimize power loss [95, 97].

For example, in Siano et al. [98] evaluate the maximum wind energy exploitation in a distribution network under different active management schemes during a given time horizon. The algorithm integrates active management schemes such as coordinated voltage control, energy curtailment and power factor control. Ochoa et al. [99] propose a multi-period AC optimal power flow technique to offer a means of measuring the impact of ANM on connectable renewable capacity while respecting voltage statutory limit. A range of technologies, including coordinated voltage control of

transformers and voltage regulators, adaptive power factor control and energy curtailment are embedded within the formulation.

Even though the results derived under this approach is quite promising, this approach shares the same limitation of all engineering approaches: it requires much investment in sensors and communication assets and is case-specific with difficulties to be generalized.

Due to the limitations of these four approaches, this thesis proposes a theoretical toolkit that can be easily applied to any case without losing DG penetration's optimality, namely, power loss minimization and steady-state voltage reliability. The approach adopted in this thesis is described in the Logic and Structure Section in the forward of this thesis. The rest of the thesis presents the derivation of the toolkit, demonstrates its generality and ease in application, and verifies the optimality after its application.

## **1.2 In Scope of Distribution Systems**

### **1.2.1 Distribution Systems**

Distribution systems are the next level under transmission systems in power systems. Generally, in most utility systems, distribution systems are referred to power delivery configurations that are radial, built of only 34.5 kV or below, and feed service transformers. This concept is in relative to transmission systems that are above 34.5 kV, configured as networks, and do not feed service transformers directly [38].

More generalized definition of distribution systems are found in some of today's publications [2, 11]: "distribution" means the "retail" or "service to native load" level, while "Transmission" is becoming synonymous with "wholesale level grid."

The rest of this subsection gives a brief review of the physical and equipment levels in distribution systems. Some statistics from a medium-sized power system are also listed in Table 2.

#### ***Hierarchy of distribution systems***

Distribution systems are further divided into three physical levels, primary, secondary/service distribution systems, and load/customer level, based on their voltage levels (illustrated by Figure 6).

The primary distribution level is composed of three major functional blocks: substations, feeder systems and service transformers [38]. Distributed Generation (DG), as stated in the previous subsection, is primarily connected to distribution systems at the primary distribution level. It is therefore the physical level this thesis investigated on and proposed for a planning scheme for DG penetration [14, 69].

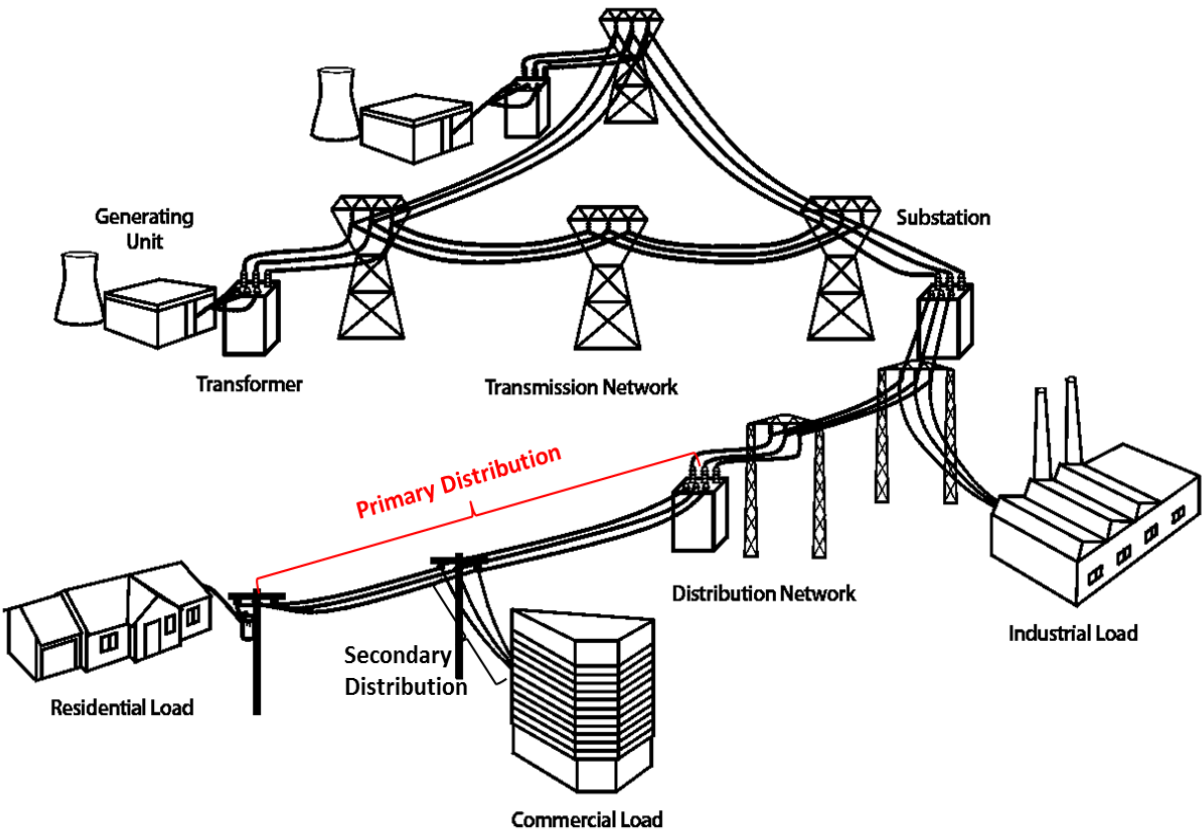


Figure 6. Hierarchy of a power system.

[2]

Table 2. Physical and Equipment Level Statistics for a Medium-Sized Power System.

<b>Level</b>	<b>Voltage (kV)</b>	<b>Number</b>	<b>Avg. Cap (MVA)</b>	<b>Total Cap (MVA)</b>
<b>Transmission</b>	345,138	12	150	1,400
<b>Sub-Transmission</b>	138,69	25	65	1,525
<b>Substations</b>	139/23.9, 69/13.8	45	44	1,980
<b>Feeders</b>	23.9,13.8	227	11	2,497
<b>Service Trans.</b>	0.12,0.24	60,000	0.05	3,000
<b>Secondary/Service</b>	0.12,0.24	250,000	0.014	3,500
<b>Customer</b>	0.12	250,000	0.005	1,250

### The Substation Level

Substations are the meeting points between the transmission grid and the distribution feeder system. The transmission and sub-transmission systems above the substation level usually form a network, with more than one power flow path between any two parts. But from distribution systems, there is only one path through the other levels of the system [100].

### The Feeder Level

Feeders, typically either overhead distribution lines mounted on wooden poles or underground buried or ducted cable sets, route the power from the substation throughout its service area. Feeders operate at the primary distribution voltage. The most common primary distribution voltage in use throughout North America is 12.47 kV, although anywhere from 4.2 kV to 34.5 kV is widely used. Worldwide, there are primary distribution voltages as low as 1.1 kV and as high as 66 kV. Some distribution systems use several primary voltages - for example 23.9 kV and 13.8 kV and 4.16 kV. A feeder is distributes power between 2 MVA to more than 30 MVA, depending on the conductor size and the distribution voltage level. Normally between two and 12 feeders emanate from any one substation [2, 70].

### The Lateral Level

Laterals, short stubs or line segments that branch off the primary feeder, represent the final primary voltage part of the power's journey from the substation to the customer. A lateral is directly connected to the primary trunk and operates at the same nominal voltage. A series of laterals tap off the primary feeder as it passes through a community, each lateral routing power to a few dozen homes. Normally, laterals do not have branches, and many laterals are only one- or two-phase.



Typically, laterals deliver from as little as 10 *kVA* for a small single-phase lateral to as much as 2 *MVA* [37, 101].

### The Service Transformers

Service transformers lower voltage from the primary voltage to the utilization or customer voltage, normally  $120/240$  two-leg service in most power systems throughout North America. In overhead construction, service transformers are single phase, between 5 *kVA* and 166 *kVA* capacity. There may be several hundred scattered along the trunk and laterals of any given feeder. Passing through these transformers, power is lowered in voltage once again, to the final utilization voltage ( $120/240$  in the U.S.) and routed onto the secondary system or directly to the customers [2, 37, 102].

### The Secondary and Service Level

Secondary circuits, fed by the service transformers, route power at utilization voltage within very close proximity to the customer, usually in an arrangement in which each transformer serves a small radial network of utilization voltage secondary and service lines, which lead directly to the meters of customers in the immediate vicinity. In the U. S., the vast majority of this system is single-phase. In European systems, much of the secondary is three-phase, particularly in urban and suburban areas [103, 104].

### ***Distribution Equipment***

In essence, there are only two major types of equipment that perform the power delivery function [37, 102, 104]:

- distribution lines, which move power from one location to another
- transformers, which change the voltage level of the power

Added to these two basic equipment types are two categories of equipment used for a very good reason:

- protective equipment, which provides safety and "fail safe" operation
- voltage regulation equipment, which is used to maintain voltage within an acceptable range as the load changes. This monitoring and control equipment is used to measure equipment

and system performance and feed this information to control systems so that the utility knows what the system is doing and can control it, for both safety and efficiency reasons.

Comparing to on transmission grids, many sophisticated devices are not commonly seen on distribution grids, such as Static Var Compensator (SVC), which can regulate voltage by adjusting local power factor. Due to their high cost, they are usually only installed on a higher voltage level to cover a larger service area [2, 37]. Communication systems, sensors and information systems, depend on which automatic control functions, are also currently not available in regular distribution systems. Regardless that some research claims the cost of these technics will eventually come down [93, 105, 106], the current status suggests that Active Network Management (ANM) is yet ready for most of distribution systems.

### **1.2.2 Feeder Systems**

Physically, the U.S. electric grid currently consists of approximately 170,000 miles of high-voltage (above 200 *kV*) electric transmission lines and associated equipment, and almost 6 million miles of lower-voltage distribution lines [2]. The size of distribution systems raises the complexity of their topology, capacity, numbers of physical components (as illustrated in Table 2), and therefore computational efforts. As shown in the Logic and Structure Section (see Figure 1), the optimization problem of DG penetration will be greatly simplified, if we can physically partition the distribution system into smaller sections and therefore reduce the size of the problem. These small sections, as are shown in the rest of this subsection, are feeder systems.

A distribution system's feeder level routes power from a relatively few utility sources (substations) to many points (service transformers), each only a short distance from the consumers it serves. Power is brought to these substations at transmission voltages somewhere between 34.5 *kV* to 230 *kV*. In turn, that power is lowered to a *primary distribution voltage* (between 2.2 *kV* and 35 *kV*), through transformers selected as appropriate for the service area [37, 104].

The feeder level is composed of individual feeder circuits, each a “neighborhood size” system operating at “primary voltage,” which nominal voltages in the range 2.4 to 19.9 *kV* phase-to-ground (4.16 – 34.5 *kV* phase-to-phase). The circuit system that must serve all the load and cover all the territory assigned to that particular substation [70].

### ***Transformers regulates feeders' voltage***

The most important equipment in substations, which gives this substation its capacity rating and “defines” the voltage of its connected distribution systems, are the substation *transformers*, which convert the incoming power from transmission voltage levels to the lower primary voltage for distribution. Individual substation transformers vary in capacity, from less than 10 *MVA* to as much as 150 *MVA* [100]. They are often equipped with tap-changing mechanisms and control equipment to vary their windings ratio so that they maintain the distribution voltage within a very narrow range, regardless of larger fluctuations on the transmission side [107] .

### ***Most feeders are the same "size"***

Most feeders are planned by *starting* with the premise that the main trunk (the initial segment out of the substation, through which all of the power is routed) will be the largest economical conductor in the conductor set. The feeder layout is arranged so this segment picks up enough load for its peak load to fall somewhere in the middle or upper half of that largest conductor's economical range. Thus, all feeders in a power system are somewhat the same "size" in terms of capacity and loading [37, 108].

### ***Topologies of Distribution Systems***

There are three fundamentally different ways to lay out a feeder system used by utilities. As shown in Figure 7, radial, loop, and network structures differ in how the distribution feeders are arranged and interconnected about a substation [37, 70].

#### **Radial feeders systems**

**More than 80% of all distribution worldwide is accomplished using *radial feeder systems***, in which there is only one path between any customer and the substation (Figure 7, left). In some cases radial feeders are designed and built as fixed radial circuits, but in a majority of cases the feeder system is physically constructed as a network (many paths from many sources), but is operated radially by opening switches at strategic points to impose a radial flow pattern [70, 109, 110]. (In Y-connected radial systems, the neutral conductor is connected through all open switch points, thus forming a network connecting feeders and substations.)

Radial circuits are almost always both the least expensive type of distribution system and the easiest to analyze and operate. Both low cost and simplicity of analysis and operation made radial systems popular in the beginning of the electric era, before computerization made analysis of complex circuit behavior reliable and inexpensive. This early popularity helped institutionalize radial circuit design as *the* way to build distribution. Although simplicity of analysis is no longer a major concern, low cost continues to make radial circuits the choice for more than 90% of all new distribution construction [2].

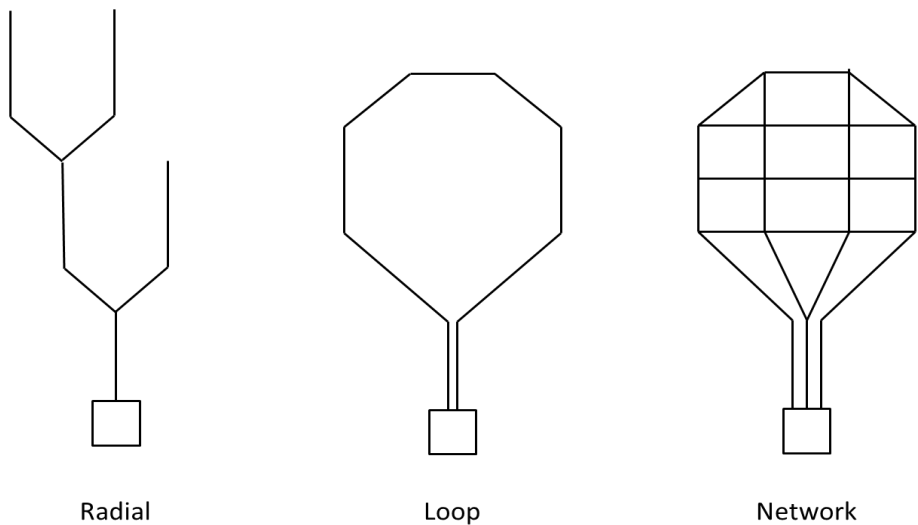


Figure 7. Topologies of feeder systems.

Loop feeders systems

Distribution can also be built and operated as *loop feeder* circuits in which the power flows into each "end" of a feeder and moves outward to customers (Figure 7, middle). This is basically a "dynamic" radial circuit, with the open point (null point) shifting as loads change. When built and protected properly, it can provide very high levels of customer reliability. Generally, loop feeder systems cost about 20% to 50% more than radial systems. Sometimes loop feeder systems are operated as open loop systems, with an open switch near the middle of the loop, in which case they are basically radial circuits [70, 111, 112].

## Feeder networks

Feeder networks consist of groups of feeders interconnected so that there is always more than one path between any two points in the feeder network (Figure 7, right). If designed with sufficient capacity and protection throughout, a feeder network can provide very high levels of customer reliability: the loss of any segment or source will not interrupt the flow of power to any customers [113-115].

Among their disadvantages, feeder networks cost considerably more than radial systems, usually 33% to 50% more in underground construction and 100% to 150% more in overhead construction, and they require much more complicated analysis and operating procedures. They also require more expensive protective devices and coordination schemes [37, 70, 104].

### *Voltage Limit versus Current Limit*

In dense urban areas, distribution systems are dominated by capacity limitations. Here, even the highest primary voltage with the largest possible conductor (1354 MCM, 34.5 kV) may not have enough capacity to serve less than two square miles, even though it can move its full thermal rating (70 MW) nearly 19.2 km before encountering Range A voltage drop limits. On the other hand, voltage drop is seldom if ever an issue in such planning [108].

At the other end of the distribution scale, in sparsely populated rural areas, voltage drop dominates the considerations which the planner must overcome. Here, load density is orders of magnitude lower than in urban areas, but the distances between nearest customers are often dozens of miles. A single feeder may have to distribute power over more than 2,960 km<sup>2</sup>. Even so, few feeders ever run up against capacity constraints [116, 117].

Moreover, in areas of dense load, feeders are usually laid out in network structures for reliability reasons; while in less populated areas, feeders are laid out in radial structure in order to keep the cost in a reasonable range [37, 104]. **Therefore, voltage limit dominates the considerations in radially laid out feeder systems.**

### *Radial Feeder Systems are Voltage Independent*

For a radial feeder system, its voltage is defined by the substation transformer at the beginning of the feeder, which is so-called feeder's primary side (Figure 7, left). (For very long feeders in rural

areas, feeders' voltages may be readjusted by several tap changers along the line.) Because radial structure restricts power flow in an emanating manner, the voltage of a radial feeder system is not affected by any other feeder systems in the nearby or far areas, even those originated from its mother substation [37, 70]. **Therefore, a radial feeder system is independent in voltage analysis.**

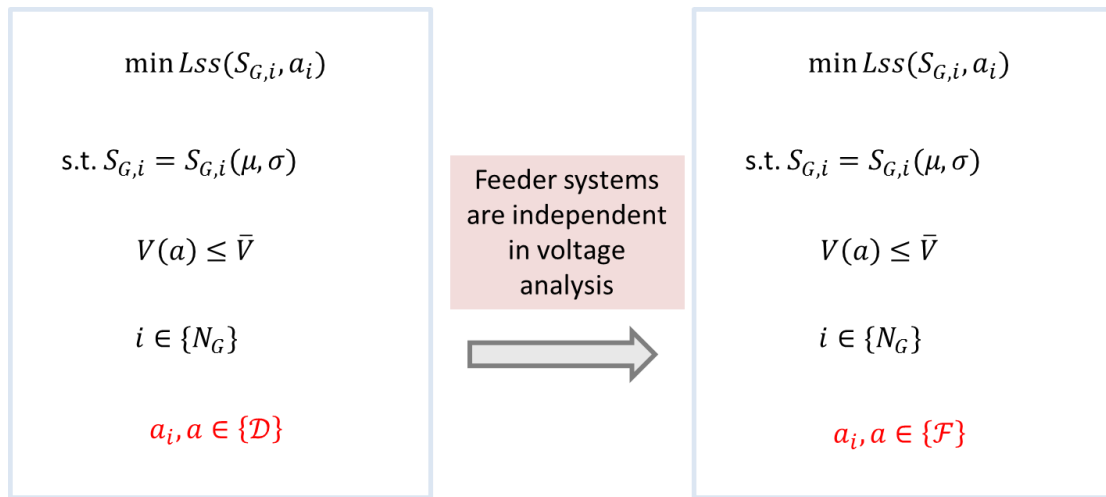


Figure 8. Voltage constrained DG penetration is simplified onto basis of feeder systems.

This figure illustrates the one step in the transformation Figure 1, where its symbols are declared.

The size of an optimization problem is defined by the region that the constraints are active. As a result, an optimization problem that encompasses the variable dimension of a distribution system, if constrained by voltage limits, should be decomposed into feeder systems. In the Logic and Structure Section, the planning scheme of DG penetration in this thesis is posed as an optimization problem with the objective of minimizing power delivery loss and a constraint of voltage rise within permissible upper limit (illustrated by Figure 1). Such a problem for DG penetration in distribution systems is decomposed as in feeder systems (illustrated by Figure 8), which greatly reduce the size, computational complexity and time of the original problem. This important property, however, has been ignored in many of the previous studies [118-124].

This size reduction of voltage-constrained optimization problems is illustrated in Figure 9. DG penetration is studied on the distribution system of São Miguel Island, Portugal. The distribution system has a capacity around 50 MVA, contains over 800 loads and 2,000 line sections and nodes (Figure 9, top). More parameter of this system is presented in Appendix D. Based on voltage independency of radial feeder systems, the original distribution system is decomposed into eight feeder systems, sized from 7 MVA to 4 MVA (Figure 9, bottom).

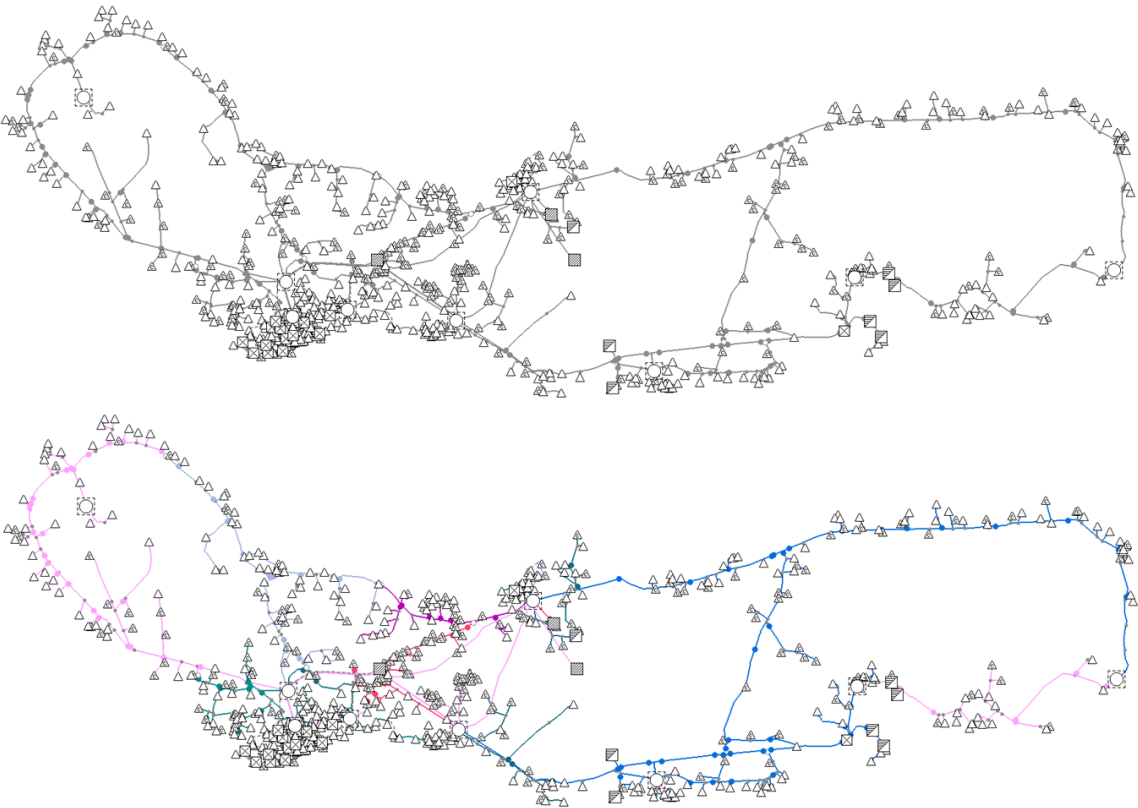


Figure 9. A **50MW** distribution system in São Miguel Island is decomposed into eight feeder systems in voltage-constrained analysis.

### A Feeder System

For demonstration convenience, the rest of this thesis exemplifies and verifies the proposed methods and results on a 10 kV two-feeder system extracted from the 50 MW distribution system in Figure 9. Its topology and parameters are shown in Figure 10 and Table 3 respectively. Due to the independency of feeder systems in voltage analysis, DG penetration is mainly tested on Feeder 1. The voltage on the primary side of Feeder 1 is set as the voltage upper limit, 1.05 p.u.. Loads in the test system are discrete and distributed over similar but not fully identical distance, which deviates from the assumption in previous sections where loads are considered continuously and uniformly distributed. The testing results shown in the later part of this thesis, however, well comply with the proposed implications.

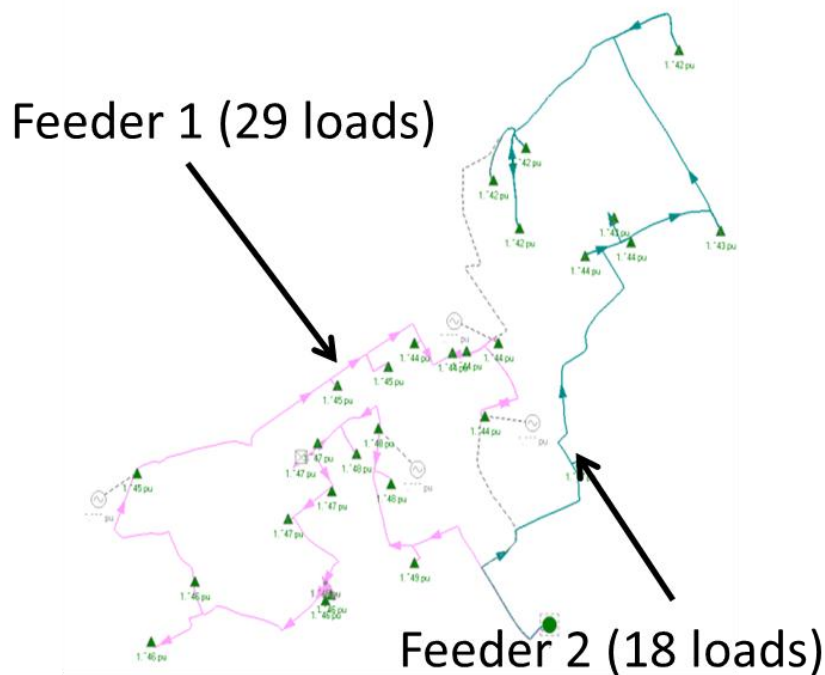


Figure 10. A 10 kV two-feeder system extracted from a 50 MW distribution system in Figure 9.



Table 3. Statistics of the two-feeder system in Figure 10.

	Total Load	Fd.1 Load	Avg. Load
$P(kW)$	1605.2	770.8	55.1
$Q(kVar)$	594.0	210.7	27.0
$r(\Omega \cdot km^{-1})$	0.160	$x(\Omega \cdot km^{-1})$	0.092

## 1.3 Models and Concepts

In many existing DG penetration studies, voltage calculation of a distribution system appears to be the most time-consuming module [72, 79-81]. These studies estimate voltage of every bus/node by running distribution power flow, which is more computational expensive than power flow used in transmission grids for three reasons: (1) the size of a distribution system, in terms of numbers of nodes, can be much greater than that of a transmission system (as illustrated by Table 2); (2) the topology of a distribution system is radial in normal operation, and therefore much more sparse than that of a transmission system; and (3) the conductor resistance of power delivery lines (feeders) in a distribution system cannot be ignored, due to the lower voltage level they operate on and the greater ratio of resistance to reactance, whereas for most of time transmission power flow only counts conductor reactance. Section 1.2 has made this problem easier by decomposing the problem from a distribution size to a feeder size.

This section further simplifies voltage calculation by introducing a new concept, which avoids the running of power flow. In the second subsection, mathematical models, from which the results of Chapter 2 and Chapter 3 are derived, is presented based on this concept.

### 1.3.1 Voltage Effective Power

#### *Deficiency of Conventional Measurements*

Many existing studies present their conclusion of DG capacity in measurements of real, reactive or apparent power. These measurements lacking of information of power factor and feeder's conductor, however, are not sufficient for voltage analysis.

While power factor's impact on capacity and loss does not vary as a function of line size, its impact on voltage does, because it depends greatly on the conductor's  $X/R$  ratio. A  $4/0$  circuit has an  $X/R$  ratio of 1.34 ( $Z = 0.37 + j0.49 \Omega \cdot km^{-1}$ ). At its thermal current limit of 340 A and at unit

power factor, this circuit creates a voltage drop of 2.7% per kilometer. Voltage drop increases to 4.1% per kilometer at 90% power factor and 4.6% per kilometer at 70% power factor (2.6 km reach). Load drops by nearly a factor of two as power factor worsens from 100% to 70%.

A similar shift in power factor would degrade the performance of a larger conductor line much more. If built with 636 MCM conductor, this same line would have an  $X/R$  ratio of nearly 4.0 ( $Z = 0.10 + j0.39 \Omega \cdot km^{-1}$ ). At its thermal limit of 770 A and at unit power factor, it creates a voltage drop of only 1.7% per kilometer. But if power factor slips to only 90%, voltage drop more than doubles, to 4.45% per kilometer. By the time power factor reaches 70% on this conductor, voltage drop is 6% per kilometer. Voltage drops by a factor of four as power factor worsens from 100% to 70%. The larger line, with a relatively high  $X/R$  ratio, is twice as sensitive to shifts in power factor.

### ***Introducing Voltage-Effective Power***

As a result, this thesis introduces a new variable in voltage analysis. In distribution systems, voltage difference over a conductor, which resistance is  $R$  and reactance is  $X$ , can be approximated by<sup>4</sup>:

Equation 1

$$\Delta V = V_1 - V_2 \approx \frac{RP_N + XQ_N}{V_2}$$

where  $V_1$  and  $V_2$  are voltages measured at the two ends of the conductor; where  $P_N$  and  $Q_N$  are net real and reactive power flowing from  $V_1$  to  $V_2$ . In a *per unit* system, Equation 1 can be expressed as

Equation 2

$$\Delta V = RP_N + XQ_N$$

if setting  $V_2$  as the base voltage.

### ***Voltage-Effective Power and Power Tangent***

Define a new concept voltage-effective power in dimension of watts ( $W$ ) as

---

<sup>4</sup> Errors caused by this approximation are very small at primary distribution level. Appendix A estimates this error by giving its mathematical expression and several numerical examples.

Equation 3

$$P^V = P(1 + K^V)$$

where  $K^V$  is defined as voltage-effective power tangent of unit dimension, and

Equation 4

$$K^V = K_\alpha \cdot K_\theta = \frac{X}{R} \cdot \frac{Q}{P}.$$

In Equation 4, angle  $\alpha$  is the power angle of the conductor, and angle  $\theta$  is the phase angle of power flowing on the conductor. Therefore,

Equation 5

$$\alpha = \arctan \frac{X}{R} = \arctan K_\alpha$$

and

Equation 6

$$\theta = \arctan \frac{Q}{P} = \arctan K_\theta.$$

By Equation 3 to Equation 6, voltage drop across a conductor in Equation 2 can be expressed by voltage-effective power  $P^V$  and conductor's resistance  $R$  as,

Equation 7

$$\Delta V = P^V \cdot R.$$

### ***Voltage-Effective Apparent Power and Power Factor***

Now define the apparent form of voltage-effective power  $S^V$  in dimension of volt-amperes (VA) as,

Equation 8

$$S^V = S \cdot PF^V,$$

where  $PF^V$  is defined as voltage-effective power factor in dimension of unit, and

Equation 9

$$PF^V = \cos(\theta - \alpha).$$

Same as in Equation 4, angle  $\alpha$  is the power angle of the conductor, and angle  $\theta$  is the phase angle of power flowing on the conductor. The two angles can be estimated by Equation 5.

Equation 8 and Equation 9 together give another form of Equation 2. With these two definitions, voltage difference can be expressed as

Equation 10

$$\Delta V = S^V \cdot Z$$

where  $Z$  is the conductor's impedance.

Equation 8 shows that the voltage-effective power factor defines the direction of voltage-effective apparent power. In circuit theory, phase angle of power flow indicates the current flowing direction: current flows forward when  $\theta \leq 180^\circ$ , and backward when  $\theta > 180^\circ$ . Whereas Equation 8 states that, **the apparent power, and thus the current, effective in causing voltage difference is determined by the difference of the conductor's power angle and power flow's phase angle,  $\alpha - \theta$ .**

### ***Real versus Apparent Form***

Defining voltage-effective power, in both the real and apparent forms, enables much easier calculation of voltage and loss profiles of feeder systems (as shown in Chapter 3 and 4). It nevertheless guarantees much higher accuracy compared to studies that deploy (Direct Current) DC model in voltage calculation [6, 120, 125-128]. The two forms have their own advantages: the real form is easy to be updated in voltage calculation, and the apparent form, due to its transformation from regular apparent power, is convenient to be used in proofs of DG penetration for loss minimization. The later chapters include more details to demonstrate these advantages. Table 4 presents the duality between voltage-effective power  $S^V$  and regular apparent power  $S$ .

Table 4.  $S$  versus  $S^V$ : Duality between regular and voltage-effective apparent power.

Variable	Associated variable	Direction indicator
$S = \sqrt{P^2 + Q^2}$ apparent power	$I$ current/ loss/ thermal rating	$\alpha$ power flow phase
$S^V = S \cdot PF^V$ voltage-effective apparent power	$V$ voltage	$\alpha - \theta$ angle difference of power flow phase and conductor's power angle

Because  $P^V$  is used more often, for convenience, this thesis refers the real form as *voltage-Effective power*, and the apparent form as *voltage-effective apparent power*.

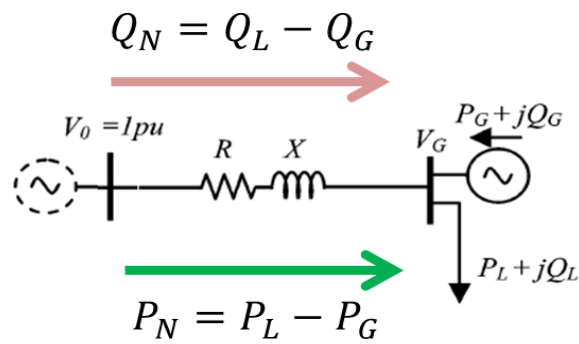


Figure 11. Line diagram for a two-bus system.

### A Simple Example

Figure 11 shows an example of a two-bus system integrated with a single DG unit. Voltage drop between feeder's primary voltage  $V_0$  and DG bus voltage  $V_G$  is calculated with  $S$  and  $S^V$  as,

$$\Delta V = V_0 - V_G \approx \begin{cases} P_N^V \cdot R \\ S_N^V \cdot Z \end{cases}$$

where  $P_N = P_L - P_G$  and  $Q_N = Q_L - Q_G$  are net real and reactive power flowing from  $V_0$  to  $V_G$ .

### 1.3.2 Induced Power Flow Model

#### *Two Major Layouts in Radial Feeder Systems*

As stated in Section 1.2, this thesis studies DG penetration for distribution systems dominated by voltage constraints, which is often decomposed by radial feeder systems. Figure 12 illustrates two different ways to lay out a radial distribution system. Each of the two configurations can be engineered to work in nearly any situation, but neither is always superior to the other in terms of reliability, cost, ease of protection, and service quality in all situations. Most planning engineers have a preference for one or the other. In fact, about 20% of utilities have standardized on the large-trunk design as their recommended guideline while another 20% prefer the multi-branch approach [37, 70, 104].

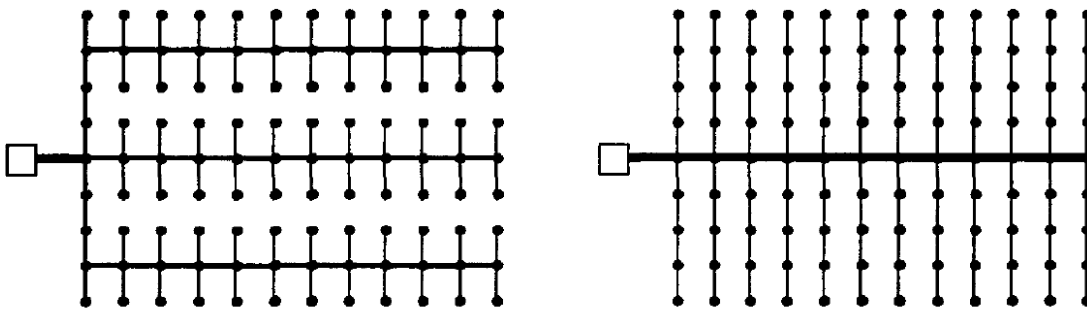


Figure 12. Two ways of routing a radial feeder to 108 service transformers.

“multi-branch” (left) and “large trunk” (right) [70].

**For convenience, the rest of the thesis uses the “large trunk” layout in deriving planning scheme for DG penetration.** However, it shows, in the meanwhile, the results derived are not limited to this type of layout. **Moreover, two assumptions are made to justify the development of the induced power flow model and other results:**

- **Laterals on the feeder are negligible.** All parameters of lateral level, such as voltage, current, and power flow, are aggregated to the primary distribution level;
- **Three-phase distribution feeders operate under balanced conditions.**

### Power Flow Model Induced from $P^V$

Consider a practical feeder system (shown in Figure 13). Because feeder's load size is much smaller than DG size, load density is treated with continuous functions, while DG density is treated with discrete functions. (For load, such as medium industry and commercial users, it can be treated the same way as DG.) This is more reasonable than previous studies, which uses continuous functions to model both DG and loads [6, 120, 125-128].

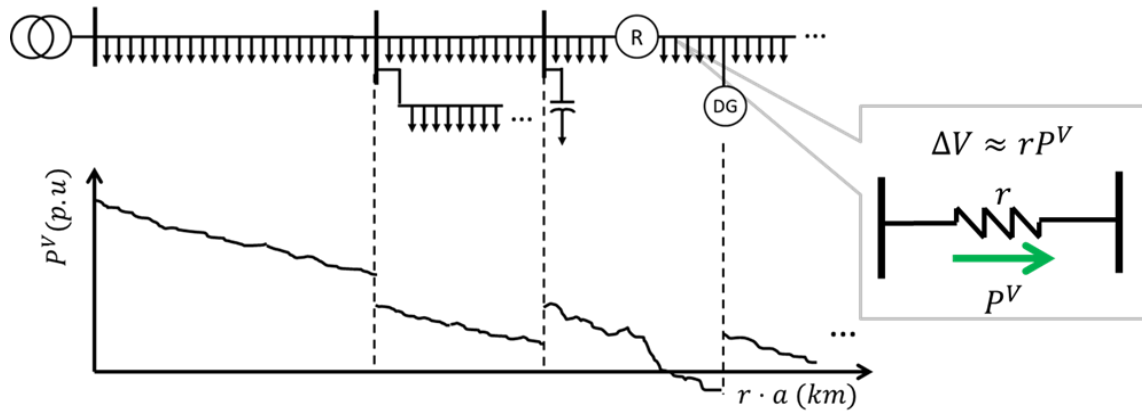


Figure 13. A practical feeder system penetrated with DG and its voltage-effective power flow.

Take load power density at location  $a$  as  $p_L(a)$  and  $q_L(a)$ , measured in  $p.u./km$ . The  $i$ th of  $N_G$  DG inserted at location  $a_i$  is of capacity  $p_G(a_i)$  and  $q_G(a_i)$ , measured in  $p.u./km$ . Hence, real and reactive power flows  $P_L$ ,  $Q_L$ ,  $P_G$  and  $Q_G$  are derived as:

Equation 11

$$P_L(a) = \int_a^l p_L(\zeta) d\zeta$$

$$Q_L(a) = \int_a^l q_L(\zeta) d\zeta$$

and

Equation 12

$$P_G(a) = \sum_i^{N_G} p_G(a_i)$$

$$Q_G(a) = \sum_i^{N_G} q_G(a_i)$$

Further assume that the feeder's conductor is uniform and the unit resistance and impedance of the feeder is  $r$  and  $z$ , measured in  $p.u./km$ .<sup>5</sup> Based on Equation 7 and Equation 10, the voltage profile  $V(z)$  of the feeder can be calculated as:

Equation 13

$$V(a) = V_0 - \int_0^a \Delta V(\zeta) d\zeta \approx V_0 - \int_0^a r P^V(\zeta) d\zeta$$

and

Equation 14

$$V(a) = V_0 - \int_0^a \Delta V(\zeta) d\zeta \approx V_0 - \int_0^a z S^V(\zeta) d\zeta$$

where  $V_0$  is the feeder's primary voltage.

### ***Tools and Implementation Environment***

In this thesis, proposed methods and derived results are verified and examined mainly through two software tools. One is MATLAB R2012b, the other is DPlan.

DPlan is geographic based integrated analysis and optimization system for distribution network. It is developed by Instituto de Optimizaçãõ Aplicada (IOA), Lisbon, Portugal, and is used in Europe. A graphical user interface of DPlan is shown in Figure 14. It runs power flow analysis in voltage and power loss analysis to evaluate and optimize performance for distribution grids.

---

<sup>5</sup> Feeder's conductor is treated as uniform based on Section 1.2.2, which presents most feeders are of "same" size. The results derived from the assumption, however, can be easily extended to the case where conductors are of difference sizes by changing the resistance and impedance in Equation 13 and Equation 14 as functions of locations on feeder,  $r(\zeta)$  and  $z(\zeta)$ .



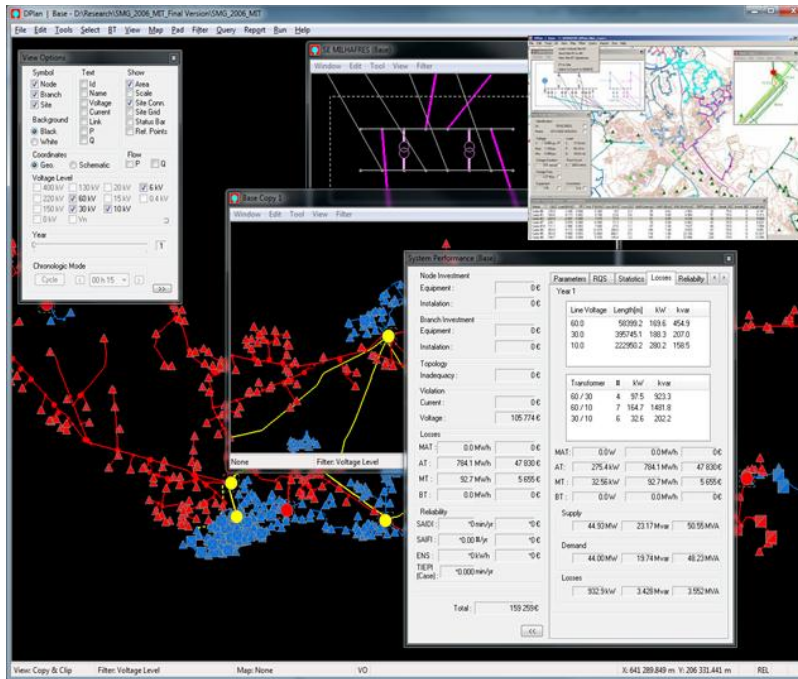


Figure 14.A screen shot from DPlan.

# Chapter 2: Mitigating Voltage Rise in DG Penetration

---

Voltage rise is the bottleneck of DG penetration in distribution grids [4, 12, 57, 58]. This chapter gives a deeper view of how DG penetration causes voltage rise and how to prevent this problem in a planning scheme. Results of this chapter serves as tools that can be applied directly in practices. Fast examination of voltage profiles in DG penetration can prevent overvoltage, save ante-post engineering cost and accelerate the progress of DG penetration.

Section 2.1 introduces ways to analyze voltage profiles on feeder systems in an easy and fast manner. It revises the *zero-point analysis*, which has been conventionally used in determining the possibility of overvoltage occurrence, and points out its inaccuracy. This section further provides a graphical method that visualizes the voltage profile change during DG penetration. An *Area Criterion* is proposed on this method as a revision of the zero-point analysis.

Section 2.2 discusses the permissible DG penetration in a distribution grid. Based on the early part of this thesis, it reveals that DG penetration should be defined on the feeder system level, instead of the whole distribution system level. Quantitative analysis is conducted and an analytical expression is derived to determine the DG penetration capacity for any given feeder system. Using this formula, distribution system planners can generate a DG penetration chart, which enables them to examine DG penetration feasibility on spot. In addition, DG penetration capacity is redefined according to the proposed formula.

Section 2.3 reveals six factors that causes voltage rise in DG penetration, including penetrating location, penetrating capacity, penetrating dispersion, feeder's conductor, load profile and feeder's primary voltage. Based on these factors, it further discusses methods used in practices to mitigate voltage rise. Two of these methods for voltage rise mitigation, demand response and reconfiguration, are highlighted in Section 2.4 by proposing their new implementation schemes.

## 2.1 Visualizing Feeder's Voltage Profile

### 2.1.1 Zero Point on Feeder

*What is a zero point?*

The vast majority of power distribution systems are radial or open loop systems, which means that they are designed so that power flows “downhill” from a single source (substation) to the customers (as illustrated by Figure 11). DG penetration creates more sources on the feeder, and leads to two cases categories depending on the relation of the generation output to the feeder’s load. Figure 15 illustrates the two cases on a Direct Current (DC) model, where the reactance of the feeder’s conductor is ignored.

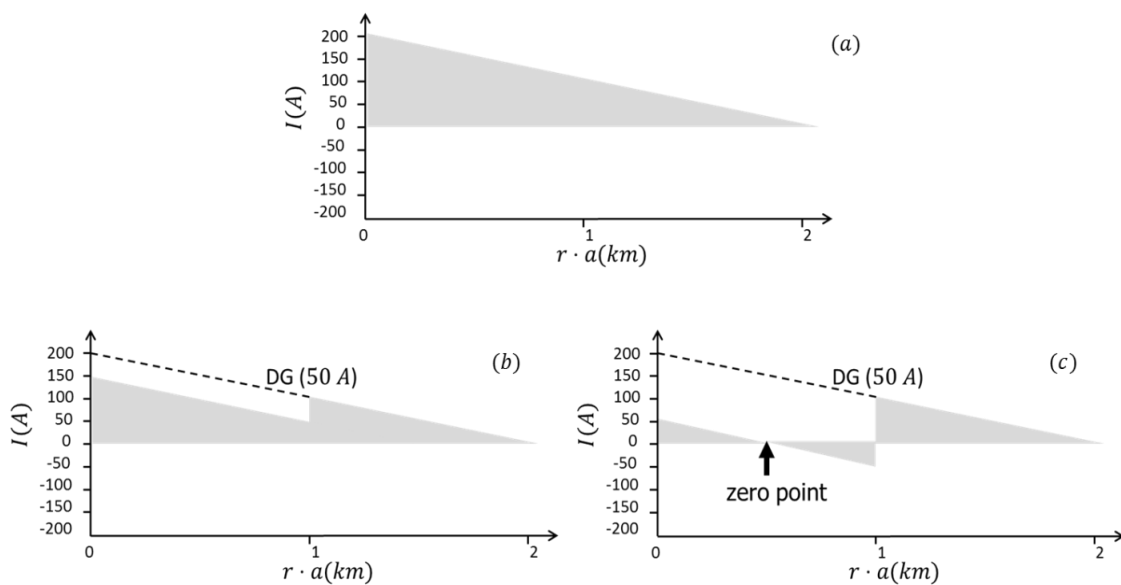


Figure 15. Zero point created by DG penetration.

(a) Current flow along a two-kilometer feeder uniformly loaded at  $100 A \cdot km^{-1}$ . (b) Penetrated with a 50 A DG unit located one kilometer from the substation, where the load downstream is 150 A. There is no zero point. Dotted line shows reduction in power flow on the feeder. (c) The DG unit produces 150 A. In this case, current flows back from the DG unit to the substation and thus a zero point is created.

1. DG output is less than the load downstream of its location. In this case the DG unit reduces current on all equipment between it and the substation, but makes no impact on the loadings on anything downstream from it, as shown in Figure 15 (b).
2. DG output is more than the load downstream of the DG location, as depicted in Figure 15 (c). Here, too, the DG unit makes no substantial impact on the loadings of any equipment downstream from it, but it reverses some of the flow on the feeder from its location back toward the substation. **Unless its output is greater than the load on the entire feeder, it creates a “zero point” between it and the substation, where current flow is rendered zero due to the back flow from the DG.**

Current flow on all points between the DG site and the zero point is reversed (as compared to the non-DG case). Flow direction on all other parts of the feeder, and all branches, remains the same. Generally, DG output and feeder load will not be correlated over time, which means that the zero point will move, perhaps over a wide portion of the feeder.

A zero point can be detected for different physical variables. For example, the DC model described by Figure 15 shows a current zero point; in AC models, zero point can be defined for real power, reactive power, and the proposed voltage-effective power and its apparent form. Locations of these zero points, unless the loads on the feeder are of identical power factors, will also move along a distance of the feeder.

### ***“Zero Point Analysis”***

One conventional way to characterize DG-feeder interaction on feeder’s voltage profile called “zero point analysis.” [4, 129, 130] This method uses zero point of real power flow as the indicator of overvoltage, which is defined as voltage higher than the feeder’s primary voltage<sup>6</sup>.

In general, it states that the closer the zero point is to the substation, the loading and power loss of the feeder is reduced, but with a great possibility the DG penetration will cause overvoltage.

In cases where the DG output exceeds the load on the entire feeder, the zero point is essentially in the upstream of the feeder source at the substation. In these and some other cases, depending on the

---

<sup>6</sup> In distribution systems, feeders’ primary voltage is usually set to be close to the upper limit of a pre-defined range (i.e.  $V_0 = \bar{V}$ ) in order to fully utilize the feeder’s load reach. Section 2.1.3 gives more detail about load reach.

amount of DG output, loadings on some points of the feeder could be higher than in the non-DG case. Typically the highest loading on the feeder in these cases is immediately upstream of the DG unit site, and if the site is far “downstream” from the substation, it is typical for this portion of the feeder to see an increase in both normal loading and fault duty, too.

The zero-point analysis provides an intuitive way to detect the overvoltage. However, it only gives a qualitative description of the likelihood of overvoltage based on zero point’s closeness to the feeder’s primary side. Accurate prediction of overvoltage’s occurrence and location cannot be deduced from this method.

The variable used for zero-point analysis is another problem. In practices, feeder load are neither uniformly distributed nor of the same power factor, which could create much error in evaluation based on current, real, and reactive zero-point analysis.

#### ***What does zero point indicate?***

Zero point is usually taken as an indicator of overvoltage by previous studies. Since its occurrence suggests reversed power flow and therefore a voltage rise somewhere in the feeder, it is regarded to be avoided as possible in any operation [104, 130]. However, analytical analysis from Equation 13 shows that it is not proper to indicate overvoltage but can be used to characterize a feeder’s overall voltage profile.

According to the critical point theorem, the maximum and minimum points of a differentiable function can be found by taking derivative of the function (or its segments). Therefore, for a voltage profile given by Equation 13

$$V(a) = V_0 - \int_0^a \Delta V(\zeta) d\zeta \approx V_0 - \int_0^a r P^V(\zeta) d\zeta$$

where  $V_0$  is the feeder’s primary voltage set at the substation, and  $V(a)$  must be within the permissible range  $\underline{V} \leq V(a) \leq \bar{V}$ . The local maximum and minimum voltages are at:

Equation 15

$$\arg_a V_{min} := \left\{ a \in [0, l] \left| \frac{\partial V(a)}{\partial a} = P^V(a) = 0, \frac{\partial^2 V(a)}{\partial a^2} > 0 \right. \right\}$$

and

Equation 16

$$\arg_a V_{max} := \left\{ a \in [0, l] \left| \frac{\partial V(a)}{\partial a} \right. \right\}$$
$$\equiv \{a \in [0, l] | \text{DG's insertion position}\}$$

Equation 15 and Equation 16 state:

1. **Zero point does not indicate overvoltage, but indicate the local minimum of the feeder's voltage profile;**
2. **Local maximum voltages appear at DG locations, where is the potential location for overvoltage;**
3. **Local minima and local maxima voltages appear alternatively.**

### 2.1.2 A Graphical Method

In a radial or loop power delivery system, electrical power flows out and “down” from the source (substation) to the consumers (load). **Although phase angle is a big factor in movement of power, as is described in any text on power flow, on a distribution system phase is normally not a major factor, and voltage alone is viewed as associated with power flow.** By contrast, in a true network voltage situation, such as the planning of a high voltage transmission grid, voltage phase-angle differences among parts of the system are a big part of the “power flow problem.” Voltage on a feeder is often depicted using a *voltage profile* of voltage at points along the circuit, as shown in Figure 16. Based on the mathematical model presented in the previous section, a graphical method for predicting voltage profile is proposed as the following for any DG penetrated feeder.

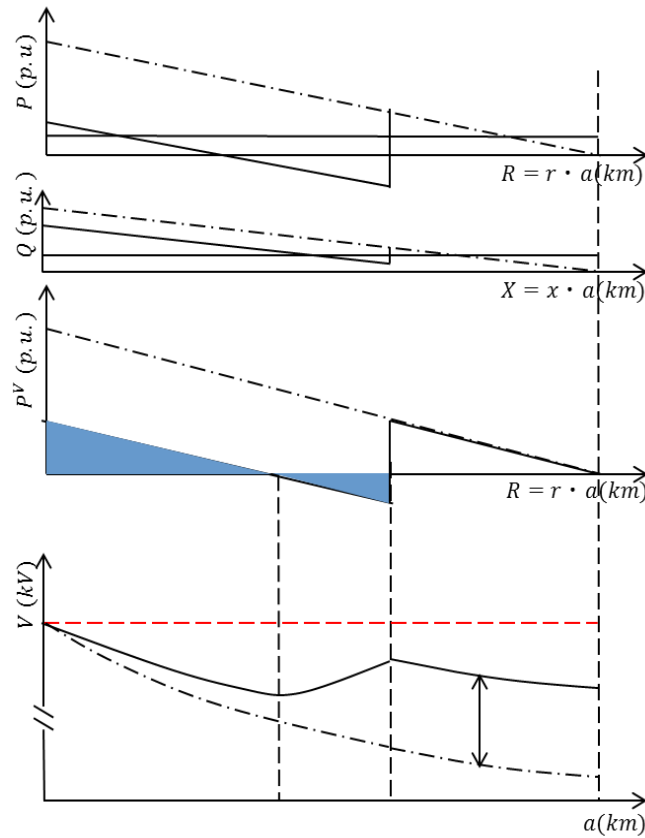


Figure 16. Voltage-effective power flow and voltage profile on a DG-integrated feeder.

From top to bottom: (1) active power density and flow on feeder, (2) reactive power density and flow on feeder, (3) voltage-effective power flow, and (4) voltage profile.

#### Outline of the Graphical Method

*Step 1.* Plot net flow of real and reactive power as the cumulative area under the net power density curves on the feeder;

*Step 2.* Plot voltage-effective power flow,  $P^V$ , on the feeder by summing up the real power flow and the  $x/r$  normalized reactive power flow in Step 1;

*Step 3.* Plot voltage profile as the difference of the feeder's primary voltage  $V_0$  minus the cumulative area under the  $P^V$  curve. Voltage decreases when  $P^V$  is positive and vice versa.

Taking the above steps, voltage profile can be predicted immediately. This process is illustrated by Figure 16: the voltage-effective power  $P^V$  can be derived from the real and reactive power flow on the feeder, according to step 1 and step 2. To plot the voltage profile based on the  $P^V$  flow chart, voltage decreases when the area under the  $P^V$  curve is positive, reaching its minimum at zero point, increases when the area under the  $P^V$  curve is negative, reaching its maximum at where DG penetrates. Because DG penetration does not affect power flow downstream from its location, the voltage profile downstream to DG location is in parallel of its original form. This finishes the plot of the voltage profile of the DG penetrated feeder.

For demonstration purpose, the example in Figure 16 assumes uniformly distributed load on the feeder of a “large-trunk” layout. The application of the proposed graphical method, however, is never limited to this assumption, and can be extended to any load type and feeder configuration.

### 2.1.3 Area Criterion

#### *Load Reach*

Load reach is measured in units of distance, usually kilometers or miles. It measures the distance that the feeder system can move power. The *load reach* of a circuit or design is the distance that it can move a certain amount of power before encountering the applicable steady-state voltage drop limit [60, 131, 132]. Obviously, the load reach of a circuit depends on the amount of power being moved. The reach of a circuit limited to moving 5 MW will be farther than if it is transporting 6 MW.

In distribution systems, feeders’ primary voltage is usually set to be close to the upper limit of a pre-defined range (i.e.  $V_0 = \bar{V}$ ) in order to fully utilize the feeder’s load reach.

#### *Determining overvoltage by voltage-effective power area*

Given this condition and based on Step 3 in the graphical method, an Area Criterion can be stated as following:

#### **Area Criterion**

*Overvoltage occurs at the location where the positive area cumulated from the feeder’s primary side is less than the negative area under the voltage-effective power flow curve.*



Figure 17 illustrates the Area Criterion: when DG is penetrated with a small capacity, which generates the blue area under the  $P^V$  curve, the negative area is less than the positive area. Therefore, the maximum voltage at DG location is not greater than the feeder's primary voltage. No overvoltage occurs. DG capacity is then increased, which creates the areas under the orange  $P^V$  curve. The induced voltage rises back to the feeder's primary voltage at where the negative area reaches equal to the positive area under the  $P^V$  curve, and continues to rise afterward. Overvoltage occurs along the distance where after the area-equal point (marked by the dash line).

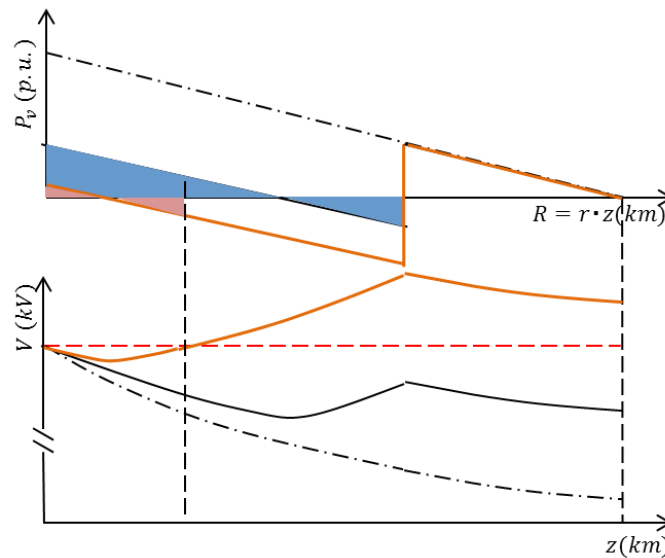


Figure 17. Relation between areas under the voltate-effective power curve and the feeder's voltage profile.

The Area Criterion points out the sufficient and necessary condition for overvoltage occurrence. **It states that, overvoltage occurs if and only if the cumulative reversed  $P^V$  flow is greater than its forward counterpart.**

The proposed method and criterion above are different from the traditional “zero point analysis”, which determines the possibility of having overvoltage on the feeder in a qualitative way. Studies following zero point analysis usually come to the conclusion that reversed power flow, real and reactive, is not preferable regardless of its value and location on the feeder [4, 129, 130]. **However,**

with the proposed method and Area Criterion, it is found that Large reversed power flow does not necessarily cause overvoltage.

## 2.2 Penetrating DG with Voltage Reliability

### 2.2.1 How Much DG can be Penetrated?

Voltage rise is the bottleneck of DG penetration in distribution grids. Therefore, many previous studies attempt to address the question of how much DG can be penetrated in a distribution grid without risking for overvoltage [10, 68, 87, 96, 123]. As presented in Section 1.1.4, there are mainly four approaches have been taken, including: distribution power flow approach, scenario approach, engineering approach, and active network planning approach. Unfortunately, all of the four approaches do not provide a complete answer to the question. Results from scenario approach are in general qualitative. A range of permissible ratio, from 20% to 35%, of DG capacity to total load capacity in a distribution grid, is recommended for DG penetration [4, 47, 76-78]; Engineering approach is heavily case dependent and hard to be extended to other situations [38, 93-95]; Active network management and power flow approaches provide more accurate and generalized solutions. However, they are usually carried out by a set of programmed processes. Users of these two approaches are not able to trace the DG penetration possibilities until the last step. Moreover, the implementation of these two approaches attaches to commercial software that requires extra investment for any DG penetration decision.

#### *An Analytical Formula*

In fact, an analytical expression can be used to determine DG penetration based on the Area Criterion. For a single DG unit located at  $a_i$ , its penetration does not cause overvoltage if and only if:

Equation 17

$$\Delta V(a) = \int_0^a P_L^V(\zeta) d\zeta - a \cdot P_G^V \geq 0$$

A little mathematical manipulation leads to

Equation 18

$$a \cdot \frac{P_G^V}{\int_0^a P_L^V(\zeta) d\zeta} \leq 1$$

Equation 18 shows that DG penetration is a function of both penetration capacity and location on the feeder. For a given feeder system and a designated DG location, system planners and utilities, with Equation 18, can find the maximum DG capacity that will not cause overvoltage. Similarly, for a DG unit to be installed on the feeder system, they can use Equation 18 to decide the farthest permissible DG location on the feeder. Although in many cases, DG units are owned and installed by individual users, which are not controlled under the utilities, utilities and policy maker can use these estimations to set standards for DG penetration. Any installation that exceeds the DG penetration limits on maximum capacity and/or farthest location will risk the system reliability for overvoltage, and thus should be avoided. And installations that stay close to the margin of these limits deserve penalization to degree.

This result can be extended to the penetration of multiple DG units. With  $N_G$  DG units, the penetration of the  $i$ th DG unit does not cause overvoltage if and only if,

Equation 19

$$\Delta V(a_i) = \int_0^{a_i} P_L^V(\zeta) d\zeta - a_i \cdot \sum_{n>i}^{N_G} P_{G,n}^V - \sum_{n \leq i} P_{G,n} \cdot a_n \leq 0$$

and

Equation 20

$$\frac{a_i \cdot \sum_{n>i}^{N_G} P_{G,n}^V + \sum_{n \leq i} P_{G,n} \cdot a_n}{\int_0^{a_i} P_L^V(\zeta) d\zeta} \leq 1$$

### ***DG Penetration Chart***

It is desirable to examine a DG penetration plan on spot without going through complicated calculation. Many commercial software packages today enable system planners and utilities to do so [104, 133, 134]. To use such software, however, may be time-consuming in the sense of requiring much data input for every implementation frame, and more importantly, does not provide the

planners an intuition of how DG penetration influences voltage profile of the distribution grid (and actually the feeder system).

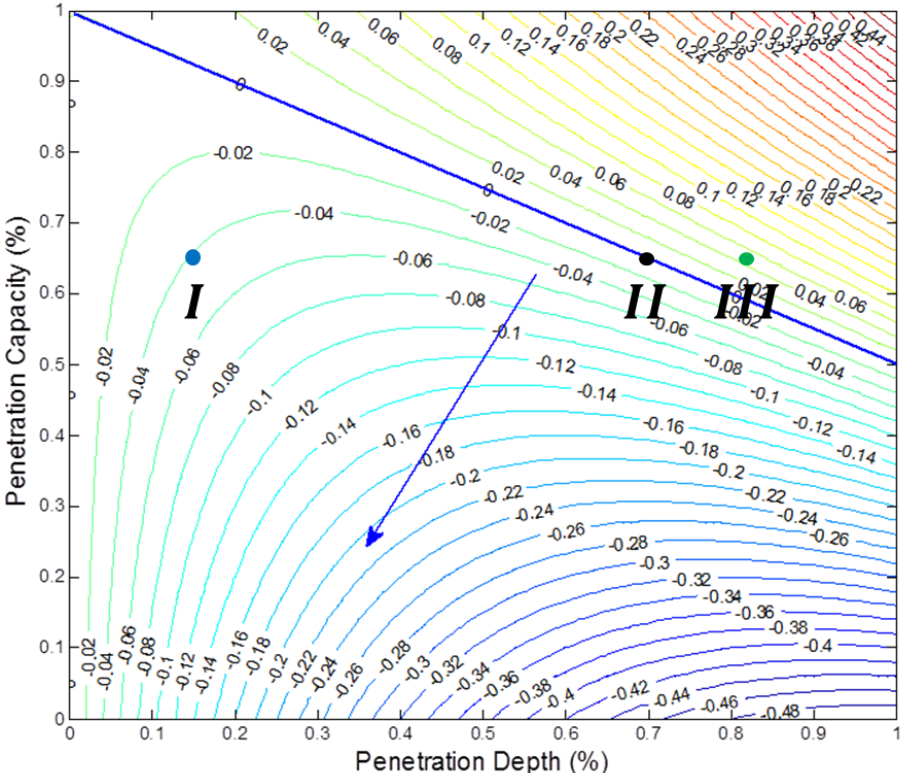


Figure 18. DG penetration chart.

This chart is generated for single DG penetration on Feeder 1, shown in the two-feeder system in Figure 9. The coordination of penetration capacity and depth are normalized by the total load on Feeder 1 and the feeder’s length. The maximum voltages of the feeder, marked on the contours, is evaluated in the *per unit* system, which basis is set as the feeder’s primary voltage.

A DG penetration chart can fulfill this task. Equation 17 is a first-order differential equation with two variables, DG capacity and location. Given the value of one variable, the other can be solved as the limit (maximum capacity or farthest distance from the feeder’s primary side) of DG penetration. For single DG penetration, a three-dimensional chart can be plotted to demonstrate how plans of various DG capacity and location influence the feeder’s maximum voltage. The two axes penetration capacity and penetration depth indicate the capacity and location of the DG unit to be

penetrated. Given any DG penetration plan, a point can be located on the contours of the chart, which indicates the maximum voltage on the feeder after DG penetration. Figure 18 shows a penetration chart for DG penetration on Feeder 1 of the test system in Figure 9.

The testing feeder system sets the primary voltage to the upper permissible voltage level (in Figure 9). The voltage plane of this DG penetration chart has three parts: upper part (warm color), a line (blue), and lower part (cold color), which respectively indicates DG capacity and location that will result in overvoltage, the feeder's primary voltage, and normal voltage (Figure 18). **Any DG penetration is voltage-reliable, in the sense of resulting normal voltage, should be located in the lower plane.**

The numbers marked on the contours indicates the safety margin and overvoltage severity of implementing a DG penetration plan. Figure 18 and Figure 19 together exemplify the use of this penetration chart. In Figure 18 (Left), three candidate sites are considered for a given DG unit of 600 kW real power output and 50 kVar reactive power output. Based on the statistics of Feeder 1

in Table 3, it is calculated the penetration capacity is  $\frac{P_G^V}{P_{L1}^V} = 65\%$ , and the penetration depth of

the three candidate sites are  $a_I = 11\%$ ,  $a_{II} = 67\%$  and  $a_{III} = 89\%$ . The three penetration plans are located in the penetration chart as shown in Figure 18. It is observed that penetrating at the first site is in the range of normal voltage and will induce a voltage with 4% margin to the upper voltage bound; at the second site will induce a voltage of the same value as feeder's primary voltage; and at the third site will cause an overvoltage. This observation is verified by testing the three penetration plan on DPlan. The three induced voltage profiles are plotted in Figure 19 (Right, bottom).

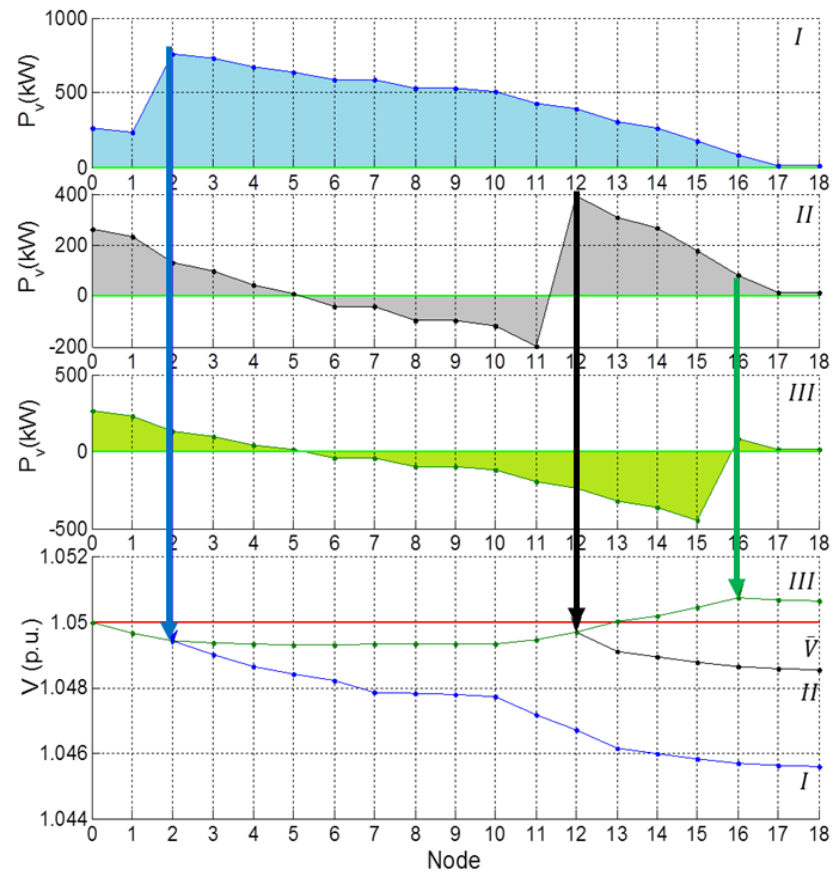
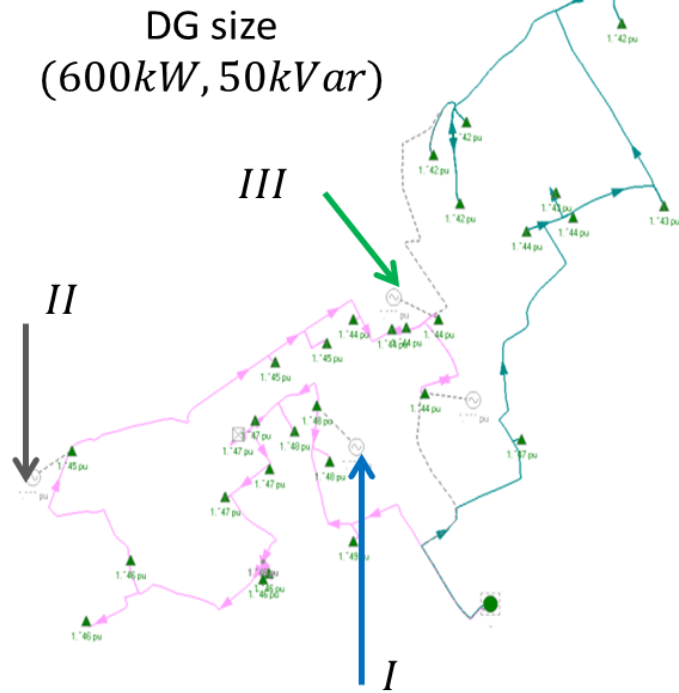
This penetration chart can be derived for more general cases.

For  $V_0 \neq \bar{V}$ , the following chart can be consulted to easily determines the voltage feasibility and margin to voltage upper limit of candidate DG. The instruction of using the chart:

1. Locate the point  $(a, c)$  for the penetration depth and capacity of candidacy, and find its relative voltage rise level on the chart, say  $\Delta\tilde{V}$  ;
2. Measure the power flow at the feeder's primary side, calculate  $\tilde{M} = \frac{\bar{V}-V_0}{P_v \cdot l}$ , where  $P_v$  is the total voltage-effective power flowing into the feeder,  $l$  is the feeder's length;

3. The DG candidacy is valid if  $M' = \tilde{M} - \Delta\tilde{V} \geq 0$  and  $M'$  gives the voltage margin to its upper limit.

For multiple DG penetration, the chart can be derived for each DG based on Equation 20. The order of penetration does not affect the resultant voltage profiles, and each DG penetration can be treated individually. This superposition property for multiple DG penetration will be proved in Section 3.3.



Voltage profiles of Feeder 1 induced from DG inserted at Node 2 (I), Node 12 (II), and Node 16 (III).

Figure 19. Voltage profiles after penetrating a single DG unit at three locations of Feeder 1 in Figure 9.

Left: the three penetration locations on the feeder; Right: the resultant voltage-effective power flow and voltage profiles.

### **2.2.2 An Accurate Definition for Permissible DG Penetration Level**

DG penetration level, defined as the ratio of penetrated DG capacity to total load in a distribution system, is frequently used in previous studies [10, 87, 135-137]. It is also used in many studies to define the viability of DG penetration plans in the sense of overvoltage occurrence. However, this conventional definition of DG penetration level has several deficiencies that may lead to inaccurate estimation, which consequently risk the voltage reliability of the DG penetrated distribution system.

First, the conventional definition of DG penetration level is estimated on the basis of a whole distribution system. Section 1.2 has shown that feeder systems are independent in voltage analysis. In radial distribution systems, a feeder's voltage is regulated by the transformer of its originated substation. DG penetration on a certain feeder does not affect the voltage profiles of any other feeders in the system. Conversely, the load of other feeders does not contribute to forming the voltage profile of the DG penetrated feeder, and hence should not be included in the definition of DG penetration level.

Secondly, DG penetration location, as an important piece of information, is not included in the conventional definition of DG penetration level. Equation 17 to Equation 20 have shown that voltage profile of a feeder is not only affected by its penetrated DG capacity, but also by its penetrated DG location. This point is also demonstrated by the example in a DG penetration chart in Figure 18: for the same DG penetration capacity, three different penetration locations can result in voltages that are normal, equal to the feeder's primary voltage, and higher than the permissible upper bound.

Finally, the physical variables that are used in conventional DG penetration definition do not contain sufficient information for voltage analysis. As stated in Section 1.2.1, conductor resistance cannot be ignored in distribution systems. This is because (1) conductors in distribution systems have a much higher ratio of resistance to reactance; and (2) distribution systems have a considerably lower voltage than transmission systems. Therefore, in an Alternative Current (AC) distribution system, both the phase angle and power flow magnitude are required to deduce voltage profiles. Previous studies use variables, including real power, reactive power, and apparent power, in describing DG penetration capacity [6, 120, 125-128], which misses either side of the AC power flow information. More importantly, none of these variables contains the information of feeders' conductor, in terms of resistance and reactance.



Because of the aforementioned deficiencies, the definition of DG penetration level is revised here. The new definition takes the following form:

Equation 21

$$\text{DG penetration level} = \left. \frac{P_G^V}{P_L^V} \right|_a$$

In Equation 21, the left side of the separator is the ratio of the voltage-effective power of DG  $P_G^V$  to that of its penetrated feeder's load  $P_L^V$ ; the right side represents the condition when the left-side variables are measured, which is the DG penetration location  $a$ .

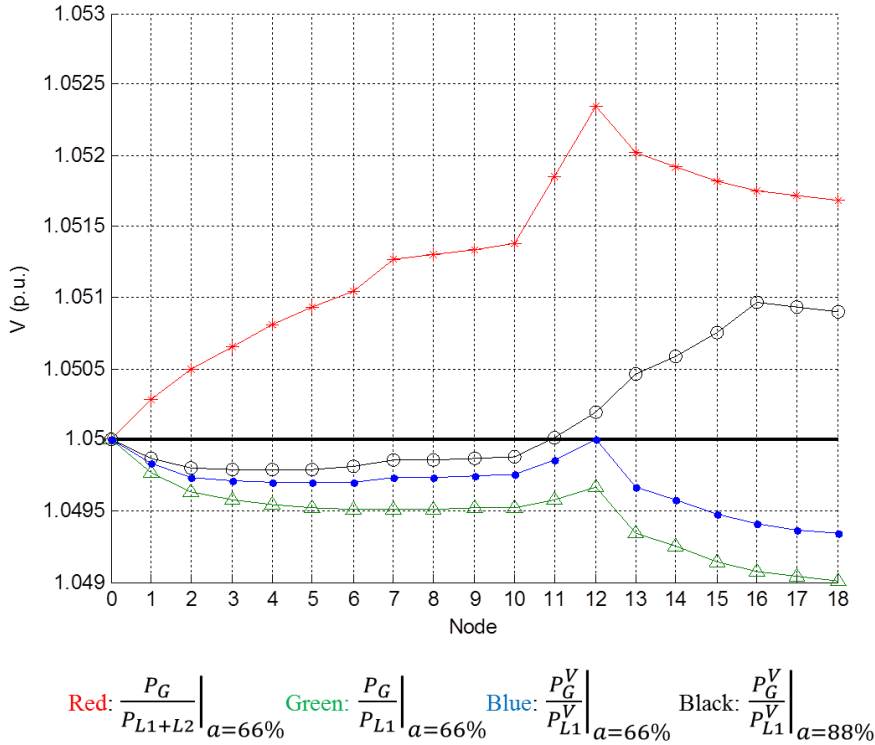


Figure 20. Voltage profile under 20% penetration rate of four types of definitions.

Figure 20 demonstrates the benefits of the revised definition of DG penetration level. It compares the voltage profiles induced by 20% DG penetration under three definitions: real power ratio of DG capacity to the system load, which is the total load on Feeder 1 and Feeder 2 (red); real power ratio of DG capacity to Feeder 1's load (green); voltage-effective power ratio of DG capacity to Feeder 1's load (blue and black). The first three voltage profiles are measured under the case of the DG unit is located on Node 12, which gives the penetration depth  $a = 66\%$ ; while the fourth voltage profile is measured when the DG unit is installed at Node 16, which gives the penetration depth  $a = 88\%$ .

Figure 20 reveals some critical factors of evaluating DG penetration level under different definitions,

1. **Evaluating on a system basis raises the penetration DG capacity, which consequently causes overvoltage.** The voltage profiles, under this definition, will not be consistent if DG penetrates on Feeder 2;
2. **Measuring DG penetration in real power may result voltage profiles drifting away from that induced from DG penetration level in voltage-effective power.** The resultant voltage profile is lower if DG power factor is smaller than load power factor (as shown in Figure 20), and vice versa.
3. **Ignoring DG penetration location may cause overvoltage.** For the same DG capacity, overvoltage is observed when DG location is moved from Node 12 to Node 16. This point has been made in the previous subsection.

Therefore, the revised definition of DG penetration in Equation 21 can give an accurate estimation of voltage profile for any DG penetration plan. Ignoring DG location, power factor, conductor information, or including irrelevant load information from other feeders may lead to inconsistent voltage estimation, and thus risk the system reliability to overvoltage.

## 2.3 Six Factors Influencing Feeder Voltage Profile

Furthermore, Equation 17 to Equation 20 show that voltage profile is determined by a few factors on DG and system characteristics, including:

- DG location,  $a$ ;

- DG output power,  $p_G(a)$  and  $q_G(a)$ ;
- DG dispersion level, inferred by  $P_G(z)$  and  $Q_G(z)$ ;
- Feeder's conductor, specifically, its resistance and reactance  $r$  and  $x$ ;
- Feeder load,  $p_L(z)$  and  $q_L(z)$ ;
- Feeder's primary voltage  $V_0$ .

These factors are not first discovered in this thesis for their influences on voltage profiles of DG penetrated feeders [4-6]. They are, however for the first time, revealed through a non-qualitative method and presented with their influences in analytical forms.

### 2.3.1 Principles of Feeder Voltage Variation

This section deploys the graphical method and the Area Criterion to investigate factors that influence voltage profile on a DG penetrated feeder. Recommendations are made to distribution system planners and policy makers on mitigating voltage rise by controlling these factors.

In the Area Criterion, positive and negative areas under the  $P^V$  curve represent cumulative forward and reversed  $P_p$  flows respectively. For this reason, cumulative forward (and reversed)  $P^V$  flow and positive (and negative) area under the  $P^V$  curve are used interchangeably in the rest of this thesis. **In addition, loads on feeders, for illustration purpose, are assumed to be uniformly distributed.** Application of the derived results, however, is not limited by the assumption and can be extended to more general cases.

#### *Factor 1: DG Output*

Figure 17 illustrates how DG output creates overvoltage by reducing the  $P^V$  flow and creating a negative area under the  $P^V$  curve. The voltage is less than the upper limit  $\bar{V}$  if the DG output is relatively small, indicated by the fact that the negative area,  $dec$ , is less than the positive area,  $abc$ . Starting from the feeder's primary side  $b$ , the voltage decreases where  $P^V(a)$  is positive, and increases from the zero point  $c$  where  $P^V(a)$  at  $f$  from where to  $c$  the area under the  $P^V$  curve,  $fgc$ , equals to the absolute value of the negative area,  $dec$ .

As shown in Figure 17, overvoltage is caused by increasing the DG output, which reduces the positive area and increases the negative area under the  $P^V(a)$  curve. The net area change is depicted as the parallelogram,  $aa'd'd$ . The voltage starts to exceed the upper limit  $\bar{V}$  at  $f$  where the negative

area  $c'gf'$  equals the positive area  $a'bc$ , and reaches its maximum at  $e$ . Regardless of the DG output, the local minimum voltage occurs at the zero point,  $c$ . And the voltage profiles downstream of  $e$  are paralleled in shape, in other words, have the same changing rate. This is because DG insertion changes the  $P^V$  flow of its upstream and has no effect on that of its downstream.

**Proposition V.1:** Overvoltage can be eliminated by controlling DG maximum output.  
**Recommendation 1:** The DG should be controlled so that less reversed than forward  $P^V$  flow is generated throughout the feeder.

The above proposition and recommendation is verified on the test system in Figure 10. A DG unit is installed at Node 12 of Feeder 1. Figure 21 shows the voltage-effective power flow and voltage profiles on Feeder 1 measured in DPlan under three DG output  $I(600kW, 50kVar)$  ,  $II(800kW, 50kVar)$  and  $III(600kW, 250kVar)$ .

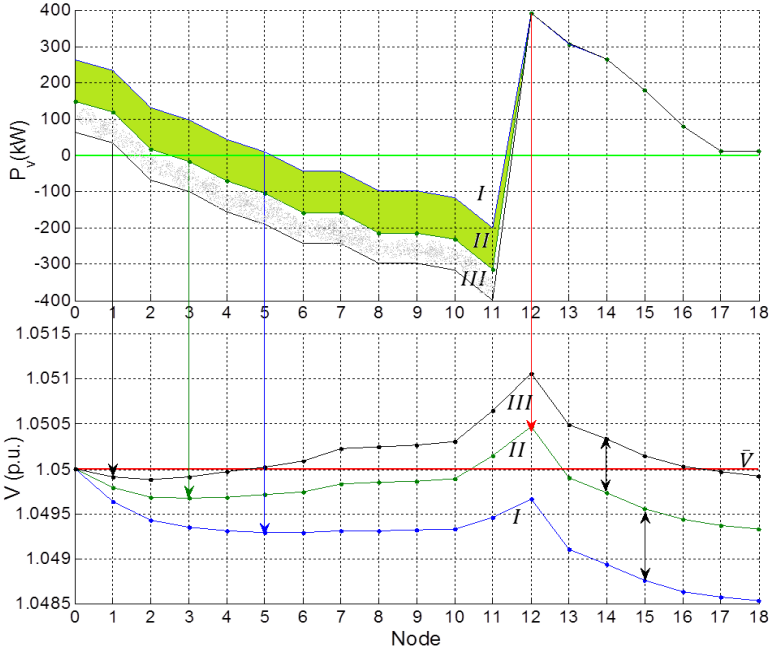


Figure 21. Voltage profiles of Feeder 1 under three setups of DG output.  $I(600kW, 50kVar)$ ,  $II(800kW, 50kVar)$  , and  $III(600kW, 250kVar)$ .

As shown in Figure 21, the voltage measurement from DPlan, which estimates voltage through AC power flow, performs what is predicted from the proposed graphical method and Area Criterion in Section 2.1.2 and Section 2.1.3.

In addition, for every setting of DG output, the voltage profile varies according to the Area Criterion: reaching its local minimum and maximum at the zero point and DG location respectively, and exceeding its upper limit when the negative area is larger than the positive area under the  $P^V$  curve in upstream of DG location. By increasing the output of DG real power from setup *I* to *II* by 200 kW, it raises up the voltage profile more than increasing the reactive power of DG output by the same amount from setup *I* to *III*. This is because the feeder's ratio of reactance to resistance  $x/r$  is less than one. In addition, because changing DG output does not affect the  $P^V$  flow downstream to the DG location, the downstream voltage profiles are paralleled for all the three setups.

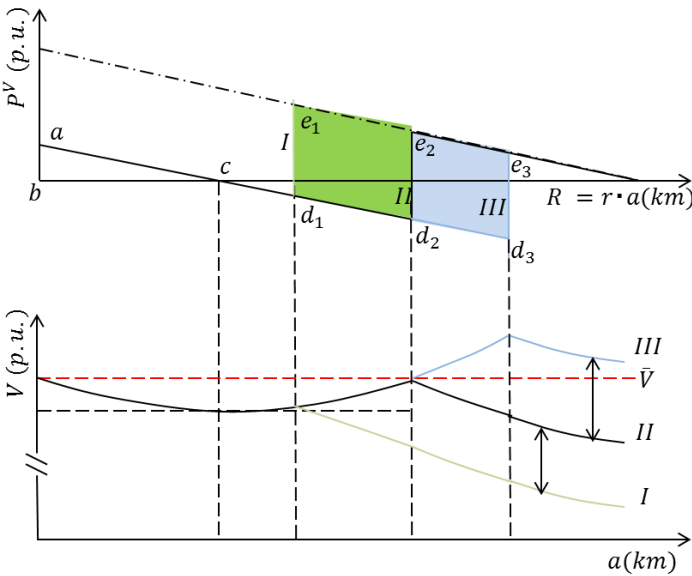


Figure 22. Voltage-effective power flow (top) and voltage profile (bottom) varying with DG location.

A DG unit is inserted at  $e_1$ ,  $e_2$  and  $e_3$  and induces a voltage profile that is under the upper limit *I*, hitting the upper limit *II* and over the upper limit *III*.

### **Factor 2: DG Location**

The voltage profile on a feeder is affected by DG location. Figure 22 illustrates this fact by inserting a DG unit at three locations,  $e_1$ ,  $e_2$  and  $e_3$  on the feeder.

It is observed that, in the three locations, the positive areas  $abc$  under the  $P^V$  curve are the same, so are the voltage profiles in the upstream of DG location. This is because DG location does not affect the amount of  $P^V$  flowing into the feeder. However, the deeper the DG unit is inserted on the feeder, the less its output can be absorbed by the loads downstream, indicated by the larger negative area induced. As shown in Figure 22, moving the DG unit from location  $e_1$  to  $e_2$  and to  $e_3$  produces the negative area  $e_1d_1d_2e_2$  and  $e_2d_2d_3e_3$ , which lifts the downstream voltage profile up parallel from  $I$  to  $II$  and to  $III$ .

**Proposition V.2:** The deeper a DG is located at a feeder, the more likely it will cause overvoltage.  
**Recommendation 2:** Given its output, DG should be allocated no deeper than a location to where the induced cumulative  $P^V$  flow equals to zero.

This result is verified through the example shown in Figure 19. A DG unit sized of (600kW, 50kVar) is inserted at Node 2, Node 12 and Node 16 of Feeder 1 respectively. The induced voltage-effective power and voltage profiles are plot in Figure 19 (Right).

The results shown in Figure 19 verify Proposition V.2, that is, the deeper a DG unit is inserted on a feeder, the more likely it will cause overvoltage. Inserting a DG unit at Node 2 does not generate any reversed  $P^V$  flow and results in a monotonically decreasing voltage profile. By pushing the DG unit further down to Node 12, the voltage profile is raised to a higher value without hitting the upper limit, which can be predicted from the fact that the negative area is less than the positive area under the  $P^V$  curve throughout the feeder. Overvoltage occurs when the DG unit is inserted at Node 16, the very end of the feeder, where DG output cannot be absorbed by the two loads downstream and a large reversed  $P^V$  flow is generated. In this case, the negative area under the  $P^V$  curve is much larger than the positive area upstream to Node 16, and the voltage profile hits the voltage upper limit near Node 13, where the positive and negative areas break even. In addition, as stated in

Proposition V.2, the voltage profiles of the three cases are the same at upstream and in parallel at downstream to DG on the feeder.

**Factor 3: DG Dispersion**

Previous studies have discussed DG dispersion effects; namely, whether installing one DG unit of a large size is better or worse than installing two or more DG units of smaller sizes. Through simulations and field tests, some studies show that dispersion of DG helps prevent overvoltage, but they fail to provide theoretic support for such statements [4, 129, 138]. The following analysis explains how DG dispersion can improve voltage profiles and why the statements of previous studies are sometimes not true. Figure 24 depicts three cases: one large size DG unit located at  $f$ ; three small DG units of the total size same as the large DG unit and inserted upstream of  $f$ ; and two small DG units of the same total size and inserted downstream of  $f$ .

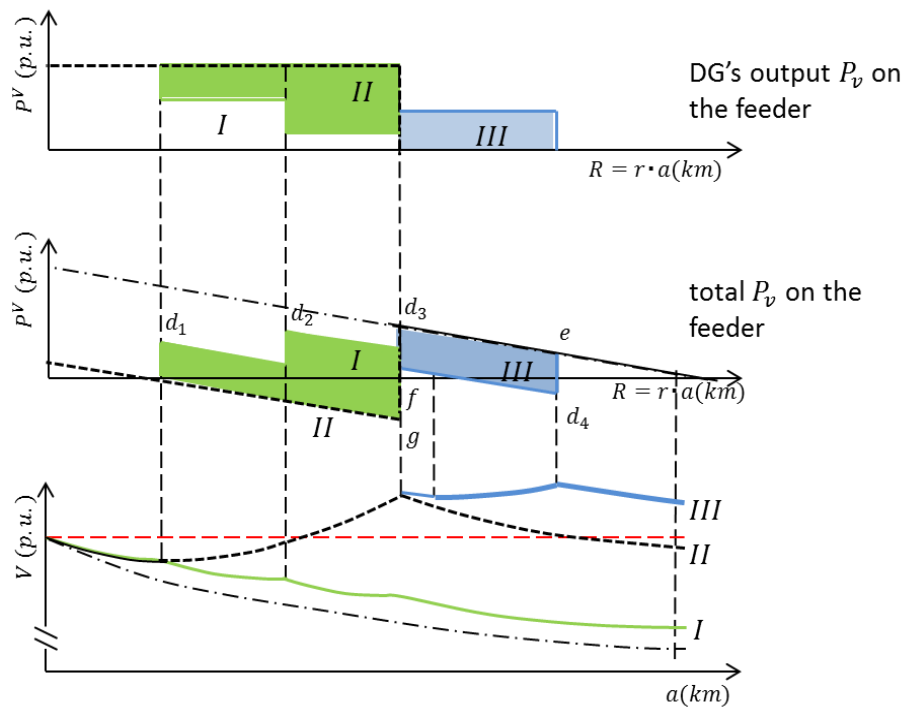


Figure 23. Voltage-effective power flow and voltage profiles varying with DG dispersion level.

(Top) Voltage-effective power flow resulting from (a) three small DG units, (b) one large DG unit, and (c) two medium DG units, of which the total sizes are the same. (Middle) Voltage-effective power flow of the three dispersion levels of DG. (Bottom) Voltage profiles of (a), (b) and (c) shown as *I*, *II* and *III* respectively.

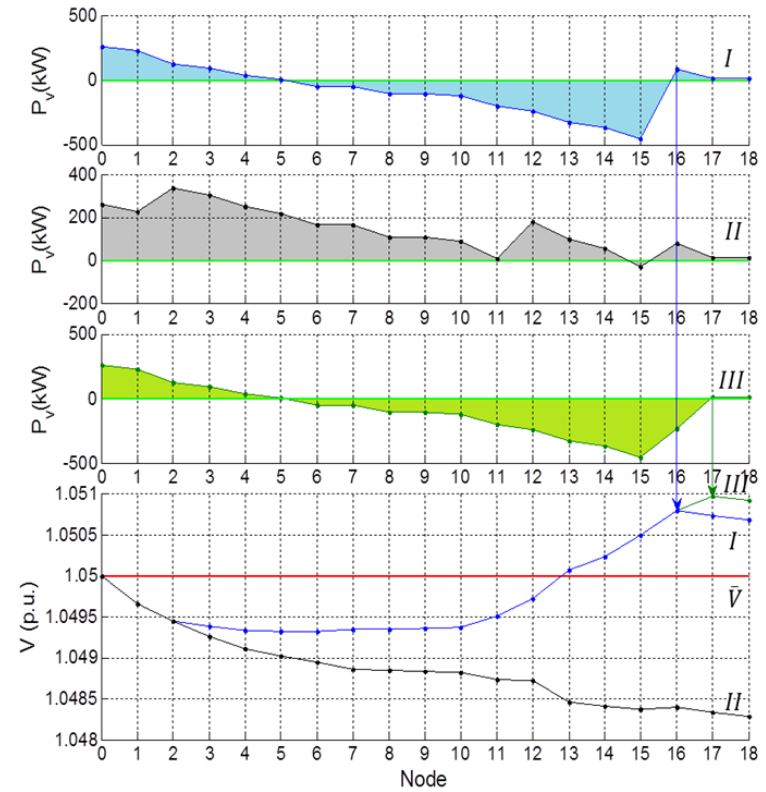
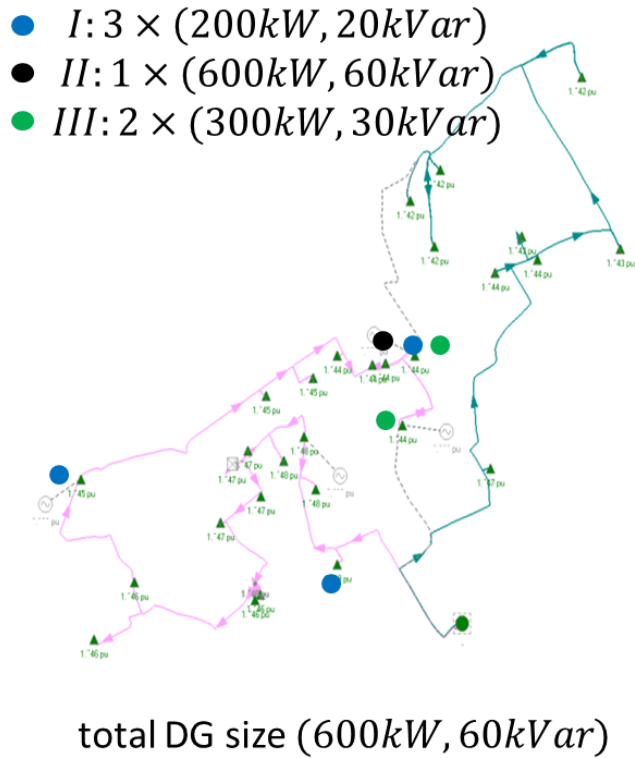


Figure 24. Voltage profiles of Feeder 1 under three levels of DG dispersion.

A large DG unit (*I*), three small DG units (*II*), and two medium DG units (*III*).



Figure 23 shows that dispersion may sometimes be used to avoid overvoltage. For example, in case *I*, the DG output is absorbed by the loads upstream of  $f$ , which reduces the reversed  $P^V$  flow. However, dispersion may also worsen the voltage profile. Case *II* verifies this point: when dispersion spreads DG deeper on the feeder, the DG output may exceed their downstream loads, resulting in more reversed  $P^V$  flow and thus raising voltage.

**Proposition V.3:** Spreading DG capacity does not necessarily mitigate overvoltage.

**Recommendation 3:** Dispersion of DG capacity improves a voltage profile only when it reduces the reversed  $P^V$  flow on the feeder.

Influences of DG dispersion level on voltage profiles are verified through three cases: *I*. a large DG unit sized of (600 kW, 60 kVar) and inserted at Node 16; *II*. three small DG units, each sized of (200 kW, 20 kVar), and inserted at Node 2, Node 12 and Node 16 respectively; *III*. two small medium DG units, each sized of (300 kW, 30 kVar) and inserted at Node 16 Node 17 respectively. Case *II* disperses the DG capacity to the upstream in Case *I*, and Case *III* disperses the DG capacity to the downstream in Case *I*. Their induced voltage-effective power and voltage profiles are measured from Dplan (in Figure 24).

Proposition V.3 is demonstrated by Figure 24, Right: dispersion that spreads the DG output to more loads over long distance on a feeder (as in Case *II*) improves the voltage profile, whereas dispersion that spreads the DG output toward the end of the feeder (as in Case *III*), where its output power cannot be absorbed, creates more negative area under the  $P^V$  curve, and thus results in more severe overvoltage.

#### ***Factor 4: Feeder's Conductor***

Conductors' characteristics influence voltage profiles in a way different from the factors of DG side. According the graphical method, the occurrence of overvoltage is determined by the ratio of reactance to resistance  $x/r$  of a feeder's conductor; whereas the previous studies generally limit their discussion to reducing conductor resistance for voltage mitigation purpose [4, 37, 104, 116].

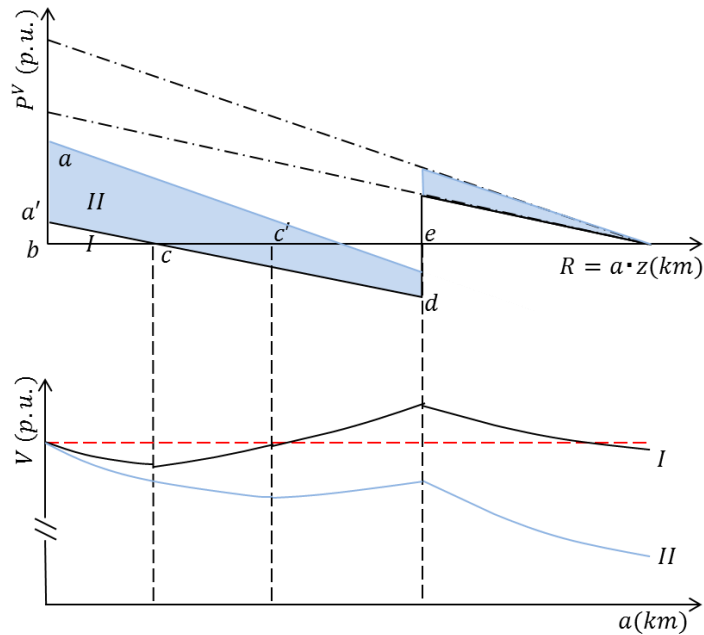


Figure 25. Voltage-effective power flow (Top) and voltage profile (Bottom) varying with the ratio of reactance to resistance  $x/r$  or load profile of a feeder.

A larger  $x/r$  or load density will result in a voltage profile of a lower value ( $II$ ).

Figure 25 illustrates this point: by increasing  $x/r$ , the zero point, where the local minimum voltage occurs, moves from  $c$  to  $c'$ . Meanwhile, the total area under the  $P^V$  curve is increased by  $aa'd$ , which brings the voltage profile to lower value throughout the feeder. In practice, the value of  $x/r$  can be adjusted by changing the feeder's spacing (for overhead feeders) and insulation (for underground feeders), which affect reactance  $x$ , or by changing the conductor's materials and size, which determine resistance  $r$ . In the latter case, the resultant voltage profile is flatter than that induced from reactance adjustment. This is because the value of the unit resistance  $r$  defines the dimension of the horizontal axis,  $a \cdot r(km)$ , in a  $P^V$  plot and thus determines the magnitude of the voltage profile. In distribution system planning where other constraints (such as cost and land-of-use) exist, it is worthwhile to notice that overvoltage can be prevented by trading off these factors and choosing a conductor of an appropriate ratio of reactance to resistance.

**Proposition V.4:** Overvoltage can be prevented by planning for the feeder's layout and conductor.

**Recommendation 4:** The resultant ratio of reactance to resistance should induce less reverse than forward  $P^V$  flow on the feeder.

**Factor 5: Load Profile**

Loads affect a voltage profile differently depending on their locations on a feeder. Loads upstream to DG location determine the voltage drop measured from the feeder's primary side; loads downstream to DG determine how much DG output can be absorbed and consequently how much reversed  $P^V$  flow is induced. Therefore, to prevent overvoltage, a feeder should have enough loads upstream to DG to produce voltage drop and downstream to DG to reduce reserved  $P^V$  flow. Figure 25 and Figure 26 illustrate how the voltage profile is affected by changing load density and feeder's length respectively.

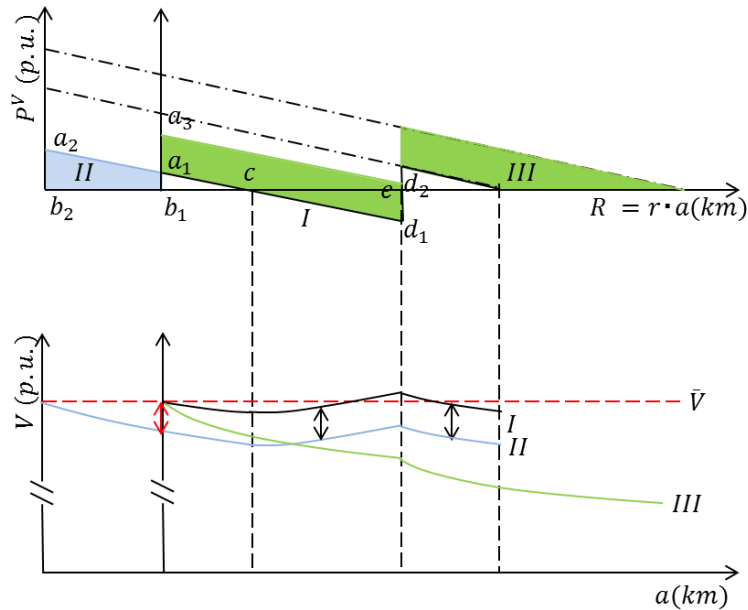


Figure 26. Voltage-effective power flow (Top) and voltage profile (Bottom) varying with load profile.

Adding a new feeder section of the same load density to the upstream (II) and downstream (III) to DG respectively results in voltage profile of lower values.

As shown in Figure 25, increasing load density results in a steeper  $P^V$  curve that creates larger positive area and smaller negative area, which mitigates overvoltage according to the Area Criterion. In practice, this tactic can be implemented through demand response programs [139-141]. On the other hand, as shown in Figure 26, adding a loaded feeder section to the upstream or downstream of DG mitigates overvoltage by adding an extra positive area under the new  $P^V$  curve. Although this approach has not been adopted as often as changing load density through demand response, it would be a promising tactic given recent development in remote control switching devices and communication technologies that enables convenient and timely reconfiguration of distribution networks [35, 95, 142].

#### ***Factor 6: Primary Voltage Settings***

Finally, the settings of voltage regulating equipment, such as tap transformers and voltage regulators, directly influence the voltage profile on a feeder [100]. By adjusting any of the settings, the voltage profile starting from the adjusted location can be brought down, *in paralleled to the original one*, to a lower level throughout the feeder.

### **2.3.2 Practical Methods to Voltage Control**

In practice, the six factors influencing a feeder's voltage profile can be realized in a few forms. As later chapters will discuss the two determinants, that is, how to size and locate DG units, this subsection give a brief view of other available means of mitigating voltage rise in DG penetrated distribution systems. Some of these means are used in the system planning stage: a planner can provide a better "DG penetrating environment" by upgrading conductors, refining feeder's configuration, and installing some online device to adjust real power and reactive power; whereas the other means are used in operation to recalibrate voltage profile after DG units penetrated: they include DG output control, reactive power control (Var control), load profile adjustment and online reconfiguration.

#### ***Primary Tap Adjustment***

The most common practice used to mitigate voltage rise is primary tap changing, which decreases the secondary voltage of the feeder's supply transformer by selecting an appropriate tap position. The work principle and effect of this method is stated in Factor 6, primary voltage settings. It is usually in conjunction with Automatic Voltage Control (AVC) relay. The AVC relay continuously

monitors the output voltage from the transformer, a tap change command will be initiated when the voltage is above the preset limits [34, 143]. Previous studies show that, for a 11 kV feeder system, lowering the voltage at the primary substation from 103% to 100% of nominal reduces the voltage rise to just below the permitted +6% voltage limit [4].

Before changing tap of a feeder's primary side, a system operator must ensure that this action will not adversely impact on any of its customers. If there are other feeders connected to the same transformer, the voltage profile along these circuits may be depressed. Also, if the generator is not exporting power, the system voltages will be depressed.

As a comparison, On-Load Tap Changers (OLTC) installed along the feeder and performing, such as stepping-up transformers, are seldom used in voltage rise mitigation, despite of their popularity in correcting excessive voltage drop. This is because the design of OLTC intends to step up voltage and its transforming ratio is greater than one. The flipped use of OLTC is prohibited, for the reason that it is designed for conventional passive distribution systems that are without generation and keep power flow in one direction. Retrofitting an OLTC for bi-directional flow applications can be more expensive than installing a "real" transformer and loses its original cost advantage [60, 102, 104].

### ***DG Output Control***

#### Power Factor Control

In Power Factor Control (PFC),  $P/Q$  of DG units is maintained constant, any fluctuation in real power  $P$  brings about proportional variation of voltage.

In practice, a grid-connected DG needs to fulfill the specific requirement depending on the regulation of the country. For example, in the Danish, DG power factor is confined between 1.00 and 0.95 lagging. The German grid code specifies different reactive power limits according to voltage value at interconnection (with a power factor ranging between 1.00 and 0.925 lagging). The Irish grid code requires a power factor between 0.835 leading and 0.835 lagging when the active power output level is below 50% of the rated capacity. In Italy and the UK, the power factor at a DG terminal should be between 0.95 leading and 0.95 lagging [2, 14, 144].

The amount of reactive power that can be imported/absorbed is generally governed by the parameters of the generator. Typically a synchronous generator can import reactive power at a 0.95

power factor. Wind turbines, with uncompensated induction generators, can import reactive power at around a 0.9 power factor [31, 36, 73].

#### DG Output Curtailment

This method is much often used with DG of Varying Energy Resources (VERs). Currently, due to the inflexibility of the voltage control strategies, a distribution system operator trips whole DG sets from the network to solve the voltage rise problem. This operation largely wastes the potential renewable energy and reduces the profit of DG. Therefore DG power output curtailment is proposed as a straight forward method to solve voltage variation problems by reducing DG power production [18, 24, 145]. The work principle of this method is explained by Proposition V.2. This method is the further implementation of sizing a DG unit in operation after the planning stage.

#### ***Reactive Power Control (Var Control)***

##### Shunt Reactance

According to Proposition V.2, one solution to the voltage rise problem created by excessive DG output is to increase the reactive load by using shunt reactances. Shunt reactances inject negative Vars into the feeder at their locations, improving the power factor upstream of them. This reduces the voltage-effective power flow on the circuits between its location and the feeder's primary side, and thus mitigates voltage rise [12, 108, 119].

##### Series Reactance

Series reactance works as the “reactive impedance in combination with reactive load” duo. Placed in series with a distribution line, they counteract or “cancel” DG output reactive power, lowering voltage rise. In addition, series reactance can mitigate flicker and voltage regulation problems [31, 85].

Series reactances, the same as series capacitor, have a downside, including a not entirely undeserved reputation for causing intermittent operating problems. In some cases, they can exacerbate “ringing” (a type of voltage resonance following major changes in load level or switching or just for no apparent reason at all), voltage transients, and something like ferro-resonance in nearby transformers. Such problems are very rare, but they do occur. More likely but

still rare are situations where a series reactance will cause big voltage drop at on a feeder when DG output is at low, off-peak condition [66, 108, 146].

### Power Electronics

Power Electronics (PE) devices can, if properly designed and applied, essentially force voltage, power factor, and phase angle of power flow in a circuit to exactly correspond to the planners' and operators' wishes. At present, PE solutions are generally expensive compared to the other options for voltage performance improvement. They are included here for completeness's sake, and because in really "messy" cases where dynamics, phase, or circular flow issues abound, they often provide effective and even elegant solutions [33, 35, 36, 45, 147].

### ***Load Profile Adjustment***

#### Demand Response

Demand Response (DR) refers to cooperative activities between the utilities and their customers to implement options for system performance improvement. Conventionally, DR is used to temporarily reduce the total power consumption increase, hence maintaining network safety and stability, maximizing energy efficiency [42, 139, 148]. This technique has been increasingly employed on Low Voltage (LV) networks for mitigating voltage rise by increasing end-user energy consumption [141]. The requirement for DR applications is that the loads agree to be modulated when necessary, convinced to use more energy during off peak hours.

As an example, a DR system consisting a central controller, and four load controllers has been applied on an 11kV distribution network with a 2.6MW wind power generator [85]. Each load controller governs a balanced three phase load at 415V network. The central controller monitors the voltage on the 415V network; the load controller will switch in its load as soon as the voltage is greater than the preset limits. This work demonstrated that DR can be used to mitigate voltage variation problems with minimum network reinforcement and minimum constraint of DG output.

#### Energy storage

Energy storage is under the same principle of DR, as explained by Factor 5, but with more flexibility and usually shorter response time, and more predictable responsive capacity. These devices use a Power Conversion System (PCS) to connect to distribution systems. They can source

or sink both real and reactive power to compensate for voltage variations in the short or medium term. It has been demonstrated that approximately 1 *MWh* storage per *MW* of wind power is enough to reduce at least 10% of the local voltage rise in weak networks [10, 41, 76]. For longer durations of voltage problems, excessive energy storage capability is required with a high capital cost [96].

Energy storage devices include pumped hydro storage, compressed air energy storage (CAES), hydrogen, lead acid batteries, super-conducting magnetic energy storage (SMES), flywheel and capacitors. Currently, energy storage technologies are at various stages of development and deployment. Pumped hydro and lead acid batteries are the most widespread storage technology deployed on power systems; they are technically and commercially mature [2, 10].

### ***Conductor Upgrading***

#### Larger Wire

The work principle of conductor upgrading is straightforward by Proposition V.4. Larger wire size often does prove to be an effective means of alleviating voltage rise. Particularly in situations where the plan is for a new feeder, the marginal cost of the next size wire is generally quite small [108]. In situations where wire size is below 500 *MCM*, and hence conductor's resistance is the dominant part of the impedance, upgrading conductor or cable size in one or more segments might prove an economical way to "buy" improved voltage performance.

In most cases where the existing or planned wire size is larger than about 600 *MCM*,  $R/X$  ratio is so small that increasing the wire size does not provide a great amount of voltage rise improvement for the money [104, 108]. In addition, larger wire size always means higher fault current. This may mean that upgrades in the capacity of breakers, reclosers, and sectionalizers are now required. But despite these caveats, larger conductor works particularly well when the existing or proposed wire size is small, and it reduces loss, an added benefit [37, 56].

#### Closer Phase Spacing

The reactive component of impedance in a line segment is a function of the phase spacing. Larger phase spacings produce a higher  $X$ . One way that the voltage performance of a feeder can be extended is to reduce the phase spacing, thereby reducing reactive impedance, and consequently



improving voltage rise performance. Usually, this is not an option open to a planner: changing phase spacing is probably not feasible, and even if so, is prohibitively expensive [2, 101].

The only exception happens when building a new feeder with a higher rating than needed. Actually, this setting is deployed by many utilities in order to accommodate future upgrades to higher voltage [56]. For example, several utilities in the southern U.S. build new 12.47 kV feeders to 34.5 kV standards. The difference in crossarm width for a typical horizontal overhead pole among their designs is three feet (nine versus twelve feet), which results in an increase in reactive impedance. Planners often forget to take this high reactance and encountered voltage problems in the detailed design of feeder systems [101].

### ***Configuration Refinement***

#### Network reconfiguration

Network reconfiguration refers to the process of closing/opening the Normal Open Point (NOP) between two radial feeders to form a “ring” operation. This technique has been widely used for network loss reduction and load balance. Artificial intelligence techniques, such as, fuzzy logic and genetic algorithm (GA) have been applied to maximize load ability margin and minimize system loss [149-154].

Reconfiguration is a new topic in voltage control on DG connected networks [50, 55]. It is very attractive in the sense that they often cost nothing in terms of capital additions, crew time for modifications, or commitment to future configuration (i.e., the feeders can always be switched back to their original configuration in the future). Applications of reconfiguration are worth exploring even when some slight amount of money would need to be spent to add a line segment, switch, or other equipment to facilitate the purpose.

With reconfiguration, a distribution feeder system is therefore a rather dynamic entity, in that its switching pattern is changing from year to year in response to DG and load growth in some of the areas it serves. One result of this (completely justifiable) approach to distribution system planning is that in many parts of the power system, all the feeders in the area will be loaded to their maximum capability [150, 153]. This is near optimal and very sound planning, because what has been purchased in the past and installed is being fully utilized.

### Artful Use of Feeder Configuration

While reconfiguration refers to dynamical adjustment on the base configuration, here we think of a more static approach of making change on the base configuration for the long term, which is not reversible.

The role of a distribution feeder is to provide power flow pathways from the source (the substation) to the set of service transformers in its service area. In many (most) cases, a distribution planner has much freedom with respect to how s/he arranges the configuration, selecting and refining the exact configuration of a feeder, the plan for how pathways split on their way from the one source to the many consumers, of how its trunk branches and its laterals stem from them to carry power from the source throughout the service territory [37, 46].

Voltage is only one of several factors a planner has to juggle in layout of a feeder, and protection, reliability, and other needs may dictate that one configuration cannot be used instead of another [104, 155]. But planners should always consider these options, and strangely they often neglect to consider such changes in configuration within a single feeder as a solution to voltage and minor overloading problems. Such changes often result in a better distribution of loading.

### *Hybrid and Cooperative Methods*

Due to the complexity of the existing DG connected networks, a single control strategy is often insufficient in solving complex voltage problems. Therefore, hybrid and cooperative methodologies are widely employed, compared with single control strategy. Hybrid and cooperative approaches manage different aspects and various situations on the network. State estimation and overall decision making strategies play a vital role in the overall system [35, 96, 97, 156, 157].

## **2.4 Two Innovative Approaches for Voltage Mitigation**

Section 2.3 presents a few methods that are used to realize the six factors improve voltage profiles of DG penetrated feeders. All of these methods ultimately mean spending money, and each has other implications that gain or lose advantage in other categories of importance to the planner. Table 5 gives an overview of their pros and cons [37, 131]. It is not hard to observe that the methods resorted to at the planning stage, such as improving feeder layout and larger wire, have better overall performance than the ones that are implemented in operation. This is because more

flexibility appears in the planning stage, and the methods of this stage build the “foundation” of feeder system configuration where the later methods can exercise on.

Table 5. Means to mitigate voltage rise in DG penetrated distribution systems. [37, 131]

Measure	Mitigating Effect	Initial Cost	Operation Cost
Reconfiguration	Grey	Green	Green
Feeder Layout	Grey	Grey	Green
Larger wire	Green	Grey	Green
Demand Response	Green	Grey	Yellow
Shunt Reactance	Green	Grey	Red
Series Reactance	Green	Grey	Grey
DG Output Control	Green	Green	Red
Power Electronics	Yellow	Red	Grey
Storage	Red	Red	Red

Color Chart	
Excellent	Yellow
Good	Green
Poor	Red
Depends	Grey

However, in the operational stage, there are two methods, Demand Response (DR) and reconfiguration, appear to have performance compelling to the other methods. As stated in Section 2.3, these two methods have several privileges:

- Low capital investment. As always, performance and cost are in compromise in voltage rise mitigation. Methods that can effectively mitigate voltage rise usually require sophisticated devices, power electronics for example, hence high capital investment [4, 47, 76-78]. As a comparison, the only necessary device needed for reconfiguration is controllable switches, which cost is coming down recently. Similarly, DR can be implemented with simple load shedding devices [95, 106]. For highly cooperative customers, even these devices are optional. Utilities can depend on customer’s full cooperation, with delay and responsive rate taken into account, to instruct their use of electricity [158, 159].

- High operational flexibility. The voltage mitigation effects of operational methods are typically limited to their location and size [72, 79-81]. This becomes a problem when demand profile and some DG output, which are Variable Energy Recourses (VERs), varies over time. Accordingly, the location and severity of overvoltage changes over the feeder and time. For this reason, a system planner usually needs to size and locate the devices for the worst case, which raises initial cost and operational complexity. Conversely, reconfiguration and DR have very high operational flexibility: they are not distributed over the whole configuration, and can be resorted anywhere when needed; they hardly have capacity limit (for DR, its capacity is as much as the total load over a feeder system).
- Good effects of voltage rise mitigation. When used smartly, DR and reconfiguration can effectively mitigate voltage rise in a short time [154, 160]. In particular, DR will not cause voltage flicker, protection reset, fault current and other power quality concerns that are often seen in other operational methods [45, 114].

Despite these advantages, so far DR and reconfiguration have not been studied much for their use in voltage rise mitigation. This is partially because they are emerging concepts with “smart grid” that encourages advanced algorithms and use of controllable devices, which becomes more affordable recently. This section aims at shedding some thoughts on these two methods, by proposing their possible implementing schemes.

For DR, it presents the strategies of calling load adjustment and compares the voltage mitigation effect under different pricing structures. The results will be interesting to utilities and DR providers to design DR programs and to implement them for DG penetrated systems.

For reconfiguration, this section presents a set of guidelines to adjusting DG connected feeders. The results can be used in any software package, while they are straightforward enough for system operators to apply on site for simple feeder systems.

This work, however, is not completed and is included here for the provision of future extension of this thesis. Their results should be solidified with real load data. More case studies and comprehensive cost-and-benefit modeling apart from voltage mitigation effect are also deserved. However, this section suggests a direction from where the continued work of this thesis may emanate.

## 2.4.1 Demand Response for Voltage Rise Mitigation

### *Cost Effectiveness of DR on Voltage Rise mitigation*

In order to evaluate DR's cost-effectiveness in voltage rise mitigation, effectiveness in voltage rise mitigation and cost resulting from DR are defined respectively.

The effectiveness in voltage rise mitigation is defined as: the total reduced overvoltage through DR. According to Equation 17 and Equation 19, voltage difference can be calculated by the cumulative area under the  $P^V$  curve over the distance where DR is implemented. Therefore, the effectiveness in voltage rise mitigation through a DR's call is measured by the increased cumulative area upstream to DG location, illustrated as the shadowed area in Figure 25.

The costs of DR depend on types of program. DR has two primary categories: time-based rates and incentive-based demand response [42, 161]. Time-based rates are usually implemented under the context of electricity markets. By implementing price differentials across different time periods, they seek to avoid dispatch of expensive peak generations and ancillary services, and thus to improve market efficiency [162]. Incentive-based DR programs offer payments for end users to reduce their electricity usage during periods of system need or stress [163, 164]. Here only incentive-based DR programs are considered.

Pricing structures of incentive-based DR programs primarily take three forms [42, 163]:

1. Flat monetary or credit rewards for contracted duration and capacity, say  $\$100/MW$  for one year participation;
2. Monetary or credit rewards proportional to demand adjusted for a contracted price in  $\$/MWh$ ;
3. Monetary or credit rewards proportional to times of response for a contracted price in  $\$/\# \text{ of response}$ .

The second pricing structure can infer the other two pricing structures and as well it can represent other factors, such as power delivery loss. Therefore, the discussion in this subsection is mainly based on this pricing structure.

Given the definitions above, we propose to evaluate DR's cost-effectiveness in voltage rise mitigation by the incremental ratio of DR's benefit (voltage regulating effectiveness) to its cost, denoted as  $\partial B / \partial C (V/\$)$ . Incremental benefit/cost evaluation is straightforward and no exotic computation or systems are needed for its application. Moreover, this method separates prioritization of DR implementation into incremental decisions, isolates the "very high cost-effective" decisions from other decisions, and permits a DR provider to look at the efficacy of money spent after each decision has been made.

### ***DR Strategies of Voltage Rise mitigation***

This section explores how to prioritize DR implementation on loads at different locations of a feeder to mitigate voltage rise resulting from DG. Two typical feeder configurations, so-called "large-trunk" and "multi-branch", are studied, as shown in Figure 12. Other configurations, such as loop and meshed network, can be engineered to either of the two configurations in nearly any situation [37, 70, 104].

**Apart from the assumption made in Section 1.2.2 and Section 1.3.2, we further assumes the following facts for illustration convenience.** The proposed DR strategies and conclusion on DR pricing structures, however, are not limited by the assumptions and can be extended to more complex situations.

- **Loads on a lateral can be aggregated to a single load on the primary feeder**
- **Only real power is changed under DR, i.e. DR does not affect reactive power consumption;**
- **All end users have the same margin of adjusting their electricity consumption under calls of DR.**

Same as defined in Section 2.1.2, *depth* is used to describe load and DG location on a feeder, with a symbolical expression as  $a \cdot r$  (km), where  $a$  (km) is the distance from the beginning of the feeder and  $r$  (p. u./km) is the unit resistance of feeder's conductor. The deeper an end user is located, the further s/he is electrically away from the beginning and the nearer to the end of the feeder.

### Voltage Rise Mitigation by DR on Feeders of Large-Trunk Configuration

Figure 27 depicts the voltage-effective power flowing on a feeder of big-trunk configuration. Based on the definition of DR's effectiveness, the feeder can be partitioned into two zones,  $Z_I$  and  $Z_{II}$ .  $Z_I$  covers loads downstream to DG location, and  $Z_{II}$  covers those upstream to DG location. Given that the DG is inserted at depth  $a_G$ , for an end user at depth  $a$  who increases electricity consumption by  $\Delta P$  (p. u.), the reduced overvoltage can be calculated as:

Equation 22

$$\Delta V_h = \begin{cases} a_G \cdot \Delta P^V, \forall a \in Z_I \\ a \cdot \Delta P^V, \forall a \in Z_{II} \end{cases}$$

where  $\Delta P^V = \Delta P$ . It can be observed that in  $Z_{II}$  the deeper DR is called, the more effective it is on voltage rise mitigation by generating a greater area under the  $P^V$  curve. However, for all loads in  $Z_I$ , their DR effectiveness  $\Delta V$  is the same regardless of depth.

Given the result, DR's cost-effectiveness is estimated under three forms of the adjusted-demand-based pricing structure.

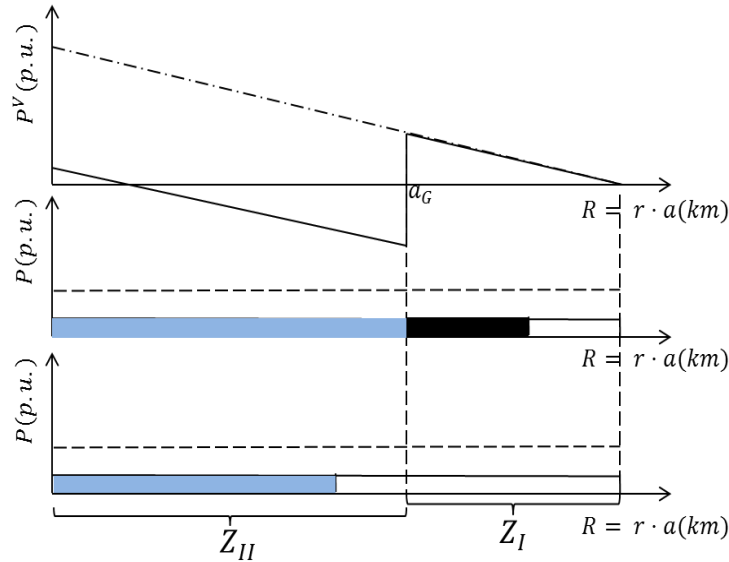


Figure 27. DR's priority regions defined by its cost-effectiveness on voltage rise mitigation.

(Top) Voltage-effective power flow of a feeder with a DG at depth  $a$ ; (Middle) Power contributes to voltage rise mitigation (blue) is less than power increased by end users in Region I (blue and black); (Bottom) Power increased by end users in Region II fully contributes to voltage rise mitigation (blue).

### Flat Cost and Constant for All Depth

The most basic form is a flat price,  $c$  ( $\$/p.u. \cdot hr$ ), for all end users regardless of their depth on a feeder. Therefore, the DR cost of an end user at depth  $h$  to respond  $\Delta P$  ( $p.u. \cdot hr$ ) is  $\Delta C_h = c \cdot \Delta P \cdot T$ , where  $T$  ( $hr$ ) is the DR implementing interval. Its cost-effectiveness is measured by incremental benefit/cost defined in Section III as:

Equation 23

$$\left. \frac{\partial B}{\partial C} \right|_h = \frac{\Delta V_a}{\Delta C_a} = \begin{cases} a_G/c, \forall a \in Z_I \\ a/c, \forall a \in Z_{II} \end{cases}$$

Loads at depth  $a$  of higher cost-effectiveness have higher priority to be called in DR for voltage rise mitigation purpose. Equation 23 shows when DR's cost is flat and constant along the feeder, loads in  $Z_I$  have higher priority of DR implementation than those in  $Z_{II}$ . By defining a *priority region*,  $Z^*$ , as the region where the loads having top priority, the guidelines for DR implementation can be summarized as below:

#### **Guideline A**

1.  $Z^* = \begin{cases} Z_{II} & \text{iff all loads in } RI \text{ have reached their} \\ & \text{DR capacity,} \\ Z_I & \text{otherwise.} \end{cases}$
2. In  $Z_I$ , a load at a shallower location have a higher priority than those at deeper locations;
3. In  $Z_{II}$ , a load at deeper location have a higher priority than those at shallower locations.

Guideline A.1 and A.2 are directly derived from Equation 23. Guideline A.3 is based on the fact that the demand adjusted not only contributes to voltage reduction upstream to DG, but also increases power delivery loss. Therefore, for loads in  $Z_{II}$  of a same cost-effectiveness, minimizing loss becomes the objective.



Flat Cost Varying with Depth

Despite of its implementation ease and plausible fairness, a flat DR price identical to all customers on the feeder may result in frequent calls to a certain group of end users. As shown by Equation 23 and Guideline A , for voltage rise mitigation within a certain range, end users in  $Z_I$  will be always called for the maximum cost-effectiveness. It is not fair to concentrate the responsibility of voltage rise mitigation on some end users simply because they cannot choose their depth on the feeder. To enhance fairness, studies have made the frequency of DR calling as a constraint or penalization cost, when optimizing DR strategy for different purposes [148, 165-167]. This approach, however, makes the original nonlinear problem more time-consuming and less likely to be solved. In practice, an alternative is to partition the service area into regions of different DR prices. In a feeder system, this approach can be applied by setting multi-level DR prices along the feeder, as shown in Figure 28.

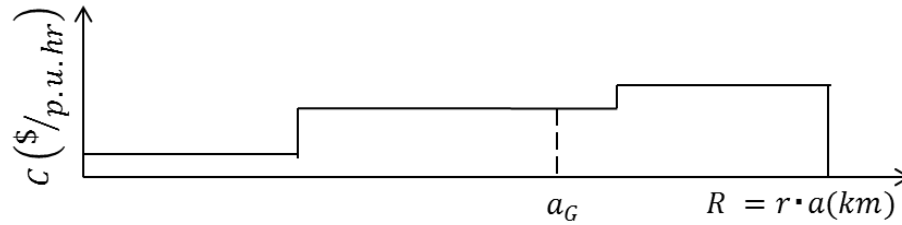


Figure 28. DR cost varying with depth on feeder.

As shown in Figure 28, if the DR cost is  $c_1 (\$/p.u.hr)$  in  $Z_I$  and  $c_2 (\$/p.u.hr)$  in  $Z_{II}$ , and  $c_1 > c_2$ , the guidelines for most-effective DR implementation of voltage rise mitigation can be summarized as:

**Guideline B**

1.  $Z^* = \begin{cases} Z_I & \text{if } a_G > a \cdot c_1/c_2, \forall a \in Z_{II}, \\ Z_{II} & \text{otherwise.} \end{cases}$
2.  $Z^*$  is changed if and only if all loads of  $Z^*$  have reached their capacity for demand response;
3. In  $Z_I$ , a load at a shallower location has a higher priority than those at deeper locations.

For more levels of DR costs, the guidelines can be easily extended to apply. It can be observed from the Guideline B.1 that the ratio of DR costs between the two regions,  $c_1/c_2$ , serves as a weight in estimating DR's cost effectiveness in  $Z_I$ . This property enables a DR provider to prioritize end users at designated locations by applying different DR prices along the feeder. Certain end users, which may be preferred by a DR provider due to their response flexibility, capacity and etc., can be identified with high cost-effectiveness in voltage rise mitigation even if they are shallow on the feeder. However, the fairness, represented by the frequency called by DR, is still a problem. Once the DR prices are set, the DR-calling frequency of certain regions will be always higher than that of others.

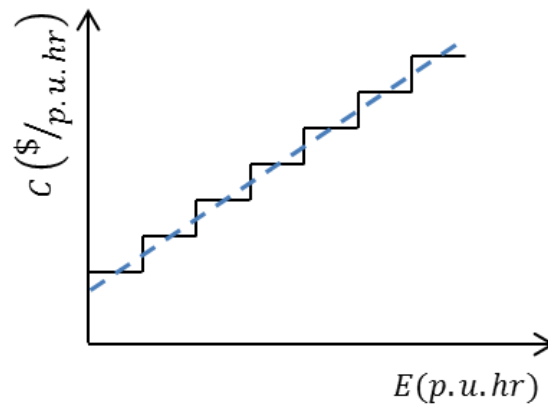


Figure 29. Linear cost function of DR.

Cost per MW increases linearly with the energy that an end user has responded to DR calls. The practical pricing structure (step) can be approximated to a linear continuous function (dash),  $c = c \cdot E + k$ , for convenience.

#### Cost as a Function of Energy Response

DR price that is set as a function of adjusted energy,  $c = c(E) (\$/p.u. \cdot hr)$ , can result in more uniform DR-calling frequency regardless of end-user depth. A linear cost function, as an example of this pricing structure, is depicted in Figure 29.

For an end user at depth  $h$  that has responded with  $E$  ( $p.u. \cdot hr$ ), the DR cost for another demand adjustment  $\Delta P$  ( $p.u.$ ) is  $\Delta C_h = c(E + \Delta P \cdot T) \left( \$/p.u. \cdot hr \right)$ . Therefore, the cost-effectiveness under this form of DR price is:

Equation 24

$$\frac{\partial B}{\partial C} \Big|_a = \frac{\Delta V_a}{\Delta C_a} = \begin{cases} \frac{a_G}{c(E + \Delta P \cdot T)}, \forall a \in Z_I \\ \frac{a}{c(E + \Delta P \cdot T)}, \forall a \in Z_{II} \end{cases}$$

The guidelines for DR to regulate voltage on the feeder are summarized below:

**Guideline C**

1.  $Z^* = a$ , if  $a > a' \cdot \frac{c(E + \Delta P \cdot T)}{c(E' + \Delta P' \cdot T)}$ ,  $\forall a, a' \in Z_I, Z_{II}$ ;
2.  $Z^*$  is updated for every incremental  $\Delta P$  of DR.

Guidelines above reveal two advantages of this pricing structure. First, it increases the fairness to end users. Under this pricing structure, the priority of DR implementation is adjusted by end-user responding frequency. For users that are frequently called and respond, their DR cost is increased, which raises the priority of other users by  $\frac{c(E + \Delta P \cdot T)}{c(E' + \Delta P' \cdot T)}$  in the next call. Second,

it retains the advantage of allowing a DR provider to set preferences of end user to call in DR implementation.

***Voltage Rise mitigation on Multi-branch Configuration***

This subsection investigates DR strategies for voltage rise mitigation on a multi-branch feeder. For simplicity, a feeder system of only two branches is considered, as shown in Figure 30. The derived results, however, can be extended to more branches and emanating levels.

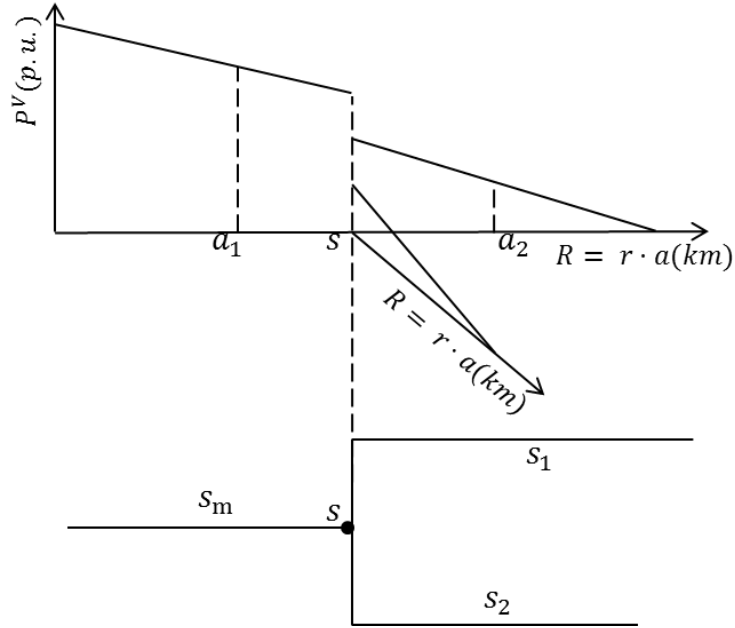


Figure 30. A two-branch feeder circuit.

(Top) Voltage-effective power flow; (Bottom) Feeder's topology. The main trunk  $s_m$  emanates at depth  $s$  into branches  $s_1$  and  $s_2$ .

On the multi-branch feeder shown in Figure 30, we consider two cases: (a) DG is inserted on the main trunk,  $s_m$ , at depth  $a_1$ , and (b) DG is inserted on a branch,  $s_1$ , at depth  $a_2$ . In the first case, the feeder model can be converted to a big-trunk model by aggregating voltage-effective power flow  $P_v$  on the branches. And DR's cost-effectiveness can be analyzed with the approach presented in Guideline A.

In the second case, the feeder can be partitioned into three zones,  $Z_I$ ,  $Z_{II}$  and  $Z_{III}$ , on which DR has different cost-effectiveness, as shown in Figure 31.  $Z_I$  covers the loads downstream to the DG location,  $a_2$ .  $Z_{II}$  covers those upstream to  $a_2$  on the branch  $s_1$  and on the main trunk,  $s_m$ .  $Z_{III}$  covers loads on the other branch,  $s_2$ . Given that the main trunk splits into branches at depth  $s$ , by increasing demand by  $\Delta P(p.u. \cdot hr)$  at depth  $a$ , voltage on the feeder is reduced by:

Equation 25

$$\Delta V_a = \begin{cases} a_G \cdot \Delta P^V, \forall a \in Z_I \\ a \cdot \Delta P^V, \forall a \in Z_{II} \\ s \cdot \Delta P^V, \forall a \in Z_{III} \end{cases}$$

where  $\Delta P^V = \Delta P$ . It can be observed that in  $Z_{II}$  the deeper where DR is called from, the more effective it is on voltage rise mitigation by generating a greater area under the  $P^V$  curve. For all loads in  $Z_{II}$  and  $Z_{III}$ , their DR effectiveness is the same regardless of depth.

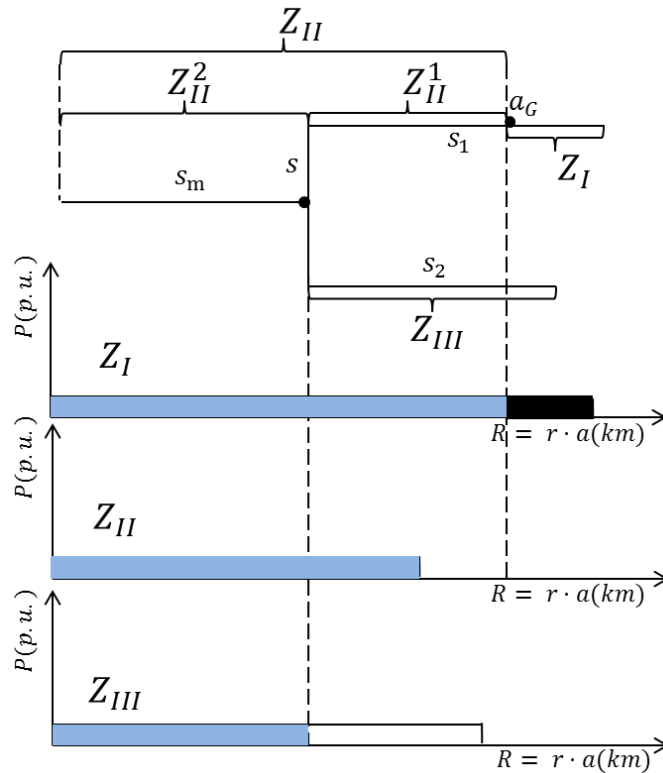


Figure 31. DR's priority regions when DG is inserted at a branch of a feeder.

(Top) Three priority regions of a two-branch feeder with a DG at depth  $a$ ; (Bottom) Power contributes to voltage rise mitigation (shadow) is less than power increased by end users in Region I and III (shadow and dark); and power increased by end users in Region II fully contributes to voltage rise mitigation (shadow).

From Equation 25, for a flat DR price,  $c$  ( $\$/p.u. \cdot hr$ ), along the feeder, the DR cost-effectiveness of end users at depth  $a$  is

Equation 26

$$\left. \frac{\partial B}{\partial C} \right|_a = \frac{\Delta V_a}{\Delta C_a} = \begin{cases} a_G/c, \forall a \in Z_I \\ a/c, \forall a \in Z_{II} \\ s/c, \forall a \in Z_{III} \end{cases}$$

Equation 26 shows that  $RI$  has a higher priority than  $Z_{II}$  of DR implementation simply due to  $a_G > a$ .  $Z_{III}$ , however, has a higher priority compared to  $Z_{II}$  if and only if  $s > a$ . Based on the fact, we can further partition  $Z_{II}$  into two sub-regions  $Z_{II}^1$ , which is the part of  $Z_I$  on the branch  $s_1$ , and  $Z_{II}^2$  which is the part of  $Z_I$  on the main trunk  $s_m$ , as shown in Figure 31. The guidelines for DR implementation on the feeder are summarized as below:

**Guideline D**

1. The priority of DR implementation on the feeder is  $Z_I \rightarrow Z_{II}^1 \rightarrow Z_{III} \rightarrow Z_{II}^2$ ;
2.  $Z^* = Z_I$ . And  $Z^*$  is changed if and only if all loads in  $Z^*$  have reached their capacity for demand response;
3. In  $Z_{II}$ , a load at a deeper location has a higher priority than those at shallower locations.
4. In  $Z_I$  and  $Z_{III}$ , a load at a shallower location has a higher priority than those at deeper locations.

The DR strategies under the other two forms of DR prices can be derived in a similar way as shown in subsection A and therefore are not repeated here.

Guideline D.1 reveals an important fact: voltage rise on a DG-integrated feeder can be mitigated by implementing DR on the other branches,  $Z_{III}$ . This is an important property. A multi-branch feeder covers diversified service areas and each of its branches is likely to have a different profile of loads and renewable DG output. Voltage problems resulting from imbalanced demand and DG output on one branch may be alleviated by a reversed situation of other branches.

Guideline D.3 is directly derived from Equation 26. Guideline D.4 is based on the fact that the demand in respond to DR's call increases power delivery loss, and loss minimization becomes the objective in the case.

## *Summary*

This subsection proposes DR strategies under different pricing structures to mitigate voltage rise. At the same time, these DR pricing structures are compared by their voltage mitigation effectiveness and fairness among customers. Some critical observations are:

- 1. Flat DR cost for end users may cause either low cost-effectiveness or poor fairness;**
- 2. DR's price as a function of end-user response energy can increase the fairness and allows DR providers to set preference for end-user groups;**
- 3. Voltage rise on a DG-integrated branch can be effectively mitigated by implementing DR on the other branches in a multi-branch configuration.**

## **2.4.2 Reconfiguration in Voltage Regulation**

### *Background*

Reconfiguration is conventionally thought of as a resort of fault isolation and power flow rerouting in emergent situations [149-154]. With the recent development of control and automation technologies, reconfiguration is becoming recognized as a means to in order to improve system performance, such as to reduce power delivery loss and balance load among power delivery equipment [149, 154, 168, 169]. Voltage management, as a possible application of reconfiguration, has the advantage of little impact on customers, high flexibility of implementing location and capacity [50, 55]. The applications and benefits of reconfiguration are summarized in Table 6.

### *Sectionalizing Switch, Sectionalizer and Closer*

Reconfiguration is implemented with the action of sectionalizing switches. In primary distribution systems, sectionalizing switches are used for both protection, to isolate a fault, and for configuration management, to reconfigure the network. Figure 32 shows a schematic diagram of a simplified primary circuit of a distribution system together with sectionalizing switches.

Figure 32, shows a part of a primary distribution system, consists of two substations  $S_1$  and  $S_2$  and feeder systems emanating from them. Load points, where the service transformers are tapped off from the primary circuit, is not depicted for illustration convenience. There are two types of switches in the system: normally closed switches (blue) connecting the line sections  $b_1$  to  $b_6$ , and normally opened switches (white) on the tie-lines connecting either two primary feeders  $b_7$ , or two

substations  $b_8$ , or loop-type laterals  $b_9$ . Distribution systems are normally operated as radial networks; however, configuration is changed during operation by changing the state of some sectionalizing switches. For example, in Figure 32, switches  $b_7$  and  $b_8$  can be closed and  $b_3$  and  $b_6$  can be opened to transfer load from one feeder to another.

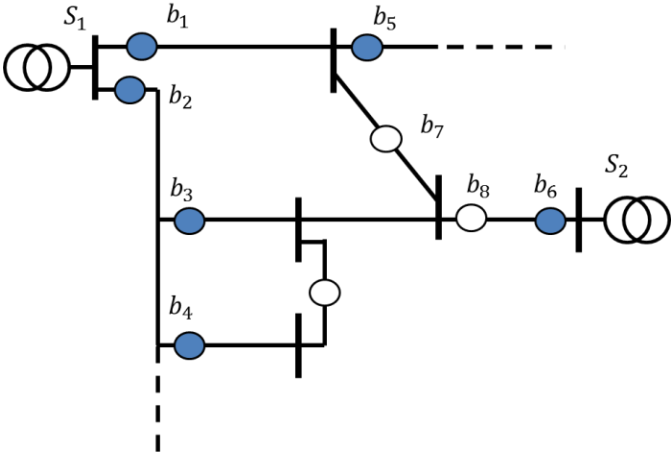


Figure 32. Schematic diagram of partial distribution system at primary level.

Load on feeders are assumed to be aggregated from their secondary level and are not depicted. The configuration is up to change depending on the alternative operation of the normally closed switches (blue) and normally opened switches (white).

Every complete operation consist a pair of switching operation, that is, one open and one close operation. For clarity, a normally closed switch that takes opening action is referred to as a *sectionalizer*; a normally opened switch that takes closing action is referred to as a *closer*. This definition of sectionalizers and closers can also be inferred from their functions in system protection: a sectionalizer is used for fault isolation, and a closer is used for reconnection of load in faulted region to another delivery source. Ideally, the sectionalizer and closer should act simultaneously. In practice, either acts ahead of the other. For protection purpose, sectionlizers acts first to prevent fault propagation [101, 104]. This section focuses on reconfiguration’s application on overvoltage mitigation, the first priority is reliability, and to prevent customers from even short blackout, it suggests closers act first.



### Work principle

The nature of reconfiguring distribution system is to change the power flow on feeders. Factor 5 in Section 2.3.1 has explained the work principle. Voltage rise can be mitigated through reconfiguration that adjusts power flow on the feeder concerned to a desirable form.

After reconfiguration, DG units on a feeder may be connected to the same source (substation) or to a different one. As the circuit shown in Figure 32, if a DG unit were connected between  $b_1$  and  $b_5$ , its supply source is  $S_1$ . After reconfiguration, this DG unit is connected to the same source if opening  $b_1$  and closing  $b_7$ ; whereas it will be supplied by  $S_2$  if opening  $b_1$  and  $b_3$  then closing  $b_7$  and  $b_8$ . Any reconfiguration consists of multiple operation can be decomposed into these two types of reconfiguration. It is also worthy to notice that, on any “ring” of a primary distribution circuit, reconfiguring DG units to the same source changes the original  $P^V$  flow direction (see Figure 33), which make equivalent of connecting the DG units to another source. We derive the voltage mitigation strategies for these two cases one by one.

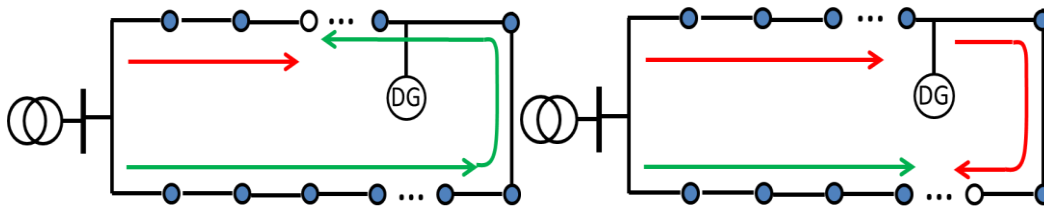


Figure 33. Voltage-effective power flow in reconfiguration on a circuit loop.

(Left) Before reconfiguration, the DG unit sees voltage-effective power flows from its right to left; (Right) After reconfiguration, the DG unit sees the voltage-effective power flows from its left to right. In both cases, the DG unit is supplied with the same substation.

Table 6. Reconfiguration applications and their benefits.  
[21, 154, 170, 171]

	<b>Substation Load Balancing</b>	<b>Feeder Load Balancing</b>	<b>Primary Distribution System Loss Reduction</b>	<b>Fault Identification and Service Restoration</b>	<b>Voltage Management</b>
<b>Reconfiguration Application</b>	Substation loads are monitored and loads (i.e. sections of feeders) are switched from one substation to another or within the same substation to prevent a substation transformer from becoming overloaded. Switching could be done by time periods within a day, daily, weekly, or seasonally.	Feeder loads are monitored and loads (i.e. sections of feeders) are switched from one a feeder to another to prevent a feeder from becoming overloaded. Switching could be done by time periods within a day, daily, weekly, or seasonally.	Loss are reduced through better feeder configuration and transformer loading.  The adjustments to feeder configuration and transformer loading are accomplished by monitoring feeder and transformer loads, and switching loads from one feeder to another.	Reconfiguration is used to remotely detect, locate, and isolate faulted feeder sections, and restore service to unfaulted sections. Service restoration is achieved by switching loads on outage to adjacent energized feeders.	When system-wide generation shortages/oversupply invokes voltage drop/rise excessive of acceptable range, loads (i.e. sections of feeders) are switched from one feeder to another to maximize the number of customers served at acceptable voltage.
<b>Justifications (Benefits)</b>	Transformer aging is slowed, increasing its lifetime, thereby deferring a capital expenditure to increase substation capacity.	Lifetime of existing feeders is prolonged, therefore deferring capital expenditure to increase feeder capacity.	Reduced loss can result in generator fuel savings and possibly some reduction in needed generation capacity.	Faster restoration of service reduces the amount of unserved energy and reduces the duration of outages for customers.	Less load will be served at sub-standard voltages so there is less chance for customer equipment damage or performance deterioration.
<b>Principal Benefit</b>	Capital expenditure deferral.	Capital expenditure deferral.	<ul style="list-style-type: none"> <li>• Fuel savings</li> <li>• Capital expenditure deferral (generation capacity deferral).</li> </ul>	<ul style="list-style-type: none"> <li>• Reduction of utility revenue loss</li> <li>• Higher customer reliability (in terms of distribution outage durations).</li> </ul>	Lower risk of customer damage and potential suits against the utility.

***DG connected to the same source after reconfiguration***

The general principle is to reconfigure the circuit so that more forward voltage-effective power  $P^V$  is induced than its reversed counterpart. According to the Area Criterion (in Section 2.2.2), overvoltage happens when the negative area under  $P^V$  gets greater than the positive area that is cumulated from a feeder's primary side. Therefore, in the case DG is still connected to the same source after reconfiguration, and the direction of  $P^V$  flows the same, the sectionalizer should trip off least load at DG downstream to retain the positive  $P^V$  flow at DG upstream; whereas the closer should add load to DG upstream to absorb excessive DG output, that flows reversely to the feeder's primary side.

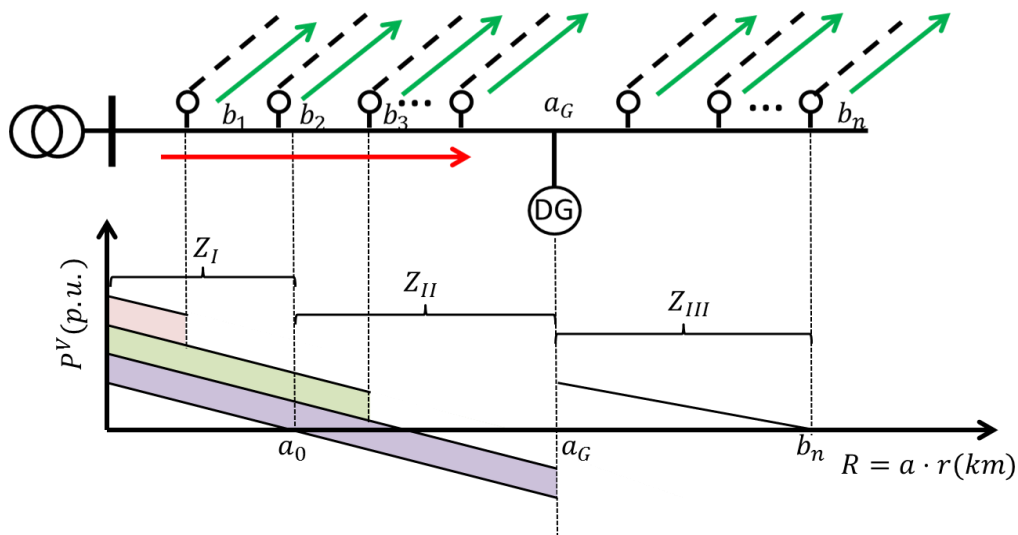


Figure 34. Priority zones on DG connected feeder for closers to trip on.

Figure 34 illustrates this strategy by a partial circuit of a feeder system. To mitigate the voltage rise caused by DG penetration, a sectionalizer opens at the other end of the feeder. Closers, from  $b_1$  to  $b_n$  closes by priority until overvoltage is mitigated, according to the Area Criterion, which induces negative area is less than positive area under voltage-effective power  $P_v$  curve.

The priority is assigned by the cost and benefit for each branch's connection to the DG-integrated feeder. The primary cost is considered here as the number of switching operation, which leads to switching devices depreciation, system disturbance and its induced maintenance cost.

Using the marginal benefit/cost approach, as discussed in Section 2.4.1, the feeder can be divided into three zones:  $Z_I$  from the feeder's primary side to the zero point of the original  $P^V, a_0$ ;  $Z_{II}$  from  $a_0$  to DG location  $a_G$ ; and  $Z_{III}$  from  $a_G$  to the end of the feeder. Quantifying the benefit of closing  $b_i$  by the voltage rise it mitigates, its marginal benefit/cost is:

Equation 27

$$\frac{\partial B}{\partial C} = \Delta V_i = \begin{cases} P_i^V b_i, i \in Z_I, Z_{II} \\ P_i^V a_G, i \in Z_{III} \end{cases}$$

where  $P_i^V$  is the total load on branch  $b_i$  to be tripped onto the DG connected feeder.

The guideline for closers' operation is expressed with an optimization formulation of Equation 28. Closers should operate from the one from near DG location to far, until the overvoltage is not observed.

Equation 28

$$\begin{aligned} & \min \|i\| \\ & s. t. \sum_i \Delta V_i \geq V_G - \bar{V} \end{aligned}$$

### ***DG connected to an alternative source after reconfiguration***

In this case, reconfiguration is completed by sectionalizing DG from its original source and connecting the sectionalized DG-integrated section to a new source (see Figure 35). This reconfiguration can be decoupled into two steps: (1) tripping off the DG unit from the original source (Sectionalization); and (2) reconnecting it to an alternative source (Reconnection). The sequence of the two steps does not indicate the actual operational sequence of switching the devices.

According to Proposition V.2 in Section 2.3.1, the deeper DG is located on a feeder, the more negative area is induced under  $P^V$  curve, which indicates the likelihood of voltage rise. Because  $P^V$  reverses its direction after reconfiguration, the nearer sectionalizer is to the original primary side,

the farther DG is away from the end of the feeder's new configuration. For example in Figure 35, after opening  $a_i$ ,  $P^V$  flowing through the DG unit changes direction. The DG location is the shallowest in the new configuration when sectionalizer  $a_1$  is chosen, which according to the Area Criterion mitigates voltage rise most effectively.

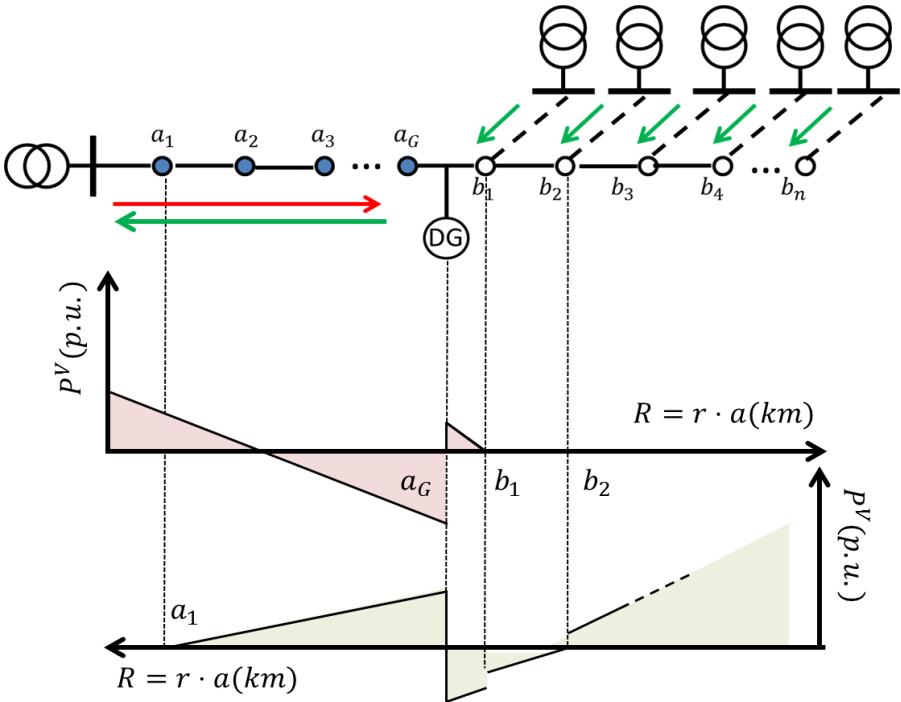


Figure 35. Voltage-effective power change after DG reconnected to a different substation.

Different from the reconfiguration that connecting DG to the same source, which may trip loads of multiple branches onto the DG connected circuit (as shown in Figure 34), for DG reconnection to a supply source, only one closer is chosen. This is because distribution systems operate in radial, and reconnection cannot generate loops. The closer is chosen based on the area criterion, expressed as

Equation 29

$$P_i^V b_i \geq V_G - \bar{V}$$

In case multiple branches satisfied the criterion, the choice is prioritized by the connection that generates the minimum total absolute area under  $P^V$  curve, which indicates the minimum loss.

### ***Future Work***

The reconfiguration strategies presented provides some thoughts of how to mitigate voltage rise fast and effectively. However, when they are to be applied in practice, voltage mitigation and device operation frequency are no longer the only benefit and cost, and there are other factors needs to be taken into consideration [153, 169, 172-174]. The future work will include the following points in the presented strategies:

- How to cooperate with existing network restoration strategies;
- How to decide the operating sequences when multiple operations are undertaken on the network;
- How to cooperate with other voltage control techniques.

# Chapter 3: Minimizing Power Delivery Loss in DG Penetration

---

The great interest in DG impact on power delivery loss can be exemplified by the link of utility operation in the chain of power industry. Most utilities have an economic incentive to reduce loss in their networks. For example, in Spain's wholesale market, utilities buy the energy loss that are consumed in their networks, and consumers pay the utilities the energy they consume times a standard loss coefficient, which is set for a regulatory period of several years. This means that the utilities buy real loss, but they receive payments for an amount of standard loss [163]. For these utilities in Spain and many other markets, the incentive is the cost difference between real and standard loss. If real loss is higher than standard ones, the utilities are economically penalized, or, if the opposite happens, they obtain a profit. Since the installation of DG will impact power delivery loss, it will have a direct consequence on the utilities profit.

In this chapter, four important rules are proposed for DG placement and sizing to reach minimum power delivery loss in distribution systems. Compared with previous studies that assess loss in a particular scenarios of DG penetration, these rules reveals the evolution of loss in a feeder as a function of different parameters, such as DG location, size, dispersion and output variance. For conciseness, the mathematical development of these rules is presented in Appendix B.

This chapter starts the discussion with placing a single DG unit on a feeder system. Section 3.1 and Section 3.2 derive optimal DG location and capacity that minimize power delivery loss. It shows that a DG unit should be placed at the location where the apparent power flow on the feeder equals to half capacity of the DG unit, summarized by the *Half Capacity Rule*. Moreover, at a given DG location, the DG output that induces minimum power delivery loss must provide voltage support, stated by the *Equal Voltage Rule*. These two rules are verified on feeders of some typical load distributions and on our test system.

Section 3.3 presents the *Superposition Rule* for applying the multiple-DG-units placement. This rule is for the first time proved mathematically and for general cases. One of its contributions is to significantly reduce the computational efforts in DG placement as demonstrated by a numerical example.

Section 3.4 further extends the DG penetration strategies for Variable Energy Resources (VERs). The *DG Variance Rule* is proposed for DG placement considering long-term demand variance and non-constant and undispatchable DG output. It shows that DG location is dominated and pushed toward a feeder's primary side by DG output variance.

The results proposed in this chapter will be interesting to, as mentioned in the beginning, utilities that operate networks and gain profit from reducing power delivery loss. Utilities that own DG units can apply these rules in DG placement; for those who have DG in their network but do not have ownership, the proposed rules can assist them to choose from candidate proposals and set instructions on DG installment by customers.

A wider impact from the results presented in this chapter is envisioned on both upstream and downstream of utilities in power industry. The proposed rules imply some flaws and potential improvement in current DG connection standards, which can be referred to by policy makers to improve future power system efficiency. They also provide marketing information for DG manufacturers that a certain range of DG capacities are to the interests of utility customers in the sense of loss reduction.

## 3.1 Optimal DG Location

### 3.1.1 Half Capacity Rule

With a DG unit of known capacity, utilities want to know where to install the unit on a feeder system so that the induced power delivery loss is minimized. The rule for choosing DG location is stated in Proposition L.1 and illustrated by Figure 36.

**Proposition L.1 (Half Capacity Rule)** To minimize power delivery loss on a feeder, the DG unit should be placed at the location where the feeder's load apparent power flow equals to half of DG rated apparent power (which is its thermally limited capacity).

Proposition L.1 can be expressed in Equation 30, with proof presented in Appendix B.

Equation 30

$$2S_L(a^*) = S_G$$



where  $S_L$  is load apparent power flow on the feeder and  $S_G$  is the thermally limited capacity of the single DG unit.

Section 1.3.2 has shown that power flow on a feeder is cumulated by load density from the feeder's end to its primary side (see Equation 11). Therefore, according to Proposition L.1, the optimal DG location is determined by DG capacity and its downstream load only.

An important assumption of Proposition L.1 is the DG unit runs at its full capacity in operation. If the DG unit tends to run at an output different from its capacity, that output should be transferred to apparent power and replace its thermally limited capacity in setting the optimal location. Furthermore, this output is static, in other words, the DG unit is not a Variable Energy Resource (VER), which will be discussed in Section 3.4.

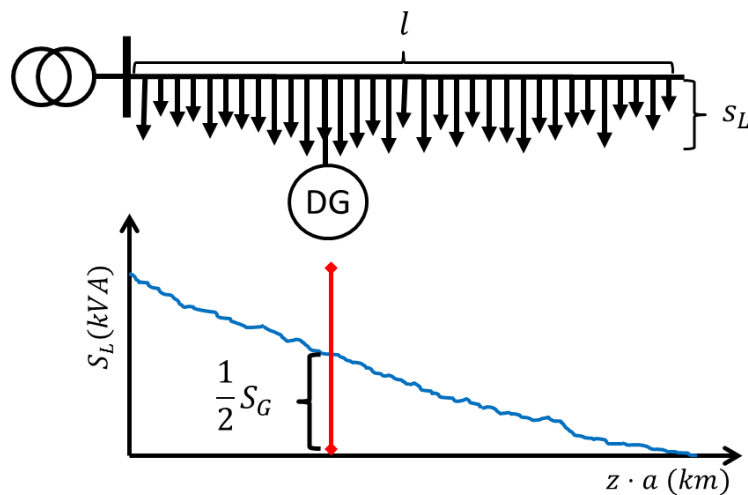


Figure 36. Optimal DG location that induces minimum power delivery loss.

Proposition L.1 and the other rules presented in the rest of this chapter are applicable to feeder configuration more general than shown in Figure 36. Since it is derived from feeder's power flow (as presented in Appendix B), when there are other devices on the feeder, for example capacitor banks, their effects can be modeled into load apparent power flow on the feeder (see Figure 13). For the feeder is of the multi-branch configuration (see Figure 12), the apparent power flow on the other

branches is determined by their loads and will not be affected by the apparent power flowing on the DG connected feeder. Therefore, the total power delivery loss is calculated in the same way as for the feeder is of the large-trunk configuration.

### ***When Subject to Voltage Constraint***

DG penetration is subject to voltage constraint. Proposition V.2 in Section 2.3.1 states that overvoltage occurs when a DG unit is installed too far away from the feeder's primary side. Therefore, when voltage rise appears as a concern, the new optimal DG location  $a_V^*$  is calculated as

Equation 31

$$a_V^* = \min\{a^*, a_{max}\}$$

where in bracket  $a^*$  is the optimal DG location calculated from the half capacity rule and  $a_{max}$  is the maximum DG penetration depth calculated from Equation 18. The new optimal location is the shallower of the two. Proof of Equation 31 is given in Appendix B.

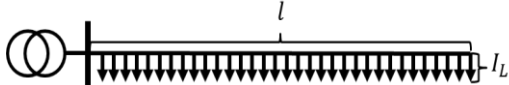
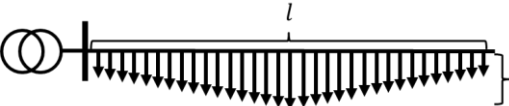
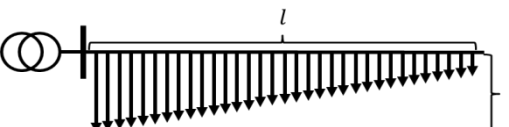
## **3.1.2 Examples and Implications**

### ***Numerical examples***

Optimal DG locations in previous studies are often proposed in two forms. One is an analytical expression for general cases; the other is rules of thumb for some specific types of load distribution. While the Half Capacity Rule and Equation 30 belongs to the first type, results in previous studies are in a much more complex form and formulated under Direct Current (DC) models, which requires load and DG measurements of current in Amperes that is usually not available [6, 120, 125-128]. Results proposed in the second type usually intend to be used as rule of thumb in practices. For example, Table 7 presents optimal DG locations when DG supplies all load on the feeder when the load is distributed uniformly, centrally and decreasingly.

The optimal DG locations shown in the last column of Table 7 verifies the Half Capacity Rule. Table 8 presents its simulation on a feeder of 20 nodes and with total load of 1000 kVA. The second row shows the total power delivery loss induced by placing DG at each node on the feeder. In each load distribution, the DG location that induces minimum loss is where the load apparent power flow equals to half of the DG thermally limited capacity, as shown in the third row. And this optimal location is the same as that calculated by Table 7.

Table 7. Optimal DG location for three typical load distributions.  
[125]

Cases (Assuming that DG supplies all the loads in each case)	$LSS_L$ (Power loss before adding DG)	$LSS$ (Power loss after adding DG)	Power loss reduction (%)	Optimal DG location
 <p>Uniformly distributed load</p>	$\frac{1}{3} I_L^2 r l^3$	$\frac{1}{12} I_L^2 r l^3$	75%	$\frac{l}{2}$
 <p>Centrally distributed load</p>	$\frac{23}{960} I_L^2 r l^5$	$\frac{1}{320} I_L^2 r l^5$	87%	$\frac{l}{2}$
 <p>Decreasingly distributed load</p>	$\frac{2}{15} I_L^2 r l^5$	$0.01555 I_L^2 r l^5$	88%	$\left(1 - \frac{\sqrt{2}}{2}\right) l$

Despite its ease of use, when a DG unit is placed according to this “rule of thumb,” the induced actual power delivery loss is not the minimum. This is because the practical load distribution is not as standard as the types defined. In addition, these rules are set based on the assumption of a DG penetration capacity, which needs to be adjusted for use and increases their implementation complexity.

As a comparison, the proposed Half Capacity Rule has the advantage of applicability to any load distribution and installed DG capacity. Table 9 verifies this advantage through the feeder system shown in Section 1.2.2 (see Figure 10 and Table 3). Power loss is simulated for the feeder system by varying DG locations under three DG penetration capacities. The minimum power loss is induced at the DG location exactly described by the Half Capacity Rule.

### ***Implications and Potential Applications***

The Half Capacity Rule provides a general guideline for utilities and policy makers to set standards and candidate sites for DG installment. Although Equation 30 mathematically presents the same

complexity as running repetitive power flow to examine feeder loss of connecting DG at each node on the feeder, it provides an intuition for system planners and policy makers, enabling them to envision the possible optimal location without going through complex calculation and running computer programs.

This result can also be useful to DG manufacturers and designers that intend to market their products to certain areas. Known the load distribution in the area and permissible DG connection sites, they can determine, by reversing the Half Capacity Rule, what DG sizes would be the local utilities' interest to minimize their power delivery loss and thus earn a greater profit.

Table 8 .Power loss varying with DG location on feeders of three load distributions.

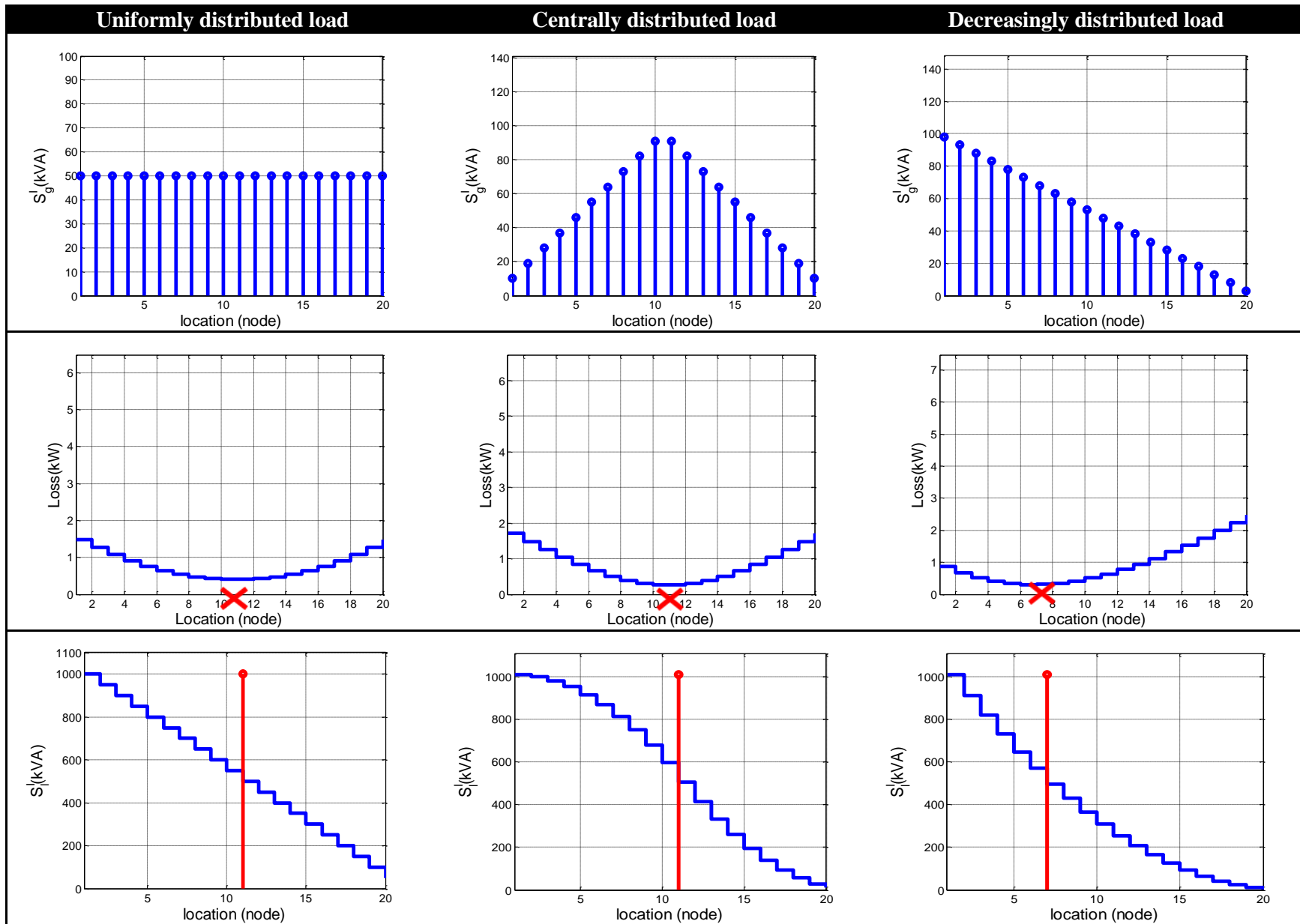
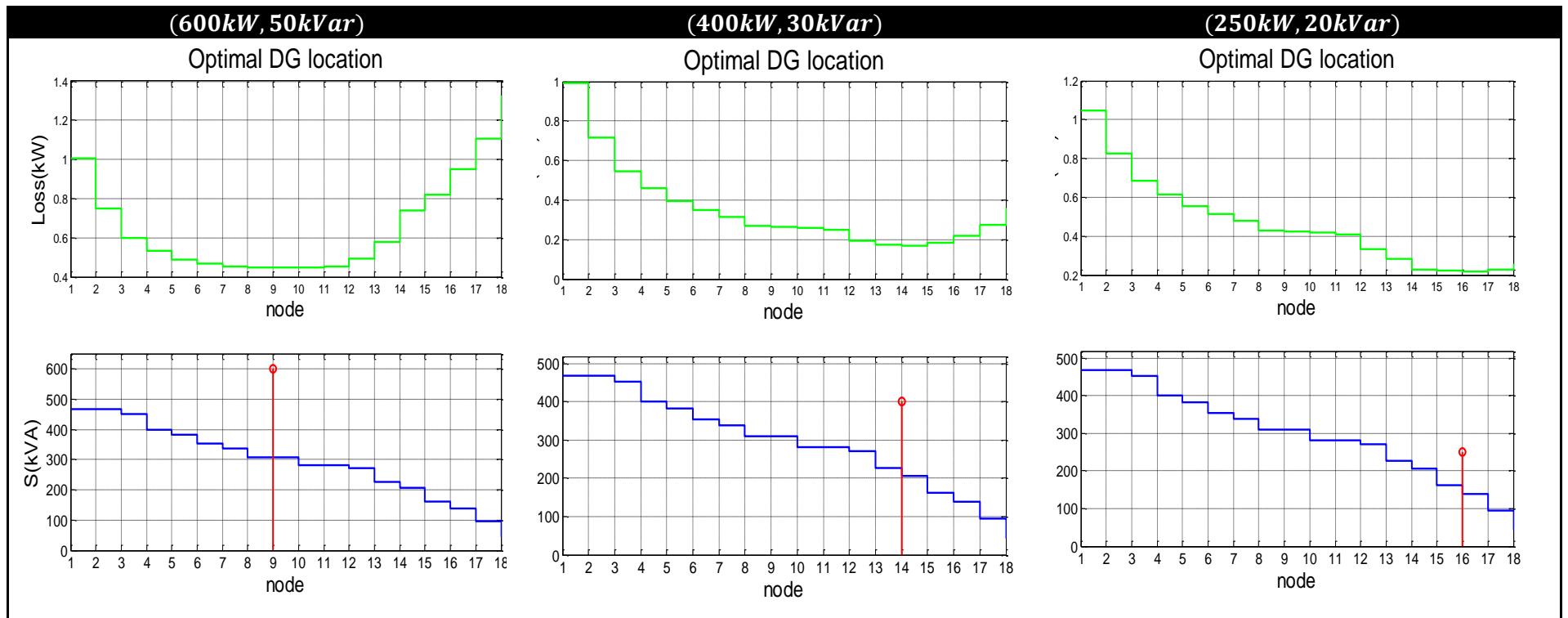


Table 9. Optimal DG location for three DG capacities penetrated on the feeder system in Figure 10.



## 3.2 Optimal DG Capacity

### 3.2.1 Equal Voltage Rule

In DG planning and operation, one case could be to decide DG capacity or output at a given site. This may happen when utilities are DG owners and want to size local generation at chosen site; or customers have DG ownership but utilities are responsible to set instructions guiding the customers' choices of DG units. More importantly, when DG units are dispatchable, utilities could be incentivized to get the right to control DG output through natural ownership or energy market. The rule of choosing DG capacity/output for minimum power delivery loss is summarized by the Equal Voltage Rule.

**Proposition L.2 (the Equal Voltage Rule)** A feeder's power delivery loss reach the minimum when the feeder's DG output voltage is the same as its primary voltage.

Proposition L.2 is illustrated by Figure 37 and proved in Appendix B. For a feeder with its load distribution known, the voltage drop purely caused by load at the given DG location can be measured as  $\Delta V_L(a_G)$ . The optimal DG output that induces minimum power delivery loss should cause the same amount of voltage rise, namely,  $\Delta V_G = \Delta V_L$ .

By the definition of voltage-effective power from Equation 8 to Equation 10, DG output/capacity is

Equation 32

$$S_G^V = \frac{\Delta V_L(a_G)}{Z(a_G)}$$

where  $Z(a_G)$  is the total impedance measured from the feeder's primary side to the DG location, and is calculated as

Equation 33

$$Z(a_G) = \int_0^{a_G} z(\zeta) d\zeta$$

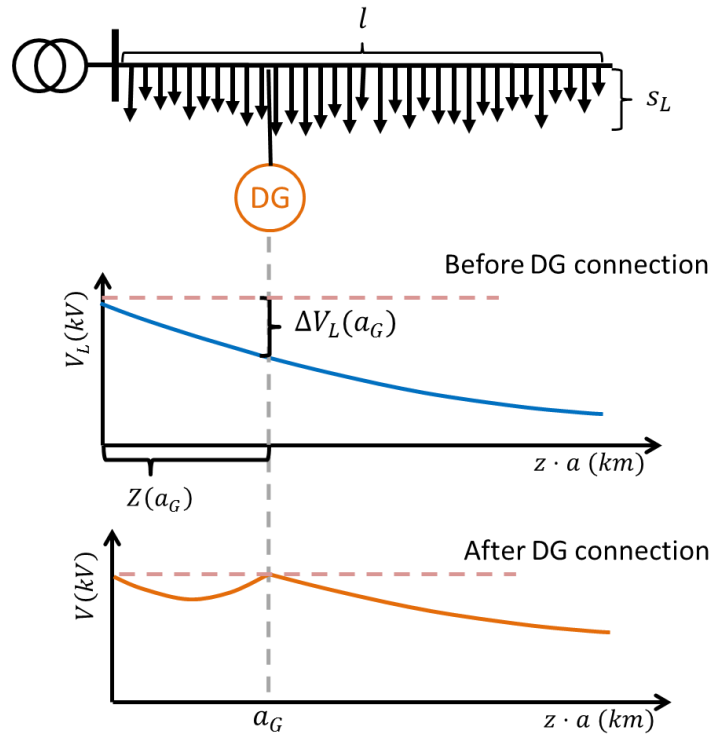


Figure 37. Equal Voltage Rule for choosing DG output/ capacity at a given location.

Compared to results presented in previous studies that contains multiple measurements and complicated calculations [5, 6, 120, 125-127], Equation 32 presents the optimal DG output/capacity in a concise form and reveals that:

- **The optimal DG output depends on both DG thermal rating and power factor** (see Equation 8 and Equation 9);
- **DG voltage is an indicator that could be directly used to determine its optimal output.**

Proposition L.2 and Equation 32 are generally applicable to feeder systems of any configuration and load distribution. It is worthy to notice that the computational complexity of Equation 32 is constant, one, which significantly reduces the computational time of the optimal DG output/capacity comparing to the existing approaches discussed in Section 1.1.5.



## 3.2.2 Examples and Implications

### *Numerical examples*

Table 10 verifies the Equal Voltage Rule on a 20-node feeder of 1000 kVA total load. The DG unit is placed at the middle of the feeder, Node 10. The first row shows three load distributions: uniform, central and decreasing. Power loss and DG output voltages are measured, through power flow program in DPlan, by varying the apparent voltage-effective power of the DG unit,  $S_G^V(a_G)$ , and are shown in the second and the third row. In the third row, a DG output in apparent voltage-effective power can be found that generates DG output voltage as the same value of the feeder's primary voltage, 10kV. In the second row, this apparent voltage-effective power induces the minimum power loss. The fourth row displays the feeder's voltage profiles when the DG unit is operated at the optimal values. It can be observed that **the optimal DG output that induces minimum power delivery loss supports the feeder's voltage at the same time**. This fact can be summarized by Corollary L.2

**Corollary L.2** For a DG unit installed at the chosen location of a feeder system, the following two statements are equivalent:

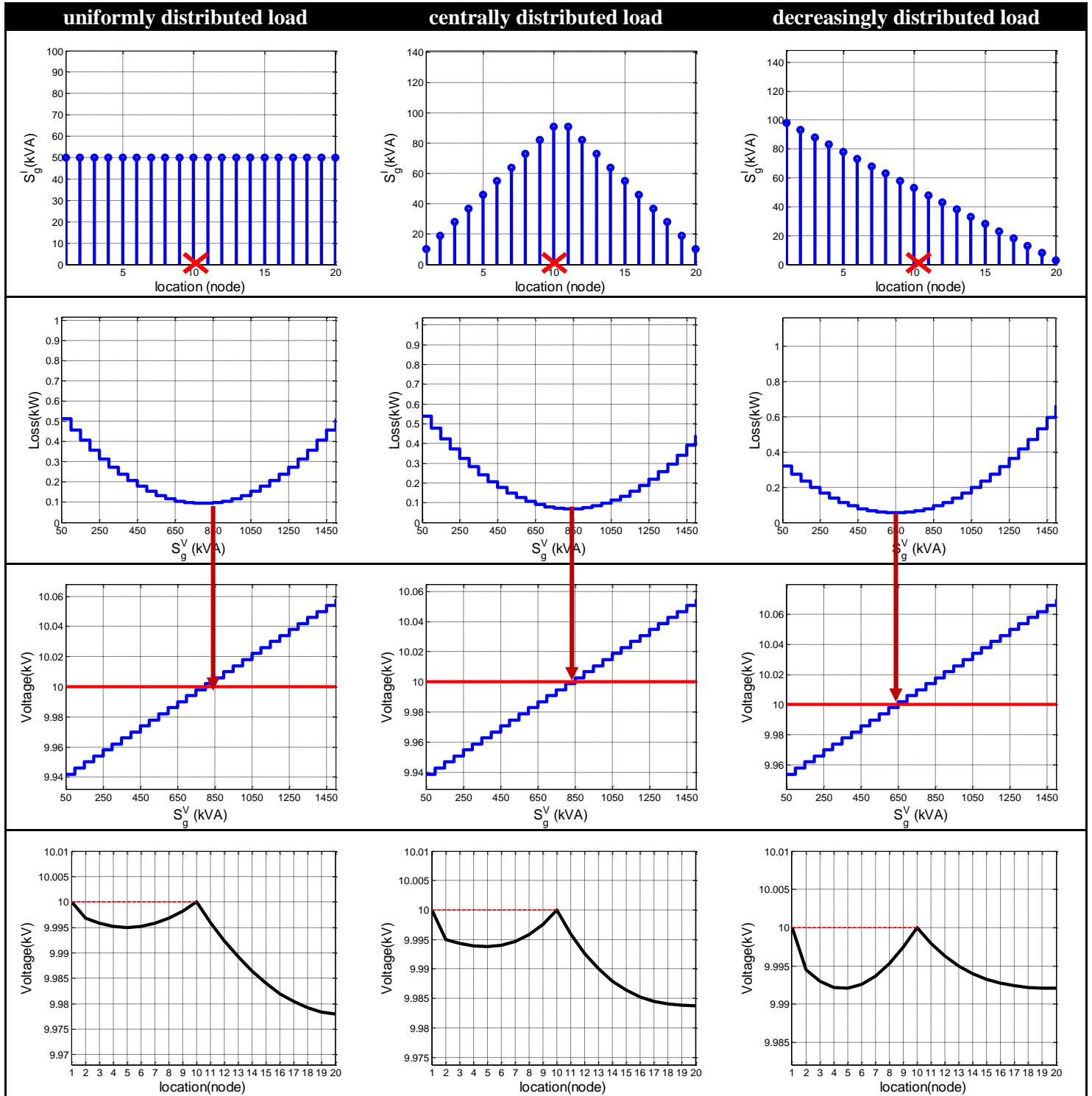
- the DG unit operates at an output minimizing the feeder's power loss
- the DG output voltage is measured the same as its feeder's primary voltage

### *Implications*

#### Simplifying the DG optimization problem

The Equal Voltage Rule states that for any DG unit that is sized in planning or operated in real time to minimize power delivery loss, its output voltage is the same as the feeder's primary voltage. According to Equation 16, the DG output voltage is the local maximum on the feeder's voltage profile. Therefore, when it equals to the feeder's primary voltage, the feeder system's voltages are all within the permissible range. By this fact, the original DG optimization formulation in the Logic and Structure Section (see Figure 1) can be further simplified by taking away the voltage constraint, which is automatically implied by the objective function of minimizing power delivery loss (illustrated by Figure 38).

Table 10. Power delivery loss and voltage profiles under varying DG capacity/output.  
The DG unit is connected at the middle of the feeder.



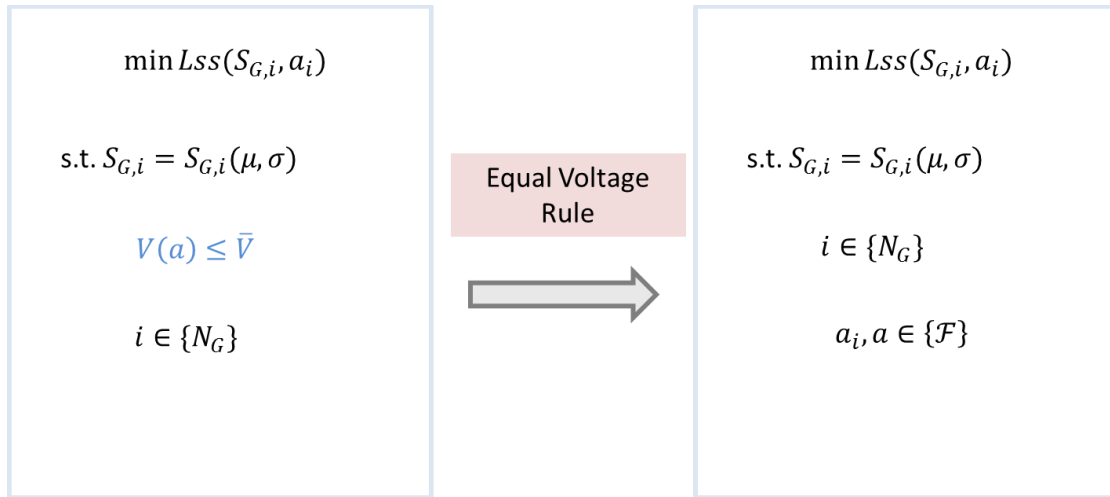


Figure 38. Voltage constraint can be implied by the Equal Voltage Rule in the DG optimization problem.

This figure illustrates the one step in the transformation Figure 1, where its symbols are declared.

For policy makers

One strong implication of the proposed results to policy makers is the need of revising the existing DG interconnection standards, represented by the IEEE Standard 1547.

In recognition of the potential adverse impacts of DG on distribution systems and the need for uniform criteria and requirements for the interconnection of DG, the industry collaborated with the Institute of Electrical and Electronics Engineers (IEEE) to create IEEE Standard 1547, first released in 2003 and later incorporated into the Energy Policy Act of 2005 [2, 14]. The standard’s primary intent is to ensure that DG units do not have negative impacts on other customers or equipment connected to the grid; it applies to the inter connection of all generation with aggregate capacity of 10 MVA or less to the distribution system.

IEEE Standard 1547 forbids DG units from actively regulating the voltage at their interconnection point; whereas the other standards and local government policies promote DG penetration by

emphasizing their potential benefits of reducing power delivery loss [13, 27, 74]. According to Corollary L.2, thus these two facts contradict each other, because DG output voltage is predetermined when it is operated and sized to reach the minimum loss. Therefore, unless IEEE Standard 1547 revises its voltage regulation limits, DG penetration will not be able to realize its full benefits.

#### For utilities and system operators

In the planning stage, the Equal Voltage Rule can assist utilities to choose DG units or set instruction for end-user DG installment. In addition, it implies the placement strategies for voltage control devices. Corollary L.2 states that optimal DG output power, power factor and voltage are interrelated. This fact can be utilized in Active Network Management (ANM) (which is introduced in Section 1.1.5) and simplifies the coordination of voltage control devices and DG units. Operating DG at the feeder's primary voltage can provide voltage support along the feeder and minimize power delivery loss at the same time. Voltage control devices can therefore be placed between the DG units and provide extra support and regulation. Much capital investment on voltage control devices can be saved in this sense.

One can also envision great applications of the proposed results in electricity market operation. So far DG is only studied as an energy supply resource in existing research [75, 139]. This is because most distribution systems penetrated with DG are connected to the main grid, which provides reliability and security services. The fine tuning of these distribution systems, such as voltage reliability and fault protection, are treated locally and decoupled from the reliability and other service market operations. However, the Equal Voltage Rule points out the possibility of DG provision of local voltage reliability service and therefore the formation of local reliability markets. Because utilities have the incentive to reduce the power delivery loss, as explained in the beginning of this chapter, they will provide voltage support service at the same time. Operating DG in this way automatically couples the energy market and reliability market by aligning their operation timelines.

One possible pricing structure for distribution energy market with DG is derived. By definition of voltage-effective power, Equation 32 can be written into its real power form as

Equation 34

$$P_G^V = \frac{\Delta V_L(a_G)}{R(a_G)}$$

where  $R(a_G)$  is the total resistance measured from the feeder's primary side to the DG location  $a_G$  and is calculated by

Equation 35

$$R(a_G) = \int_0^{a_G} r(\zeta) d\zeta$$

From Equation 34 and Equation 35, power loss reduced at the optimal DG output/capacity is

Equation 36

$$\Delta L_{SS}^* = \frac{\Delta V_L(a_G)^2}{R(a_G)}$$

Therefore, for DG units operating at other output, the cost can be calculated as the extra loss from the maximum loss reduction  $\Delta L_{SS}^*$ .

All of the above implications to policy makers and utilities are worthy to be explored in future work.

### 3.3 Penetration of Multiple DG Units

The Half Capacity Rule and Equal Voltage Rule are proposed in Section 3.1 and Section 3.2 for a single DG unit placement on a feeder system. They are applicable to general cases regardless of the DG unit's type, the feeder's configuration and load distribution. They are expressed in concise mathematical forms in Equation 30 and Equation 32. This section shows that these two rules can be extended to multiple-DG-unit placement with the same forms of their mathematical expressions.

#### 3.3.1 Superposition Rule

##### *For optimal DG locations*

One possible case of multiple DG units placement happens when penetrating DG under political requirements and economic incentives. As discussed in Section 1.1.4, local governments have been promoting DG penetration recently by providing various stipends and compensations. DG owners

and utilities receive these economic benefits often based on the DG penetration capacity or percentage under their ownership. Therefore, given a set of DG units with a predetermined total capacity, they have the flexibility of deciding locations of DG installment. Assuming  $N_G$  DG units of chosen capacities are to be installed on a feeder system, to achieve the minimum power delivery loss, the optimal location for the  $i$ th DG unit,  $a_i^*$ , should satisfy:

Equation 37

$$2\tilde{S}(a_i^*) = S_{G,i}$$

where  $\tilde{S}(a_i^*)$  is the apparent power flow on the feeder after the placement of the  $i$ th DG unit, and is measured as

Equation 38

$$\tilde{S}(a_i^*) = S_L(a_i^*) - \sum_{i+1}^{N_G} S_{G,n}$$

Note that the  $i$ th DG unit is counted by node distance from the primary side but not the placement order.

Equation 37 states that the Half Capacity Rule applies to the placement of multiple DG units as to that of a single DG unit. The apparent power flow on the feeder that measures half of the  $i$ th DG thermally limited capacity/output, however, is not the net load apparent power flow. **Instead, it is the resultant apparent power flow after the placement of all the DG units downstream to the  $i$ th unit**, expressed by the second term of Equation 38. This fact is summarized by the Superposition Rule for optimal DG placement and illustrated by Figure 39.

**Proposition L.3a (Superposition Rule for optimal DG placement)** To induce minimum power delivery loss on the feeder, each time a DG unit should be placed at the location where the apparent power flow resultant from its downstream DG placement measures the half of its thermally limited capacity.

According to Proposition L.3a, the first placed the DG unit is the one that is farthest from the feeder's primary side and is counted as the  $N_G$  th unit by distance. The Half Capacity Rule for a single DG unit applies to its placement.

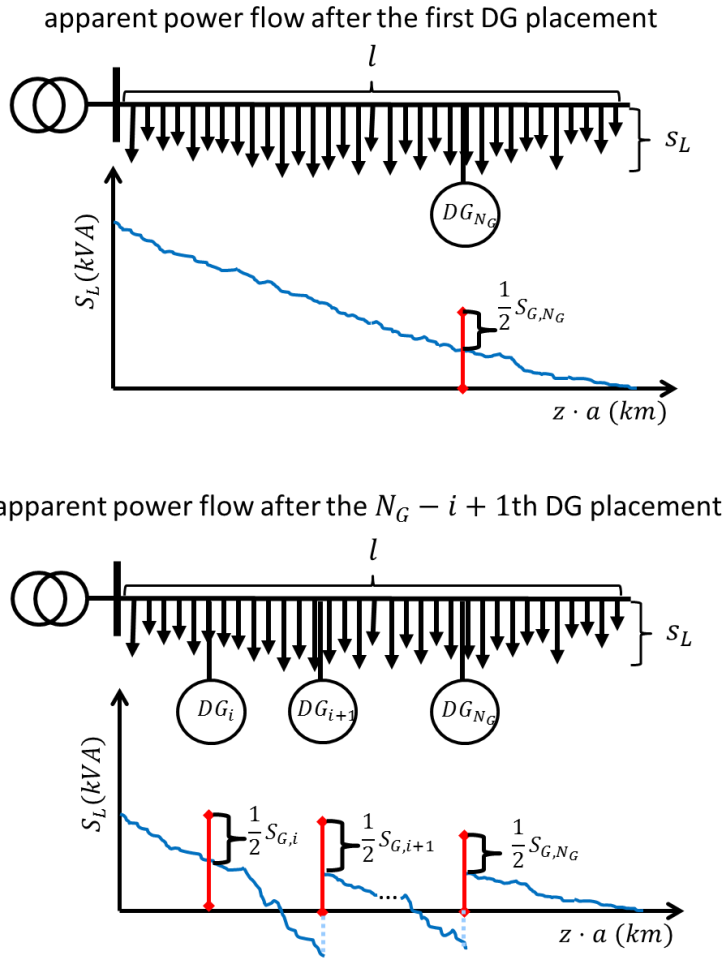


Figure 39. Optimal locations for placing multiple DG units on a feeder system.

The DG units are known for their thermal ratings/output. The placement follows the Half Capacity Rule and the Superposition Rule, starting from the DG unit farthest from the feeder's primary side.

*For optimal DG output/capacities*

A feeder may have a few sites that is planned to install DG units. In the planning stage, utilities may be incentivized to determine what capacities of DG units to be installed so that minimum power delivery loss are induced; whereas the same objective will be retained in the operation stage, in particular under a market mechanism, how much DG output is optimal if the DG units are dispatchable. Assuming the DG locations are known and the  $i$ th DG location is  $a_i$ , then the optimal DG output is determined by

Equation 39

$$S_{G,i}^V = \frac{\Delta\tilde{V}(a_i)}{Z(a_i)}$$

where  $\Delta\tilde{V}(a_i)$  is the feeder's voltage profile with the  $i$ th DG import no power and measures as

Equation 40

$$\Delta\tilde{V}(a_i) = \Delta V_L(a_i) - \sum_{n \neq i}^{N_G} \Delta V_G(a_i)$$

The above two equations can be stated by Proposition L.3b.

**Proposition L.3b (Superposition Rule for optimal DG sizing)** The power delivery loss on a feeder is minimized if and only if the output voltage of every DG unit measures the same as the feeder's primary voltage.

Notice that the optimal sizing and placement of multiple DG units are distinct by their superposition rules. In optimal DG placement, the apparent power flow is superposed only at downstream of the DG unit to be placed, as calculated by the second term in Equation 37; whereas in optimal DG sizing, the voltage profile, and hence apparent voltage-effective power  $S^V$  on the feeder, is superposed at the both upstream and downstream of the DG unit concerned, which is expressed by the second term of Equation 40. In other words, **when operating at the optimal output that minimizes the power delivery loss on the feeder, the DG voltage measures the same as the feeder's primary voltage before and after any other units start to import power; the voltage profile is supported along the feeder at the same time.** Figure 40 illustrates Proposition L.3b.



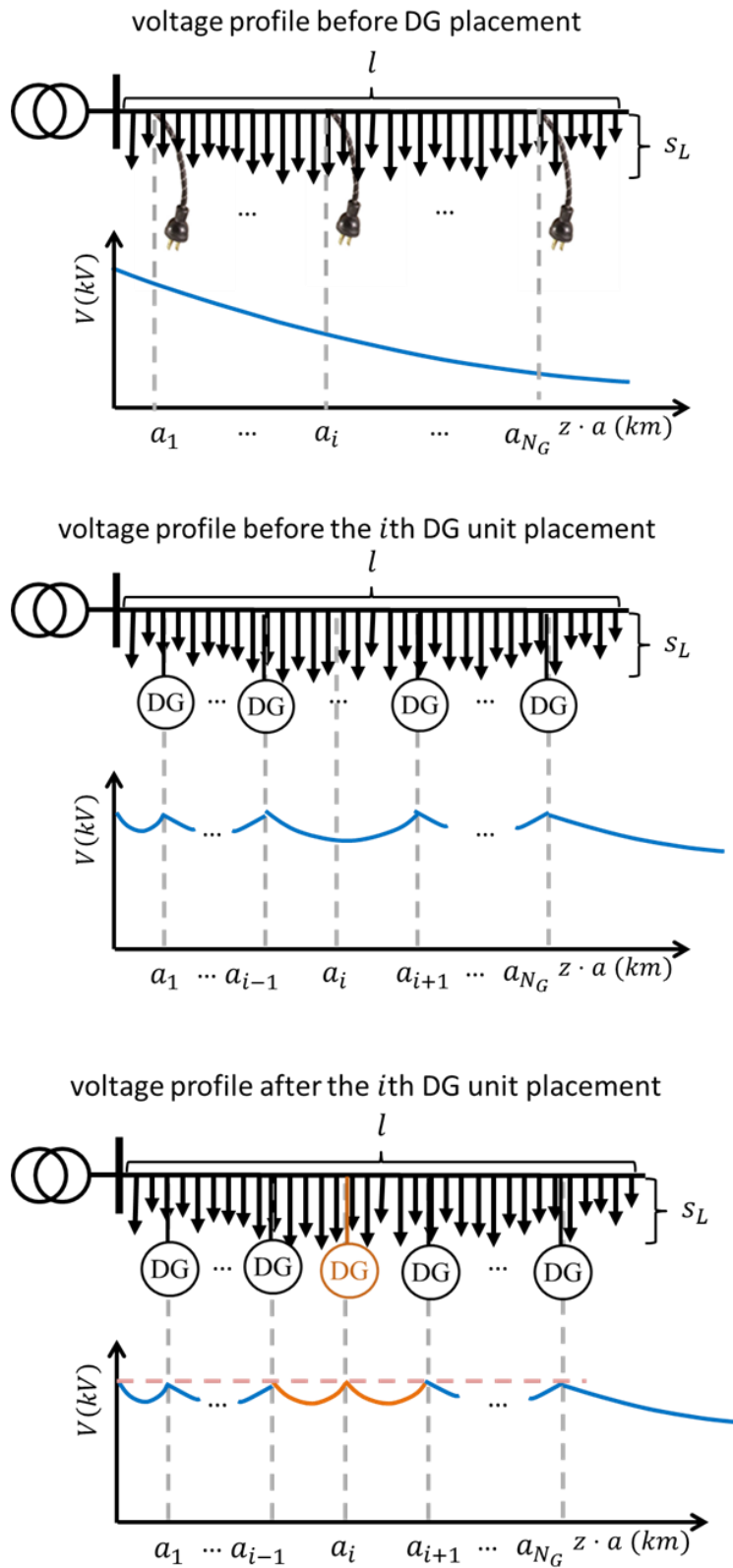


Figure 40. Optimal capacity/output of multiple-DG-unit sizing on a feeder system. The DG units are installed at given locations. The sizing follows the Equal Voltage Rule and the Superposition Rule.

### 3.3.2 Numerical Examples and Computational Complexity

#### *The Superposition Rule for optimal DG placement*

##### Computational complexity

A straightforward algorithm for Proposition L.3a is dynamic programming. According to Equation 37 and Equation 38, calculating the optimal location of the  $N_G$  th DG unit, with the load apparent power flow on the feeder, in the first step will generate the apparent power flow to calculate the optimal location of the  $N_G - 1$  th unit. This process can be carried on until the first DG unit, which located the nearest to the feeder's primary side. Given a set of chosen DG units, the order of these units based on their distance away from the feeder's primary side is also part of the placement. Therefore, the optimal placement contains two steps:

##### **Optimal placement of multiple DG units**

1. Deciding the order of the DG units. If there are  $N_G$  unit, the unit that is to be placed the nearest to the feeder's primary side is numbered as 1; and the one that is farthest from the feeder's primary side is numbered as  $N_G$ ;
2. Deciding the optimal DG locations for a chosen order of DG units.

With the Superposition Rule and the Half Capacity Rule, optimal DG locations can be obtained with much less computational efforts. Consider if there are  $N_G$  units to be placed onto a feeder of  $x$  candidate sites. The  $N_G$  units are consist of  $m$  DG sizes, and each size has  $N_m$  units. That is

Equation 41

$$N_G = \sum_m N_m$$

The computational complexity of the proposed process can be calculated as:

Equation 42

$$f_1 = \frac{N_G!}{\prod_m (N_m)!} + N_G$$

where the first and the second term calculates the computational complexity of the first and second step of the proposed process. As a comparison, the computational complexity of repetitive power flow, which is conventionally used in optimal DG placement and introduced in Section 1.1.5, is

Equation 43

$$f_2 = N_G^x$$

Table 11 compares the complexity of the two approaches for different DG groups and feeder length (or the numbers of available DG installment sites). It is observed that the computational time increases significantly with the growth of the feeder's length (the column of  $f_2$ ); whereas the computational time of the proposed approach is independent of the feeder's length and only a function of the DG unit groups. In practice, the length of a primary feeder, in terms of its nodes connecting to the next voltage level, ranges from tens to hundreds. This property of the proposed DG placement process presents great advantage over the conventional approach.

Table 11. Computational complexity comparison of the proposed DG placement process and repetitive power flow.

#	$N_G$	$N_1$	$N_2$	$x$	$f_1$	$f_2$
1	5	2	3	20	15	$9.50 \times 10^{13}$
2	5	2	3	40	15	$9.09 \times 10^{27}$
3	5	2	3	60	15	$8.67 \times 10^{41}$
4	10	5	5	20	262	$10^{20}$
5	10	5	5	40	262	$10^{40}$
6	10	5	5	60	262	$10^{60}$

#### A numerical example

The proposed process of optimal DG placement is verified through the test system shown in Section 1.2.2 (See Figure 10 and Table 3). Parameter of the DG units to be placed are included in Table 12.

Table 12. Parameters of DG units by their capacity and number per group.

$N_G$	$N_1$	$N_2$	$P_1, Q_1(kW, kVar)$	$P_2, Q_2(kW, kVar)$
4	2	2	(100,10)	(130,15)

Four DG units of two capacity/output are to be placed on the test system (Feeder 1). In the first step, all the possible sequences, in terms of their distance to the feeder's primary side, are determined. Figure 41 shows the sequences and their minimum power delivery loss (which mathematical expression shown in Appendix B). From the sequences that do not cause overvoltages, the one that induces the minimum power delivery loss is adopted, which in this case is the Sequence 4, with the numbering of DG units shown on the left of Figure 41.

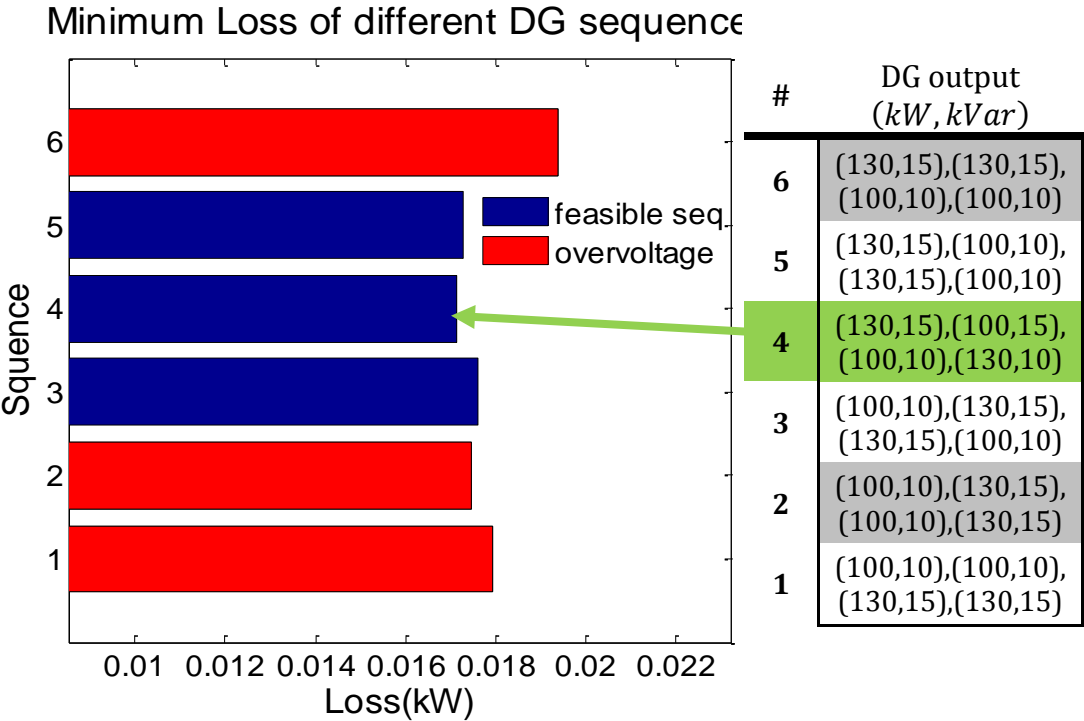


Figure 41. Possible sequences of DG placement on the test system in Figure 10 and DG groups in Table 12.

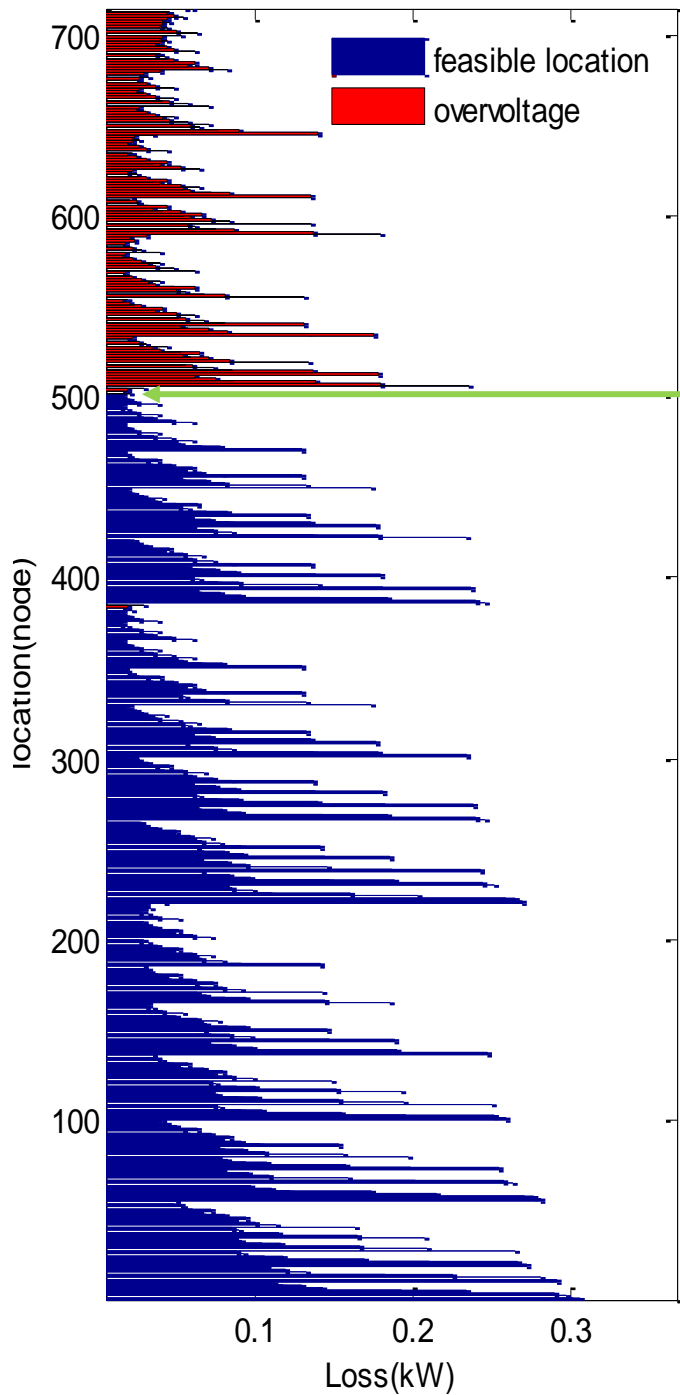
(Left) Possible DG sequences and their induced minimum loss. (Right) The DG placement of each sequence.

The next step is to apply the Superposition Rule and the Half Capacity Rule to find out the optimal locations for the selected sequence.

Figure 42 shows power loss on the feeder of all possible DG placements for Sequence 4 by running repetitive power flow. Over seven hundred cases are examined. The optimal placement is then found as the 501th row in the table on left, with the minimum power loss of  $17W$ . Several conditions are set in the program, including (1) more than one DG unit cannot be placed at the same node; (2) the DG units cannot be placed nearer than Node 2 nor farther than Node 17, which is the second last node; and (3) at least the space of two nodes is needed for the placement of next DG unit. These conditions further reduce the computational size of the repetitive power flow approach, as shown in Equation 2.

Using the proposed process of optimal DG placement, however, only takes four iterations to complete according to Equation 42. The same optimal placement is found with the application imposition of the identical conditions set in the repetitive power flow. This process is demonstrated and verified by Figure 43. It can be observed that, from the bottom figure, every time a DG unit is placed at where its half thermally limited capacity equals the load apparent power flow superposed by all its downstream DG units. The Half Capacity Rule and Superposition Rule are verified by this fact.

Loss of different DG location at sequence 4



#	DG location(Node)				Loss(kw)
701	9	11	13	15	0.064
681	8	10	12	14	0.083
661	7	10	12	14	0.071
641	6	11	15	17	0.023
621	6	9	13	16	0.032
601	6	8	12	14	0.066
581	5	11	13	16	0.028
561	5	9	12	15	0.050
541	5	8	11	14	0.081
521	5	7	11	15	0.072
501	4	11	15	17	0.017
481	4	9	13	16	0.026
461	4	8	12	14	0.061
441	4	7	12	15	0.051
421	4	6	15	17	0.024
401	4	6	10	12	0.180
381	3	11	15	17	0.017
361	3	9	13	16	0.027
341	3	8	12	14	0.061
321	3	7	12	15	0.052
301	3	6	15	17	0.024
281	3	6	10	12	0.180
261	3	5	13	16	0.039
241	3	5	9	14	0.095
221	3	5	7	9	0.269
201	2	10	12	14	0.073
181	2	8	13	16	0.040
161	2	7	13	17	0.038
141	2	7	9	15	0.086
121	2	6	10	17	0.071
101	2	6	8	10	0.258
81	2	5	10	13	0.156
61	2	5	7	14	0.123
41	2	4	11	13	0.163
21	2	4	8	11	0.266
1	2	4	6	8	0.305

Figure 42. DG placement and induced power loss on the test system in Figure 10 with the DG groups in Table 12.

(Left) All possible DG placements and their induced power delivery loss. (Right) DG locations of each placement and their induced loss.

### Superposition Property of Multiple DG Placement

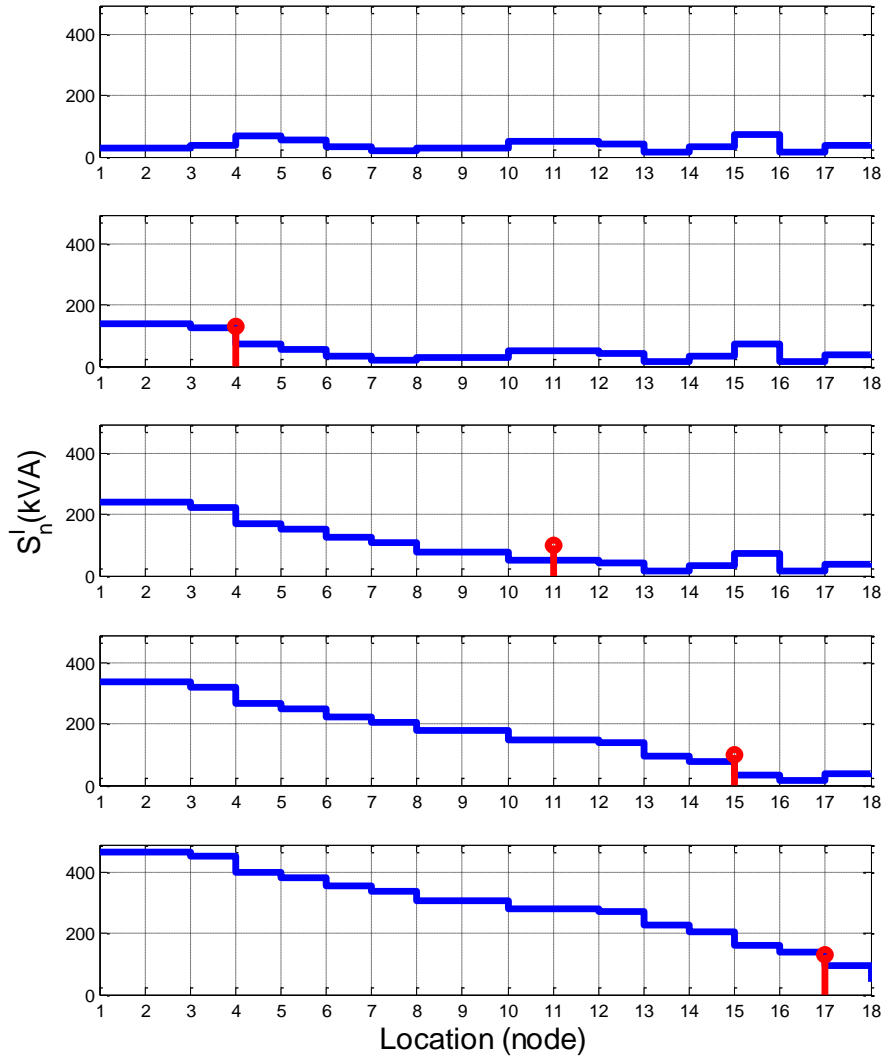


Figure 43. Apparent power flow on the feeder system in Figure 10 after the placement of every DG unit at their optimal locations.

The placement starts with the last unit (bottom) to the first unit (second).

### *The Superposition Rule for optimal DG sizing*

#### Computational complexity

The Superposition Rule for optimal DG capacities are carried out by solving Equation 39. Given the DG locations, which are numbered by their distance from the feeder's primary side, the optimal DG capacities should satisfy:

Equation 44

$$Z(a_i) \cdot \sum_{n \leq i} S_{G,n}^V + \sum_{n > i} (S_{G,n}^V \cdot Z(a_n)) = \Delta V_L(a_i)$$

where  $\Delta V(a_i)$  is the voltage drop caused by load measured at the  $i$ th location. The first term on left represents the voltage rise induced by the  $i$ th DG unit and the ones at its upstream. The second term on left represent that induced by the ones at its downstream. For  $N_G$  units, there are  $N_G$  equations in the above form, which can be solved in one iteration through a matrix function in Equation 45.

Equation 45

$$\underline{S_G^V} \cdot \underline{Z(a)} = \underline{\Delta V_L(a)}$$

where  $S_G^V$  is the vector of DG capacities in apparent voltage-effective power;  $\Delta V(a)$  is the vector voltage drop caused by load measured at the DG locations; and  $Z(a)$  is the resistance matrix measured at the DG locations, which dimension is  $N_G$  by  $N_G$ . Therefore, the computational complexity of the proposed method for optimal DG capacities/output is:

Equation 46

$$f_1 = 1$$

Equation 46 shows that the proposed method has a constant computational complexity, which does not vary with the DG groups, numbers or the feeder's length. These factors do affect the computational space of the method. As the number of DG units becomes greater, the resistance matrix has a squared growth of size. However, this should not become an issue because of the linear form of Equation 45.



As a comparison, using repetitive power flow to determine optimal DG sizes, as discussed in Section 1.1.5, causes a significantly greater time. For  $N_G$  units with  $m$  choices of capacities, the complexity is calculated by Equation 47.

Equation 47

$$f_2 = (N_G)^m$$

It shows that the computational complexity is exponential of the DG capacities. In operation, when the utilities need to decide the DG output, which has continuous ranges of values, this computational time becomes even more significant. Table 13 demonstrates this fact by comparing the computational iterations of using the proposed method and repetitive power flow in sizing different DG groups.

Table 13. Computational complexity comparison between the proposed DG sizing method and repetitive power flow.

#	1	2	3	4	5	6
$N_G$	5	5	5	10	10	10
$m$	3	5	10	3	5	10
$f_1$	1	1	1	1	1	1
$f_2$	125	3125	$9.77 \times 10^6$	$10^3$	$10^5$	$10^{10}$

Variables in the first column follow the notation in Equation 47.

#### A numerical example

The proposed method of optimal DG sizing is verified on the test system in Figure 10. Three sites that are to be connected with DG distributes evenly on Feeder 1, at Node 5, Node 9 and Node 13. The DG capacity is set to be within the range from 30 kVA to 310 kVA and of an incremental step of 10 kVA. Namely, the DG capacities are chosen from 30 kVA, 40 kVA, 50 kVA... and 310 kVA.

Using repetitive power flow, the power delivery loss for all possible DG capacity combinations are found in Figure 44. The optimal DG capacities that induce minimum power loss are obtained in the left table. Figure 45 shows the optimal DG capacities obtained through the proposed DG sizing method. These DG capacities are in apparent voltage-effective power, which equal to DG thermally limited capacities when the DG units operate at the feeder's impedance angle. The optimal DG capacities/output obtained from the two approaches are the same. Their computational time, nevertheless, differs over 25,000 times.

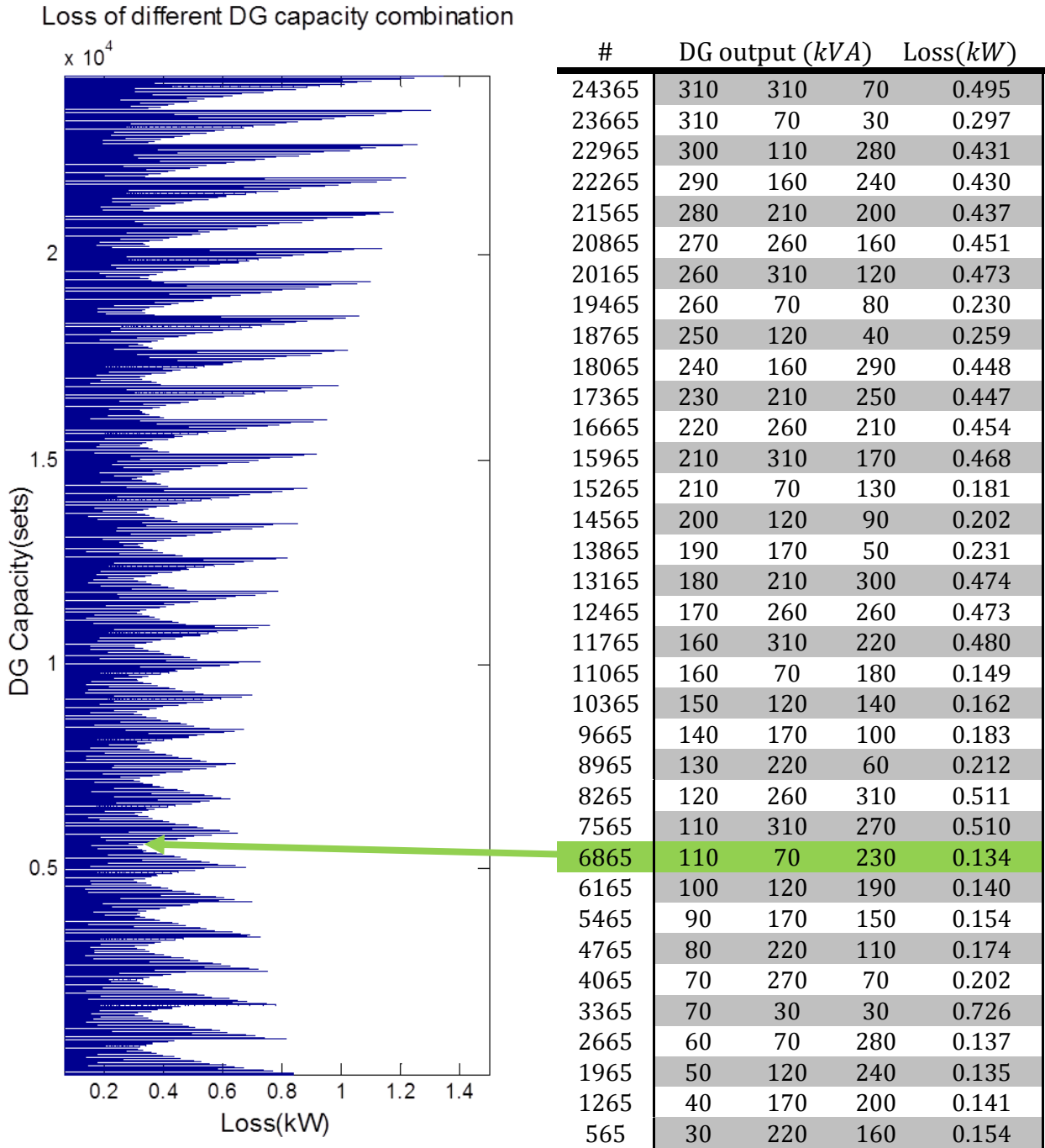


Figure 44. Optimal DG capacities and their induced power deliver loss.

The results are tested on the system in Figure 10 with three DG units to be connected at Node 5, Node 9 and Node 13. (Left) Combinations of DG capacities and their induced power loss; (Right) DG thermally limited capacities/output of each combination, assuming all the three units operate at feeder's impedance angle, and their induced power loss.

Moreover, the Equal Voltage Rule is verified in Figure 45. With the DG units operate at their optimal capacities, the resultant voltage profile is raised back to the feeder's primary voltage at every DG location. **For this reason, there is no need to examine overvoltage when determining the optimal DG capacities.**

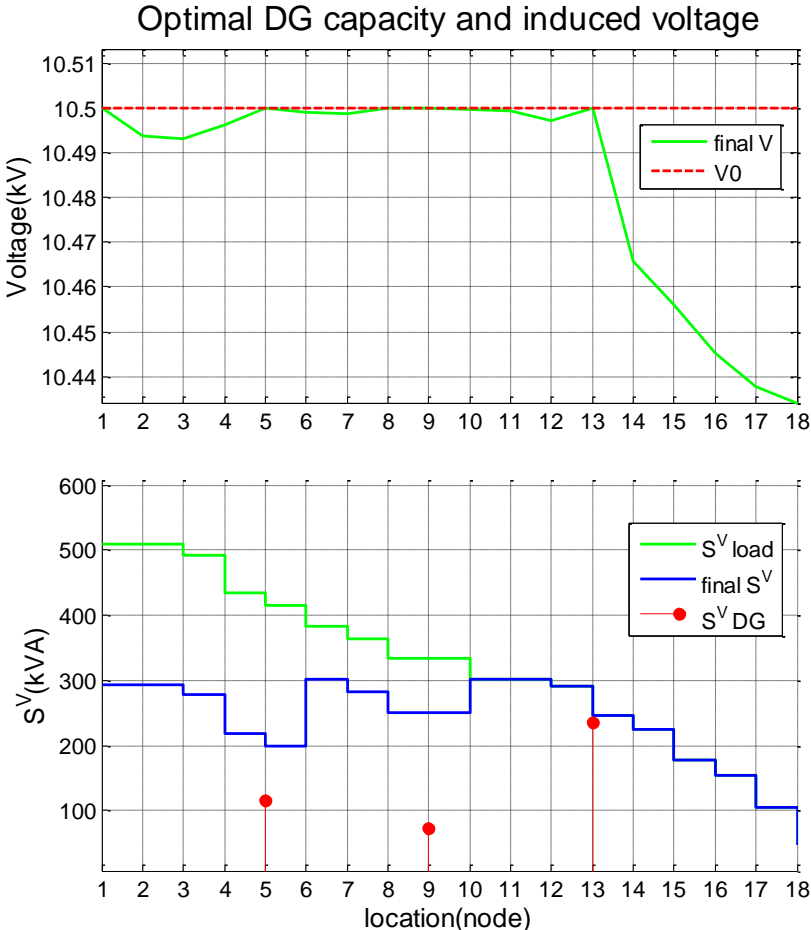


Figure 45. Optimal DG capacities/output and their induced voltage profile.

(Top) the voltage profile when the DG units import no power to the feeder and when they operate at the optimal output; (Bottom) the apparent voltage-effective power flow on the feeder of load and of load superposed with optimal DG output.

## Conclusion

The Superposition Rule for optimal DG capacities and locations makes the Half Capacity Rule and the Equal Voltage Rule applicable to multiple-DG-unit placement. This enables the system planners and operators to visualize, in even more complicated situations, the influence of DG penetration on power delivery loss. **It is worthy to notice that the Superposition Rule works on all the DG units in voltage but only on the units downstream in current.** Equation 38 and Equation 40 explain this statement. In optimal DG placement, the Half Capacity rule is implemented by examining the apparent power flow, which is in pair of current physically. According to Proposition L.3a, DG units are placed from the end until the primary side of the feeder, which updates apparent power flow only at the downstream every time a unit is placed. Conversely, the Equal Voltage Rule is implemented on the voltage profile throughout the feeder. By Equation 45, all DG output/capacities are computed at the same time. Stopping any DG units will still retain the voltage of the other DG units at the feeder's primary voltage.

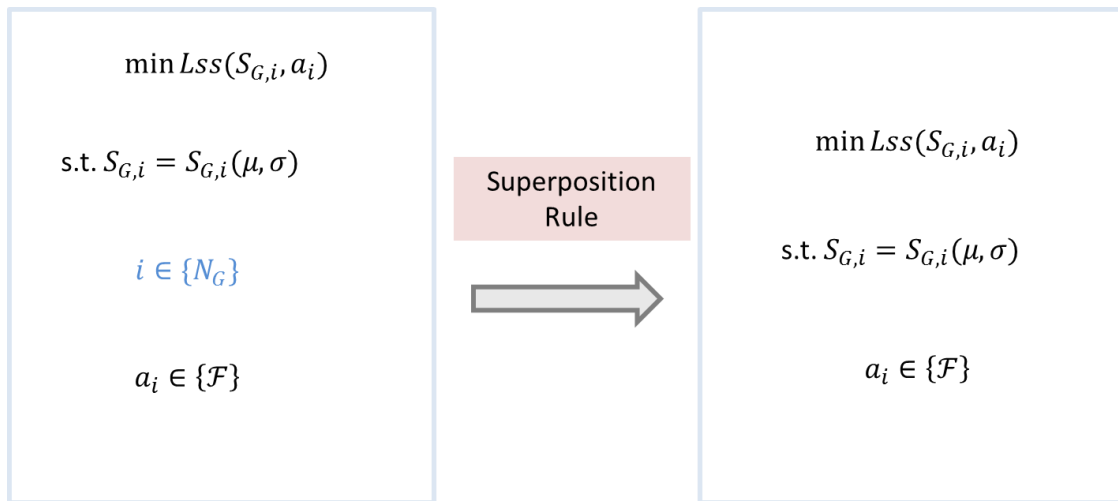


Figure 46. Optimal DG placement and sizing of multiple DG units is simplified into the same problem of a single DG unit under the Superposition Rule.

This figure illustrates the one step in the transformation Figure 1, where its symbols are declared.

Computational complexity is greatly reduced by the Superposition Rule. Comparing to repetitive power flow [72, 79-81], which is conventionally adopted in DG sizing and placement, the computational complexity of the proposed methods stay constant, regardless of the feeder's length, DG operation range and group size. This fact can be utilized to further simplify the optimization problem posed in the Logic and Structure Section (see Figure 1): the optimization problem of multiple DG units can be reduced to that of a single DG unit (see Figure 46).

## **3.4 Optimal Location of Variable Energy Resources (VERs)**

### **3.4.1 DG Variance Rule**

In the previous sections, a set of rules is proposed for DG placement and sizing in static situations, which means the load and DG output remain constant. In practice, the static assumption is hardly ever true. On one hand, electricity demand in a service area is growing over years, while the load profile changes on a daily and seasonal basis. On the other hand, DG is usually penetrated in the form of Variable Energy Resources (VERs)<sup>7</sup>, such as wind and solar energy, which output is not dispatchable and only predictable in a limited timescale and accuracy. These dynamic situations could make rules that are proposed for static situations no longer lead to the optimality.

Conventionally in DG placement, the variance of load and VER output are treated in several different ways: worst case, average case and statistical method. The worst case method locates VERs by minimizing the maximum possible power delivery loss, which is usually considered to happen under several combinations load and VER output, including [124, 175]

- maximum load and minimum VER output
- maximum load and maximum VER output
- minimum load and minimum VER output
- minimum load and maximum VER output

This method assumes the maximum power delivery loss dominate the total power loss in the long term. Hence DG location optimized under these worst cases induces minimum total power loss. However, in most cases, due to the immediate nature of VERs, their output only reaches a certain

---

<sup>7</sup> The DG penetration is considered in the form of VER in this Section. Therefore, DG and VER are used interchangeably.

value for a very short time. The power loss induced under these situations are not representative enough to be used in DG placement for the overall power loss minimization in the long term.

Alternatively, the average case method is adopted that averages the load and VER output over a planning time period, for example ten to twenty years. Although taking into account of all possible load and VER output, this method treats all their occurring possibility as the same. The optimal DG locations obtained with this method could induce great loss in some worst cases, as discussed above, despite of their short occurrence [123, 128, 176].

Statistical methods do not have the problems of the worst case and average case method. One typical form of this method is probabilistic power flow [177, 178]. For every DG placement, it simulates all possible load and VER output by their occurring frequency. Therefore, power loss induced under different situations is completely studied with their intensity and lasting time period. One and predominate deficiency of this method is its computational time. As shown in Section 3.3.2 and by Equation 41, the repetitive power flow could take a long time even in the statistic situation, not to mention when the situations are multiplied by dynamic load and VER output.

Because of the deficiencies of all these three methods, another method is used in some previous studies that minimize the expectation of the power delivery loss [98, 179, 180]. By its definition, expected value of power loss models the complete occurrence and its frequency of a load set. However, when applying it in DG placement, previous studies find it hard to be combined concisely into the model of VER output, which usually turn the method takes almost the same effort as the statistical method thus loses its advantage.

### ***Optimal DG placement under dynamic situation***

This thesis proposes the optimal DG location to be determined through Equation 48 that minimizes expected power delivery loss with varying load and VER output.

Equation 48

$$2\mathbf{E}[S_L(a^*)] = \mathbf{E}[S_G] + \widetilde{\mathbf{Var}}(S_G)$$

where  $E[S_L(a^*)]$  is the expected value of apparent load flow on the feeder;  $E[S_G]$  is the expected output of the DG unit to be placed; and  $\widetilde{\mathbf{Var}}(S_G)$  is the normalized VER variance, which is

Equation 49

$$\widetilde{\text{Var}}(S_G) = \frac{\text{Var}(S_G)}{\mathbf{E}[S_G]}$$

Notice that the normalized VER variance has the dimension of DG expected apparent power, that is,  $kVA$ . This unifies the unit system on the both sides of Equation 48.

Equation 47 and Equation 48 are general applicable to any type of probability distribution of load and VER output. They are proved in Appendix B. Their physical meaning is stated by the Modified Half Capacity Rule.

**Proposition L.4 (Modified Half Capacity Rule)** For minimum power loss over a time period, the DG unit should be placed at the location where half of the expected value plus normalized variance of its apparent power output measures the same as the expected apparent load flow on the feeder over the time period.

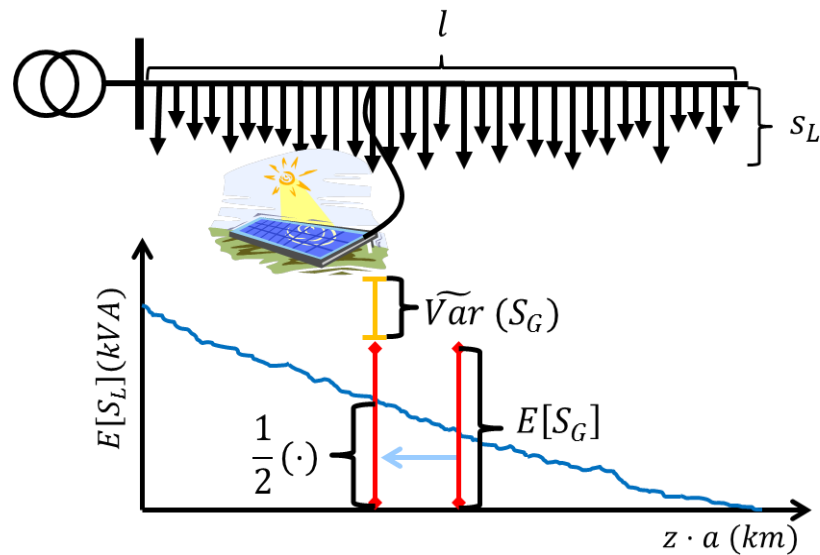


Figure 47. The Modified Half Capacity Rule for optimal Variable Energy Resources (VERs).

The optimal VER location is where the expected apparent power flow of load measures the half of the expected output plus the normalized variance of the VER.

Furthermore, two corollaries about DG variance's influences on the optimal DG locations can be derived from Proposition L.4. The proposed rules are illustrated by Figure 47.

**DG Variance Rule**

**Corollary L.4a** The greater its VER variance, the near a DG unit should be placed to the feeder's primary side.

**Corollary L.4b** Load flow variance does not affect the optimal DG location.

One condition for Equation 47, Equation 48 and the proposed rules to work is the VER output is independent of its location. This condition is well justified by the geographic and time scale of the DG placement problem. On one hand, VER output may be a function of its location when the geographic scale is wide enough. For example, output of solar panels is expected to be higher if located in Arizona than in Ohio. On the other hand, this output difference is exacerbated within a short timeframe. The output of two nearby solar panels may become different because of a cloudy passing by shadowing on one of them. For the problem posed in this thesis, however, the DG placement is scaled on the basis of feeder systems, as discussed in Section 1.1.5. The geographical condition along a feeder system does not vary much over the long term. Hence, VER variance is independent of its location.

***When subject to voltage constraint***

The chosen optimal DG location should guarantee that its induced voltage profile is within the permissible voltage range. Section 3.1.1 applies Proposition V.2 to modify the obtained optimal DG location in the static situation (see Equation 31). In the dynamic situation, the voltage constraint should be considered in the worst case so that overvoltage will not happen even by small probability. Based on Proposition V.1, the case that is likely to cause the worst rise at DG locations happens at minimum load and maximum VER output. Therefore, according to Equation 18, the maximum DG penetration depth is

Equation 50

$$a \leq \frac{\int_0^a P_{L,min}^V(\zeta) d\zeta}{P_{G,max}^V}$$



This value is compared with the optimal DG location obtained from Equation 48, and the actual DG location is decided by Equation 31.

### ***Optimal placement of multiple VERs***

The DG Variance Rule and Modified Half Capacity Rule can be extended to the case of multiple VER placement. For  $N_G$  units, the optimal placement of the  $i$ th unit, counted from the feeder's primary side, should satisfy Equation 51, which is obtained by applying the Superposition Rule on Equation 47 and Equation 48. The proof is shown in Appendix B.

Equation 51

$$2E[\tilde{S}(a_i^*)] = E[S_{G,i}] + \widetilde{\text{Var}}(S_{G,i})$$

where  $\tilde{S}(a_i)$  is the apparent load power flow superposed by VER units at the  $i$ th unit's downstream, and is calculated as

Equation 52

$$E[\tilde{S}(a_i^*)] = E[S(a_i^*)] - \sum_{i+1}^{N_G} E[S_{G,n}]$$

These optimal locations should be recalibrated by the voltage constraint. The actual DG location is

Equation 53

$$a_i^* = \min\{a_i^*, a_{max,i}\}$$

where  $a_{max,i}$  is the maximum penetration depth of the  $i$ th unit calculated in the worst case, when load reaches minimum and VER output reaches maximum. It is calculated as

Equation 54

$$a_i \leq \frac{\int_0^{a_i} P_{L,min}^V(\zeta) d\zeta - \sum_{n \leq i} P_{G,n} \cdot a_n}{\sum_{n > i}^{N_G} P_{G,n,max}^V}$$

The above equation can be carried out with the process proposed in Section 3.3.1 and by only changing the static values of load and DG output into their expected value and normalized variance.

It is worthy to notice that the DG Variance Rule is only proposed for optimal VER placement but not for VER sizing. This is because the dynamic characteristic of VER indicates its output is not dispatchable. When to size a VER unit, its output then is treated as a static value and therefore can be found with the process proposed for DG units of constant or dispatchable output.

### **3.4.2 Examples and Implications**

#### *A numerical example*

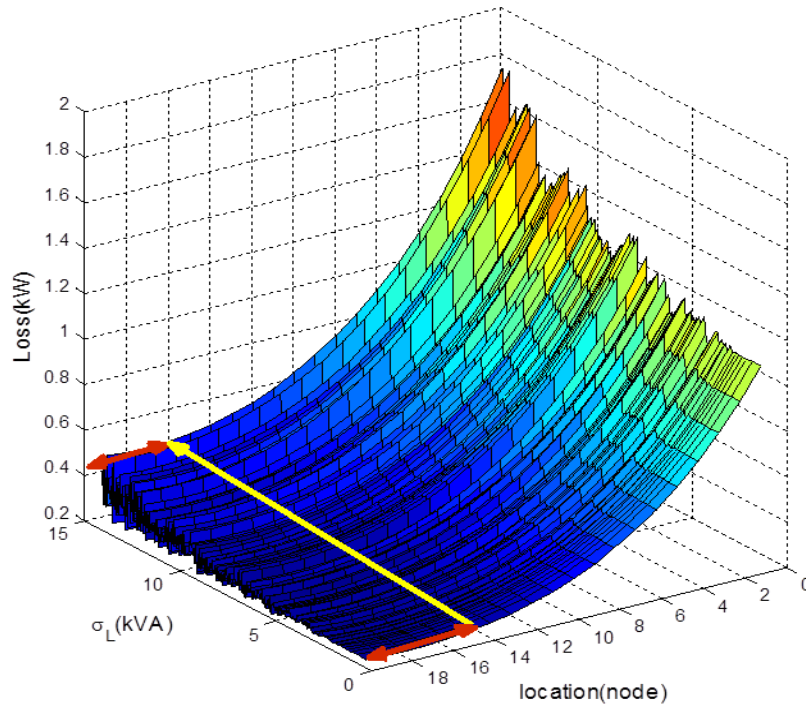
The Modified Half Capacity Rule and the DG Variance Rule is verified on the test system in Section 1.2.2 (described by Figure 10 and Table 3). The VER unit to be placed has expected output equals to 400 kVA. This output is measured in apparent voltage-effective power, which equals to the apparent power, according to Equation 8 and Equation 9, when the unit operates at the impedance power angle.

Figure 48 presents the power loss varying with the variance of load and VER output. For presentation clarity, the variance is depicted with the standard deviation as its square root value. In addition, the load standard deviation is plotted on node basis. The testing feeder has eighteen nodes, which makes the total load variance on the feeder in a comparable scale with the variance of VER output ( $\sigma_L: 15 \times 18 = 270 \text{ kVA}$  and  $\sigma_G: 280 \text{ kVA}$ ). The top figure verifies Corollary L.4b that load variance does not influence the optimal DG location, as it stays at Node 16. Conversely, as the VER output becomes more variable, shown in the bottom figure, the optimal DG location moves toward the feeder's primary side from Node 14 to Node 11.

#### *Advantages and Implications*

Simplicity and ease of application are one obvious advantage of the proposed rules for optimal VER placement. Comparing to the methods in previous studies, the proposed rules models the dynamic characteristic of load and VER output in a set of concise formulation. The power delivery loss are minimized for numerous possibilities of load and VER output with much less computational efforts. All the rules proposed for static situations, including the Half Capacity Rule and the Superposition Rule, are still applicable to dynamic situations together with the DG Variance Rule. Utilities can locate the optimal DG sites with the proposed rules without going through massive computation and even manually.

Loss under constant DG output and varying load



Loss under constant load and varying DG output

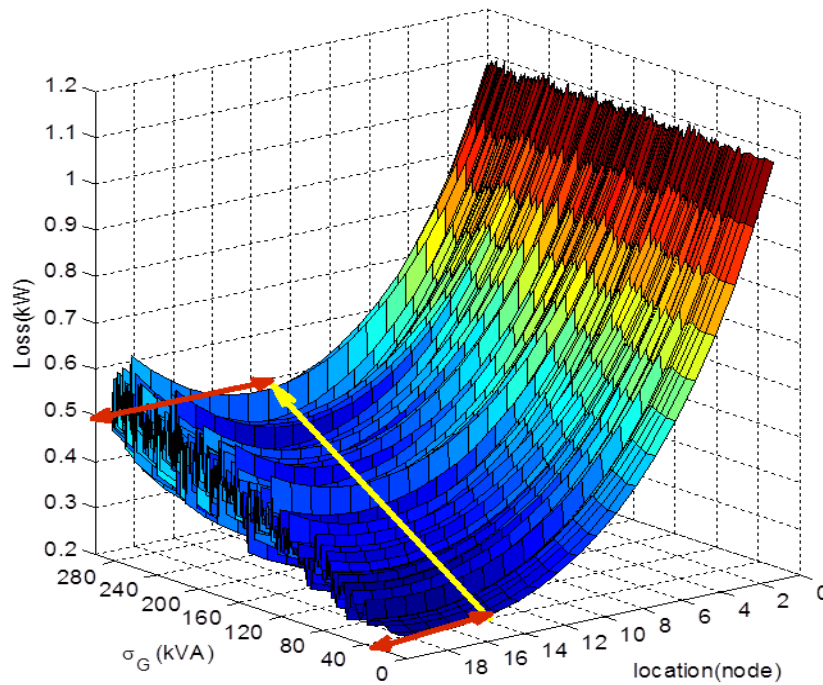


Figure 48. Optimal Variable Energy Resources (VERs) locations tested on the feeder system in Figure 10. (Top) the optimal VER location does not vary with the load variance. The load variance is measured on node basis; (Bottom) the optimal VER location moves toward the feeder's primary side as the VER variance becomes greater.

More importantly, the proposed rules provides system planners and utilities an intuition how VER penetration affects system power delivery loss in the long term. **For VERs of great intermediacy in the service area, utilities should retain the DG sites that are close to the feeder’s primary side for their connection, and use the sites that are farther away for DG units of more stable output. On the other hand, the load variance of local demand demographic should not be a concern of the utilities when penetrating DG in the area.** As stated by the DG Variance Rule, only the variance of VER output but not that of load can influence the optimal DG location.

With the DG Variance Rule, the original problem of DG placement posed in the Logic and Structure Section can be further simplified (see Figure 1). Its complexity is equalized to a problem of static load and VER output. This fact is illustrated by Figure 49, which finishes the last step of the problem transformation.



Figure 49. With the DG Variance Rule, the DG placement and sizing problem of VERs is equalized into the one of static output.

This figure illustrates the one step in the transformation Figure 1, where its symbols are declared.

# Chapter 4: the Overall Planning Scheme

---

In this chapter, an overall planning scheme is proposed for DG penetration in distribution systems, which complete the task of this thesis. The rules and methods presented in Chapter 2 for penetrating DG within the permissible voltage range and those presented in Chapter 3 for penetrating DG to get minimum power loss are utilized in this chapter to achieve both objectives.

The proposed planning scheme in this chapter aims at finding optimal DG locations, capacities and operational points, in terms of output power and power factor. While the first two results are sought for DG penetration in the planning stage, optimal DG operational points are needed in the system operation through distributed and central control or market mechanisms. Therefore, although claimed as a “planning scheme,” application of the proposed scheme can be extended to the post stage of DG penetration in distribution system operation.

One primary advantage of the proposed planning scheme is its computational simplicity and ease of implementation. The original problem in Logic and Structure Section posed for DG penetration presents great complexity (see Figure 1). This complexity is reduced step by step with the rules and methods proposed in all previous of this thesis (illustrated by Figure 8, Figure 38, Figure 46, and Figure 49). The proposed planning scheme solves the final simplified problem and therefore requires much less computational time and space. In addition, the proposed planning scheme presents a straightforward implementing flow (shown in Figure 50), which is easily programed and compatible with the existing planning tools.

The three sections of this chapter described the three steps in the planning scheme: estimating optimal DG location and capacity, refining DG location considering its varying output, and determining optimal DG operational point. Because DG penetration subject to the voltage constraint should be planned on a feeder system basis (which is proved in Section 1.1.5), each step is demonstrated and verified through the testing feeder system presented in Section 1.2.2. The proposed planning scheme, however, is applicable to the planning scale of any whole distribution system. Program code for implementing the proposed planning scheme is included in Appendix C.

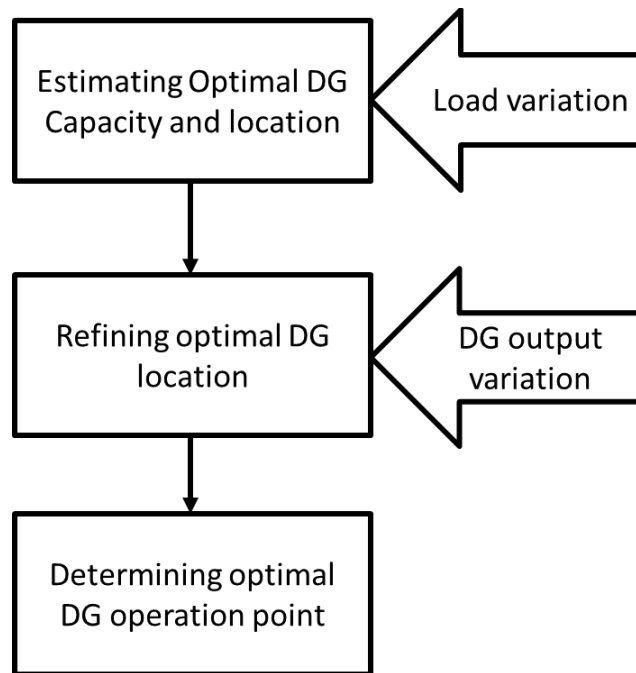


Figure 50. Overall planning scheme for DG penetration in distribution systems.

## 4.1 Estimating optimal DG capacity and location

### *Assumptions and Applications*

Chapter 3 proposes the rules for DG placement and sizing respectively. With these rules, optimal DG locations and capacities/output can be found assuming the other set of variables are known. As discussed in Chapter 3, these cases happen when utilities only have partial flexibility in DG planning, namely, the penetration capacities or sites are predetermined for political reason or end users' free willing [2, 10]. However, an even earlier planning stage should be included for a complete planning scheme. That is when utilities are granted full flexibility of DG placement and sizing at the same time. Figure 51 illustrate this step in the proposed planning scheme.

The necessity of starting with this stage not only appear as it is the real case when DG are penetrated on a green field and utilities are fully responsible of their service area planning, but also

for two other reasons. First, the minimum power delivery loss result, as the objective of DG penetration, is less when the free variables include both DG capacities and locations than when one set of the variables are predetermined [43, 181]. **Therefore, the DG penetration plan obtained under full flexibility can be used as a reference to price the cost on the part where the utilities do not have control.** For example, end users may be charged for their installed DG capacities that deviate from what are suggested for lower power delivery loss. Moreover, a connection fee can be imposed for different locations on a feeder system, much like the nodal pricing structure in transmission system, so that DG installment that causes more power loss is responsible of more compensation to the system operation party. The cost of these sub-optimality induced by partial planning flexibility can be inferred from the DG plan under the full flexibility.

The second reason is from the view of implementation. The program that solves both optimal DG capacity and location simultaneously is always capable of solving for one set when the other set is known. Actually, less computational time and space is needed for the same program to work at the DG plans with less flexibility. Hence, estimating both optimal DG location and capacity is the first step of the proposed planning scheme.

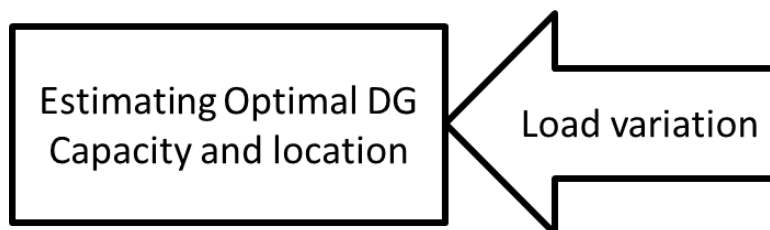


Figure 51. Step one: estimating optimal DG capacity and location for each feeder systems.

Only load variation is considered in this step.

Furthermore, this step is carried on a feeder system basis. As discussed in Section 1.2.2, a primary constraint for DG penetration at the primary distribution level is voltage rise. Feeder systems are independent systems in voltage analysis, because they operate in radial and their only voltage

control source is the transformer in their supply substation. With this condition, the optimal DG locations are sought for each feeder in the distribution system to be penetrated.

As shown in Figure 51, load variation is considered in this step. DG units are placed and sized for the minimum power loss for the long term. For optimal DG capacities and locations under varying load and their lasting time period, the expected value of power delivery loss are minimized. **DG capacity defines the upper limit of DG output. And DG output variation is considered in the operation stage but not in this step.**

### *Mathematical Model*

Assuming there are  $N_G$  DG units to be penetrated on a feeder system, for the  $i$ th unit counted from the feeder's primary side by distance, its location,  $a_i^*$ , and capacities,  $\overline{S_{G,i}}$ , are obtained by solving Equation 55, Equation 56 and Equation 57.

Equation 55

$$2 \sum_{i+1}^{N_G} \overline{S_{G,n}} + \overline{S_{G,i}} = 2E[S_L(a_i^*)]$$

Equation 56

$$Z(a_i^*) \cdot \sum_{n \leq i} \overline{S_{G,n}^V} + \sum_{n > i} (\overline{S_{G,n}^V} \cdot Z(a_n^*)) = \Delta V_L(a_i^*)$$

Equation 57

$$\overline{S_{G,i}^V} = \overline{S_{G,i}} \cdot \cos(\alpha - \theta_{min,i})$$

It can be observed that Equation 55 is derived from the Half Capacity Rule and Equation 56 is derived from the Equal Voltage Rule, which determines the optimal DG locations (Equation 37 and Equation 38) and capacities (Equation 39 and Equation 40) respectively, and both of them are modified with the Superposition Rule for multiple-DG-unit planning.

**It should be noticed that no voltage upper constraint is included in the above equations.** This is because according to the Equal Voltage Rule, DG output that induce minimum power loss give voltages that measure the same as the feeder's primary voltage, which is set within the permissible voltage range.



Since the Equal Voltage Rule only gives optimal DG capacities in voltage-effective power, Equation 57 transforms this value into DG thermal rating in apparent power, according to the definition of voltage-effective power (Equation 9). To find the maximum DG apparent power under the given DG apparent voltage-effective capacity, its voltage-effective power factor,  $\cos(\alpha - \theta)$ , needs to be set to the minimum possible value. Since in the primary distribution level, the feeder's impedance angle  $\alpha$  is usually much greater than DG power factor angle  $\theta$  (which is discussed in Section 1.2.1), the minimum voltage-effective power factor is obtained when  $\theta$  is minimum.

With some mathematical manipulations, Equation 56 and Equation 57 can be combined into a matrix equation of dimension  $N_G$  by  $N_G$  (see Equation 45). Therefore, there will be  $2N_G$  equations for  $2N_G$  variables of  $N_G$  optimal DG locations and  $N_G$  optimal DG capacities, which guarantees the existence of the solution.

### ***An Example***

This planning step is demonstrated in Figure 52 by penetrating a single DG unit in the testing feeder system in Section 1.2.2. The load expected value is set as its original value in the test system. Load standard deviation is 15 kVA at every node of Feeder 1. The minimum power factor angle of the DG unit is  $0^\circ$ , when the units operates at unit power factor.

The top figure shows that the optimal DG location and capacity are found as Node 4 and 400 kVA by solving Equation 55 and Equation 56. The bottom figure shows the power loss induced from different combinations of DG locations and capacities and the minimum power loss is attained at the combination obtained from the top figure.

The algorithm of this planning step can also be demonstrated by the top figure. Section 3.1.2 shows that solving Equation 55 needs to run a searching program on the load profile, which complexity depends on the feeder's length. On the other hand, solving for Equation 56 and Equation 57 is a matrix division operation of only one step, as shown in Section 3.2.2. For multiple-DG-unit planning, solving all these equations simultaneously may be implemented through a revolving process. Figure 53 shows the flow chart of this process.

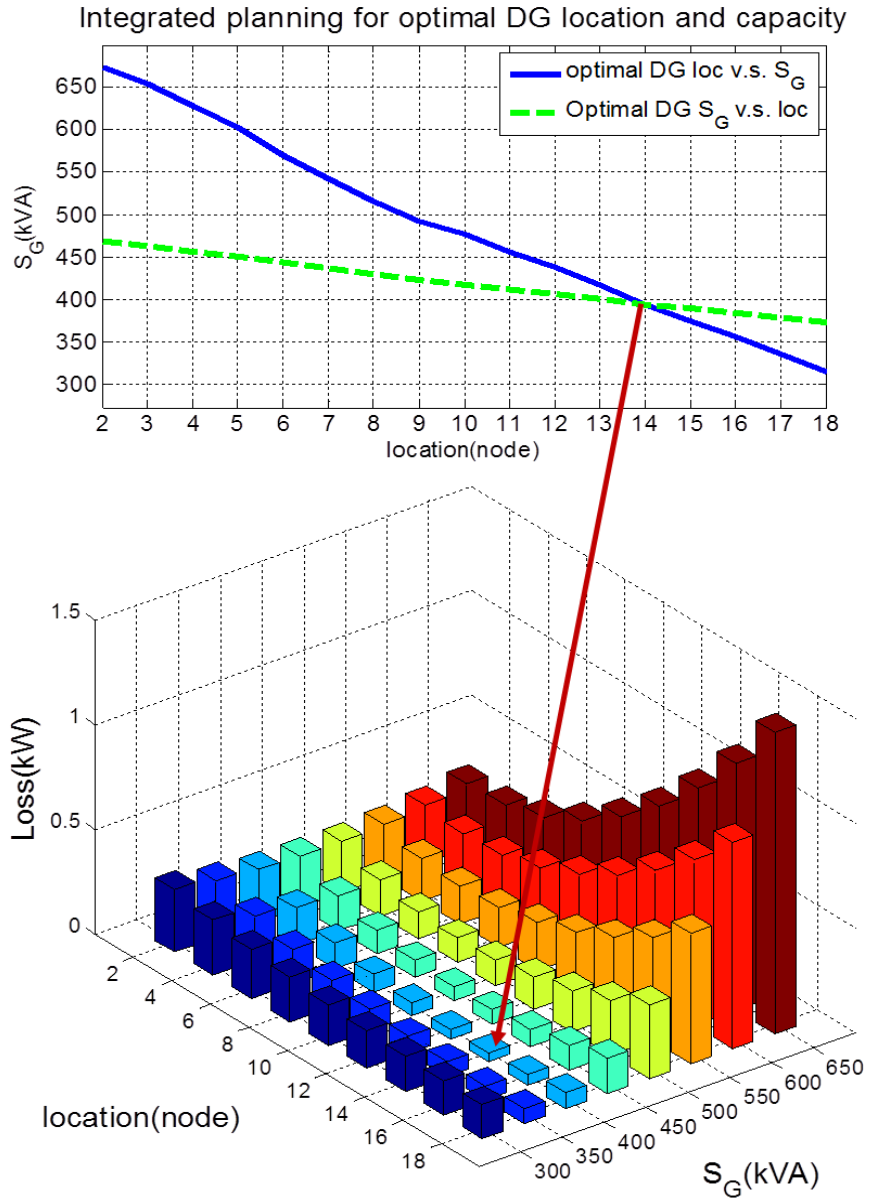


Figure 52. Optimal DG placement and sizing for the test system in Figure 10.

(Top) Traces of optimal DG location at given DG capacities and optimal DG capacities at given DG locations, derived from Equation 55 and Equation 56. (Bottom) Power delivery loss induced at various combinations of DG capacities and locations. The minimum power loss is induced by the DG placement where the two traces meet in the top figure.

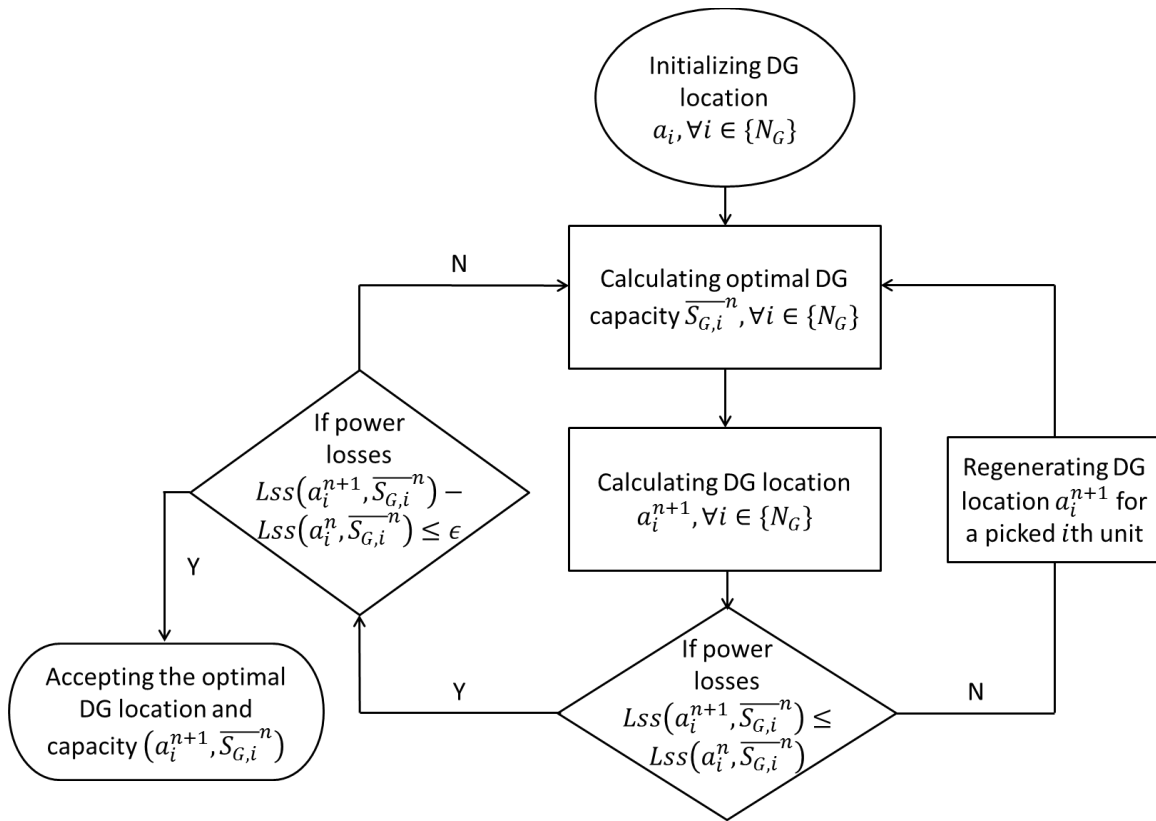


Figure 53. Algorithm of the first planning step.

In this process, an initial condition is set for optimal DG locations, then optimal DG capacities can be solved immediately. Next, the obtained DG capacities are used to find the optimal DG locations. The initial DG locations and the obtained optimal locations are used to compute power delivery loss, which is the cost function in this process. If the power loss is reduced, then the computed optimal locations move toward to the final optimal point, which is the intersecting point of the two traces in the top figure. This new set of locations is adopted for the next iteration of DG capacity calculation. Or else, the obtained locations move away from the optimal solution and are abandoned. The next iteration starts with a set of locations chosen different from the initial DG locations. The iteration is stopped when the difference of the cost function is reduced to a preset small value. The whole process is similar to tracing a point on the two curves of optimal DG location and capacity, as shown in the top figure, in a revolving manner toward its intersecting point. It is also in principle

similar to the simplex method in optimization algorithms. However, it consumes much less computational time and space. **This is because the searching space is defined on the DG capacities and locations which lead to minimum power loss, according to Equation 55 to Equation 57; while a general simplex algorithm searches globally of all possible DG capacity and locations.** The searching space of the proposed algorithm hence is much smaller.

## 4.2 Refining optimal DG location

### *Mathematical Model*

After the optimal DG capacities are obtained from the planning step one, the next step is to refine the optimal DG location considering DG output variation, which is related to each unit's capacity. Figure 54 illustrates this planning step.

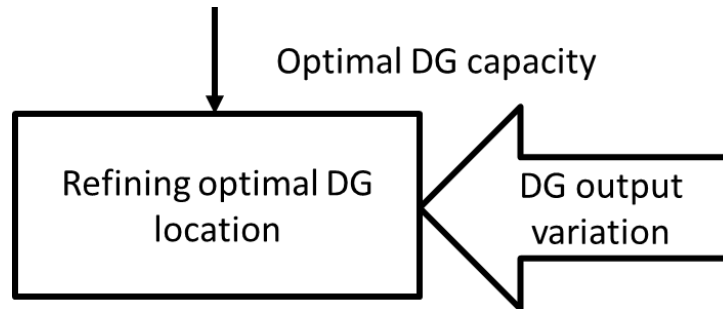


Figure 54. Step two: with the obtained optimal DG capacity and predicted DG variation, recalibrating optimal DG location.

Equation 58 presents the mathematical model of this step. It is derived from the Modified Half Capacity Rule for multiple-DG-unit placement (see Equation 51 and Equation 52).

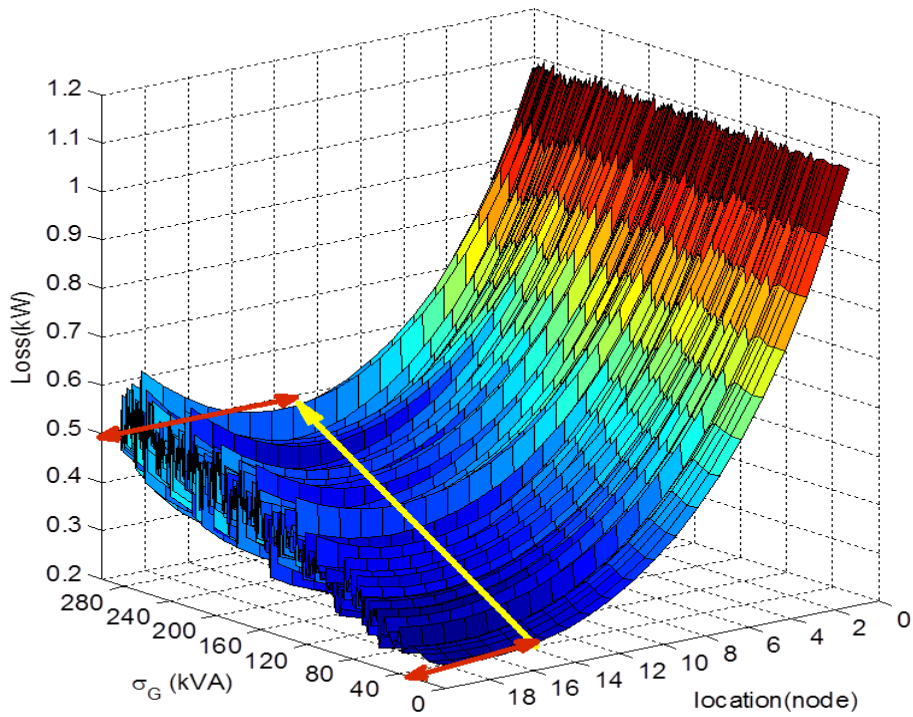
Equation 58

$$2E[S(a_i^*)] = 2 \sum_{i+1}^{N_G} E[\overline{S_{G,n}}] + E[\overline{S_{G,l}}] + \frac{Var(\overline{S_{G,l}})}{E[\overline{S_{G,l}}]}$$

Since the optimal DG capacities and their associated output variation are known, the right side of this equation can be combined into one constant. **There are  $N_G$  equations for  $N_G$  units to be placed. Every equation finds the optimal DG location for one unit, and it can be solved independently of other equations.** The only additional condition is that the distances of the DG locations from the feeder's primary side should be in the same order of their indices, that is,  $a_i < a_{i+1}$ . In other words, the 1<sup>st</sup> unit is the one that is nearest to the feeder's primary side, and the  $N_G$ th unit is the one that is located farthest from there. This property greatly reduces the computational time and space.

Similar to in the planning Step One, the mathematical model in this step does not include voltage upper constraint for the optimal DG location searching. This is explained by the DG Variance Rule (Corollary L.4a) and the Factor 2 of DG influence on voltage (Proposition V.2). According to Corollary L.4a, the optimal DG location obtained after considering DG output variation is closer to the feeder's primary side than the one that is obtained from the first planning step, which treats DG output as static. On the other hand, Proposition V.2 states that locating DG units deeper on the feeder is more likely to cause overvoltage than shallower. Because the DG locations obtained in the first planning step are within the permissible voltage upper limit, which is implied by the Equal Voltage Rule, at the locations found in this step that are shallower on the feeder DG will only output lower voltages.

The proposed mathematical model is verified on the testing feeder system in Section 1.2.2, and its results are shown in Figure 55. The expected DG output is assumed to be 75% of the DG capacity, which is 300 *kVA* given the optimal DG capacity found in Figure 52 is 400 *kVA*. It is observed that the original optimal DG location is Node 14 when the DG output is static at its full capacity of 400 *kVA*. The refined node index of optimal DG location becomes smaller as the DG output variation increases. The bottom figure depicts the resultant voltage profiles on the feeder at the refined DG locations. According to Proposition V.2, the front part of the voltage profiles are the same, and lower voltages are induced by optimal DG placement of smaller node indices. The upper voltage constraint is met automatically in the refining process of optimal DG locations.



Voltage profiles varying with DG location ( $S_G = 400$  kVA)

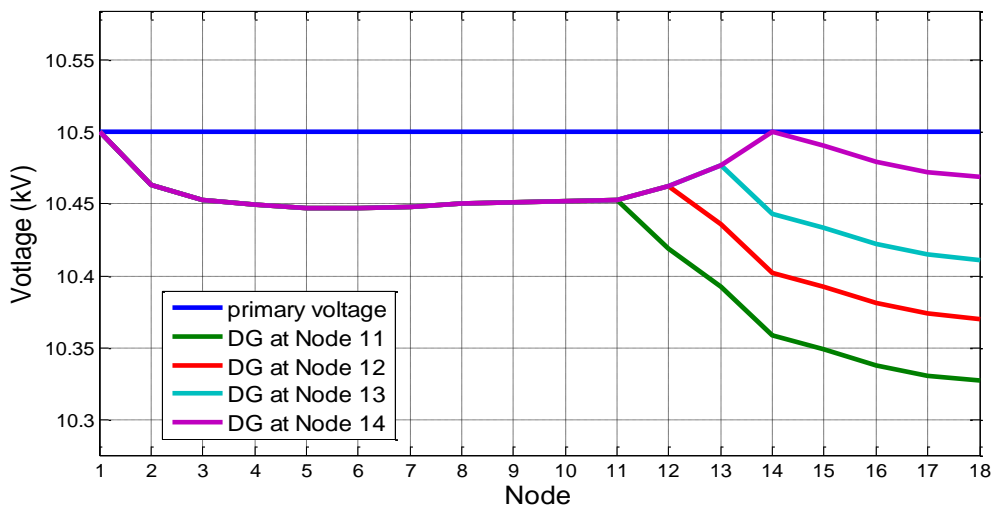


Figure 55. Recalibration of optimal VER location automatically satisfies the voltage constraint.

(Top) Power delivery loss increase as the VER standard deviation increases from 0 kVA to 280 kVA. The result is tested on the optimal DG capacity obtained in Figure 52. (Bottom) DG output voltage decreases as it is located closer to the feeder's primary side from Node 14 to Node 11.

### 4.3 Determining optimal DG operational point

#### *Assumptions and Applications*

The solution to DG penetration in a distribution system is never completed at the end of the planning stage. Conventionally, the DG units are penetrated according to the “fit and forget policy.” Once their connection capacities and locations are determined, little care is given to their operational performance. Even if DG locations and capacities are chosen for some long-term benefits, typically minimum power delivery loss, DG performance is likely not to be optimal for some range of load and power generation conditions. For this reason, DG penetration needs to be studied for the post-planning stage. Figure 56 illustrates this planning step.

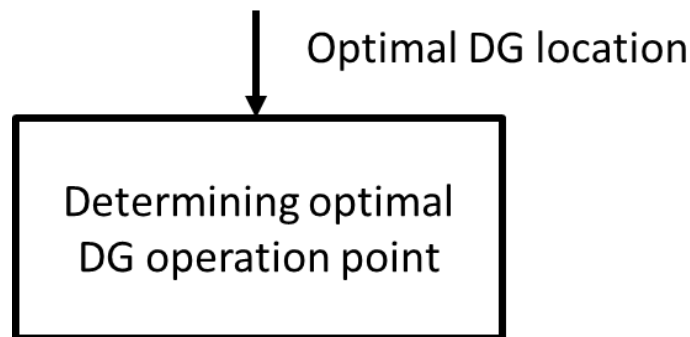


Figure 56. Step three: Determining optimal VEG operational point.

Given the optimal DG location, the DG unit may be controlled in real-time to induce minimum power delivery loss.

In operation, DG output can be controlled in various forms through a number of mechanisms. Technically, DG output can be adjusted through curtailing its real power or adjusting its power factor with the apparent output power fixed. For example, wind turbine output can be controlled by pitch control on the turbine blades; solar panel output can be smoothed by discharging the energy spikes into integrated storage. Power electronics, mechanical, and storage devices are needed to realize these processes. In terms of implementing mechanisms, DG output can be controlled through central coordination by system operators, local adjustment by intelligent agent devices installed on every unit. A more autonomous method of DG control is to incentivize end user

participation through market mechanisms. Cost of extra power loss can be charged to the end users who operate away from the optimal DG operation point. Under the same principle of DG placement cost, discussed in Section 4.1, DG influence on the distribution systems is monitored and optimized, through this transaction, not only in the stage when the units are installed but also throughout their whole lifetime.

### ***Mathematical Model***

Equation 59 presents the mathematical model of this planning step. It is straightforward from the definition of apparent voltage-effective power (see Equation 8 and Equation 9). According to the Equal Voltage Rule, minimum power loss are induced when the DG output should raise voltage at its location to the value of the feeder's primary side. For the  $i$ th DG unit, its optimal location is determined in planning Step Two as  $a_i^*$ , and the voltage drop when the unit imports no power,  $\Delta\tilde{V}(a_i^*)$ , can be measured. Hence, there are two free variables that can be controlled: the DG output apparent power  $S_{G,i}$  and DG power factor  $\cos(\theta)$ .

Equation 59

$$\theta = \cos^{-1}\left(\frac{\Delta\tilde{V}(a_i^*)}{S_{G,i}Z(a_i^*)}\right) + \alpha$$

### ***An Example***

This planning step is demonstrated on the testing feeder system in Section 1.2.2 following the testing results in Figure 52 and Figure 55. The optimal DG capacity determined in the first planning step is 400 kVA. Let the standard deviation of the DG unit under study be 200 kVA and expected value be 300 kVA. Then following the second planning step, the final optimal DG location is at Node 12.

Under various power generation conditions, the DG power factor can be controlled to minimize power delivery loss on the feeder. Figure 57 depicts this DG power factor curve when the original voltage drop at Node 12 measures as 0.5% of the primary voltage (i.e. 50 kV given the test system operates at 10 kV).



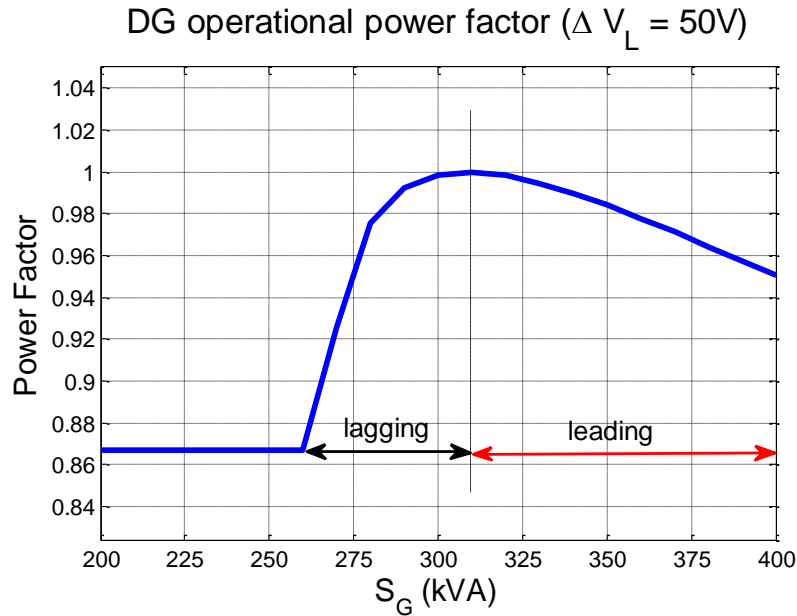


Figure 57. Optimal DG operational point for a given voltage profile.

The curve is computed for the test system in Figure 10 at Node 12 (obtained in Figure 52). The voltage drop from the feeder's primary side measured at DG location is 50 V when the DG unit imports zero power. The power delivery loss is minimized when the DG unit operates on the curve.

It is observed that the optimal DG power factor is a constant value when the DG output is less than 260 kVA at non-ideal generation conditions. This is because to raise the output voltage with limited output power, a DG unit needs to operate at its minimum lagging voltage-effective power factor, 0.865 in this example, to get unit voltage-effective power factor. According to its definition, it is reached when the unit's power factor angle,  $\theta$ , aligns with the impedance power angle of the feeder's conductor,  $\alpha$ . For the conductors in the test system (see Figure 10), the impedance power angle is about  $29^\circ$ . Therefore, the optimal DG power factor is 0.87 when DG output power is less than 258 kVA in this example.

After being constant, the optimal DG power factor curve first increases, reach the unit power factor, then decreases. The DG unit operates at lagging power factor in region where the curve rises, and

vice versa. This is because a voltage-effective power factor has two solutions of the DG operational angle  $\theta$ , which are derived from the positive and negative difference of  $\alpha - \theta$  (see Equation 9).

**Although operating on the whole curve mathematically gives the minimum power delivery loss, the operational range for most of the generators is greater than power factor of 0.9.** Therefore, when the DG unit generates power less than 268 kVA, the power factor should be adjusted to its lower limit.

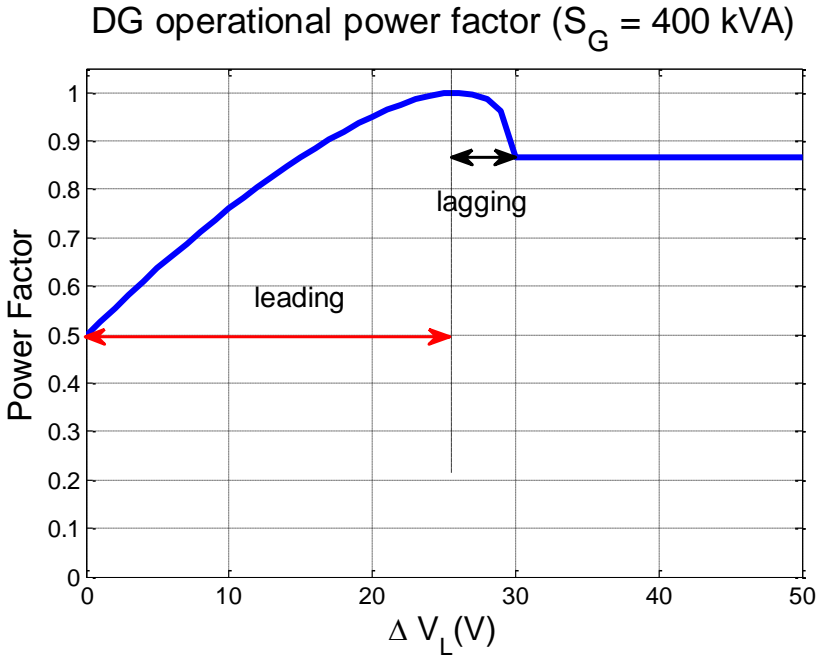


Figure 58. Optimal DG power factor when DG operates at its full capacity.

At the obtained optimal DG capacity and location, 400 kVA and Node 12 (in Figure 52 and Figure 55), the optimal power factor for the DG unit is calculated for varying DG apparent voltage-effective power, which implies DG output voltage.

For DG types of more stable output, utilities may want to find their optimal power factors at a constant output levels. Because voltage data can be measured easily in today’s distribution systems,

such a chart of optimal power factors can assist system operators to determine the DG operational point under different conditions of load and other units' output in a fast and convenient manner.

Figure 58 shows this chart for the test system, when the DG unit operates at its full capacity 400 kVA. It can be observed that the optimal power factor first rises to 1, then decreases, and stays constant after reaches 0.88. In the rising region, the DG unit operates at leading power factor; in the decreasing region, it operations at lagging power factor. In the constant region, the DG unit operates power factor angle,  $\theta$ , that aligns with the impedance power angle of the feeder's conductor,  $\alpha$ , so that the voltage-effective power factor becomes 1. Similar to Figure 57, system operators are more likely to refer to the top curve in practice due to the permissible operational range of today's available DG units.

Similar to applying Figure 57, although operating on the whole curve mathematically gives the minimum power delivery loss, the actual operation of the generation is limited to their operational range. In this example, for most of the generators under, the power factor may set as 0.9, which is presumably the lower limit, when the voltage difference is less than 17 V and greater than 29 V.

# Chapter 5: Conclusion

---

## *Problem Statement*

Distributed Generation (DG), or embedded generation, that generates power of from kilowatts to tens of megawatts presents great benefits and substantial positive social impacts to utilities, system operators and electricity consumers [10-12]. Research and practices during the past several decades have been conducted endeavoring to penetrate DG for its maximum benefits and minimum adverse impact. The existing approaches, however, have a few deficiencies. One is their proposed DG penetration plans are limited to specific system configurations and capacities, and therefore are hard to be applied to other situations [4, 47, 76-78]. On the other hand, studies with statistic approach that attempt to conclude characteristics of optimal DG penetration are usually inaccurate and tends to lose its optimality in application to specific scenarios [10, 30, 73, 74]. In addition, those methods that run programs to solve for DG penetration plans are usually computationally expensive due to the extensive sizes of distribution systems and stochastic characteristics of DG output from Variable Energy Resources (VERs) [72, 79-81]. Other studies taking engineering approaches or active network planning that considers coordination of distribution system components requires considerable investment in sensors, communication assets, and retrofitting equipment with control functionalities [38, 93-95].

Due to the great interests in DG penetration and the deficiencies of previous studies, this thesis proposes a planning scheme for DG penetration in distribution systems that maximizes DG penetration's benefits, in terms of power delivery loss reduction, and restricts its adverse impact of steady-state voltage rise. A unique approach is taken to simplify the DG penetration problem with two sets of rules that describes interaction of DG penetration and power delivery loss and voltage profiles in distribution systems (illustrated by Figure 1).

## *Assumptions and Study Scope*

This thesis restricts its discussion on DG penetration in the distribution systems operating at primary distribution voltage (between 2.2 kV and 35 kV) (Section 1.2.1). A general assumption made in this thesis is that DG is penetrated at an originally healthy primary distribution system. In other words, conditions are taken for granted that a distribution system before DG penetration

should satisfy, and are not imposed to the system after DG penetration. For instance, before DG penetration voltage profiles of feeders in distribution systems decrease monotonically, with the power flow drawn by loads along the feeders. By configuration layout and engineering methods, such as choosing feeders' conductors and connecting bank capacitors to the feeders, system planner need to ensure the voltage throughout the feeder is above the lower limit of the predetermined voltage range. After DG penetration, feeders have power imported on their delivery paths to end users, and therefore have voltages raised at DG locations. This voltage rise need be mitigated to lower than the upper limit of the predetermined voltage range. In derivation of the planning scheme for DG penetration, this thesis assumes the original system is well designed and has voltage profiles all above the predetermined lower limit. DG penetration will only cause voltage rise, and therefore only the upper limit is imposed for the voltage profiles of feeders.

Apart from this general assumption, primary distribution systems have a few common characteristics taken for assumptions in the development of the rules and the planning scheme in this thesis.

- System topologies are planned in mesh and operated in radial. In other words, there is only path between any customers and the substation in normal operation (Section 1.2.1);
- Feeders' voltages in the system are regulated by the transformers in substations on their primary side (Section 1.2.2);
- All feeders are somewhat the same "size" in terms of capacity and loading (Section 1.2.2);
- Feeders' primary voltage is usually set to be close to the upper limit of a pre-defined range in order to fully utilize the feeder's load reach<sup>8</sup> (Section 2.1.3).

Two more assumptions are made for the derivation of the power flow model in this thesis (Section 1.3.2):

- Laterals on the feeder are negligible;
- Three-phase distribution feeders operate under balanced conditions.

---

<sup>8</sup> This assumption is made for convenience of the application of rules and methods derived in this thesis, and is taken for granted in the numerical examples. The feasibility of these results, however, does not depend on this assumption and can be adjusted to situations where this assumption does not hold.

### *Original Contributions*

The major contribution of this thesis is proposing a planning scheme for DG penetration in distribution systems that maximizes DG penetration's benefits, in terms of power delivery loss reduction, and restricts its adverse impact of steady-state voltage rise. Comparing to existing studies on DG penetration, the proposed planning scheme has the following advantages:

- Providing the base line of DG penetration. In practices, there are many more constraints and objectives for DG penetration. These constraints can be complied with the proposed planning scheme in need of adjusting to a comprehensive system configuration and wider timeframe;
- General applicability. Instead of providing a DG penetration plan for a specific distribution system, the proposed planning scheme can applied to any distribution systems regardless of their configurations and capacities without losing results' optimality;
- Requiring much less computational efforts. With two sets of rules proposed of DG penetration interacting with system power delivery loss and voltage profiles, this thesis transforms a complex DG penetration problem into one of exponentially less computational space and time (quantified by Equation 42 to Equation 47).

More intellectual merits of this thesis appear in the development of the proposed planning scheme where a few concepts, methods and rules are derived. Their application is never limited in the planning scheme, but can be used in combination or separately to suit any specific DG penetration situation. These concepts, methods and rules provides the users an intuition how DG penetration affects the performance of a distribution system. The policy makers, regulators, industries and utilities will be able to use this toolkit, without going through complicated computations, as guidelines to make policies, standards and decisions in DG penetration and related business.

One concept proposed is voltage-effective power (Section 1.3.1). This concept maps the power parameters in complex domain, in terms of magnitude and phase, to real domain, and therefore enables fast estimation of voltage profiles in primary distribution systems.

Based on voltage-effective power, a *graphical method* is proposed that visualizes the voltage profile change during DG penetration (Section 2.1.2). Moreover, the zero-point analysis, which has been conventionally used in determining the possibility of overvoltage occurrence, is revised by an *Area*

*Criterion* with improved accuracy in overvoltage estimation (Section 2.1.3). Existing definition of DG penetration level contents ambiguity and tends to risk system voltage reliability. This thesis provides guidelines for specifying DG penetration level, and presents a DG penetration chart for distribution planner to examine DG penetration feasibility (Section 2.2).

The rules for DG penetration interacting with system voltage profiles are summarized as below (Section 2.3):

**Proposition V.1:** Overvoltage can be eliminated by controlling DG maximum output.

**Proposition V.2:** The deeper a DG is located at a feeder, the more likely it will cause overvoltage.

**Proposition V.3:** Spreading DG capacity does not necessarily mitigate overvoltage.

**Proposition V.4:** Overvoltage can be prevented by planning for the feeder's layout and conductor.

With these rules, two innovative methods for voltage rise mitigation, Demand Response (DR) and reconfiguration, are further studied and presented with implementation strategies (Section 2.4). Comparing to the conventional methods, they have the advantages of low capital investment, high operational flexibility, and good effects of voltage rise mitigation.

In addition to the voltage rules, DG penetration for maximum benefit of power delivery loss reduction should follow the rules below:

**Proposition L.1 (Half Capacity Rule)** To minimize power delivery loss on a feeder, the DG unit should be placed at where the feeder's load apparent power flow equals to half of DG thermally limited capacity. (Section 3.1.1)

**Proposition L.2 (the Equal Voltage Rule)** A feeder's power delivery loss reach the minimum when the feeder's DG output voltage is the same as its primary voltage. (Section 3.2.1)

**Corollary L.2** For a DG unit installed at the chosen location of a feeder system, the following two statements are equivalent (Section 3.2.1):

- the DG unit operates at an output minimizing the feeder's power loss
- the DG output voltage is measured the same as its feeder's primary voltage

**Proposition L.3a (Superposition Rule for optimal DG placement)** To induce minimum power delivery loss on the feeder, each time a DG unit should be placed at where the apparent power flow resultant from its downstream DG placement measures the half of its thermally limited capacity. (Section 3.3.1)

**Proposition L.3b (Superposition Rule for optimal DG sizing)** The power delivery loss on a feeder is minimized if and only if the output voltage of every DG unit measures the same as the feeder's primary voltage. (Section 3.3.1)

**Proposition L.4 (Modified Half Capacity Rule)** For minimum power loss over a time period, the DG unit should be placed at where half of the expected value plus normalized variance of its apparent power output measures the same as the expected apparent load flow on the feeder over the time period. (Section 3.4.1)

**Corollary L.4a (DG Variance Rule)** The greater its VER variance, the near a DG unit should be placed to the feeder's primary side. (Section 3.4.1)

**Corollary L.4b (DG Variance Rule)** Load flow variance does not affect the optimal DG location. (Section 3.4.1)

### ***Recommendations***

From these rules, some recommendations are made for the utilities that plan for or have started connecting DG to their networks, and for policy makers that set up standards and regulations for DG penetration. These recommendations can also be interesting to related business. For instance, DG manufacturers may use them as a reference to market certain DG technologies (renewable or conventional) and sizes according to the targeted distribution systems.

- The risk of overvoltage should be determined by DG penetration on basis of each feeder system instead of a whole distribution system. (Section 1.2)
- In service areas that sometimes could have low demand, DG should be penetrated so that high DG capacities and shallow DG locations (defined as close to the feeder's primary side) do not appear at the same time. (Section 2.3)
- In prediction of increasing DG penetration, a distribution system should be laid out with as possible larger conductors and closer phase spacing within its economic scale. (Section 2.3)



- Demand Response and network reconfiguration are promising methods to mitigate voltage rise, in terms of their high flexibility, low capital investment and good voltage mitigation effect. Future distribution systems should be planned with these functionalities. (Section 2.4)
- DG penetration capacity should be no greater than half of the apparent power profile of a feeder system. (Section 3.1)
- DG units operated for minimum power delivery loss automatically provide voltage support throughout feeders up to the primary voltage. IEEE 1547 that prohibits voltage regulation from DG should be revised in order to achieve higher system operation efficiency. (Section 3.2 and Section 3.3)
- Both the rated power and power factor of DG units should be monitored in distribution system operation for system efficiency and voltage reliability. (Section 4.3)

### ***Future Work***

The primary future work of this thesis is to expand the current framework of the proposed planning scheme to suit more comprehensive situations and wider timeframes. As stated at the beginning of this thesis, the planning scheme proposed only involves one major objective, power delivery loss reduction, and constraint, voltage upper limit, for DG penetration. In practices, many other constraints from all perspectives of policy, economic and technics exist. Incorporating these constraints into the proposed planning scheme can be carried out by software implementations, DG connection standards, and market instruments.

A potential direction is to price the DG penetration initial and operation cost with the planning scheme. DG penetration plans that deviates from what is generated by the planning scheme can be charged with initial costs that would be need for investment on voltage rise mitigation devices; DG units operation that deviates from the suggested optimal operational points can be penalized according to the extra power delivery loss induced. The results that provided by the planning scheme is not just a “hard standard” for utilities and system operators, but more a “reference” that can be used with flexibility to measure the actual performance and quantify its optimality.

More other future works are stated in each section where the rules and methods are proposed. For example, the strategies for Demand Response (DR) and reconfiguration on voltage rise mitigation should be solidified with real load data and system configurations. They are not repeated here for conciseness.

# Appendix A

This appendix calculates and simulates the error of Equation 1, which approximates the voltage difference in distribution network. The concept of voltage-effective power is developed.

## Mathematical Expression

Equation 1

$$\Delta V = V_1 - V_2 \approx \frac{RP_N + XQ_N}{V_2}$$

Figure 59 shows the approximated voltage difference  $\Delta V$ , which is induced under inductive power flow and capacitive power flow respectively. In the diagram,  $V_1$  is the voltage at the beginning of the conductor section, which resistance and reactance are  $R$  and  $X$ ; and  $V_2$  is the voltage at the end. The power transmission angle is denoted as  $\theta$ , which cosine value is the power factor of the net real power  $P_N$  and net reactive power  $Q_N$  flowing on the conductor. When current  $I$  is lagging voltage  $V_1$ , or equivalently  $\theta < 0$ , the power flowing on the conductor is inductive; otherwise, the power flowing on the conductor is capacitive. When  $\theta$  is small enough, which is required in distribution systems for efficient power transmission, Equation 1 can be used to calculate  $\Delta V$ .

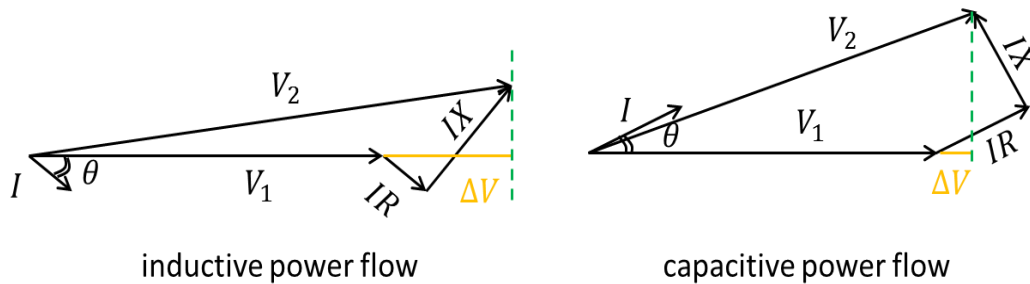


Figure 59. Approximation of voltage drop over a conductor section.

From Figure 59, the accurate mathematical relation between the voltages of the conductor section,  $V_1$  and  $V_2$ , can be derived as:

Equation 60

$$V_1 = \left[ \left( V_2 + \frac{P_N R - Q_N X}{V_2} \right)^2 + \left( \frac{Q_N R + P_N X}{V_2} \right)^2 \right]^{\frac{1}{2}}$$

If known  $V_1$ ,  $V_2$  on the other end of the conductor section can be obtained by solving Equation 60 as

Equation 61

$$V_2 = \left( \frac{c_3 - 2c_1}{2} + \frac{\sqrt{c_3^2 - 4c_1c_3 - 4c_2^2}}{2} \right)^{\frac{1}{2}}$$

where  $c_1 = Q_N X + P_N R$ ;  $c_2 = P_N X - Q_N R$ ; and  $c_3 = V_1^2$ .

With Equation 61, the voltage difference  $\Delta V$  is then can be expressed as a function of  $V_1$  and power flow  $P_N$  and  $Q_N$  on the conductor section. Voltage profile of a feeder of changing power flow is calculated by

Equation 62

$$V(a) = V_0 - \int_0^a \Delta V(\zeta) d\zeta = V_0 - \int_0^a \Delta V(P_N(\zeta), Q_N(\zeta)) d\zeta$$

Notice that neither Equation 1 nor Equation 61 models shunt capacitors on the conductor section. These are usually small values that can be ignored in distributions systems of radial structures in the suburban and rural areas. The shunt capacitance becomes not ignorable for underground cables which are usually used in distribution networks in urban area. This type of distribution systems are not in the scope of this thesis, as defined in Section 1.2.1.

### ***Simulation***

The approximation errors induced of Equation 1's deployment is demonstrated on the test system introduced in Section 1.2.1 (see Figure 9). The errors are estimated on two voltage levels, 10 kV and 30 kV. Parameters of the test system is listed in Table 14.

Table 14, Parameters of the test system in Figure 9.

$V$ (kV)	$p_N$ (kW/km)	$q_N$ (kVar/km)	$r$ ( $\Omega$ /km)	$x$ ( $\Omega$ /m)
10	20	50	0.160	0.092
30	50	25	0.402	0.394

$p_N$  and  $q_N$  are net real and reactive power flow averaged on the testing distance.  $r$  and  $x$  are unit resistance and reactance of the conductor in the test system.

Figure 60 shows the actual voltage profiles measured over 10 km in the test system. In either case, voltage decreases monotonically when no DG imports power to the system.

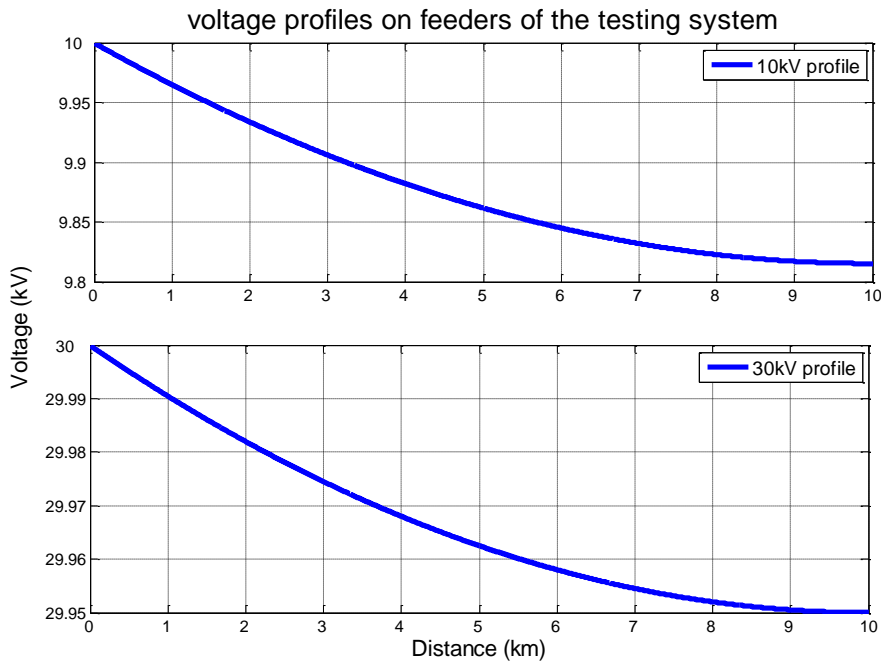


Figure 60. Actual voltage profiles measured the test system (Figure 9).

Voltage profile on a 10 kV feeder (Top) and a 30 kV feeder (Bottom).

Comparing the voltage profiles in Figure 60 with the ones approximated by Equation 1, the errors are plotted in Figure 61. It shows that the voltage errors are less than 0.02% for 10 kV feeders and  $3.33 \times 10^{-5}\%$  for 30 kV feeders. In either the 10 kV and 30 kV case, the approximation errors

stop to increase when the measurements exceed a certain distance. Therefore, **these approximation errors are upper constrained**. Moreover, **the approximation errors measured on feeders operated on a higher voltage, 30 kV, is smaller than those on a lower voltage, 10 kV**.

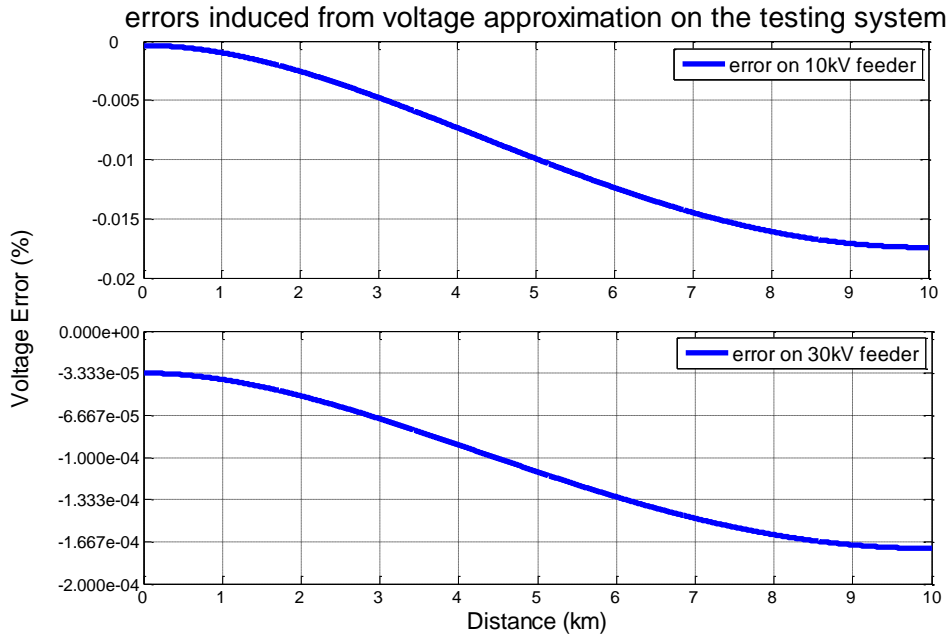


Figure 61. Errors induced by voltage approximation of Equation 1.

The actual voltage profile values over the tested distance are plotted in Equation 59. The voltage errors are normalized on their primary voltage 10 kV and 30 kV respectively.

Another approximation in this thesis treats the loads as small values comparing to DG as continuous variable. Therefore, voltage can be calculated with the integral operator over the distance of concern on the feeder as in Equation 13.

$$V(a) = V_0 - \int_0^a \Delta V(\zeta) d\zeta \approx V_0 - \int_0^a r P^V(\zeta) d\zeta$$

Errors of approximating lumped loads to continuously distributed loads are examined on the test system and plotted in Figure 62. The total loads are the same in either the 10 kV and 30 kV case.

The voltages are measured for loads lumped into 100 spots (green dash line) and 10 spots (red lines). Comparing them to the approximated voltage (blue line) that treats loads as continuously distributed, the errors are of very small value, less than  $1.5 \times 10^{-3}\%$  and  $5 \times 10^{-4}\%$  for the 10 kV feeders and 30 kV feeders respectively.

For less lumped loads (such as  $1/100$  lumped ones), the errors are hardly observable. For more lumped loads, the upper envelope of the errors traces those of the continuous loads. **Therefore, voltage profiles calculated from treating the loads as continuously distributed represents the trend of errors' changing regardless of loads' lumpiness.**

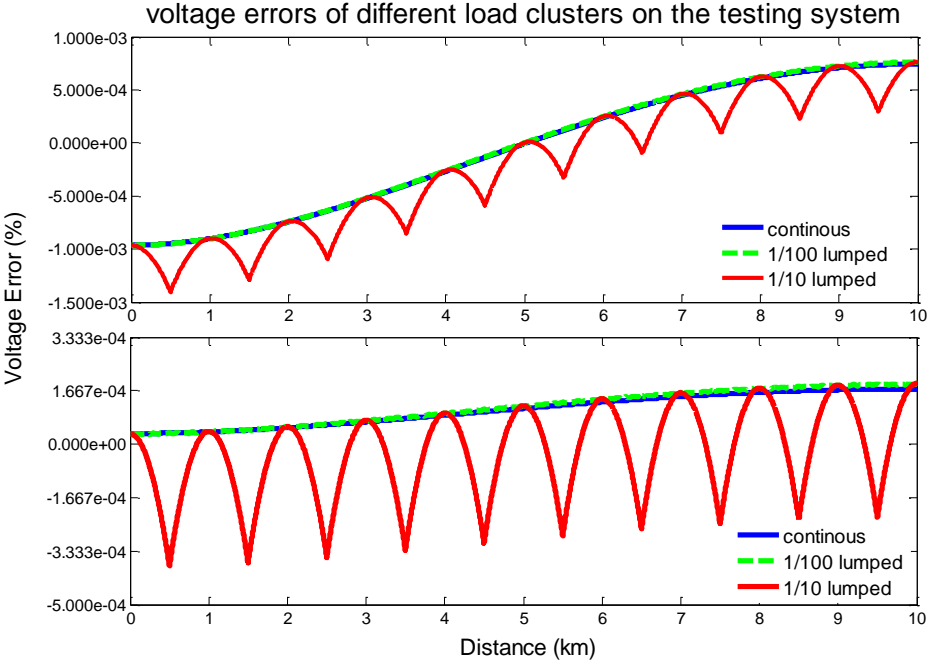


Figure 62. Errors of approximating scattered loads to continuous loads.

The voltage profiles are generated based on the parameters of the test system (see Table 14). The errors are plotted for a 10 kV feeder (Top) and a 30 kV feeder.

# Appendix B

---

This appendix presents the mathematical development of the equations and their derived propositions and rule in Chapter 3.

## B.1 Proof of Half Capacity Rule

**Proposition L.1 (Half Capacity Rule)** To minimize power delivery loss on a feeder, the DG unit should be placed at where the feeder's load apparent power flow equals to half of DG thermally limited capacity.

Proposition L.1 is expressed as

Equation 30

$$2S_L(a^*) = S_G$$

where  $S_L$  is load apparent power flow on the feeder and  $S_G$  is the thermally limited capacity of the single DG unit.

*Proof:*

Given the unit resistance of a feeder's conductor is  $r \Omega \cdot km^{-1}$ , the power delivery loss on the feeder from the primary side until location  $a$  km and are calculated by the Joule's Heating Law:

Equation 63

$$L_{SS}(a) = \int_0^a I_N(\zeta)^2 r(\zeta) d\zeta$$

where  $I_N(\zeta)$  is the net current flowing on location  $\zeta$ .

Given  $I_L(a)$  is current of load on the feeder at location  $a$  and  $I_G$  is the output current of the DG unit at location  $a_G$ , the net current on the feeder can be expressed as

Equation 64

$$I_N(a) = \begin{cases} I_L(a) - I_G, & \text{if } a < a_G \\ I_L(a), & \text{otherwise} \end{cases}$$

According to the critical point theorem<sup>9</sup>, the total loss on a feeder of length  $l$  km is minimized by placing a DG unit at location  $a_G$  that satisfies

Equation 65

$$\frac{\partial L_{SS}}{\partial a_G} = \underbrace{\frac{\partial}{\partial a_G} \int_0^{a_G} (I_L(\zeta) - I_G)^2 \cdot r(\zeta) d\zeta}_{\text{term1}} + \underbrace{\frac{\partial}{\partial a_G} \int_{a_G}^l I_L(\zeta)^2 \cdot r(\zeta) d\zeta}_{\text{term2}} = 0$$

By the Leibniz Integral Rule<sup>10</sup>, the two terms in Equation 65 are

Equation 66

$$\text{Term1} = (I_L(a_G) - I_G)^2 r(a_G)$$

and

Equation 67

$$\text{Term2} = -I_L(a_G)^2 r(a_G)$$

Substitute Equation 66 and Equation 67 into the minimum loss condition of Equation 65, it renders

Equation 68

$$2I_L(a_G)I_G - I_G^2 = 0$$

Because  $I_G \neq 0$ , and at location  $a$ , Equation 68 can be manipulated mathematically into

Equation 69

$$2I_L(a_G) \cdot \Delta V(a_G) = I_G \cdot \Delta V(a_G)$$

---

<sup>9</sup> **Fermat's Theorem (Critical Point Theorem):** Local maxima and minima of a function can occur only at its critical points. Let  $f: (a, b) \rightarrow \mathbb{R}$  be a function and suppose that  $x_0 \in (a, b)$  is a local extreme of  $f$ . If  $f$  is differentiable at  $x_0$  then  $f'(x_0) = 0$ .

<sup>10</sup> **Leibniz Integral Rule:** Let  $f(x, t)$  be a function such that both  $f(x, t)$  and its partial derivative  $f_x(x, t)$  are continuous in  $t$  and  $x$  in some region of the  $(x, t)$  plane, including  $a(x) \leq t \leq b(x)$ ,  $x_0 \leq x \leq x_1$ . Also suppose that the functions  $a(x)$  and  $b(x)$  are both continuous and both have continuous derivatives for  $x_0 \leq x \leq x_1$ . Then for  $x_0 \leq x \leq x_1$ :

$$\frac{d}{dx} \left( \int_{a(x)}^{b(x)} f(x, t) dt \right)$$



where  $\Delta V(a_G)$  is the voltage difference at the DG location  $a_G$  from the feeder's primary voltage . It is measured when the DG unit import current of  $I_G$ .

By definition of apparent power, the optimal DG location  $a^*$  is obtained by rewriting Equation 69 as

Equation 30

$$2S_L(a^*) = S_G$$

In search of such a location  $a^*$ , the alternative expression of Equation 30 is

Equation 70

$$a^* = S_L^{-1}\left(\frac{1}{2}S_g\right)$$

where  $S_L^{-1}(\cdot)$  is the inverse function of the apparent load power profile,  $S_L(\cdot)$ , on the feeder.

*Q.E.D.*

Notice that Equation 30 calculates the optimal DG location with apparent power instead of current. It is necessary to transform from the current expression in Equation 30 to the apparent power expression of Equation 68 for two reasons:

1. The ease of application. In distribution system operation, data available are more often in the form of power, either for load or DG, than current;
2. The accuracy and optimality of the DG location. Power is more controllable than current in DG penetration integration. While load consumes a same amount of real and reactive power, which gives a constant apparent power  $S_L(a)$ , current flowing on the feeder  $I_L(a)$  changes to  $I_N(a)$  after DG penetration, because of the voltage change caused by DG output. Equation 69 recovers the changed current to the constant apparent power flow by multiplying on its both sides the voltage drop induced after DG penetration.

***Power delivery loss reduction at the optimal DG location***

According to the Joule's Heating Law, the original loss induced by load on the feeder is  $LSS_0$  and is written as

Equation 71

$$LSS_0 = \int_0^l I(\zeta)^2 r(\zeta) d\zeta$$

Because DG penetration does not affect the power flow and thus loss downstream of the DG unit, the loss reduction can be examined on the feeder only over the distance from its primary side to the DG location. Therefore, by placing the DG unit at  $a^*$  derived from Equation 70, the loss reduction is

Equation 72

$$\Delta LSS = LSS_0 - LSS|_{a_G=a^*} = 2I_G \int_0^{a^*} I_L(\zeta) r(\zeta) d\zeta - I_G^2 \int_0^{a^*} r(\zeta) d\zeta$$

Because feeders in distribution systems are usually of a uniform unit resistance, that is  $r(\zeta) = r$ , Equation 72 is simplified as

Equation 73

$$\Delta LSS = 2I_G r \left[ \int_0^{a^*} I_L(\zeta) d\zeta - \frac{I_G}{2} a^* \right]$$

Since

Equation 74

$$\int_0^{a^*} I_L(\zeta) d\zeta = I_0 a^* - \int_{I_L(a^*)}^{I_0} \zeta dI_L = I_0 a^* - \int_{\frac{I_G}{2}}^{I_0} \zeta dI_L$$

where  $I_0 = I_L(0)$  is the total current drawn by load at the feeder's primary side.

The loss reduction is therefore,

Equation 75

$$\Delta L_{SS} = 2I_G r \left[ \left( I_0 - \frac{I_L}{2} \right) I_L^{-1} \left( \frac{I_G}{2} \right) - \int_{\frac{I_G}{2}}^{I_0} \zeta dI_L \right]$$

## B.2 Proof of Equal Voltage Rule

**Proposition L.2 (the Equal Voltage Rule)** A feeder's power delivery loss reach the minimum when the feeder's DG output voltage is the same as its primary voltage.

Proposition L.2 is expressed mathematically as Equation 32.

Equation 32

$$S_G^V = \frac{\Delta V_L(a_G)}{Z(a_G)}$$

where  $S_G^V$  is the voltage-effective apparent power of the DG unit;  $\Delta V_L(a_G)$  is the voltage drop purely caused by load at the given DG location;  $Z(a_G)$  is the total impedance measured from the feeder's primary side to the DG location, and is calculated as

Equation 33

$$Z(a_G) = \int_0^{a_G} z(\zeta) d\zeta$$

**Proof:**

Given the unit resistance of a feeder's conductor is  $r \Omega \cdot km^{-1}$ , the power delivery loss on the feeder from the primary side until location  $a \text{ km}$  and are calculated by the Joule's Heating Law:

Equation 63

$$L_{SS}(a) = \int_0^a I_N(\zeta)^2 r(\zeta) d\zeta$$

where  $I_N(\zeta)$  is the net current flowing on location  $\zeta$ .

Given  $I_L(a)$  is current of load on the feeder at location  $a$  and  $I_G$  is the output current of the DG unit at location  $a_G$ , the net current on the feeder can be expressed as

Equation 64

$$I_N(a) = \begin{cases} I_L(a) - I_G, & \text{if } a < a_G \\ I_L(a), & \text{otherwise} \end{cases}$$

According to the critical point theorem, the loss is minimized by operating the DG unit at output current  $I_G$  that satisfies

Equation 76

$$\frac{\partial L_{ss}}{\partial I_G} = \underbrace{\frac{\partial}{\partial I_G} \int_0^{a_G} (I_L(\zeta) - I_G)^2 \cdot r(\zeta) d\zeta}_{\text{term1}} + \underbrace{\frac{\partial}{\partial I_G} \int_{a_G}^l I_L(\zeta)^2 \cdot r(\zeta) d\zeta}_{\text{term2}} = 0$$

Based on the Leibniz Integral Rule, the two terms of Equation 76 are

Equation 77

$$\text{Term1} = -2 \int_0^{a_G} r(\zeta)(I_L(\zeta) - I_G) d\zeta$$

and

Equation 78

$$\text{Term2} = 0$$

**This mathematical manipulation reduces the integral of a second order expression to first order.**

Substituting Equation 77 and Equation 78 into Equation 76, the optimal DG output satisfies:

Equation 79

$$\int_0^{a_G} r(\zeta)(I_L(\zeta) - I_G) d\zeta = 0$$

Assuming the conductor has constant ratio of reactance to resistance  $x/r$ , which is often true in distribution systems as discussed in Section 1.2.2. Equation 79 can be written as

Equation 80

$$\int_0^{a_G} r(\zeta) I_L(\zeta) d\zeta = I_G \int_0^{a_G} r(\zeta) d\zeta$$

The left side of the Equation 80 calculates the voltage drop on loads from the feeder's primary side ( $a = 0$ ) to DG location  $a_G$ ; the right side calculates the voltage rise caused by DG import power. By definition of voltage-effective power, Equation 80 can be written as

Equation 81

$$\int_0^{a_G} r(\zeta) (P_L^V(\zeta) - P_G^V) d\zeta = 0$$

Note that current is a complex variable in Equation 80, while voltage-effective power is a real variable. Transforming Equation 80 to Equation 81 reduces the integral operation from the complex domain to real domain. Solving Equation 81, the optimal DG output is,

Equation 34

$$P_G^V = \frac{\Delta V_L(a_G)}{R(a_G)}$$

where  $\Delta V_L(a_G)$  representing the voltage drop on loads from the feeder's primary side to the DG location  $a_G$ .  $R(a_G)$  is the feeder's resistance measured over the same distance, and is calculated by

Equation 35

$$R(a_G) = \int_0^{a_G} r(\zeta) d\zeta$$

By the equivalency of the apparent and real form of voltage-effective power (see Equation 7 and Equation 10), Equation 34 can be rewritten as

Equation 32

$$S_G^V = \frac{\Delta V_L(a_G)}{Z(a_G)}$$

where  $Z(a_G)$  is the total impedance measured from the feeder's primary side to the DG location, and is calculated as

Equation 33

$$Z(a_G) = \int_0^{a_G} z(\zeta) d\zeta$$

*Q.E.D.*

### ***Power delivery loss reduction by optimal DG output***

According to the Joule's Heating Law, the original loss induced by load on the feeder is  $LSS_0$  and is given by Equation 63. With DG penetration, current flowing on a feeder is expressed by Equation 64.

Because DG penetration does not affect the power flow and thus loss downstream of the DG unit, the loss reduction can be examined on the feeder only over the distance from its primary side to the DG location. Assuming DG output current  $I_G^*$  satisfies the Equal Voltage Rule (by Equation 32 or Equation 34), then the loss reduction induced is

Equation 82

$$\begin{aligned} \Delta LSS &= LSS_0 - LSS|_{I_G=I_G^*} = 2I_G \int_0^{a_G} I_L(\zeta)r(\zeta) d\zeta - (I_G^*)^2 \int_0^{a_G} r(\zeta) d\zeta \\ &= \frac{1}{R(a_G)} \left[ 2 \left( \int_0^{a_G} I_L(\zeta)r(\zeta) d\zeta \right)^2 - \left( \int_0^{a_G} I_L(\zeta)r(\zeta) d\zeta \right)^2 \right] \end{aligned}$$

By definition of voltage-effective power, Equation 82 can be rewritten as

Equation 83

$$\Delta LSS = \frac{\Delta V_L(a_G)^2}{R(a_G)}$$

where  $\Delta V_L(a_G)$  is the voltage drop purely caused by load at the given DG location  $a_G$ ;  $R(a_G)$  is the total resistance measured from the feeder's primary side to the DG location, expressed in Equation 35.

### B.3 Proof of Superposition Rule

**Proposition L.3a (Superposition Rule for optimal DG placement)** To induce minimum power delivery loss on the feeder, each time a DG unit should be placed at where the apparent power flow resultant from its downstream DG placement measures the half of its thermally limited capacity.

The mathematical form of Proposition L.3a is given in Equation 37. The optimal location of the  $i$ th DG,  $a_i^*$ , should satisfy

Equation 37

$$2\tilde{S}(a_i^*) = S_{G,i}$$

where  $\tilde{S}(a_i^*)$  is the apparent power flow on the feeder after the placement of the  $i$ th DG unit. Assuming  $N_G$  DG units of chosen capacities  $S_{G,n}$  are to be installed on a feeder system of load,  $\tilde{S}(a_i^*)$  is

Equation 38

$$\tilde{S}(a_i^*) = S_L(a_i^*) - \sum_{i+1}^{N_G} S_{G,n}$$

where  $S_L(a_i)$  is the apparent load power flow at DG location  $a_i^*$ .

#### **Proof:**

Given the unit resistance of a feeder's conductor is  $r \Omega \cdot km^{-1}$ , the power delivery loss on the feeder from the primary side until location  $a$  km and are calculated by the Joule's Heating Law:

Equation 63

$$LSS(a) = \int_0^a I_N(\zeta)^2 r(\zeta) d\zeta$$

where  $I_N(\zeta)$  is the net current flowing on location  $\zeta$ .

Current flowing on the feeder connected of  $N_G$  DG units can be expressed as

Equation 84

$$I_N = \begin{cases} I_L(a) - \sum_1^{N_G} I_{G,n}, & \text{if } a < a_1 \\ \vdots & \\ I_L(a) - \sum_i^{N_G} I_{G,n}, & \text{if } a < a_i \\ \vdots & \\ I_L(a), & \text{if } a > a_{N_G} \end{cases}$$

where  $I_L(a)$  is the current induced by load at location  $a$ ;  $I_{G,i}$  is the current output of the  $i$ th DG unit, which location is  $a_i$ . Substituting Equation 84 into Equation 63, the feeder's total power delivery loss is calculated as

Equation 85

$$\begin{aligned} LSS &= \int_0^l (I_L(\zeta) - I_G(\zeta))^2 r(\zeta) d\zeta \\ &= \int_0^{a_1} \left( I_L(\zeta) - \sum_1^{N_G} I_{G,n} \right)^2 r(\zeta) d\zeta + \int_{a_1}^{a_2} \left( I_L(\zeta) - \sum_2^{N_G} I_{G,n} \right)^2 r(\zeta) d\zeta + \dots \\ &\quad + \int_{a_{N_G-1}}^{a_{N_G}} (I_L(\zeta) - I_{G,N_G})^2 r(\zeta) d\zeta + \int_{a_{N_G}}^l I_L(\zeta)^2 r(\zeta) d\zeta \end{aligned}$$

According to the critical point theorem, the feeder's total power delivery loss is minimized when placing the  $i$ th DG is located at  $a_i$  that satisfies,



Equation 86

$$\frac{\partial L_{SS}}{\partial a_i} = \frac{\partial}{\partial a_i} \left[ \int_{a_{i-1}}^{a_i} \left( I_L(\zeta) - \sum_i^{N_G} I_{G,n} \right)^2 r(\zeta) d\zeta + \int_{a_i}^{a_{i+1}} \left( I_L(\zeta) - \sum_i^{N_G} I_{G,n} \right)^2 r(\zeta) d\zeta \right] = 0, \forall i$$

Based on the Leibniz Integral Rule,

Equation 86 can be written as

Equation 87

$$\left( I_L(a_i) - \sum_i^{N_G} I_{G,n} \right)^2 r(a_i) - \left( I_L(a_i) - \sum_{i+1}^{N_G} I_{G,n} \right)^2 r(a_i) = 0, \forall i$$

After some mathematical manipulations,

Equation 88

$$\left( 2 \sum_{i+1}^{N_G} I_{G,n} + I_{G,i} \right) I_{G,i} \cdot r(a_i) = 2I_L(a_i)I_{G,i} \cdot r(a_i), \forall i$$

Because  $I_{G,i} \cdot r(a_i) \neq 0$ , canceling off the term on both sides of Equation 88 gives

Equation 89

$$2\tilde{I}(a_i) = I_{G,i}$$

where  $\tilde{I}(a_i)$  is the load current at location of the  $i$ th DG unit,  $a_i$ , superposed by the current output of DG units downstream to the  $i$ th DG unit, and is expressed as

Equation 90

$$\tilde{I}(a_i) = I_L(a_i) - \sum_{i+1}^{N_G} I_{G,n}$$

Assuming the voltage at the DG location  $a_G$  drops from the feeder's primary voltage of amount  $\Delta V(a_G)$ , Equation 89 can be rewritten as

Equation 91

$$2\tilde{I}(a_i) \cdot \Delta V(a_i) = I_{G,i} \cdot \Delta V(a_i)$$

By definition of apparent power, this naturally leads to

Equation 37

$$2\tilde{S}(a_i^*) = S_{G,i}$$

and

Equation 38

$$\tilde{S}(a_i^*) = S(a_i^*) - \sum_{i+1}^{N_G} S_{G,n}$$

where  $S_L(a_i)$  is the apparent load power flow at DG location  $a_i^*$ ;  $S_{G,n}$  are thermal/ apparent power capacities of the  $n$ th DG unit.

*Q.E.D.*

**Proposition L.3b (Superposition Rule for optimal DG sizing)** The power delivery loss on a feeder is minimized if and only if the output voltage of every DG unit measures the same as the feeder's primary voltage.

The mathematical expression of Proposition L.3b is given by Equation 39. Assuming the DG locations are known and the  $i$ th DG location is  $a_i$ , then the optimal DG output is determined by

Equation 39

$$S_{G,i}^V = \frac{\Delta\tilde{V}(a_i)}{Z(a_i)}$$

where  $\Delta\tilde{V}(a_i)$  is the feeder's voltage profile with the  $i$ th DG import no power and measures as

Equation 40

$$\Delta\tilde{V}(a_i) = \Delta V_L(a_i) - \sum_{n \neq i}^{N_G} \Delta V_G(a_i)$$

**Proof**

Given the unit resistance of a feeder's conductor is  $r \Omega \cdot km^{-1}$ , the power delivery loss on the feeder are calculated by the Joule's Heating Law in Equation 63. For a feeder connected with  $N_G$  DG units at locations  $a_1, a_2, \dots, a_{N_G}$ , the induced current on the feeder is expressed by Equation 84. Therefore, the power delivery loss on the feeder can be expressed with Equation 85.

According to the Leibniz Integral Rule, the feeder's power delivery loss is minimized when operating the  $i$ th DG unit at output current  $I_{G,i}$  such that

Equation 92

$$\begin{aligned} \frac{\partial L_{SS}}{\partial I_{G,i}} = -2 \left[ \int_0^{a_1} \left( I_L(\zeta) - \sum_1^{N_G} I_{G,n} \right) r(\zeta) d\zeta + \int_{a_1}^{a_2} \left( I_L(\zeta) - \sum_2^{N_G} I_{G,n} \right) r(\zeta) d\zeta + \dots \right. \\ \left. + \int_{a_{i-1}}^{a_i} (I(\zeta) - I_{G,N_G}) r(\zeta) d\zeta \right] = 0, \quad \forall i \end{aligned}$$

Some mathematical manipulation on Equation 92 gives

Equation 93

$$I_{G,i} \int_0^{a_i} r(\zeta) d\zeta = \underbrace{\int_0^{a_i} I_L(\zeta) r(\zeta) d\zeta}_{term1} - \sum_1^{i-1} \underbrace{\left[ I_{G,n} \int_0^{a_n} r(\zeta) d\zeta \right]}_{term2} - \sum_{i+1}^{N_G} \underbrace{I_{G,n} \int_0^{a_i} r(\zeta) d\zeta}_{term3}, \quad \forall i$$

For Equation 93, the left side represents voltage drop caused by the  $i$ th DG. On the right side, *Term 1* represents voltage drop caused by the load; *Term 2* and *term 3* represents the voltage rise caused by DG output upstream and downstream to the  $i$ th unit respectively.

By definition of voltage-effective power, Equation 93 can be written as

Equation 94

$$P_{G,i}^V = \frac{\Delta\tilde{V}(a_i)}{R(a_i)}$$

where  $R(a_G)$  is the total resistance measured from the feeder's primary side to the DG location, expressed by Equation 35; and  $\Delta\tilde{V}(a_i)$  is the feeder's voltage profile with the  $i$ th DG import no power and measures as

Equation 40

$$\Delta\tilde{V}(a_i) = \Delta V_L(a_i) - \sum_{n \neq i}^{N_G} \Delta V_G(a_i)$$

which is equivalent to the left side of Equation 93.

By the equivalency of the apparent and real form of voltage-effective power (see Equation 7 and Equation 10), an alternative form of Equation 94 is

Equation 39

$$S_{G,i}^V = \frac{\Delta\tilde{V}(a_i)}{Z(a_i)}$$

where  $Z(a_i)$  is the total impedance measured from the feeder's primary side to the DG location, and is calculated by Equation 33.

*Q.E.D.*

### ***Power delivery loss reduction by optimal DG output***

Equation 83 gives the power loss reduction by operating a single DG unit at the optimal output. By Proposition L.2, it can be written as

Equation 95

$$\Delta L_{SS} = \frac{\Delta V_L(a_G)^2}{R(a_G)} = \frac{\Delta V_G(a_G)^2}{R(a_G)}$$

Given this result, for a feeder with  $N_G - 1$  DG units connected, adding one more DG unit at location  $a_i$  will reduce power delivery loss by

Equation 96

$$\Delta L_{SS_i} = \frac{\Delta \tilde{V}(a_i)^2}{R(a_i)} = \frac{\Delta V_{G,i}(a_i)^2}{R(a_i)}$$

where  $\Delta \tilde{V}(a_i)$  is the feeder's voltage profile with the  $i$ th DG import no power, so it is the voltage will be raised by the unit operating at the optimal output. Therefore, the total power loss reduction induced from simultaneously operating  $N_G$  units at their optimal output can be calculated as

Equation 97

$$\Delta L_{SS} = \sum_1^{N_G} \Delta L_{SS_i} = \sum_1^{N_G} \frac{\Delta \tilde{V}(a_i)^2}{R(a_i)}$$

**This result is summarized as the superposition rule of power loss reduction under optimal DG output.**

### **B.4 Proof of DG Variance Rule**

**Proposition L.4 (Modified Half Capacity Rule)** For minimum power loss over a time period, the DG unit should be placed at where half of the expected value plus normalized variance of its apparent power output measures the same as the expected apparent load flow on the feeder over the time period.

Proposition L.4 and the DG Variance Rule (Corollary L.4a and Corollary L.4b) can be presented with the same mathematical expression:

Equation 48

$$2\mathbf{E}[S_L(a^*)] = \mathbf{E}[S_G] + \widetilde{\mathbf{Var}}(S_G)$$

where  $E[S_L(a^*)]$  is the expected value of apparent load flow on the feeder;  $E[S_G]$  is the expected output of the DG unit to be placed; and  $\widetilde{\mathbf{Var}}(S_G)$  is the normalized VER variance, which is

Equation 49

$$\widetilde{\mathbf{Var}}(S_G) = \frac{\mathbf{Var}(S_G)}{\mathbf{E}[S_G]}$$

**Proof**

For load varying with time, the total power loss on a feeder is evaluated as the expected value over the probability distribution region of load current profile,  $I_L(a)$ , and the DG output current  $I_G$ .

Equation 98

$$\mathbf{E}[Lss] = \int_{I_L(a)} \int_{I_G} Lss(I_L(a), I_G) \Omega(I_L(a), I_G) dI_G dI_L(a)$$

where  $\Omega(I_L(a), I_G)$  is the joint Probability Distribution Function (PDF) of current of load and DG on the feeder.

According to the Critical Point Theorem, the expected total loss is minimized by placing the DG unit at location  $a_G$  that satisfies

Equation 99

$$\frac{\partial \mathbf{E}[Lss]}{\partial a_G} = \frac{\partial}{\partial a_G} \int_{I_L(a)} \int_{I_G} Lss(I_L(a), I_G) \Omega(I_L(a), I_G) dI_G dI_L(a) = 0$$

According to Leibniz Integral Rule, Equation 99 is calculated as

Equation 100

$$\frac{\partial \mathbf{E}[Lss]}{\partial a_G} = \int_{I_L(a)} \int_{I_G} \left[ \frac{\partial}{\partial a_G} Lss(I_L(a), I_G) \right] \Omega(I_L(a), I_G) dI_G dI_L(a) = 0$$

It has been proved by Equation 66 to Equation 68 that

$$\frac{\partial}{\partial a_G} LSS(I_L(a), I_G) = (2I_L(a_G)I_G - I_G^2) r(a_G)$$

Therefore, Equation 100 is simplified as

Equation 101

$$\frac{\partial \mathbf{E}[LSS]}{\partial a_G} = \int_{I_L(a)} \int_{I_G} \underbrace{(I_G^2 - 2I_L(a_G)I_G)r(a_G)}_{\text{term 1}} \Omega(I_L(a), I_G) dI_G dI_L(a)$$

*Term 1* is a function of the DG location  $a_G$  and is independent of other locations  $a$  on the feeder. Hence, Equation 101 can be reduced to integral on the probability distribution region of  $I_L(a_G)$  only, instead of on the load current profile of the whole feeder  $I_L(a)$ . That is,

Equation 102

$$\frac{\partial \mathbf{E}[LSS]}{\partial a_G} = \int_{I_L(a_G)} \int_{I_G} (I_G^2 - 2I_L(a_G)I_G)r(a_G) \Omega(I_L(a_G), I_G) dI_G dI_L(a_G) = 0$$

Since the load current at DG location  $a_G$  and DG output are not correlated variables, the joint PDF of the two variables can be written as the product of their distribution probability  $\omega_L(a_G)$  and  $\omega_G$ :

Equation 103

$$\Omega(I_L(a_G), I_G) = \omega_L(a_G) \cdot \omega_G$$

Substitute Equation 103 into Equation 101, it renders

Equation 104

$$2 \left( \int_{I_L(a_G)} I_L(a_G) \omega_L(a_G) dI_L(a_G) \right) \left( \int_{I_G} I_G \omega_G dI_G \right) = \left( \int_{I_L(a_G)} \omega_L(a_G) dI_L(a_G) \right) \left( \int_{I_G} I_G^2 \omega_G dI_G \right)$$

By definition of expected value and property of probability density function, Equation 104 is rewritten as

Equation 105

$$2\mathbf{E}[I_L(a_G)]\mathbf{E}[I_G] = 1 \cdot \mathbf{E}[I_G^2]$$

By the equivalency of the second cumulant and variance of a random variable, the left side of Equation 105 is

Equation 106

$$\mathbf{E}[I_G^2] = \frac{\mathbf{E}[I_G]^2 + \mathbf{Var}(I_G)}{\mathbf{E}[I_G]} = \mathbf{E}[I_G] + \widetilde{\mathbf{Var}}(I_G)$$

where  $\widetilde{\mathbf{Var}}(I_G)$  is DG current's variance normalized by its expected value, and is expressed as

Equation 107

$$\widetilde{\mathbf{Var}}(I_G) = \frac{\mathbf{Var}(I_G)}{\mathbf{E}[I_G]}$$

Relaxation of Equation 107 gives its apparent power form that finds optimal DG location  $a^*$  in Equation 48. This relaxation is elaborated in the end of this subsection.

Equation 48

$$2\mathbf{E}[S_L(a^*)] = \mathbf{E}[S_G] + \widetilde{\mathbf{Var}}(S_G)$$

where

Equation 49

$$\widetilde{\mathbf{Var}}(S_G) = \frac{\mathbf{Var}(S_G)}{\mathbf{E}[S_G]}$$

*Q.E.D.*

### ***Implementation of Modified Half Capacity Rule***

In the Modified Half Capacity Rule, notice that the expected apparent load flow does not equal to the flow of expected apparent load density. In other words, apparent load power flow needs to be estimated inside the expectation operator,



Equation 108

$$\mathbf{E}[S_L(a^*)] = \mathbf{E} \left[ \int_{a^*}^l s_L(\zeta) d\zeta \right]$$

and

Equation 109

$$\mathbf{E}[S_L(a^*)] \neq \int_{a^*}^l \mathbf{E}[s_L(\zeta)] d\zeta$$

This is because of the functional non-variance property of expected value<sup>11</sup>. Therefore, when implementing the Modified Half Capacity Rule, all possible values of load power flow should be estimated and then is the apparent load power flow's expected value.

***Error induced under the apparent power form***

Transforming from Equation 106 to Equation 48 is justified by the two reasons stated at the end of Section B.1: the application ease, and the accuracy and optimality of DG location. This transformation, however, requires a relaxation that generates ignorable but still errors. Both the relaxation and its induced error are discussed here.

Multiplying both sides of Equation 105 by squared expected value of voltage drop on loads at the DG location, it renders

Equation 110

$$2\mathbf{E}[I_L(a_G)]\mathbf{E}[I_G]\mathbf{E}[\Delta V_L(a_G)]^2 = \mathbf{E}[I_G^2]\mathbf{E}[\Delta V_L(a_G)]^2$$

By the equivalency of the second cumulant and variance of a random variable, Equation 110 is written as

Equation 111

$$2(\mathbf{E}[I_L(a_G)]\mathbf{E}[\Delta V_L(a_G)])(\mathbf{E}[I_G]\mathbf{E}[\Delta V_L(a_G)]) = \mathbf{E}[I_G^2] \left( \mathbf{E}[\Delta V_L(a_G)^2] - \mathbf{Var}(\Delta V_L(a_G)) \right)$$

---

<sup>11</sup> In general, the expectation operator and functions of random variables do not commute; that is  $\mathbf{E}[g(X)] = \int_{\Omega} g(X) dP \neq g(\mathbf{E}[X])$ . A notable inequality concerning this topic is Jensen's inequality, involving expected values of convex (or concave functions).

By definition of covariance, the left side of Equation 111 is expanded as

Equation 112

$$\begin{aligned} & (\mathbf{E}[I_L(a_G)]\mathbf{E}[\Delta V_L(a_G)])(\mathbf{E}[I_G]\mathbf{E}[\Delta V_L(a_G)]) \\ &= \left( \mathbf{E}[I_L(a_G) \cdot \Delta V_L(a_G)] - \mathbf{Cov}(I_L(a_G), \Delta V_L(a_G)) \right) \left( \mathbf{E}[I_G \cdot \Delta V(a_G)] - \mathbf{Cov}(I_G, \Delta V_L(a_G)) \right) \end{aligned}$$

Because of voltage on a distribution feeder is controlled within a predefined range and has little variation, the covariance of load current, DG current and voltage at the DG location is ignorable. Therefore, the left side of Equation 111 is relaxed to

Equation 113

$$\begin{aligned} & (\mathbf{E}[I_L(a_G)]\mathbf{E}[\Delta V_L(a_G)])(\mathbf{E}[I_G]\mathbf{E}[\Delta V_L(a_G)]) \approx \mathbf{E}[I_L(a_G) \cdot \Delta V_L(a_G)]\mathbf{E}[I_G \cdot \Delta V(a_G)] \\ &= \mathbf{E}[S_L(a_G)]\mathbf{E}[S_G] \end{aligned}$$

For the same reason, voltage variance at the DG location can be ignored. Hence, the right side of Equation 111 is relaxed to

Equation 114

$$\begin{aligned} & \mathbf{E}[I_G^2] \left( \mathbf{E}[\Delta V_L(a_G)^2] - \mathbf{Var}(\Delta V_L(a_G)) \right) \approx \mathbf{E}[I_G^2]\mathbf{E}[\Delta V_L(a_G)^2] \\ &= \mathbf{E}[I_G^2 \cdot \Delta V_L(a_G)^2] - \mathbf{Cov}(I_G^2, \Delta V_L(a_G)^2) \\ &\approx \mathbf{E}[I_G^2 \cdot \Delta V_L(a_G)^2] \\ &= \mathbf{E}[S_G^2] \end{aligned}$$

From all above steps, the analytical expression of the error induced from the relaxation of the whole transformation is

Equation 115

$$\begin{aligned} \xi &= 2\mathbf{E}[I_L(a_G)\Delta V_L(a_G)]\mathbf{Cov}(I_G, \Delta V_L(a_G)) + 2\mathbf{E}[I_G\Delta V_L(a_G)]\mathbf{Cov}(I_L(a_G), \Delta V_L(a_G)) \\ &\quad - \mathbf{E}[I_G^2]\mathbf{Var}(\Delta V_L(a_G)) - \mathbf{Cov}(I_G^2, \Delta V_L(a_G)^2) - 2\mathbf{Cov}(I_L(a_G), \Delta V_L(a_G))\mathbf{Cov}(I_G, \Delta V_L(a_G)) \end{aligned}$$

***Proof of Modified Half Capacity Rule for multiple-DG-unit placement***

For  $N_G$  units, the optimal placement of the  $i$ th unit, counted from the feeder's primary side, should satisfy

Equation 51

$$2\mathbf{E}[\tilde{S}(a_i^*)] = \mathbf{E}[S_{G,i}] + \widetilde{\mathbf{Var}}(S_{G,i}), \forall i$$

where  $\mathbf{E}[\tilde{S}(a_i^*)]$  is expected value of the load power flow superposed by DG output downstream of the  $i$ th unit, and is calculated by

Equation 52

$$\mathbf{E}[\tilde{S}(a_i^*)] = \mathbf{E}[S(a_i^*)] - \sum_{i+1}^{N_G} \mathbf{E}[S_{G,n}]$$

and  $\widetilde{\mathbf{Var}}(S_{G,i})$  is the apparent power output variance of the  $i$ th DG unit normalized by its expected value, and is expressed by

Equation 49

49

$$\widetilde{\mathbf{Var}}(S_{G,i}) = \frac{\mathbf{Var}(S_{G,i})}{\mathbf{E}[S_{G,i}]}$$

***Proof***

For a feeder connected with  $N_G$  DG units, its expected value of delivery power loss is evaluated on the probability distributions of all DG output and loads, and is expressed as

Equation 116

$$\mathbf{E}[L_{SS}] = \int_{I_L(a)} \int_{J_G} L_{SS}(I_L(a), J_G) \Omega(I_L(a), J_G) dJ_G dI_L(a)$$

where  $\mathcal{J}_G = \{I_{G,1}, I_{G,2}, \dots, I_{G,N_G}\}$  represents the set of DG current output; and  $\Omega(I_L(a), \mathcal{J}_G)$  represents the joint Probability Distribution Function (PDF) of current output of loads and all the DG units on the feeder.

According to the Critical Point Theorem, the expectation of power delivery loss is minimized if placing the  $i$ th DG unit at location  $a_i$  that satisfies

Equation 117

$$\frac{\partial \mathbf{E}[L_{ss}]}{\partial a_i} = \int_{I_L(a)} \int_{\mathcal{J}_G} \left[ \frac{\partial}{\partial a_i} L_{ss}(I_L(a), \mathcal{J}_G) \right] \Omega(I_L(a), \mathcal{J}_G) d\mathcal{J}_G dI_L(a) = 0, \quad \forall i$$

In the proof of Section B.3,

**Equation 86** to Equation 88 shows that

$$\frac{\partial}{\partial a_i} L_{ss}(I_L(a), \mathcal{J}_G) = 2 \left( \sum_{i+1}^{N_G} I_{G,n} - I_L(a_i) I_{G,i} \right) I_{G,i} \cdot r(a_i) + I_{G,i}^2 \cdot r(a_i), \quad \forall i$$

Hence, Equation 117 is written as,

Equation 118

$$\underbrace{2 \int_{I_L(a)} \int_{\mathcal{J}_G} \left( I_L(a_i) - \sum_i^{N_G} I_{G,n} \right) I_{G,i} \cdot \Omega(I_L(a), \mathcal{J}_G) d\mathcal{J}_G dI_L(a)}_{\text{term1}} \\ = \int_{I_L(a)} \int_{\mathcal{J}_G} I_{G,i}^2 \cdot \Omega(I_L(a), \mathcal{J}_G) d\mathcal{J}_G dI_L(a)$$

Notice that integral in *term 1* only has load current variable at location  $a_i$ , which reduces the integral region. And this term is simplified as

Equation 119

$$\begin{aligned}
term1 &= \int_{I_L(a_i)} \int_{J_G} I_L(a_i) I_{G,i} \Omega(I_L(a_i), J_G) dJ_G dI_L(a_i) \\
&\quad - \int_{I_L(a)} \int_{J_G} \left( \sum_i^{N_G} I_{G,n} \right) I_{G,i} \Omega(I_L(a), J_G) dJ_G dI_L(a)
\end{aligned}$$

Assume the load and all DG output are uncorrelated<sup>12</sup>, the joint PDF of load and DG current output is therefore decoupled:

Equation 120

$$\Omega(I_L(a_i), J_G) = \omega_L(a_i) \cdot \prod_1^{N_G} \omega_{G,n}$$

Substituting Equation 119 and Equation 120 into Equation 118 gives

Equation 121

$$\begin{aligned}
&2 \left( \underbrace{\int_{I_L(a_i)} I_L(a_i) \omega_L(a_i) dI_L(a_i) - \sum_i^{N_G} \int_{I_{G,n}} I_{G,n} \omega_{G,n} dI_{G,n}}_{term\ 1} \right) \left( \int_{I_{G,i}} I_{G,i} \omega_{G,i} dI_{G,i} \right) \\
&= \left( \int_{I_L(a_i)} I_L(a_i) dI_L(a_i) \right) \left( \int_{I_{G,i}} I_{G,i}^2 \omega_{G,i} dI_{G,i} \right)
\end{aligned}$$

By definition and linearity property of expected values, *term 1* on the left side of Equation 121 is written as,

Equation 122

$$term1 = E[I_L(a_i)] - \sum_{i+1}^{N_G} E[I_{G,n}]$$

---

<sup>12</sup> In some cases, say DG such as wind turbine, their output may be correlated. It is believed that the output of wind turbines at the tail of wind's direction is less than that at the front of the wind, mainly due the wind power has been reaped by DG gradually. This effect is assumed to be small, for the reason that only usually limited number of such VEs are integrated on a feeder system, and is ignored here.

$$= \mathbf{E} \left[ I_L(a_i) - \sum_{i+1}^{N_G} I_{G,n} \right]$$

Define  $\tilde{I}_L(a_i)$  as the load current superposed with DG current output downstream to the  $i$ th DG unit, expressed as

Equation 123

$$\tilde{I}_L(a_i) = I_L(a_i) - \sum_{i+1}^{N_G} I_{G,n}$$

Substituting Equation 122 and Equation 123 into Equation 121 renders

Equation 124

$$2\mathbf{E}[\tilde{I}_L(a_i)]\mathbf{E}[I_{G,i}] = 1 \cdot \mathbf{E}[I_{G,i}^2]$$

Following the same relaxation procedure in the proof of Modified Half Capacity Rule for a single DG unit, Equation 124 is transformed to its apparent power form that finds the optimal  $i$ th DG location  $a_i^*$ , expressed as

Equation 51

$$2\mathbf{E}[\tilde{S}(a_i^*)] = \mathbf{E}[S_{G,i}] + \widetilde{\text{Var}}(S_{G,i}), \forall i$$

where

Equation 52

$$\mathbf{E}[\tilde{S}(a_i^*)] = \mathbf{E}[S(a_i^*)] - \sum_{i+1}^{N_G} \mathbf{E}[S_{G,n}]$$

and

Equation 49

$$\widetilde{\text{Var}}(S_{G,i}) = \frac{\text{Var}(S_{G,i})}{\text{E}[S_{G,i}]}$$

*Q.E.D.*

## Appendix C

---

This appendix includes the primary parameters of the testing distribution system in Section 1.2.2

### *Data of the São Miguel Island system*

The configuration of the whole test system is shown in Figure 9. The parameters of two major components in the system, transformers and feeders, are summarized in Table 17 and Table 18. Since this thesis demonstrates its proposed methods on feeder-system level, only general information is included here of the overall distribution system. Some extra information, such as parameters of feeder's conductors, is presented in Table 14 in Appendix A.

Table 15. Number of Components.

nodes	line sections	substations	supply	loads
<b>1,956</b>	1,957	9	39	781

supply includes all transformers at substation that sources the feeders in the system and DG units when they are connected in tests.

Table 16. System Capacity.

substation capacity (MVA)	load capacity (MVA)	capacity margin	
		real power (MW)	reactive power (MVar)
<b>194.000</b>	234.504	62.959	28.253

capacity margin = supply capacity – load capacity, where supply capacity equals to substation capacity when no DG is penetrated in the system.

Table 17. Transformers.

voltage levels (kV)	60 / 30	60 / 10	60 / 6	30 / 10	total
---------------------	---------	---------	--------	---------	-------

<b>number</b>	4	7	4	6	25
<b>power rating (MVA)</b>	50	76	40	28	194

Table 18. Feeders.

<b>voltage level (kV)</b>	<b>overhead (m)</b>	<b>underground (m)</b>	<b>total (m)</b>
<b>60.0</b>	58399.2	0.0	58399.2
<b>30.0</b>	373137.2	22607.8	395745.0
<b>10.0</b>	76346.4	146603.9	222950.2
<b>Total</b>	507882.8	169211.7	677094.5

*Data of the testing feeder system*

The configuration of the testing feeder system is given in Figure 10.

Table 19. Power Balance.

	<b>apparent power (kVA)</b>	<b>real power (kW)</b>	<b>reactive power (kVar)</b>
<b>supply</b>	1,110.276	978.968	523.770
<b>load</b>	1,068.312	959.595	469.539
<b>loss</b>	57.587	19.373	54.231

Table 20. Power Delivery Loss.

	<b>real power (kW)</b>	<b>reactive power (kVar)</b>	<b>energy (MWh)</b>
<b>total feeder loss</b>	3.0	1.2	8.6
<b>total trans. loss</b>	16.4	53.0	55.2
<b>total loss</b>	19.4	54.2	63.7

Table 21. Operation Status Measured at Feeders' Substations.

<b>feeder system</b>	<b>load</b>		<b>real power (kW)</b>	<b>loss</b>	
	<b>power rating (kVA)</b>	<b>power factor (cos<math>\theta</math>)</b>		<b>dissipation %</b>	<b>energy (MWh)</b>
<b>Feeder 1</b>	469.4	0.985	0.990	0.214	2.820
<b>Feeder 2</b>	537.4	0.929	2.022	0.405	5.757

The power factors are measured at where the power is injected into the feeders, namely feeders' primary side.



Table 22 presents the load capacity at every nodes of the feeder system. In each numerical example Table 23 gives the power delivery status for the two feeders in the test system. The parameters are presented on basis of line sections. The voltage basis here is 10 kV, with  $V_1$  and  $V_2$  defined as the voltages of each section's two ends.

Table 22. Load Capacity.

ID	Apparent Power (MVA)	Real Power (MW)	Reactive Power (MVar)	Power Factor $\cos\theta$
2PT0018	630	43.9	17.4	0.930
2PT0081	200	10.8	5.1	0.904
2PT1057	–	264.0	152.5	0.866
2PT0016	315	22.0	8.7	0.930
2PT0017	630	33.9	16.0	0.904
2PT0019	500	34.9	13.8	0.930
2PT0020	630	43.9	17.4	0.930
2PT0236	315	27.7	16.0	0.866
2PT0316	315	22.0	8.7	0.930
2PT0325	315	27.7	16.0	0.866
2PT0328	315	16.9	8.0	0.904
2PT0329	630	43.9	17.4	0.930
2PT0362	160	11.2	4.4	0.930
2PT0402	315	16.9	8.0	0.904
2PT1199	315	16.9	8.0	0.904
2PT1015	400	21.5	10.2	0.904
2PT1052	315	27.7	16.0	0.866
2PT1050	400	27.9	11.0	0.930
2PT1122	100	5.4	2.5	0.904
2PT1123	630	55.4	32.0	0.866
2PT1182	315	16.9	8.0	0.904
2PT1235	100	7.0	2.8	0.930
2PT1253	100	7.0	2.8	0.930
2PT1284	315	22.0	8.7	0.930
2PT1385	250	22.0	12.7	0.866

<b>2PT1389</b>	630	43.9	17.4	0.930
<b>2PT0425</b>	250	17.4	6.9	0.930
<b>2PT1440</b>	500	26.9	12.7	0.904
<b>2PT0327</b>	315	22.0	8.7	0.930

In this thesis, the load consumption is scaled to a percentage under a certain circumstance, for example 50% of the full capacity. These specific scales are stated in the numerical examples.

Table 23. Feeder Power Delivery Status.

line section ID	length (m)	current (A)	power flow		power delivery loss		Voltage (p. u.)	
			real (kW)	reactive (kVar)	real (kW)	reactive (kVar)	V <sub>1</sub>	V <sub>2</sub>
<b>Feeder 1</b>								
10_LXHIOV_240_S	882.0	25.8	462.462	80.190	0.2825	0.1615	1.05000	1.04932
10_LXHIOV_240_S	233.7	19.6	350.414	58.222	0.0430	0.0246	1.04842	1.04829
10_LXHIOV_050_S	7.0	0.3	5.369	2.506	0.0000	0.0000	1.04842	1.04842
10_LXHIOV_240_S	322.2	21.1	377.327	65.786	0.0689	0.0394	1.04863	1.04842
10_LXHIOV_050_S	103.3	1.3	21.477	9.718	0.0004	0.0001	1.04842	1.04840
10_LXHIOV_240_S	435.9	5.2	92.475	20.000	0.0057	0.0033	1.04679	1.04672
10_LXHIOV_240_S	486.8	2.3	41.711	8.637	0.0013	0.0007	1.04672	1.04669
10_LXHIOV_035_S	219.9	0.4	6.952	1.939	0.0001	0.0000	1.04672	1.04671
10_LXHIOV_240_S	714.0	14.9	267.954	40.481	0.0765	0.0438	1.04789	1.04757
10_LXHIOV_240_S	77.6	15.5	278.698	39.113	0.0090	0.0051	1.04793	1.04789
10_LXHIOV_240_S	675.7	12.5	224.044	36.856	0.0509	0.0291	1.04757	1.04732
10_PHCA#_016_S	409.1	1.3	21.921	7.100	0.0027	0.0002	1.04757	1.04745
10_LXHIOV_240_S	593.3	24.9	445.265	83.329	0.1772	0.1013	1.04932	1.04887
10_LXHIOV_240_S	365.2	22.0	394.317	68.559	0.0852	0.0487	1.04887	1.04863
10_LXHIOV_050_S	243.4	1.0	16.910	6.998	0.0006	0.0001	1.04887	1.04884
10_LXHIOV_050_S	502.7	0.4	6.951	0.697	0.0002	0.0000	1.04669	1.04666
10_LXHIOV_240_S	450.8	7.7	136.297	30.503	0.0129	0.0074	1.04690	1.04679
10_LXHIOV_240_S	220.8	18.6	333.470	53.695	0.0367	0.0210	1.04829	1.04816
10_LXHIOV_240_S	371.7	17.0	305.591	47.600	0.0519	0.0296	1.04816	1.04797
10_LXHIOV_240_S	341.1	8.9	158.214	33.107	0.0130	0.0075	1.04699	1.04690
10_LXHIOV_240_S	947.2	11.4	202.087	40.573	0.0588	0.0336	1.04732	1.04699
10_LXHIOV_240_S	50.9	15.5	278.698	39.113	0.0059	0.0034	1.04795	1.04793
10_LXHIOV_240_S	50.3	17.0	305.591	47.600	0.0070	0.0040	1.04797	1.04795
<b>Feeder 2</b>								
10_LXHIOV_120_S	1,073.2	29.5	499.146	199.106	0.9119	0.2851	1.05000	1.04814
10_LXHIOV_120_S	444.1	21.7	364.490	146.589	0.2031	0.0635	1.04625	1.04568
10_LXHIOV_240_S	1,183.5	5.5	100.259	5.563	0.0175	0.0100	1.04568	1.04549
10_LXHIOV_240_S	596.2	1.0	17.430	2.362	0.0003	0.0002	1.04534	1.04532
10_LXHIOV_240_S	404.9	3.5	61.363	12.131	0.0023	0.0013	1.04538	1.04534
10_LXHIOV_240_S	206.9	26.8	447.728	189.341	0.0716	0.0409	1.04642	1.04625
10_PHCA#_016_S	160.6	3.5	55.447	31.397	0.0082	0.0007	1.04625	1.04612
10_LXHIOV_120_S	1,044.3	28.1	470.514	194.821	0.7997	0.2500	1.04814	1.04642
10_LXHIOV_240_S	983.4	4.0	72.522	6.006	0.0076	0.0044	1.04549	1.04538

# Appendix D

---

This appendix includes the MATLAB code used in the simulations of this thesis, and settings and output of DPlan that is interfaced with MATLAB.

```

%%%%%%%%%%%%%%%%%%%%%%%%%%%%%%%%%%%%%%%%%%%%%%%%%%%%%%%%%%%%%%%%%%%%%%%%
%%%%%%%%
%Tree plot of data of DPlan
%JK Wang, 111912
% The same version as beta1,edited for 39 feeders plot
of whole S.M. island
% Updated for Matlab 2012b, which imports data in a
whole cell array
%%%%%%%%%%%%%%%%%%%%%%%%%%%%%%%%%%%%%%%%%%%%%%%%%%%%%%%%%%%%%%%%%%%%%%%%
%%%%%%%%
% approx: power flow used to calculate Pv is Pv - losses

function [A,XY] =
FdTr_final3(flag,data,NdEq,desid,rtid)
    % Function head for exporting data for plots

%function
[NdLst,EdgLst,TrLst,Vnum,lvlnum,Enum]=FdTr(flag,data,NdEq,desid,rtid)
%flag:    (double/binary) == 0 point measurement,e.g.
voltage; == 1 section measurement, e.g. power
%Vnum:    (double) node/vertex number
%Enum:    (double) feeder/edge number
%lvlnum:  (double) depth/level number
%NdLst:   (cell matrix) node list: {'node name'}No table
of figures entries found.{voltage}{node depth}
%        size = Vnum * 3
%EdgLst:  (double matrix) edge list: [in source id][out
destiny id]
%        size = Edgnum * 2
%TrLst:   (double matrix) tree structure of the input
distribution system
%        (node id)(parent)(number of
children)[(Children)()...]
%        size = Vnum * 2+
%data:    (cell array) import data: total col# = 14
%NdEq:    (cell array) connected nodes with no voltage
drop in between in conjunction box
%rtid:    (string) name of the root node||cannot
detected by parent depth=0
%        due to the massive naming of line sections. A
program determines

```

```

%        root by depth == 0 is FdTr_final1.m
%desid:   (string) name of the destiny node||='null'
including braches;o.w.
=====
%load
data
        %data for testing purpose
%load textdata
=====
% All list in this program is vertical (i.e. row
sequenced)
% Data import
x2r =
0.092/0.16;
        % x to r ratio
Vlim =
1.05;
        % maximum voltage allowed
% change cvol to column of parameter interested
if flag
    cvol =
9;
        %voltage effective power
else
    cvol =
13;
        %voltage
end

Enum = size(data,1);
fv = data(:, [2,1,cvol,cvol+1]); %swap node of a line
section, power is measured at end node
%Combine equivalent nodes
% =====
%NdEq = [{'EDXX001NI5'}, {'EDXX001NIB'},
{'EDXX001NIE'}, {'EDXX001NI8'}]';
if ~isempty(NdEq)
    for kk = 2:size(NdEq,1)
        NdTmp = cell(Enum,2);
        NdTmp(:, :) = NdEq(kk);
        [m n]= find(cellfun(@strcmp,fv(:,1:2),NdTmp),1);
        idx = sub2ind(size(fv),m,n);

```

```

        fv(idx) = NdEq(1);
    end
end
%% build edge list and node list
%flag: (double/binary) == 0 point measurement, e.g.
voltage; == 1 section measurement, e.g. power
clear NdLst
clear EdgLst
Vnum = 1;
for i = 1:Enum*2
    if i==1
        NdLst(Vnum,1:2+flag) = [fv(i,1),fv(i,3:3+flag)];
        EdgLst(i,1)= Vnum;
    else
        % Power flow counts on the in source
        if i> Enum
            ii = i - Enum;
            ij = 2;
        else
            ii = i;
            ij = 1;
        end
        NdTmp = cell(Vnum,1);
        NdTmp(:, :) = fv(ii,ij);
        NdEst =
find(cellfun(@strcmp,NdLst(:,1),NdTmp),1);
        if isempty(NdEst)
            Vnum = Vnum + 1;
            cind = flag+ij*(~flag)+2;
            NdLst(Vnum,1:2+flag)=
[fv(ii,ij),fv(ii,cind:cind+flag)];
            EdgLst(ii,ij) = Vnum;
        else
            EdgLst(ii,ij) = NdEst;
        end
    end
end
end
if flag
    NdLst(:,2) = num2cell(cell2mat(NdLst(:,end)).*x2r+
cell2mat(NdLst(:,end-1)));
    NdLst(:,3) = [];
end

```

```

end
%% generate tree structure/list
if ~isempty(rtid)
    NdTmp = cell(Vnum,1);
    NdTmp(:, :) = {rtid};
    rt = find(cellfun(@strcmp,NdLst(:,1),NdTmp),1);
else
    display('Cannot find the root node.')
    return
end
if ~isempty(desid)
    NdTmp = cell(Vnum,1);
    NdTmp(:, :) = {desid};
    des = find(cellfun(@strcmp,NdLst(:,1),NdTmp),1);
    if isempty(des)
        display('Cannot find the destination node.')
        return
    end
end
clear TrLst
TrLst = [(1:Vnum)',zeros(Vnum,2)];
TrLst = genTr(EdgLst,rt,TrLst);
%leaves' children # = 0, root parent = 0
% for i = 1:Enum
% %     Ndid = EdgLst(i,1);
% %     Ndch = EdgLst(i,2);
%     Ndid = EdgLst(i,2);
%     Ndch = EdgLst(i,1);
%     TrLst(Ndid,3)= TrLst(Ndid,3) + 1;
%     Chnum = TrLst(Ndid,3);
%     TrLst(Ndid,Chnum + 3)= Ndch;
%     TrLst(Ndch,2) = Ndid;
% end
%% generating Node list with (x,y)=(node depth/level,
voltage)
if strcmp(desid, '')
    mainfd = 0;
else
    mainfd = 1;
end
switch mainfd
    case 0

```

```

lvlnum = 0;
clear Q
if TrLst(rt,3)==0
    display('isolated node')
    return
else
    NdLst(rt,3) = {lvlnum};
    Chnum = TrLst(rt,3);
    Q(:,1) = TrLst(rt,4:Chnum+2);
    lvlnum = lvlnum + 1;
    Q(:,2) = lvlnum;
    NdTmp = cell(size(Q,1),1);
    NdTmp(:,:)= {lvlnum};
    NdLst(Q(:,1),3) = NdTmp;
    while size(Q,1)~=0
        lvlnum = Q(1,2);
        NdLst(Q(1,1),3) = {lvlnum};
        NxtNd = Q(1,1);
        if TrLst(NxtNd,3)~=0
            Chnum = TrLst(NxtNd,3);
            QTmp = TrLst(NxtNd,4:Chnum +
3)';
            %can't use 'end' instead of
            'chnum +3'; end can be 0
            QTmp(:,2) = lvlnum + 1;
            Q = [Q; QTmp];
        end
        Q(1,:) = [];
    end
end
case 1
% find a defined feeder

    lvlnum = 1;
    NdLst(des,3) =
{lvlnum};
%set
the destiny level = 1 (not=0 to distinguish from other
NdLst unassigned elements)and flip with root level at
last;
    NdPnt = TrLst(des,2);
    while NdPnt~=0
        lvlnum = lvlnum + 1;

```

```

        if lvlnum == 46
            display('there')
        end
        NdLst(NdPnt,3) = {lvlnum};
        NdPnt = TrLst(NdPnt,2);
    end
    Brch = cellfun(@isempty,NdLst(:,3));
    Brch = find(Brch==1);

NdLst(Brch,:)=[];
    %delete branches
    lenmfd =
size(NdLst,1);
    % length of main/defined feeder
    NdLst(:,3) = num2cell(abs(cell2mat(NdLst(:,3))-
lenmfd));
end
%% Plot voltage figure
XY = cell2mat(NdLst(:,2:3));
XY(:, [1,2])=
XY(:, [2,1]);
    % swap columns

figure
hold on
switch mainfd
    case 0
        A = zeros(Vnum, Vnum);
        for i = 1:Enum
            A(EdgLst(i,1),EdgLst(i,2)) = 1;
        end
        gplot(A,XY,'.-')
    case 1
        A = [];
        [x,ind] = sort(XY(:,1));
        XY = XY(ind,:);
        plot(x,XY(:,2),'.-');
end
if flag
    plot(x,zeros(lenmfd,1),'LineWidth',2,'Color','green')
    ylabel('P_v(kW)');
else

```

```

plot(x,Vlim*ones(lenmfd,1),'LineWidth',2,'Color','red')
    ylabel('V (p.u.)')
end
% Shaded area can be implemented by the following
program; Multiple
% shadows needs extra efforts of programming, and is
implemented by post
% graph with paint board at the time of 0707
% if mainfd
%     ymax = max(max(ref,XY(:,2)));
%     ymin = min(min(ref,XY(:,2)));
%     shadedplot(x',XY(:,2) ',ref','g');
% end
% ylim([ymin-0.002,ymax+0.002])
% xlim([0,lenmfd-1])
xlabel('Node');
set(gca,'XTick',0:1:lenmfd-1)

%ylable ('Q (kVar)')
grid on

```

---

```

%generate a tree list by a recursive function
function TrLst = genTr(EdgLst,prnt,TrLst)
%function TrLst = genTr(EdgLst,prnt,TrLst,des)
% TrLst    (double matrix) tree structure of the input
distribution system
%         (node id) (parent) (number of
children) [(Children) () ...]
%         size = Vnum * 2+
%EdgLst:  (double matrix) edge list: [in source id][out
destiny id]
%         size = Edgnum * 2
%rtid:    (string) name of the root node
[r,c] = find(EdgLst== prnt);
rc = [r,c];
if TrLst(prnt,2)== 0 %if root
    Chnum = size(r,1); %minors its parent branch
else
    [r1,c1] = find(EdgLst(r,:) == TrLst(prnt,2));

```

```

    rc(r1,:)=[]; %delete parent branch
    r = rc(:,1);
    c = rc(:,2);
    Chnum = size(r,1);
end
TrLst(prnt,3) = Chnum;
if Chnum == 0
    display(prnt)
end
for i = 1:Chnum
    if c(i) == 1
        Chld = EdgLst(r(i),2);
    else
        Chld = EdgLst(r(i),1);
    end
    % if child == destiny or reach the end (child is the
node's parent, pointing back to its parent branch)
%     if (Chld == des)
%         display('reach destiny')
%         return
%     end

```

---

```

    TrLst(prnt,3+i) = Chld;
    TrLst(Chld,2) = prnt;
%     TrLst = genTr(EdgLst,Chld,TrLst,des);
    TrLst = genTr(EdgLst,Chld,TrLst);

end

%%%%%%%%%%%%%%%%%%%%%%%%%%%%%%%%%%%%%%%%%%%%%%%%%%%%%%%%%%%%%%%%%%%%%%%%%%
%Tree plot of all feeders in a system stored under the
same folder
%Feeder data are stored in .txt form
%JK WANG, 091212
%%%%%%%%%%%%%%%%%%%%%%%%%%%%%%%%%%%%%%%%%%%%%%%%%%%%%%%%%%%%%%%%%%%%%%%%%%
function sysplt(folder)

dirListing =
dir(folder);
    % get the names of all files. dirListing is a
struct array.

```



```

for i =
1:length(dirListing)
    % loop through the files and open
    if
~dirListing(i).isdir
        % skip hidden system files
        fileName =
fullfile(folder,dirListing(i).name);
        % use full path because the folder may not be the
active path
        %format of file may prevent loading: #tab, edit must
be done in excel(not in txt or matlab), decimal accuracy
        dirListing(i).name
        aa = importdata(fileName)
        data = aa.data;
        textdata = aa.textdata;
        [A,XY] =
FdTr_beta1(flag,data,textdata,NdEq,desid,rtid)
        end
end

```

---

```

function [X,Y,Z] = unplot(filename)
%%To unplot data from a matlab figure (.fig) files
generated
% using version 7 or later. It can be used for both 2D
and 3D plots
% Example usage:
% To unplot 2D graphs
% [x,y] = unplot('example2D.fig')
% To unplot 3D graphs
% [x,y,z] = unplot('example3D.fig')

% Pradyumna
% January 2012

if nargin==1
    fig1 = load (filename,'-mat');
    a =
fig1.hgS_070000.children.children(1,1).properties;
    if isfield(a,'ZData')
        % unploting 3D plot

```

```

        Y =
fig1.hgS_070000.children.children(1,1).properties.YData;
        X =
fig1.hgS_070000.children.children(1,1).properties.XData;
        Z =
fig1.hgS_070000.children.children(1,1).properties.ZData;
    else
        % unploting 2D plot
        Y =
fig1.hgS_070000.children.children(1,1).properties.YData;
        X =
fig1.hgS_070000.children.children(1,1).properties.XData;
    end
else
    disp('Usage unplot(''filename.fig''). See ''help
unplot'' for more details');
end

```

---

```

load
data
        % data for testing purpose

load textdata
% All list in this program is vertical (i.e. row
sequenced)
% Data import
vcol = 14;
fv = [textdata(:,1:2),num2cell(data(:,vcol-
1:vcol))];
        %get information from the
two data matrices
imported
        %process voltage information
Enum = size(fv,1);
% Combine equivalent nodes
NdEq = [{'EDXX001NI5'}, {'EDXX001NIB'},
{'EDXX001NIE'}, {'EDXX001NI8'}]';
for kk = 2:size(NdEq,1)
    NdTmp = cell(Enum,2);
    NdTmp(:,:)= NdEq(kk);
    [m n]= find(cellfun(@strcmp,fv(:,1:2),NdTmp),1);
    for i = 1:size(m,1)

```

```

fv(m(i),n(i))=NdEq(1);
                                % assignment only works when
appears once
    end
end
%% build edge list and node list
clear NdLst
clear EdgLst
Vnum = 1;
for i = 1:Enum*2
    if i==1
        NdLst(Vnum,1:2) = [fv(i,1),fv(i,3)];
        EdgLst(i,1)= Vnum;
    elseif i<= Enum
        NdTmp = cell(Vnum,1);
        NdTmp(:, :) = fv(i,1);
        NdEst =
find(cellfun(@strcmp,NdLst(:,1),NdTmp),1);
        if isempty(NdEst)
            Vnum = Vnum + 1;
            NdLst(Vnum,1:2)= [fv(i,1),fv(i,3)];
            EdgLst(i,1) = Vnum;
        else
            EdgLst(i,1) = NdEst;
        end
    else
        NdTmp = cell(Vnum,1);
        NdTmp(:, :) = fv(i-Enum,2);
        NdEst =
find(cellfun(@strcmp,NdLst(:,1),NdTmp),1);
        if isempty(NdEst)
            Vnum = Vnum + 1;
            NdLst(Vnum,1:2)= [fv(i-Enum,2),fv(i-Enum,4)];
            EdgLst(i-Enum,2) = Vnum;
        else
            EdgLst(i-Enum,2) = NdEst;
        end
    end
end
end
%% generate tree structure/list
clear TrLst

```

```

TrLst = [(1:Vnum)', zeros(Vnum,1)];
for i = 1:Enum
    Ndid = EdgLst(i,1);
    TrLst(Ndid,2)= TrLst(Ndid,2) + 1;
    Chnum = TrLst(Ndid,2);
    TrLst(Ndid,Chnum + 2)=EdgLst(i,2);
end
%% generating Node list with (x,y)=(node depth/level,
voltage)
NdTmp = cell(Vnum,1);
NdTmp(:, :) = {'EDXX001N99'};
rt = find(cellfun(@strcmp,NdLst(:,1),NdTmp),1);
lvlnum = 0;
clear Q
if TrLst(rt,2)==0
    display('isolated node')
    return
else
    NdLst(rt,3) = {lvlnum};
    Chnum = TrLst(rt,2);
    Q(:,1) = TrLst(rt,3:Chnum+2);
    lvlnum = lvlnum + 1;
    Q(:,2) = lvlnum;
    NdTmp = cell(size(Q,1),1);
    NdTmp(:, :)={lvlnum};
    NdLst(Q(:,1),3) = NdTmp;
    while size(Q,1)~=0
        lvlnum = Q(1,2);
        NdLst(Q(1,1),3) = {lvlnum};
        NxtNd = Q(1,1);
        if TrLst(NxtNd,2)~=0
            Chnum = TrLst(NxtNd,2);
            QTmp = TrLst(NxtNd,3:Chnum + 2)';
            QTmp(:,2) = lvlnum + 1;
            Q = [Q; QTmp];
        end
        Q(1,:) = [];
    end
end
end
%% Plot voltage figure
A = zeros(Vnum, Vnum);

```

```

for i = 1:Enum
    A(EdgLst(i,1),EdgLst(i,2)) = 1;
end
YX = cell2mat(NdLst(:,2:3));
gplot(A, [YX(:,2) YX(:,1)])

```

---

```

%comparison of approximation and actual voltage
calculation 2/23/2013
%vs: actual value
%vsa: Pr+Qx/Vs or Pr+Qx/V0 | (:,1) continous 1/10000;
(:,2) 1/100 lumped; (:,3) 1/10 lumped
function [vs,vsa] = appxcmp(pd,qd,v0,r,x)
p = pd.*ones(10000,1);
q = qd.*ones(10000,1);
Ptot = pd*10000;
Qtot = qd*10000;

% 1/100 lump load
p2 = zeros(10000,1);
q2 = zeros(10000,1);
% p2(1:100:end) = pd.*100;
% q2(1:100:end) = qd.*100;
p2(51:100:end) = pd.*100;
q2(51:100:end) = qd.*100;

% 1/10 lump load
p3 = zeros(10000,1);
q3 = zeros(10000,1);
% p3(1:1000:end) = pd.*1000;
% q3(1:1000:end) = qd.*1000;
p3(501:1000:end) = pd.*1000;
q3(501:1000:end) = qd.*1000;

p = [p,p2,p3];
q = [q,q2,q3];

% P(1,:) = Ptot.*ones(1,3) - p(1,:);
% Q(1,:) = Qtot.*ones(1,3) - q(1,:);
P(1,:) = Ptot.*ones(1,3);

```

```

Q(1,:) = Qtot.*ones(1,3);
c3(1,:) = v0^2.*ones(1,3);
vsa(1,:) = v0.*ones(1,3);
for i = 1:10000
    if i > 1
        P(i,:) = P(i-1,:) - p(i,:);
        Q(i,:) = Q(i-1,:) - q(i,:);
        c1(i,:) = Q(i, :).*x + P(i, :).*r;
        c2(i) = P(i,1).*x - Q(i,1).*r;
        c3(i,:) = vs(i-1)^2;
        %vsa(i,:) = vsa(i-1,:) - c1(i, :)./vsa(i-1,:);
        vsa(i,:) = vsa(i-1,:) - c1(i, :)./v0;
    else
        c1(i,:) = Q(i, :).*x + P(i, :).*r;
        c2(i) = P(i,1).*x - Q(i,1).*r;
    end
    vs(i) = sqrt(1/2*c3(i) - c1(i,1) + sqrt(1/4*c3(i)^2
- c1(i,1)*c3(i) - c2(i)^2));
end
k;

```

---

```

%comparison of approximation and actual voltage
calculation 2/23/2013
%vs: Pr+Qx/Vs or Pr+Qx/V0
%vs: actual value | (:,1) continous 1/10000; (:,2) 1/100
lumped;
%
(:,3) 1/10 lumped; (:,4) consider
susceptance
function [vs,vsa] = appxcmp2(pd,qd,v0,r,x,qb)
p = pd.*ones(10000,1);
q = qd.*ones(10000,1);
Ptot = pd*10000;
Qtot = qd*10000;

% 1/100 lump load
p2 = zeros(10000,1);
q2 = zeros(10000,1);
% p2(1:100:end) = pd.*100;
% q2(1:100:end) = qd.*100;
p2(51:100:end) = pd.*100;

```

```

q2(51:100:end) = qd.*100;

% 1/10 lump load
p3 = zeros(10000,1);
q3 = zeros(10000,1);
% p3(1:1000:end) = pd.*1000;
% q3(1:1000:end) = qd.*1000;
p3(501:1000:end) = pd.*1000;
q3(501:1000:end) = qd.*1000;

p = [p,p2,p3,p];
q = [q,q2,q3,q-qb];

% P(1,:) = Ptot.*ones(1,3) - p(1,:);
% Q(1,:) = Qtot.*ones(1,3) - q(1,:);
P(1,:) = Ptot.*ones(1,4);
Q(1,1:3) = Qtot.*ones(1,3);
Q(1,4) = Qtot - 10000*qb;
c3(1,:) = v0^2.*ones(1,4);
vs(1,:) = v0*ones(1,4);
vsa(1) = v0;
for i = 1:10000
    if i > 1
        P(i,:) = P(i-1,:) - p(i,:);
        Q(i,:) = Q(i-1,:) - q(i,:);
        c1(i,:) = Q(i,1).*x + P(i,1).*r;
        c2(i,:) = P(i,1).*x - Q(i,1).*r;
        c3(i,:) = vs(i-1)^2;
        %vsa(i,:) = vsa(i-1,:) - c1(i,1)./vsa(i-1,:);
        vsa(i) = vsa(i-1) - c1(i,1)./v0;
    else
        c1(i,:) = Q(i,1).*x + P(i,1).*r;
        c2(i,:) = P(i,1).*x - Q(i,1).*r;
    end
    vs(i,:) = sqrt(1/2.*c3(i,:) - c1(i,1) +
sqrt(1/4.*c3(i,1).^2 - c1(i,1).*c3(i,1) - c2(i,1).^2));
end
k;

%this function converts density to flow by a psuedo-
integral

```

```

% ds    |l|x1 density distriubted on a feeder of |l|
nodes
% flow |l|x1 flow on the feeder
function flow = d2f(ds)
l = size(ds,1); %get number of nodes
flow = zeros(l,1);
for k = 1:l
    flow(k) = sum(ds(k:end));
end

```

```

% this function calculates the power flow integrated
with DG
% in a DG model, input qg and Qld as 0
% works with single DG and multiple DGs
function [Pn,Qn] = dgintS(pg,qg,Pld,Qld,a)
% a    |Ng|x1 DG's locations
% pg   |Ng|x1 real power of Ng DG
% qg   |Ng|x1 reactive powere of Ng DG
% Pld  |l| x1 real power load flow
% Qld  |l| x1 reactive power load flow
% Ng   number of DG
% l    number of nodes

```

```

l = size(Pld,1);

pgnew = zeros(l,1);
pgnew(a) = pg;
qgnew = zeros(l,1);
qgnew(a) = qg;
Pg = d2f(pgnew);
Qg = d2f(qgnew);
Pn = Pld - Pg;
Qn = Qld - Qg;

```

```

% this function returns all possible sequence given
% DG's types and numbers for each type
function seqIg = dgorder(dgtype, typesz)
%dgtype |typenum| x 1 types for DG

```

```

%typeze |typename| x 1 numbers for each type
%Ig |dgnum| x seqnum all possible sequence
%typename scaler total number of types
%dgnum scaler total number of DG

typename = size(dgtype,1);
dgnum = 0;
% get the dg's number
for k = 1:typename
    dgnum = dgnum + typesz(k);
end

seqIg = zeros(dgnum,1);
j = 0; %counter
for k = 1:typename
    m = j + 1;
    j = j + typesz(k);
    seqIg(m:j) = repmat(dgtype(k),typesz(k),1);
end

seqIg = perms(seqIg);
seqIg = unique(seqIg,'rows');
seqIg = seqIg';

%%%%%%%%%%%%%%%%%%%%%%%%%%%%%%%%%%%%%%%%%%%%%%%%%%%%%%%%%%%%%%%%%%%%%%%%
%%%%%%%%%%%%%%%%%%%%%%%%%%%%%%%%%%%%%%%%%%%%%%%%%%%%%%%%%%%%%%%%%%%%%%%%
%Tree plot of data of DPlan
%JK Wang, 111912
% The same version as beta1,edited for 39 feeders plot
of whole S.M. island
% Updated for Matlab 2012b, which imports data in a
whole cell array
%%%%%%%%%%%%%%%%%%%%%%%%%%%%%%%%%%%%%%%%%%%%%%%%%%%%%%%%%%%%%%%%%%%%%%%%
%%%%%%%%%%%%%%%%%%%%%%%%%%%%%%%%%%%%%%%%%%%%%%%%%%%%%%%%%%%%%%%%%%%%%%%%
% approx: power flow used to calculate Pv is Pv - losses
% returns: NdLst:(cell matrix) node list: {'node
name'}{P}{Q}{node depth}
% size = Vnum * 4

```

```

function NdLst =
FdTr_lss(data,NdEq,desid,rtid) %
Function head for exporting data for plots

%function
[NdLst,EdgLst,TrLst,Vnum,lvlnum,Enum]=FdTr(flag,data,NdEq,desid,rtid)
%flag: (double/binary) == 0 point measurement,e.g.
voltage; == 1 section measurement, e.g. power
%Vnum: (double) node/vertex number
%Enum: (double) feeder/edge number
%lvlnum: (double) depth/level number
%NdLst: (cell matrix) node list: {'node
name'}{P}{Q}{node depth}
% size = Vnum * 4
%EdgLst: (double matrix) edge list: [in source id][out
destiny id]
% size = Edgnum * 2
%TrLst: (double matrix) tree structure of the input
distribution system
% (node id)(parent)(number of
children)[(Children)()...]
% size = Vnum * 2+
%data: (cell array) import data: total col# = 14
%NdEq: (cell array) connected nodes with no voltage
drop in between in conjunction box
%rtid: (string) name of the root node||cannot
detected by parent depth=0
% due to the massive naming of line sections. A
program determines
% root by depth == 0 is FdTr_finall.m
%desid: (string) name of the destiny node||='null'
including braches;o.w.
=====

Enum = size(data,1);

%import length, P, and Q
fv = data(:, [2,1,5,9,10]); %swap node of a line section,
power is measured at end node
%Combine equivalent nodes

```

```

% =====
%NdEq = [{'EDXX001NI5'}, {'EDXX001NIB'},
{'EDXX001NIE'}, {'EDXX001NI8'}]';
if ~isempty(NdEq)
    for kk = 2:size(NdEq,1)
        NdTmp = cell(Enum,2);
        NdTmp(:, :) = NdEq(kk);
        [m n] = find(cellfun(@strcmp, fv(:, 1:2), NdTmp), 1);
        idx = sub2ind(size(fv), m, n);
        fv(idx) = NdEq(1);
    end
end
%% build edge list and node list
%flag: (double/binary) == 0 point measurement, e.g.
voltage; == 1 section measurement, e.g. power
clear NdLst
clear EdgLst
Vnum = 1;
for i = 1:Enum*2
    if i==1
        NdLst(Vnum, 1:4) = [fv(i, 1), fv(i, 3:end)];
        EdgLst(i, 1) = Vnum;
    else
        % Power flow counts on the in source
        if i > Enum
            ii = i - Enum;
            ij = 2;
        else
            ii = i;
            ij = 1;
        end
        NdTmp = cell(Vnum, 1);
        NdTmp(:, :) = fv(ii, ij);
        NdEst =
find(cellfun(@strcmp, NdLst(:, 1), NdTmp), 1);
        if isempty(NdEst)
            Vnum = Vnum + 1;
            cind = 3;
            NdLst(Vnum, 1:4) = [fv(ii, ij), fv(ii, cind:end)];
            EdgLst(ii, ij) = Vnum;
        else

```

```

        EdgLst(ii, ij) = NdEst;
    end
end
end

NdLst(:, 2:end) = num2cell(cell2mat(NdLst(:, 2:end)));

%% generate tree structure/list
if ~isempty(rtid)
    NdTmp = cell(Vnum, 1);
    NdTmp(:, :) = {rtid};
    rt = find(cellfun(@strcmp, NdLst(:, 1), NdTmp), 1);
else
    display('Cannot find the root node.')
    return
end
if ~isempty(desid)
    NdTmp = cell(Vnum, 1);
    NdTmp(:, :) = {desid};
    des = find(cellfun(@strcmp, NdLst(:, 1), NdTmp), 1);
    if isempty(des)
        display('Cannot find the destination node.')
        return
    end
end
clear TrLst
TrLst = [(1:Vnum)', zeros(Vnum, 2)];
TrLst = genTr(EdgLst, rt, TrLst);
%leaves' children # = 0, root parent = 0
% for i = 1:Enum
% %     Ndid = EdgLst(i, 1);
% %     Ndch = EdgLst(i, 2);
%     Ndid = EdgLst(i, 2);
%     Ndch = EdgLst(i, 1);
%     TrLst(Ndid, 3) = TrLst(Ndid, 3) + 1;
%     Chnum = TrLst(Ndid, 3);
%     TrLst(Ndid, Chnum + 3) = Ndch;
%     TrLst(Ndch, 2) = Ndid;
% end

```

```

%% generating Node list with (x,y)=(node depth/level,
voltage)
if strcmp(desid, '')
    mainfd = 0;
else
    mainfd = 1;
end
% the program of generating a full tree need to be
rewrite
switch mainfd
case 0
    lvlnum = 0;
    clear Q
    if TrLst(rt,3)==0
        display('isolated node')
        return
    else
        NdLst(rt,3) = {lvlnum};
        Chnum = TrLst(rt,3);
        Q(:,1) = TrLst(rt,4:Chnum+2);
        lvlnum = lvlnum + 1;
        Q(:,2) = lvlnum;
        NdTmp = cell(size(Q,1),1);
        NdTmp(:,:)={lvlnum};
        NdLst(Q(:,1),3) = NdTmp;
        while size(Q,1)~=0
            lvlnum = Q(1,2);
            NdLst(Q(1,1),3) = {lvlnum};
            NxtNd = Q(1,1);
            if TrLst(NxtNd,3)~=0
                Chnum = TrLst(NxtNd,3);
                QTmp = TrLst(NxtNd,4:Chnum +
3)';
                %can't use 'end' instead of
'chnum +3'; end can be 0
                QTmp(:,2) = lvlnum + 1;
                Q = [Q; QTmp];
            end
            Q(1,:) = [];
        end
    end
case 1
% find a defined feeder

```

```

    lvlnum = 1;
    NdLst(des,5) =
{lvlnum}; %set
the destiny level = 1 (not=0 to distinguish from other
NdLst unassigned elements)and flip with root level at
last;
    NdPnt = TrLst(des,2);
    while NdPnt~=0
        lvlnum = lvlnum + 1;
        NdLst(NdPnt,5) = {lvlnum};
        NdPnt = TrLst(NdPnt,2);
    end
    Brch = cellfun(@isempty,NdLst(:,5));
    Brch = find(Brch==1);

NdLst(Brch,:)=[];
    %delete branches
    lenmfd =
size(NdLst,1);
    % length of main/defined feeder
    NdLst(:,5) = num2cell(abs(cell2mat(NdLst(:,5))-
lenmfd));
end

=====
%generate a tree list by a recursive function
function TrLst = genTr(EdgLst,prnt,TrLst)
%function TrLst = genTr(EdgLst,prnt,TrLst,des)
% TrLst (double matrix) tree structure of the input
distribution system
% (node id) (parent) (number of
children) [(Children) () ...]
% size = Vnum * 2+
%EdgLst: (double matrix) edge list: [in source id][out
destiny id]
% size = Edgnum * 2
%rtid: (string) name of the root node
[r,c] = find(EdgLst== prnt);
rc = [r,c];
if TrLst(prnt,2)== 0 %if root

```

```

    Chnum = size(r,1); %minors its parent branch
else
    [r1,c1] = find(EdgLst(r,:) == TrLst(prnt,2));
    rc(r1,:)=[]; %delete parent branch
    r = rc(:,1);
    c = rc(:,2);
    Chnum = size(r,1);
end
TrLst(prnt,3) = Chnum;
%% Enable the code to see branches
% if Chnum == 0
%     display(prnt)
% end
for i = 1:Chnum
    if c(i) == 1
        Chld = EdgLst(r(i),2);
    else
        Chld = EdgLst(r(i),1);
    end
    % if child == destiny or reach the end (child is the
node's parent, pointing back to its parent branch)
    %     if (Chld == des)
    %         display('reach destiny')
    %         return
    %     end

    TrLst(prnt,3+i) = Chld;
    TrLst(Chld,2) = prnt;
%     TrLst = gentr(EdgLst,Chld,TrLst,des);
    TrLst = gentr(EdgLst,Chld,TrLst);

end

% This function calculte voltage difference given
current flow
function dv = i2dv(ifl, r, intv)
%dv     |1| x 1     voltage drop from the feeder's
primary side
%ifl    |1| x 1     current flow
%intv   |1| x 1     interval between each section
l = size(ifl,1);

```

```

dv = zeros(1,1);
flsec = ifl.*intv;
for k = 1:l
    dv(k) = sum(flsec(1:k)).*r;
end
=====
% compare load density in San Miguel
function dnst = lddnst(data)
S = data(:,1);
PF = data(:,2);
L = data(:,3);
theta = acos(PF);
P = S.*cos(theta);
Q = S.*sin(theta);
p = P./L;
q = Q./L;
p_pu = p./S;
q_pu = q./S;
dnst = [p,q,p_pu,q_pu]
end
=====
%this function calculate loss on the feeder for given
current density
% and unit resistance

function [Ltot,L] = lsscal(ifl,r,intv)
%ids(A)   |1| x 1   current density
%r        scaler   unit resistance
%intv(km) |1| x 1   interval length between nodes
l = size(ifl,1);
L = zeros(1,1);
L = ifl.^2.*r.*intv;
Ltot = sum(L);
=====
%this function display the verification of optimal
location and capacity
%for minimum loss of a DG-integrated feeder
function lss = lsscmp(ids,ig, a, r)
% ids    |1| x 1   current density on the feeder of |1|
nodes

```



```

% ifl    |l| x 1 current flow on the feeder of |l| nodes
% ig     double current output of DG
% a      DG's location
l = size(ids);
if a > l
    display('Infeasible location')
    return
end
ifl = zeros(l,1);
idsg = ids;
idsg(a) = ids(a) - ig;
lss = 0;
for k = 1:l
    ifl(k) = sum(idsg(k:end));
    lss = lss + (ifl(k)^2)*r;
end

```

---

```

%this function display the verification of optimal
location and capacity
%for minimum loss of a DG-integrated feeder
function lss = lssopt(ids, r)
% ids    |l| x 1 current density on the ffeeder of |l|
nodes
% ifl    |l| x 1 current flow on the feeder of |l| nodes
% vpf    |l| x 1 voltage at dg's location
% ig     double current output of DG
% a      DG's location
% l      integer number of nodes
% itot   total load (A)
% deltg  dg capacity increment
% n      types of DG capacity

l = size(ids,1);
ll = (1:l:1)';
itot = sum(ids);

```

```

%% Generating loss plot of DG capacity

```

```

LP2 = 3;
dl = round(1/(LP2+1)); %increment of number of nodes;
dg is not inserted at the end of the feeder
lp2 = zeros(LP2,1);
for k = 1:LP2
    lp2(k) = dl*k;
end

dig = itot/l; %use the same resolution of location
illustration.
ig = zeros(l,1);
for k = 1:l
    ig(k) = dig*k;
end

for k2 = 1:LP2
    lss1 = zeros(l,1);
    vpf = zeros(l,1);
    for k1= 1:l
        ifl = zeros(l,1);

        idsg = ids;
        idsg(lp2(k2)) = ids(lp2(k2)) - ig(k1);
        for k = 1:l
            ifl(k) = sum(idsg(k:end));
        end
        lss1(k1) = sum((ifl.^2).*r);
        vpf(k1) = sum(ifl(1:lp2(k2)).*r);
    end

    subplot(LP2,1,k2);
    [AX,H1,H2]=plotyy(ig,vpf,ig, lss1);
    hold on
    plot(itot.*ones(l,1).*r)
end

```

```

%%
%
% for k = 1:n

```

```

%      ig(k) = deltg*k;
% end
% clear k
% deltg = max(ids);
% n = round(itot/deltg/10);
% ig = zeros(n,1);

lss = zeros(1,1);
for k1 = 1:l
    for k2 = 1:n
        ifl = zeros(1,1);
        idsg = ids;
        idsg(k1) = ids(k1) - ig(k2);

        for k = 1:l
            ifl(k) = sum(idsg(k:end));
            lss(k1,k2) = lss(k1,k2) + (ifl(k)^2)*r;
        end
    end
end

[ll,nn] = meshgrid(1:l:1,ig);
surf(ll,nn,lss)



---


% this function find the optimal location for any flow
input
% and given DG capacity
% this function is based on result  $I_g = 2I_{ld}(a)$ 
function [a,flag] = optDGa(Ig, ifl,amin,amax)
% I_g scaler    DG's current capacity
% ifl |l| x 1    current flow on the feeder
% flag binary    showing if minimum loss is achievable
%              flag = 0, loss is quadractic function,
global min loss
%              achievalbe;
%              flag = 1, loss is increasing function of
a, Lmin at amin

```

```

%              flag = 2, loss is decreasing function of
a, Lmin at amax
% amin double    the nearest location (node index)
permissible to locate a
%              DG to feeder's primary side
flag = 0;
b1 = find(ifl>(Ig/2));
a1 = max(b1);
b2 = find(ifl<(Ig/2));
a2 = min(b2);
if isempty(a1)
    display('DG over supplies the feeder, minimum loss
achieves at amin')
    a = amin;
    flag = 1;
    return
elseif isempty(a2)
    display('DG is very scattered, minimum loss achieves
at amax')
    a = amax;
    flag = 2;
    return
end
if a1 > a2
    display('power flow should be monotonically
decreasing')
    return

elseif a2-a1 > 1 %identical power level
    a = min(max(a2 -1, amin), amax);
elseif ifl(a1) + ifl(a2) > Ig
    a = min(max(a2, amin), amax);
else
    a = min(max(a1, amin), amax);
end



---


% this function calculates the optimal locations for Ng
DG arranged in
% given sequence pg and qg

```

```

% this function can be used for both Sg and Ig
% based on  $2\tilde{S}(a_i) = S_g$ 
% IMPORTANT:=====
% in the set of calculation. Direction of complex power
is defined as the
% direction of current. i.e. power angle larger than pi,
current reverse
% direction, which is the Pv direction.
% =====
% i is reserved for the calculation of complex power
here
function a = optMultiDGa(pg,qg, pfl,qfl,r,x, amin,amax)
% a   |Ng| x 1  locations of DG
% pg  |Ng| x 1  real capacity of DG
% qg  |pg| x 1  reactive
% pfl |l| x 1   read load flow on the feeder
% qfl |l| x 1   read load flow on the feeder
l = size(pfl,1);
Ng = size(pg,1);
a = zeros(Ng,1);
for k = Ng:-1:1
    sg = sqrt(pg(k)^2+qg(k)^2); %sg is not build as
vector
    if k == Ng
        sfl = sqrt(pfl.^2 + qfl.^2);
        [a(k),flag] = optDGa(sg,sfl,amin,amax);
        % the Ng th DG serves as the boundary condition,
        % current flow is the original load flow
    else
        % Only viable for DG model, for AC Sn ~= Sld -
Sdg, must be
        % calculated in real and reactive parts
respectively,
        % ifl = ifl - [Ig(k + 1).*ones(a(k +
1),1);zeros(l-a(k + 1),1)];
        % update current flow by reducing DG downstream
to the k th
        pfl = pfl - [pg(k + 1).*ones(a(k +
1),1);zeros(l-a(k + 1),1)];
        qfl = qfl - [qg(k + 1).*ones(a(k +
1),1);zeros(l-a(k + 1),1)];
        sfl = sqrt(pfl.^2 + qfl.^2);

```

```

%=====define complex power direction
pvfl = pfl.*r + qfl.*x;
sfl = sfl.*sign(pvfl);
%=====

        [a(k),flag] = optDGa(sg,
sfl(1:a(k+1)),amin,amax);
        % only search at the range from the primary side
to the last DG,
        % because optDGa assumes monotonically
decreasing power flow
    end
% set the minimum interval
%   if flag == 1
%       a(k) = a(k) + damin;
%   end
end


---


% This function calculate the optimal capacity for
multiple DG
% assuming the feeder has uniform x and r
% for no specification of Sgmin and Sgmax, set PFvg = 1
for use
function Sg =
optMultiDGcap(a,PFvg,Pld,Qld,x,r,intv,Sgmin,Sgmax)
% Svg  |Ng| x 1  optimal voltage-effective apparent
power of DG
% Assumption=====
%   Svg > 0 never act as pure load
%=====
% all assumptions are for the use of functions and
scripts, not to the
% general results of the thesis
%=====
% a   |Ng| x 1  locations of DG
% PFvg |Ng| x 1  voltage-effective power factor of DG
% Pn  |l| x 1   net real flow on the feeder
% Qn  |l| x 1   net reactive flow on the feeder
% intv |l| x 1  interval between each section
% x, r (double) unit reactance and resistance of
feeder's conductor
% l   nodes number(feeder length)

```

```

% Ng    DG number
% Sgmin double    permissible minimum DG cap
% Sgmax double    permissible maximum DG cap
Ng = size(a,1);

% modify the equation here with r and x into vector for
non-uniform
% conductor=====
vsec = Pld.*r + Qld.*x;

dvld = zeros(Ng,1);
alen = zeros(Ng,1);
z = sqrt(x^2+r^2); %unit impedance
for k = 1:Ng
    dvld(k) = sum(vsec(1:a(k)).*intv(1:a(k)));%Mv
    alen(k) = sum(intv(1:a(k)))*z;% km
end
A0 = repmat(alen,1,Ng);
A1 = triu(ones(Ng,Ng),0).*A0+tril(ones(Ng,Ng),-1).*A0';
Sgv = A1\dvld;%kVA

% =====

Sg = zeros(Ng,1);
for k = 1:Ng
%     if k == 1
%         pvg = pvld;
%     else
%         pvg = pvg - [z*Sg(k-1)].*ones(a(k-
1),1);zeros(1-a(k-1),1)];
%     end
%
%     Sgv =
sum(pvg(1:a(k)).*intv(1:a(k)))/(z*sum(intv(1:a(k))));%kV
A
    Sg(k) = Sgv(k)./PFvg(k);
    if Sg(k)>Sgmax
        Sg(k) = Sgmax;
    elseif Sg(k) < Sgmin

```

```

        Sg(k) = Sgmin;
    end
end
=====
% This function returns DG's votlage effectivepower
factor
function PFvg = pf2pfv(PFg,r,x)
thetag = acos(PFg);
alpha = atan(x/r);
PFvg = cos(thetag-alpha);
=====

% This function calculte voltage difference given real
and reactive flow
function dv = pq2dv(P,Q,x,r,intv)
%dv    |l| x 1    voltage drop from the feeder's
primary side
%ifl    |l| x 1    current flow
%intv    |l| x 1    interval between each section
l = size(P,1);
vsec = P.*r + Q.*x;
dv = zeros(l,1);
for k = 1:l
    dv(k) = sum(vsec(1:k).*intv(1:k));
end
=====

% This function calculte voltage difference given
apparent power and
% voltage effective power facotr
function dv = S2dv(S,PFv,x,r,intv)
%dv    |l| x 1    voltage drop from the feeder's
primary side
%s    |l| x 1    current flow
%intv    |l| x 1    interval between each section
l = size(P,1);
z = sqrt(x^2+r^2);
vsec = P.*r + Q.*x;
dv = zeros(l,1);
for k = 1:l
    dv(k) = sum(vsec(1:k).*intv(1:k));
end
=====

```

```

% This script depicts the DG voltage varying with its
location
% the test is on Figure 54 in the thesis (Losses varying
with DG output variance)
% NdLst: (cell matrix) node list: {'node
name'}{P}{Q}{node depth}
% size = Vnum * 4
% ag: |dgnum| x 1 DG's location
% vfl: |1| x |dgnum| votlage profile over the
feeder
% voltage profile of
optimal DG's location
% typenum: scaler total number of types
% dgnum: scaler total number of DG
% amin double the nearest location (node index)
permissible to locate a
% DG to feeder's primary side
% script needs clear workspace
clear
%% get P,Q, and intv from the one feeder system
[data1,txt1,data] = xlsread('10kv_one feeder');
NdEq = [{'EDXX001NI5'}, {'EDXX001NIB'},
{'EDXX001NIE'},{'EDXX001NI8'}]';
% desid = '263602CF0A9BA712';
rtid = 'EDXX001N99'; %naming sequence reversed since
here
%desid = '';
desid = '2PT0019';
NdLst = FdTr_1ss(data,NdEq,desid,rtid);

Ndata = cell2mat(NdLst(:,2:end));
[x,ind] = sort(Ndata(:,end));
Ndata = Ndata(ind,:);

% %% ideal case
% ids1 = 5*ones(50,1); %kw
% intv1 = 50*ones(50,1); %m
% pfl = d2f(ids1);
% Ndata = [intv1,pfl,zeros(50,1)];

r = 0.16;%ohm/km

```

```

x = 0.092;%ohm/km
z = sqrt(r^2+x^2);
V = 10.5;%base kV
V0 = V;%primary side voltage
Vmax = V0;
err = 0.005; %err generated by matlab approx

intv = Ndata(:,1)./1000; %km
Pld = Ndata(:,2);%kW
Qld = Ndata(:,3);%kVar
Sld = sqrt(Pld.^2 + Qld.^2);%kVA

Vnum = size(Ndata,1);
amin = 2;
amax = Vnum - 1;

% DG location, assume uniformly distributed
% dgnum = 3;
% dgintv = floor(Vnum/(dgnum + 1));
% ag = (1+dgintv):dgintv:(Vnum-dgintv);

% DG location varying range
ag = 11:1:14;
ag = ag';
anum = size(ag,1);

%% plot superposition effect
%PFg = ones(dgnum,1);
PFg = 1;
thetag = acos(PFg);
alpha = atan(x/r);
PFvg = cos(thetag-alpha);
sgmax = Sld(1)*2; % DG less than half total load
sgmin = Sld(end)/2; % DG greater than half single load
%sgintv = floor(sgmin);
sg = 379;% output at its preset full capacity

% svg = sg.*PFvg;

```

```

% pg = sg.*cos(thetag);
% qg = sg.*sin(thetag);
svg = sg*PFvg;
pg = sg*cos(thetag);
qg = sg*sin(thetag);

pvld = Pld.*r + Qld.*x;
pv = zeros(Vnum,1);
pvrec = zeros(Vnum,anum+1);
dv = zeros(Vnum,1);
Vf1 = zeros(Vnum,anum+1);

for k = 1:anum+1
    if k ==1
        pvrec(:,1) = pvld;
    else
        % pv defines as pv*r (in this prog) == sv*z
        pvrec(:,k) = pvld - [z*svg.*ones(ag(k-1),1)];
        for k1 = 1:Vnum
            dv(k1) =
sum(pvrec(1:k1,k).*intv(1:k1))./1000; %kv
            end
        end
        %pvrec(:,k) = pv;
        Vf1(:,k) = V0- dv;
end
% vf1 = V0-dv;
Vf1(1,:) = V0; %impose primary voltage at nodel, actual
v0 at node 0

figure
plot(Vf1,'LineWidth',3)
ylabel('Votlage (kV)','FontSize',16);
xlabel('Node','FontSize',16);
ylim([min(min(Vf1))*0.995 max(max(Vf1))*1.008])
xlim([1 Vnum])
grid on
title('Voltage profiles varying with DG location (S_G =
400 kVA)','FontSize',18)
set(gca,'FontSize',12)

```

```
set(gca,'XTick',1:1:Vnum)
```

---



---

```

% This script shows the relation of Sg and given power
factor

```

```

% [data1,txt1,data] = xlsread('10kv_one feeder');
% NdEq = [{'EDXX001NI5'}, {'EDXX001NIB'},
{'EDXX001NIE'}, {'EDXX001NI8'}]';
% % desid = '263602CF0A9BA712';
% rtid = 'EDXX001N99'; %naming sequence reversed since
here
% %desid = '';
% desid = '2PT0019';
% NdLst = FdTr_lss(data,NdEq,desid,rtid);
%
% Ndata = cell2mat(NdLst(:,2:end));
% [x,ind] = sort(Ndata(:,end));
% Ndata = Ndata(ind,:);
%
% intv = Ndata(:,1)./1000; %km

```

```
%% figure 56 and figure 57 in the thesis
```

```

dV = 0:50;
sg = 400;
x = 0.092;%ohm/km
r = 0.16;%ohm/km
z = sqrt(x^2+r^2);
len = 4.0498;%km length from node 1 to 11 on feeder 1
svg = dV*10./z./len;
PFvg = min(1, svg./sg);
%PF = cos(max(-pi/2, min(pi/2, acos(PFvg)+atan(x/r))));
%PF2 = cos(max(-pi/2, min(pi/2, -acos(PFvg)+atan(x/r))));
gama= acos(PFvg);
alpha = atan(x/r);
PF = zeros(1,51);
for kk = 1:51
    if gama(kk) > alpha

```

```

        PF(kk) = cos(gama(kk)-alpha);
    else
        PF(kk) = cos(alpha-gama(kk));
    end
end

```

```

figure
%plot(dV,PF,dV, PF2,'LineWidth',3,'Color','blue')
plot(dV,PF,'LineWidth',3,'Color','blue')
ylabel('Power Factor','FontSize',16);
xlabel('\Delta V_L(V)','FontSize',16);
ylim([min(PFvg)*0.95 max(PFvg)*1.05])
grid on
title('DG operational power factor (S_G = 400
kVA)','FontSize',18)
set(gca,'FontSize',12)
%set(gca,'YTick',0.8:1)

sg1 = 200:10:400;
dV1 = 20; %v
sgv1 = dV1*10/z/len; %kVA
PFv1 = sgv1./sg1;
%rr = size(PFv1,2);
PFv1 = min(1,PFv1);
gama1= acos(PFv1);

PF1 = zeros(1,21);
for kk = 1:21
    if gama1(kk) > alpha
        PF1(kk) = cos(gama1(kk)-alpha);
    else
        PF1(kk) = cos(alpha-gama1(kk));
    end
end
% PF1 = cos(acos(PFv1)+atan(x/r));

```

```

figure
%plot(sg1,PF1,sg1,PF2,'LineWidth',3,'Color','blue')
plot(sg1,PF1,'LineWidth',3,'Color','blue')
ylabel('Power Factor','FontSize',16);
xlabel('S_G (kVA)','FontSize',16);
ylim([min(PF1)*0.95 max(PF1)*1.05])
grid on
title('DG operational power factor (\Delta V_L =
50V)','FontSize',18)
set(gca,'FontSize',12)
set(gca,'XTick',200:25:400)

```

---

```

% generating contour graph for ver planning
% showing  $E\langle I(a) \rangle = E\langle I_g \rangle + \text{VAR}\langle I_g \rangle / E\langle I_g \rangle$ 
% szvar      double      size of variance set
% szrnd      double      random number size
% sigma      double      sigma of distribution
function deployed for
%
% l          double      random number generation
%            number of nodes on feeder
% ids       |l| x 1      load density
% idsrnd    |l| x |szrnd| random load density
% r         double      resistance of feeder

```

```

sigmasq = (0.1:0.5:200)';
sigma = sqrt(sigmasq);
% for testing ver's sigma, fixing load sigma
sigmald = sigma(1);

```

```

szvar = length(sigma);
szrnd = 100;

```

```

l = 20;
r = 0.01;
ids = [1.2448 1.0048 1.3345 1.2477 1.6610 1.3378
1.3587...
1.1118 0.8119 1.0170 0.9306 0.9739 1.2241
0.9755...
0.8998 1.0085 1.0640 1.1915 0.8870 1.1710]';

```

```

    ifl = zeros(1,1); %|1| x szrnd
    for k = 1:l
        ifl(k,:) = sum(ids(k:end,:),1);
    end
    ig = 1/4*ifl(1);
    igrec = zeros(szrnd,szvar);
    lss = zeros(1,szvar);
    for k1 = 1:szvar % loop of sigma changing for ig
        igrnd = zeros(1,szrnd);
        idsrnd = zeros(1,szrnd);
        for k3 = 1:szrnd
            igrnd =
normrnd(ones(1,szrnd).*ig,ones(1,szrnd).*sigma(k1));
            igrnd =
normrnd(ones(1,szrnd).*ig,ones(1,szrnd).*sigmald);
            igrnd = max(0,igrnd); %set random number
generated negative to zero
            igrnd = min(20,igrnd);%set max output for ver
            igrec(:,k1) = igrnd;
            %idsrnd =
normrnd(repmat(ids,1,szrnd),ones(1,szrnd).*sigmald)./10
+ 1;
            idsrnd =
normrnd(repmat(ids,1,szrnd),ones(1,szrnd).*sigma(k1))./1
0 + 1;
        end

% compute current flow of varying load
iflrnd = zeros(1,szrnd); %|1| x szrnd
for k = 1:l
    iflrnd(k,:) = sum(idsrnd(k:end,:),1);
end

for k2 = 1:l % loop for chaning dg location
    igftp = [ones(k2,szrnd)*diag(igrnd);zeros(1-
k2,szrnd)]; % |1| x szrnd, dg flow
    ifltp = iflrnd - igftp;
    lss(k2,k1) = mean(sum((ifltp.^2).*r,1));
end

```

end

```

[ll,sig] = meshgrid(1:1:l,sigma);
%contour(ll,sig,lss')
lssb = ((lss'./100).^2).*10;
surf(sig,ll,lssb)
ylabel('location(node)','FontSize',18);
xlabel('\sigma_ld','FontSize',16);
zlabel('Loss(kW)','FontSize',16);
set(gca, 'YTick',1:2:18)
set(gca,'FontSize',14)
title('Optimal location for a variable energy
resoure','FontSize',18)

```

---

```

% This script get the optimal location for the one
feeder system
% script needs clear workspace
clear
%% import data
[data1,txt1,data] = xlsread('10kv_one feeder');
NdEq = [{'EDXX001NI5'}, {'EDXX001NIB'},
{'EDXX001NIE'}, {'EDXX001NI8'}]';
% desid = '263602CF0A9BA712';
rtid = 'EDXX001N99'; %naming sequence reversed since
here
%desid = '';
desid = '2PT0019';
NdLst = FdTr_lss(data,NdEq,desid,rtid);

Ndata = cell2mat(NdLst(:,2:end));
[x,ind] = sort(Ndata(:,end));
Ndata = Ndata(ind,:);

intv = Ndata(:,1)./1000; %km
Pld = Ndata(:,2);
Qld = Ndata(:,3);
Sld = sqrt(Pld.^2 + Qld.^2); %kVA
Vnum = size(Ndata,1);

```



```

%% input DG's parameter
pg = 700; %kw
qg = 70; %kVar
sg = sqrt(pg^2 + qg^2);
V = 10.5; %kV
r = 0.16; %ohm/km

%% generate loss

Ltotal1 = zeros(Vnum,1);

for k = 1:Vnum
    Pg = zeros(Vnum,1);
    Pg(k) = pg;
    Pg = d2f(Pg);
    Qg = zeros(Vnum,1);
    Qg(k) = qg;
    Qg = d2f(Qg);
    Pn = Pld - Pg;
    Qn = Qld - Qg;
    Sn = sqrt(Pn.^2 + Qn.^2); %kVA

    ifl = Sn./V./sqrt(3); %A

    [L1,L2] = lsscal(ifl,r,intv); %w
    Ltotal1(k) = L1./1000.*3;
end

a = optDGa(sg,Sld);

% plot loss
h = figure;
subplot(2,1,1)
stairs(Ltotal1,'LineWidth',2,'Color','green')
xlim([1 Vnum]); % chop the first data point
set(gca,'XTick',1:1:Vnum)
ylabel('Loss (kW)', 'FontSize',16);
xlabel('node', 'FontSize',16);
title('Optimal DG location','FontSize',20)

```

```

grid on
%plot apparent flow
subplot(2,1,2)
stairs(Sld,'LineWidth',2,'Color','blue');
xlim([1 Vnum]); % chop the first data point
ylim([0 max([sg;Sld])+50]);
ylabel('S (kVA)', 'FontSize',16);
xlabel('node', 'FontSize',16);
set(gca,'FontSize',12)
hold on
stem(a,sg,'LineWidth',2,'Color','red')
set(gca,'XTick',1:1:Vnum)

```

---

```

grid on
% This memu verifies superposition theory for optimal
location
% NdLst: (cell matrix) node list: {'node
name'}{P}{Q}{node depth}
% size = Vnum * 4
% seqSg: (double) |dgnum| x seqnum all possible
sequence
% aseq: (double) |dgnum| x seqnum optimal location
for DGs at each sequence
% Lall: (double) |seqnum| x 1 loss of all DG
sequence
% ov (double) |seqnum| x 1 overvoltage
indicator for resultant
% voltage profile of
optimal DG's location
% typenum: scaler total number of types
% dgnum: scaler total number of DG
% amin double the nearest location (node index)
permissible to locate a
% DG to feeder's primary side
% script needs clear workspace
clear
%% get P,Q, and intv from the one feeder system
[data1,txt1,data] = xlsread('10kv_one feeder');

```

```

NdEq = [{'EDXX001NI5'}, {'EDXX001NIB'},
{'EDXX001NIE'}, {'EDXX001NI8'}]';
% desid = '263602CF0A9BA712';
rtid = 'EDXX001N99'; %naming sequence reversed since
here
%desid = '';
desid = '2PT0019';
NdLst = FdTr_iss(data,NdEq,desid,rtid);

```

```

Ndata = cell2mat(NdLst(:,2:end));
[x,ind] = sort(Ndata(:,end));
Ndata = Ndata(ind,:);

```

```

% %% ideal case
% ids1 = 5*ones(50,1); %kw
% intv1 = 50*ones(50,1); %m
% pfl = d2f(ids1);
% Ndata = [intv1,pfl,zeros(50,1)];

```

```

r = 0.16;%ohm/km
x = 0.092;%ohm/km
V = 10.5;%base kV
V0 = V;%primary side voltage
Vmax = V0;
err = 0.005; %err generated by matlab approx

```

```

intv = Ndata(:,1)./1000; %km
Pld = Ndata(:,2);%kW
Qld = Ndata(:,3);%kVar
Sld = sqrt(Pld.^2 + Qld.^2);%kVA

```

```

Vnum = size(Ndata,1);
amin = 2;
amax = Vnum - 1;

```

```

%generate DG sequence, GOOD DATA KEEP!!
pgn = [100 130]';
qgn = [10 15]';
dggrp = [2 2]';

```

```

% % ideal case dg
% pgn = [60 40]';
% %pgn = [50 30]';
% qgn = [0 0.01]';% to distinguish the two sets. dgorder
function bug
% dggrp = [2 2]';
% %dggrp = [3 3]';

```

```

seqpg = dgorder(pgn, dggrp);
seqqg = dgorder(qgn, dggrp);
seqsg = sqrt(seqpg.^2 + seqqg.^2);

```

```

dgnum = size(seqpg,1);
seqnum = size(seqqg,2);
Lall = zeros(seqnum,1);
ov = zeros(seqnum,1);

```

```

aseq = zeros(dgnum,seqnum);

```

```

%% calculating opt location and loss for the sequence

```

```

for k = 1:seqnum
    aseq(:,k) =
    optMultiDGa(seqpg(:,k),seqqg(:,k),Pld,Qld,r,x,amin,amax);

```

```

    [Pn,Qn] =
    dgintS(seqpg(:,k),seqqg(:,k),Pld,Qld,aseq(:,k));
    Sn = sqrt(Pn.^2 + Qn.^2);
    ifl = Sn./V./sqrt(3); %kVA

```

```

    dv = pq2dv(Pn,Qn,x,r,intv);%kV
    if min(dv) < V0-Vmax - err;
        ov(k) = 1;
    end

```

```

    [L1, L2] = lsscal(ifl,r,intv);
    Lall(k) = L1./1000.*3; %kW

```

```

end

Lnew = ov.*Lall;

hseq = figure;
barh(Lall)
hold on
barh(Lnew,'red')%identify the sequence cause over
voltage
xlabel('Loss (kW)', 'FontSize',16);
ylabel('Squence', 'FontSize',16);
xlim([min(Lall)/2 max(Lall)*1.2]); %set 20% margin of
the figure
title('Minimum Loss of different DG
sequence', 'FontSize',18)
hl = legend('feasible seq', 'overvoltage');
set(hl, 'box', 'off');
set(gca, 'FontSize',14)

% find the sequence that generates minimum loss and
doesn't cause
% overvoltage

Lnew2 = Lall;%excluding the overvoltage sequence
Lnew2(ov~=0) = max(Lall);
[Lmin,indLmin] = min(Lnew2);

% plot superposition effect
aLmin =
optMultiDGa(seqpg(:, indLmin), seqqg(:, indLmin), Pld, Qld, r,
x, amin, amax);
pgLmin = seqpg(:, indLmin);
qgLmin = seqqg(:, indLmin);
sgLmin = seqsg(:, indLmin);

hsup = figure;
for k = dgnum:-1:0

    subplot(dgnum+1,1,k+1)
    if k == dgnum
        Pn = Pld;
        Qn = Qld;
    else
        [Pn,Qn] =
dgintS(pgLmin(k+1:end), qgLmin(k+1:end), Pld, Qld, aLmin(k+1
:end));
    end
    Sn = sqrt(Pn.^2 + Qn.^2);
    % Approx: Need edit later =====
    if Pn<0
        Sn = -Sn;
    end
    %=====
%    Snew = Sn./V./sqrt(3); %kVA
    stairs(Sn, 'LineWidth',2, 'Color', 'green')
    if k == dgnum
        xlabel('node', 'FontSize',16); %only
effective agfter axis is created
    end
    xlim([1 Vnum]); % chop the first data point
    ylim([0 max(Sld)*1.05])
    set(gca, 'XTick', 1:1:Vnum)
    if k == ceil(dgnum/2);
        ylabel('S^I_n(kVA)', 'FontSize',16);
    end
%    title('Optimal DG location', 'FontSize',20)
    grid on
    if k > 0
        hold on
    end
    stem(aLmin(k), sgLmin(k), 'LineWidth',2, 'Color', 'red')
    else
        title('Superposition Property of Multiple DG
Placement', 'FontSize',20)
    end
end

%% plot minimum loss comparision graph
intvmin = 2; % minimum interval between each spot
kk = 0; % counter to calculate size of set
for k1 = amin:(amax - (dgnum - 1)*intvmin)
    for k2 = (k1 + intvmin):(amax - (dgnum-2)*intvmin)

```

```

        for k3 = (k2 + intvmin):(amax - (dgnum-
3)*intvmin)
            for k4 = (k3 + intvmin):(amax - (dgnum-
4)*intvmin)
                %
                for k5 = (k4 + intvmin):(amax -
(dgnum-5)*intvmin)
                    %
                    for k6 = (k5 + intvmin):(amax -
(dgnum-6)*intvmin)
                        kk = kk + 1;
                    end
                end
            end
        end
    end
end

Lall2 = zeros(kk,1);%kW
aall = zeros(kk,4);
ov2 = zeros(kk,1);
kk2 = 0;
for k1 = amin:(amax - (dgnum - 1)*intvmin)
    for k2 = (k1 + intvmin):(amax - (dgnum-2)*intvmin)
        for k3 = (k2 + intvmin):(amax - (dgnum-
3)*intvmin)
            for k4 = (k3 + intvmin):(amax - (dgnum-
4)*intvmin)
                %
                for k5 = (k4 + intvmin):(amax -
(dgnum-5)*intvmin)
                    %
                    for k6 = (k5 + intvmin):(amax -
(dgnum-6)*intvmin)
                        kk2 = kk2 + 1;
                        atmp = [k1 k2 k3 k4]';
                        aall(kk2,:) = atmp;
                    %
                    atmp = [k1 k2 k3 k4 k5 k6]';
                    [Pn,Qn] =
dgintS(pgLmin,qgLmin,Pld,Qld,atmp);
                    Sn = sqrt(Pn.^2 + Qn.^2);
                    ifl = Sn./V./sqrt(3); %kVA

                    dv = pq2dv(Pn,Qn,x,r,intv);%kV
                    if min(dv) < V0-Vmax - err;
                        ov2(kk2) = 1;
                    end
                end
            end
        end
    end
end

```

```

        end
        [L1, L2] = lsscal(ifl,r,intv);
        Lall2(kk2) = L1./1000.*3;
    end
end
end
end
end

Lnew2 = ov2.*Lall2;

hseq2 = figure;
barh(Lall2)
hold on
barh(Lnew2,'red')%identify the sequence cause over
voltage
xlabel('Loss (kW)', 'FontSize',16);
ylabel('location (node)', 'FontSize',16);
xlim([min(Lall2)/2 max(Lall2)*1.2]); %set 20% margin of
the figure
ylim([1 kk]);
title(['Loss of different DG location at sequence
',num2str(indLmin)], 'FontSize',18)
hl2 = legend('feasible location','overvoltage');
set(hl2,'box','off');
set(gca,'FontSize',14)

%% output table
[~,ind]=ismember(aall,aLmin','rows');
indnew = find(ind~=0); %best sequence

=====

% This memu verifies superposition theory for optimal
capacity
% NdLst: (cell matrix) node list: {'node
name'}{P}{Q}{node depth}
% size = Vnum * 4

```

```

% ag:      |dgnum| x 1      DG's location
% vfl:    |l| x |dgnum|    votlage profile over the
feeder
%
%          voltage profile of
optimal DG's location
% typenum: scaler          total number of types
% dgnum:   scaler          total number of DG
% amin double the nearest location (node index)
permissible to locate a
%          DG to feeder's primary side
% script needs clear workspace
clear
%% get P,Q, and intv from the one feeder system
[data1,txt1,data] = xlsread('10kv_one feeder');
NdEq = [{'EDXX001NI5'}, {'EDXX001NIB'},
{'EDXX001NIE'}, {'EDXX001NI8'}]';
% desid = '263602CF0A9BA712';
rtid = 'EDXX001N99'; %naming sequence reversed since
here
%desid = '';
desid = '2PT0019';
NdLst = FdTr_lss(data,NdEq,desid,rtid);

Ndata = cell2mat(NdLst(:,2:end));
[x,ind] = sort(Ndata(:,end));
Ndata = Ndata(ind,:);

% %% ideal case
% ids1 = 5*ones(50,1); %kw
% intv1 = 50*ones(50,1); %m
% pfl = d2f(ids1);
% Ndata = [intv1,pfl,zeros(50,1)];

r = 0.16;%ohm/km
x = 0.092;%ohm/km
z = sqrt(r^2+x^2);
V = 10.5;%base kV
V0 = V;%primary side voltage
Vmax = V0;
err = 0.005; %err generated by matlab approx

```

```

intv = Ndata(:,1)./1000; %km
Pld = Ndata(:,2);%kW
Qld = Ndata(:,3);%kVar
Sld = sqrt(Pld.^2 + Qld.^2);%kVA

Vnum = size(Ndata,1);
amin = 2;
amax = Vnum - 1;

% DG location, assume uniformly distributed
dgnum = 3;
dgintv = floor(Vnum/(dgnum + 1));
ag = (1+dgintv):dgintv:(Vnum-dgintv);
ag = ag';%

%% plot superposition effect
PFg = ones(dgnum,1);
thetag = acos(PFg);
alpha = atan(x/r);
PFvg = cos(thetag-alpha);
sgmax = Sld(1)*2; % DG less than half total load
sgmin = Sld(end)/2; % DG greater than half single load
%sgintv = floor(sgmin);
sg = optMultiDGcap(ag, PFvg, Pld, Qld, x, r, intv, sgmin,
sgmax);

svg = sg.*PFvg;
pg = sg.*cos(thetag);
qg = sg.*sin(thetag);

pvld = Pld.*r + Qld.*x;
pv = zeros(Vnum,1);
pvrec = zeros(Vnum,dgnum);
dv = zeros(Vnum,1);

for k = 1:dgnum+1
    if k ==1

```

```

        pv = pvld;
    else
        % pv defines as pv*r (in this prog) == sv*z
        pv = pv - [z*svg(k-1).*ones(ag(k-
1),1);zeros(Vnum-ag(k-1),1)];
        for k1 = 1:Vnum
            dv(k1) =
sum(pv(1:k1).*intv(1:k1))./1000; %kv
        end
    end
    pvrec(:,k) = pv;
end
vfl = V0-dv;
vfl(1) = V0; %impose primary voltage at nodel, actual
v0 at node 0

h1 = figure;
subplot(2,1,1)
plot(vfl,'LineWidth',2,'Color','green')
hold on
plot(V0*ones(Vnum,1),'--','LineWidth',2,'Color','red')
ylim([min(vfl) max(vfl)+0.2*(max(vfl)-min(vfl))]);
xlim([1 Vnum]);
h11 = legend('final V','V0');
grid on
set(h11,'box','on');
xlabel('Voltage (kV)','FontSize',14);
set(gca,'XTick',1:1:Vnum)
title('Optimal DG capacity and induced
voltage','FontSize',18)
set(gca,'FontSize',12)

subplot(2,1,2)
hold on
stairs(pvld./r,'LineWidth',2,'Color','green')
stairs(pvrec(:,dgnum)./r,'LineWidth',2,'Color','blue')
stem(ag,svg,'filled','r')
xlabel('location (node)','FontSize',14);
ylabel('S^V (kVA)','FontSize',14);
xlim([1 Vnum]); %set 20% margin of the figure

```

```

lblim = max([pvrec(:,dgnum)./r;svg;pvld./r]);
ylim([min(pvrec(:,dgnum)) max(lblim)+0.2*(lblim-
min(pvrec(:,dgnum)))]);
hl2 = legend('S^V load','final S^V', 'S^V DG');
set(hl2,'box','on');
grid on
set(gca,'FontSize',12)
set(gca,'XTick',1:1:Vnum)

%% plot minimum loss comparision graph
seqmax = max(sg)+50; % DG less than half total load
seqmin = min(sg)-50; % DG greater than half single load
seqintv = 10;

kk = 0; % counter to calculate size of set
for k1 = seqmin:seqintv:seqmax
    kk = kk+1;
end
kk = kk^3;

Lall = zeros(kk,1);%kW
sall = zeros(kk,dgnum);
kk2 = 0;
% k1~k3, assuming only 3 DG's here
for k1 = seqmin:seqintv:seqmax
    for k2 = seqmin:seqintv:seqmax
        for k3 = seqmin:seqintv:seqmax
            kk2 = kk2 + 1;
            sgnew = [k1;k2;k3];
            sall(kk2,:) = sgnew;
            pgnew = sgnew.*cos(thetag);
            qgnew = sgnew.*sin(thetag);
            [Pn,Qn] = dgintS(pgnew,qgnew,Pld,Qld,ag);
            Sn = sqrt(Pn.^2 + Qn.^2);
            ifl = Sn./V./sqrt(3); %kVA
            [L1, L2] = lsscal(ifl,r,intv);
            Lall(kk2) = L1./1000.*3;
        end
    end
end
end

```

```

% output table
[Lssmin,ind] = min(Lall);
sg2 = sall(ind,:); %best sequence
% generate fake from sg2
%[~,ind]=ismember(ceil(sall),ceil(fake),'rows');

% plot sequence
hseq = figure;
barh(Lall)
xlabel('Loss(kW)', 'FontSize',12);
ylabel('DG Capacity(sets)', 'FontSize',12);
xlim([min(Lall)/2 max(Lall)*1.2]); %set 20% margin of
the figure
ylim([1 kk]);
title('Loss of different DG capacity
combination', 'FontSize',12)
set(gca, 'FontSize',12)

```

---

```

% This memu verifies superposition theory for optimal
capacity
% NdLst: (cell matrix) node list: {'node
name'}{P}{Q}{node depth}
% size = Vnum * 4
% ag: |dgnum| x 1 DG's location
% vfl: |l| x |dgnum| votlage profile over the
feeder
% voltage profile of
optimal DG's location
% typenum: scaler total number of types
% dgnum: scaler total number of DG
% amin double the nearest location (node index)
permissible to locate a
% DG to feeder's primary side
% script needs clear workspace
clear
%% get P,Q, and intv from the one feeder system
[data1,txt1,data] = xlsread('10kv_one feeder');
NdEq = [{'EDXX001NI5'}, {'EDXX001NIB'},
{'EDXX001NIE'}, {'EDXX001NI8'}]';
% desid = '263602CF0A9BA712';

```

```

rtid = 'EDXX001N99'; %naming sequence reversed since
here
%desid = '';
desid = '2PT0019';
NdLst = FdTr_1ss(data,NdEq,desid,rtid);

Ndata = cell2mat(NdLst(:,2:end));
[x,ind] = sort(Ndata(:,end));
Ndata = Ndata(ind,:);

% %% ideal case
% ids1 = 5*ones(50,1); %kw
% intv1 = 50*ones(50,1); %m
% pfl = d2f(ids1);
% Ndata = [intv1,pfl,zeros(50,1)];

r = 0.16;%ohm/km
x = 0.092;%ohm/km
z = sqrt(r^2+x^2);
V = 10.5;%base kV
V0 = V;%primary side voltage
Vmax = V0;
err = 0.005; %err generated by matlab approx

intv = Ndata(:,1)./1000; %km
Pld = Ndata(:,2);%kW
Qld = Ndata(:,3);%kVar
Sld = sqrt(Pld.^2 + Qld.^2);%kVA

Vnum = size(Ndata,1);
amin = 2;
amax = Vnum - 1;

% DG location, assume uniformly distributed
dgnum = 3;
dgintv = floor(Vnum/(dgnum + 1));
ag = (1+dgintv):dgintv:(Vnum-dgintv);
ag = ag';%

```

```

%% plot superposition effect
PFg = ones(dgnum,1);
thetag = acos(PFg);
alpha = atan(x/r);
PFvg = cos(thetag-alpha);
sgmax = Sld(1)*2; % DG less than half total load
sgmin = Sld(end)/2; % DG greater than half single load
%sgintv = floor(sgmin);
sg = optMultiDGcap(ag, PFvg, Pld, Qld, x, r, intv, sgmin,
sgmax);

svg = sg.*PFvg;
pg = sg.*cos(thetag);
qg = sg.*sin(thetag);

pvld = Pld.*r + Qld.*x;
pv = zeros(Vnum,1);
pvrec = zeros(Vnum,dgnum);
dv = zeros(Vnum,1);

for k = 1:dgnum+1
    if k ==1
        pv = pvld;
    else
        % pv defines as pv*r (in this prog) == sv*z
        pv = pv - [z*svg(k-1).*ones(ag(k-
1),1);zeros(Vnum-ag(k-1),1)];
        for k1 = 1:Vnum
            dv(k1) =
sum(pv(1:k1).*intv(1:k1))./1000; %kv
        end
    end
    pvrec(:,k) = pv;
end
vfl = V0-dv;
vfl(1) = V0; %impose primary voltage at nodel, actual
v0 at node 0

```

```

h1 = figure;
subplot(2,1,1)
plot(vfl,'LineWidth',2,'Color','green')
hold on
plot(V0*ones(Vnum,1),'--','LineWidth',2,'Color','red')
ylim([min(vfl) max(vfl)+0.2*(max(vfl)-min(vfl))]);
xlim([1 Vnum]);
hl1 = legend('final V','V0');
grid on
set(hl1,'box','on');
xlabel('Voltage (kV)','FontSize',14);
set(gca,'XTick',1:1:Vnum)
title('Optimal DG capacity and induced
voltage','FontSize',18)
set(gca,'FontSize',12)

subplot(2,1,2)
hold on
stairs(pvld./r,'LineWidth',2,'Color','green')
stairs(pvrec(:,dgnum)./r,'LineWidth',2,'Color','blue')
stem(ag,svg,'filled','r')
xlabel('location (node)','FontSize',14);
ylabel('S^V (kVA)','FontSize',14);
xlim([1 Vnum]); %set 20% margin of the figure
lblim = max([pvrec(:,dgnum)./r;svg;pvld./r]);
ylim([min(pvrec(:,dgnum)) max(lblim)+0.2*(lblim-
min(pvrec(:,dgnum)))]);
hl2 = legend('S^V load','final S^V','S^V DG');
set(hl2,'box','on');
grid on
set(gca,'FontSize',12)
set(gca,'XTick',1:1:Vnum)

%% plot minimum loss comparision graph
seqmax = max(sg)+50; % DG less than half total load
seqmin = min(sg)-50; % DG greater than half single load
seqintv = 10;

kk = 0; % counter to calculate size of set
for k1 = seqmin:seqintv:seqmax

```



```

    kk = kk+1;
end
kk = kk^3;

Lall = zeros(kk,1);%kW
sall = zeros(kk,dgnum);
kk2 = 0;
% k1~k3, assuming only 3 DG's here
for k1 = seqmin:seqintv:seqmax
    for k2 = seqmin:seqintv:seqmax
        for k3 = seqmin:seqintv:seqmax
            kk2 = kk2 + 1;
            sgnew = [k1;k2;k3];
            sall(kk2,:) = sgnew;
            pgnew = sgnew.*cos(thetag);
            qgnew = sgnew.*sin(thetag);
            [Pn,Qn] = dgintS(pgnew,qgnew,Pld,Qld,ag);
            Sn = sqrt(Pn.^2 + Qn.^2);
            ifl = Sn./V./sqrt(3); %kVA
            [L1, L2] = lsscal(ifl,r,intv);
            Lall(kk2) = L1./1000.*3;
        end
    end
end

% output table
[Lssmin,ind] = min(Lall);
sg2 = sall(ind,:); %best sequence
% generate fake from sg2
%[~,ind]=ismember(ceil(sall),ceil(fake),'rows');

% plot sequence
hseq = figure;
barh(Lall)
xlabel('Loss (kW)', 'FontSize',12);
ylabel('DG Capacity(sets)', 'FontSize',12);
xlim([min(Lall)/2 max(Lall)*1.2]); %set 20% margin of
the figure
ylim([1 kk]);
title('Loss of different DG capacity
combination', 'FontSize',12)

```

```

set(gca, 'FontSize',12)


---




---


% plot allowed penetration level
[a,c] = meshgrid(0:0.01:1,0:0.01:1);
vd = 1/2*(a.^2) - a.*(ones(101,101)-c);
figure
[C1,h1]=contour(a,c,vd)
set(h1, 'ShowText', 'on', 'TextStep', get(h1, 'LevelStep')*2)
L = 1/3 + a.*(c.^2) + c.*(a.^2-2.*a);
figure
surf(a,c,L)


---




---


% this script generates plot for Caisheng Wang's table
in optimal
% DG's location and capacity
% ids |1| x 3 current density on the feeder of |1|
nodes
% ifl |1| x 3 current flow on the feeder of |1| nodes
% Ig 1 x 3 DG's capacity
% h the handle of plots
% ids1 uniformly distributed load
% ids2 centrally distributed load
% ids3 increasingly distributed load
v0 = 10;%kv
ids = zeros(20,3);
l = 20;
ids(:,1) = 5*ones(20,1); %total input 100
ids2 = 1:0.9:9.1;
ids(:,2) = [ids2,fliplr(ids2)]'; %total input 101
ids3 = 9.8:-0.5:0.3;
ids(:,3) = ids3'; % total input 101
intv = ones(20,1); %resistance set to 0.08 (given San
Miguel resistance is
% 0.16ohm/km) equivalent to 500m
%for optimal capacity, assuming DG is located at the
middle of the feeder
a = 1/2;

```

```

Igvar = 5:5:150;
numIg = size(Igvar,2);

idsnew = zeros(1,3);
iflnew = zeros(1,3);
Ltot = zeros(1,3); % 1 NOT 1
Lall = zeros(numIg,3);
vg = zeros(numIg,3);
optIg = zeros(1,3);
optvg = zeros(1,3);

for k = 1:3

%for optimal location, assuming DG's capacity equals
total loads on the
%feeder
    ifl = d2f(ids(:,k));
    % Ig(k) = ifl(1,k);

% get optimal DG's location
    idsnew = ids(:,k);
    for j = 1:numIg
        idsnew(a) = ids(a) - Igvar(j);
        iflnew = d2f(idsnew);
        dvg = i2dv(iflnew,0.08,intv)./1000; %kv
        vg(j,k) = v0 - dvg(a);
        [Lall(j,k),L2] = lsscal(iflnew,0.08,intv);

    end

    dvld = i2dv(ifl,0.08,intv);
    optIg = dvld(a)/(0.08*sum(intv(1:a)));%kv/km = A

    idsnew = ids(:,k);
    idsnew(a) = ids(a) - optIg;
    iflnew = d2f(idsnew);
    dvg = i2dv(iflnew,0.08,intv)./1000; %kv
    optvg(:,k) = v0 - dvg;

%
a = optDGa(Ig(k),ifl(:,k));
idsnew(:,k) = ids(:,k);
idsnew(a,k) = ids(k) - Ig(k);
iflnew(:,k) = d2f(idsnew(:,k));
[L1,L2] = lsscal(iflnew(:,k),0.08,intv);
Ltot(k) = L1;

end
Lall = Lall./10000; %kw;
for k = 1:3
% plot optimal capacity
    figure
    % subplot(3,1,1)

stairs(Igvar*10,Lall(:,k),'LineWidth',4,'Color','blue');
xlim([min(Igvar.*10) max(Igvar.*10)]);
ylim([0 max(Lall(:,k))+0.5]);
ylabel('Loss(kW)','FontSize',16);
xlabel('S^V_g (kVA)','FontSize',16);
set(gca,'FontSize',12)
grid on
set(gca,'XTick',50:200:1500)
% subplot(3,1,2)
    figure

stairs(Igvar*10,vg(:,k),'LineWidth',4,'Color','blue');
hold on

plot(v0*ones(max(Igvar).*10,1),'LineWidth',4,'Color','red')

    xlim([min(Igvar.*10) max(Igvar.*10)]);
    ylim([min(vg(:,k))-0.01, max(vg(:,k))+0.01]);
    ylabel('Voltage(kV)','FontSize',16);
    xlabel('S^V_g (kVA)','FontSize',16);
    set(gca,'FontSize',12)
    grid on
    set(gca,'XTick',50:200:1500)
% subplot(3,1,3)
    figure
    %!!!!!! Joker in plot; due to loss of accuracy in
long decimal!!!!
    optvg(1,:) = 10;

```

```

    optvg(2:end,k)= optvg(2:end,k) ./max(optvg(:,k)).*10;
    plot(optvg(:,k), 'LineWidth',4, 'Color', 'black');
    xlim([1 1]);
    ylim([min(optvg(:,k))-0.01 v0+0.01]);
    ylabel('Voltage(kV)', 'FontSize',16);
    xlabel('location(node)', 'FontSize',16);
    set(gca, 'FontSize',12)
    hold on
    set(gca, 'XTick',1:1:20)
    plot(v0*ones(a,1), '--', 'LineWidth',2, 'Color', 'red')
    grid on
end

```

---

```

% this script generates plot for Caisheng Wang's table
in optimal
% DG's location and capacity
% ids  |1| x 3  current density on the ffeeder of |1|
nodes
% ifl  |1| x 3  current flow on the feeder of |1| nodes
% Ig   1 x 3   DG's capacity
% h    the handle of plots
% ids1 uniformly distributed load
% ids2 centrally distributed load
% ids3 decreasingly distributed load
clear

```

```

v0 = 10;%kv
ids = zeros(20,3);
l = 20;
amin = 1;
amax = 20;
ids(:,1) = 5*ones(20,1); %total input 100
ids2 = 1:0.9:9.1;
ids(:,2) = [ids2,fliplr(ids2)]'; %total input 101
ids3 = 9.8:-0.5:0.3;
ids(:,3) = ids3'; % total input 101
intv = ones(20,1); %resistance set to 0.08 (given San
Miguel resistance is
% 0.16ohm/km) equivalent to 500m

```

```

%for optimal capacity, assuming DG is located at the
middle of the feeder
a = zeros(1,3);

```

```

idsnew = zeros(1,3);
iflnew = zeros(1,3);
Ltot = zeros(1,3);

```

```

for k = 1:3

```

```

%for optimal location, assuming DG's capacity equals
total loads on the
%feeder

```

```

    ifl = d2f(ids(:,k));
    Ig(k) = ifl(1);
    %***** to Plot into kVA .*10 to the original
current value *****
    %***** Only changed in plot function. Calculation
follows the original

```

```

    %plot current flow
    h(k) = figure;
    stairs(ifl*10, 'LineWidth',4, 'Color', 'blue');
    xlim([1 20]);
    ylim([0 (Ig(k)+10).*10]);
    ylabel('SlI(kVA)', 'FontSize',16);
    xlabel('location (node)', 'FontSize',16);
    set(gca, 'FontSize',12)
    grid on

```

```

    %plot load density
    h1(k) = figure;
    stem(ids(:,k).*10, 'LineWidth',4, 'Color', 'blue');
    xlim([1 20]);
    ylim([0 10*(max(ids(:,k))+5)]);
    ylabel('SgI(kVA)', 'FontSize',16);
    xlabel('location (node)', 'FontSize',16);

```

```

set(gca,'FontSize',12)
grid on
a(k) = optDGa(Ig(k),ifl,amin,amax);

for j = 1:l
    idsnew(:,k) = ids(:,k);
    idsnew(j,k) = ids(j,k)- Ig(k);
    iflnew(:,k) = d2f(idsnew(:,k));
    [Ltot(j,k),L2] = lsscal(iflnew(:,k),0.08,intv);
end

end
Ltot = Ltot.*3./10000; %kw;Assum 10kV 3phase
for k = 1:3
% % plot optimal capacity
figure
% subplot(3,1,1)
stairs(Ltot(:,k),'LineWidth',4,'Color','blue');
xlim([1 20]);
ylim([0 max(Ltot(:,k))+5]);
ylabel('Loss(kW)', 'FontSize',16);
xlabel('Location (node)', 'FontSize',16);
set(gca,'FontSize',12)
grid on
% grid on
end

figure(h(1))
hold on
stem(a(1),Ig(1)*10,'LineWidth',4,'Color','red')
%title('uniformly distributed load','FontSize',20)

figure(h(2))
hold on
stem(a(2),Ig(2)*10,'LineWidth',4,'Color','red')
%title('centrally distributed load','FontSize',20)

figure(h(3))
hold on
stem(a(3),Ig(3)*10,'LineWidth',4,'Color','red')
%title('increasingly distributed load','FontSize',)

```

# Bibliography

---

- [1] Annual Electric Power Industry Report, 2010, U.S. Energy Information Administration.
- [2] Kassakian, J.G. and R. Schmalensee, The future of the electric grid: An interdisciplinary MIT study, 2011, Technical report, Massachusetts Institute of Technology.
- [3] Sherwood, L. US solar market trends. in Proceeding of the Solar Conference. 2007. American Solar Energy Society; American Institute of Architects.
- [4] Masters, C.L., Voltage rise: the big issue when connecting embedded generation to long 11 kV overhead lines. *Power Engineering Journal*, 2002. 16(1): p. 5-12.
- [5] El-Khattam, W. and M.M.A. Salama, Impact of Distributed Generation on Voltage Profile in Deregulated Distribution System. 2002.
- [6] Conti, S., et al. Study of the impact of PV generation on voltage profile in LV distribution networks. 2001. IEEE.
- [7] Kim, T.E. and J.E. Kim. Voltage regulation coordination of distributed generation system in distribution system. in Power Engineering Society Summer Meeting, 2001. 2001.
- [8] Doyle, M.T. Reviewing the impacts of distributed generation on distribution system protection. in Power Engineering Society Summer Meeting, 2002 IEEE. 2002.
- [9] Ayres, H.M., et al., Method for determining the maximum allowable penetration level of distributed generation without steady-state voltage violations. *Generation, Transmission & Distribution, IET*, 2010. 4(4): p. 495-508.
- [10] Cossent, R., T. Gómez, and P. Frías, Towards a future with large penetration of distributed generation: Is the current regulation of electricity distribution ready? *Regulatory recommendations under a European perspective. Energy Policy*, 2009. 37(3): p. 1145-1155.
- [11] Lasseter, R.H., Smart distribution: Coupled microgrids. *Proceedings of the IEEE*, 2011. 99(6): p. 1074-1082.
- [12] Lopes, J.A.P., et al., Integrating distributed generation into electric power systems: A review of drivers, challenges and opportunities. *Electric Power Systems Research*, 2007. 77(9): p. 1189-1203.
- [13] Bluestein, J., Environmental benefits of distributed generation. *Energy and Environmental Analysis, Inc*, 2000. 16.
- [14] IEEE Standard for Interconnecting Distributed Resources With Electric Power Systems. *IEEE Std 1547-2003*, 2003: p. 0\_1-16.
- [15] Kingston, T., T. Stovall, and J. Kelly, Exploring distributed energy alternatives to electrical distribution grid expansion in southern california edison service territory. *ORNL/TM-2005/109*, 2005.
- [16] Asano, H., et al., Microgrids: an overview of ongoing research, development, and demonstration projects. *IEEE Power Energy Magazine*, 2007: p. 78-94.
- [17] Brown, R.E. and L.A.A. Freeman. Analyzing the reliability impact of distributed generation. in Power Engineering Society Summer Meeting, 2001. IEEE. 2001.
- [18] Hatziaargyriou, N.D. and A.P.S. Meliopoulos, distributed energy sources: technical challenges, in PES winter meeting2002.
- [19] Borges, C.L.T. and D.M. Falcao. Impact of distributed generation allocation and sizing on reliability, losses and voltage profile. in Power Tech Conference Proceedings, 2003 IEEE Bologna. 2003.
- [20] Kueck, J. and B. Kirby, the distribution system of the future. *the Electricity Journal*, 2003(June).

- [21] Nara, K. and J. Hasegawa, a new flexible, reliable, and intelligent electrical energy delivery system. *electrical engineering in Japan*, 1997. 121(1): p. 47-53.
- [22] Barker, P.P. and R.W.d. Mello, *Determining the Impact of Distributed Generation on Power Systems: Part 1- Radial Distribution Systems*. 2000.
- [23] Gelling, C.W., *power delivery system of the future*. *IEEE power engineering review*, 2002.
- [24] Driesen, J. and F. Katiraei, *design for distributed energy resources*. *IEEE power & energy magazine*, 2008. 6(3): p. 30-40.
- [25] Sacotte, M., et al., *benefits of using high efficiency power equipment that reduce distribution system losses*, in *CIREC seminar 2008: Smart Grids for distribution 2008*: Frankfurt.
- [26] Agustoni, A., et al., *distributed generation control methodologies and network reconfiguration: effects on voltage profile*, 2000.
- [27] Chiradeja, P. and R. Ramakumar, *An approach to quantify the technical benefits of distributed generation*. *Energy Conversion, IEEE Transactions on*, 2004. 19(4): p. 764-773.
- [28] Goswami, S.K., *distribution system planning using branch exchange technique*. *IEEE transactions on power systems*, 1997. 12(2): p. 718-723.
- [29] Gellings, C., M. Samotyj, and B. Howe, *the future's smart delivery system*. *IEEE power & energy magazine*, 2004(sept/oct): p. 40-48.
- [30] Wiser, R., G. Barbose, and C. Peterman, *Tracking the sun: The installed cost of photovoltaics in the US From 1998-2007*, 2009, Ernest Orlando Lawrence Berkeley National Laboratory, Berkeley, CA (US).
- [31] Khan, U.N. *Distributed Generation and Power Quality*. in *International Conference on Environment and Electrical Engineering*, Karpacz, Poland. 2009.
- [32] Billinton, R. and S. Jonnavithula, *optimal switching device placement in radial distribution systems*. *IEEE transactions on power delivery*, 1996. 11(3): p. 1646-1651.
- [33] Kazemi, A. and H. Andami, *FACTS devices in deregulated electric power systems*, in *2004 IEEE international conference on electric utility deregulation, restructuring and power technologies (DRPT2004)* 2004: Hong Kong.
- [34] Choi, J.-H. and J.-C. Kim, *Advanced voltage regulation method of power distribution systems interconnected with dispersed storage and generation systems*. *Power Delivery, IEEE Transactions on*, 2001. 16(2): p. 329-334.
- [35] Kueck, J.D. and B.J. Kirby, *the distribution system of the future*. *the electricity journal*, 2003.
- [36] Zavoda, F., *the key role of intelligent electronic devices (IED) in advanced distribution automation (ADA)*, in *CICED2008* 2008.
- [37] Short, T.A., *electric power distribution handbook*. 2004: CRC Press.
- [38] Willis, H.L., *Power Delivery Systems*, in *Power Distribution Planning Reference Book*, Second Edition. 2004, CRC Press.
- [39] Willis, H.L., *Power System Reliability*, in *Power Distribution Planning Reference Book*, Second Edition. 2004, CRC Press.
- [40] Turan Gönen, *Power distribution systems*. Second Edition. 2008, CRC Press INC.
- [41] Ipakchi, A. and F. Albuyeh, *Grid of the future*. *Power and Energy Magazine, IEEE*, 2009. 7(2): p. 52-62.
- [42] FERC, *Assessment of demand response and advanced metering*, in *Staff report* 2006. p. 228.
- [43] Willis, H.L., *Consumer Demand and Electric Load*, in *Power Distribution Planning Reference Book*, Second Edition. 2004, CRC Press.
- [44] Fraser, H., *The importance of an active demand side in the electricity industry*. *the electricity journal*, 2001. 14(9): p. 52-73.
- [45] Carrasco, J., et al., *power-electronic systems for the grid integration of renewable energy sources: a survey*. *IEEE transaction on industrial electronics*, 2006. 53(4).

- [46] Brown, R.E., electric power distribution reliability. 2002: Marcel Dekker Inc.
- [47] Foote, C.E.T., et al. Developing distributed generation penetration scenarios. in Future Power Systems, 2005 International Conference on. 2005.
- [48] Purchala, K., et al., Distributed generation and the grid integration issues. Imperial College London, UK, EUSUSTEL, Work Package, 2006. 3.
- [49] Driesen, J. and R. Belmans. Distributed generation: challenges and possible solutions. in Power Engineering Society General Meeting, 2006. IEEE. 2006.
- [50] Celli, G., et al. On-line network reconfiguration for loss reduction in distribution networks with Distributed Generation. in Electricity Distribution, 2005. CIRED 2005. 18th International Conference and Exhibition on. 2005.
- [51] McDonald, J., adaptive intelligent power systems: active distribution networks. Energy Policy, 2008(36): p. 4346-4351.
- [52] Nimpitiwan, N. and G.T. Heydt. Fault current issues for market driven power systems with distributed generation. in North Amer. Power Symp. 2004. Moscow, Idaho.
- [53] Amin, S.M. and B.F. Wollenberg, toward a smart grid. IEEE power & energy magazine, 2005. sept/oct 2005: p. 34-41.
- [54] Brown, R., impact of smart grid on distribution system design, in PES general meeting2008.
- [55] Choi, J.-H., J.-C. Kim, and S.-I. Moon, integration operation of dispersed generations to automated distribution networks for network reconfiguration, in 2003 IEEE bologna power tech conference2003: Bologna, Italy.
- [56] Khator, S.K. and L.C. Leung, power distribution planning: a review of models and issues. IEEE transactions on power systems, 1997. 12(3): p. 1151-1159.
- [57] Carvalho, P.M.S., P.F. Correia, and L.A.F.M. Ferreira, Distributed Reactive Power Generation Control for Voltage Rise Mitigation in Distribution Networks. IEEE transactions on power apparatus and systems, 2008. 23(2): p. 766-772.
- [58] Padilha, A., I.F.E.D. Denis, and R.M. Cirić, Voltage regulation in distribution networks with dispersed generation. 17th CIRED, 2003.
- [59] Company, P.E., Toltage Tolerance Boundary (ANSI standard), 1999.
- [60] Grainger, J.J. and S. Civanlar, Volt/Var Control on Distribution Systems with Lateral Branches Using Shunt Capacitors and Voltage Regulators Part I: The Overall Problem. Power Apparatus and Systems, IEEE Transactions on, 1985. PAS-104(11): p. 3278-3283.
- [61] Morren, J. and S.W.H. de Haan. Maximum penetration level of distributed generation without violating voltage limits. in SmartGrids for Distribution, 2008. IET-CIRED. CIRED Seminar. 2008.
- [62] Keane, A., et al., Enhanced Utilization of Voltage Control Resources With Distributed Generation. Power Systems, IEEE Transactions on, 2011. 26(1): p. 252-260.
- [63] Bae, Y.G., Analytical Method of Capacitor Allocation on Distribution Primary Feeders. Power Apparatus and Systems, IEEE Transactions on, 1978. PAS-97(4): p. 1232-1238.
- [64] Cook, R.F., Optimizing the Application of Shunt Capacitors for Reactive-Volt-Ampere Control and Loss Reduction. Power Apparatus and Systems, Part III. Transactions of the American Institute of Electrical Engineers, 1961. 80(3): p. 430-441.
- [65] Lee, S.H. and J.J. Grainger, Optimum Placement of Fixed and Switched Capacitors on Primary Distribution Feeders. Power Apparatus and Systems, IEEE Transactions on, 1981. PAS-100(1): p. 345-352.
- [66] Maxwell, M., The Economic Application of Capacitors to Distribution Feeders. Power Apparatus and Systems, Part III. Transactions of the American Institute of Electrical Engineers, 1960. 79(3): p. 353-358.
- [67] distribution, D.o.o.e.t.a., national electric delievery technologies roadmap, 2004.

- [68] Parizad, A., A. Khazali, and M. Kalantar. Optimal placement of distributed generation with sensitivity factors considering voltage stability and losses indices. in *Electrical Engineering (ICEE), 2010 18th Iranian Conference on*. 2010.
- [69] Willis, H.L., *Distributed Resources*, in *Power Distribution Planning Reference Book, Second Edition*. 2004, CRC Press.
- [70] Willis, H.L., *Distribution Feeder Layout*, in *Power Distribution Planning Reference Book, Second Edition*. 2004, CRC Press.
- [71] Command, N.F.E., *electric power distribution systems operations*, 1990, Naval Facilities Engineering Command.
- [72] Rau, N.S. and W. Yih-Heui, Optimum location of resources in distributed planning. *Power Systems, IEEE Transactions on*, 1994. 9(4): p. 2014-2020.
- [73] Dinic, N., et al. Increasing wind farm capacity. in *Generation, Transmission and Distribution, IEE Proceedings-*. 2006. IET.
- [74] Quezada, V.M., J.R. Abbad, and T.G.S. Roman, Assessment of energy distribution losses for increasing penetration of distributed generation. *Power Systems, IEEE Transactions on*, 2006. 21(2): p. 533-540.
- [75] Jupe, S.C.E. and P.C. Taylor, Distributed generation output control for network power flow management. *Renewable Power Generation, IET*, 2009. 3(4): p. 371-386.
- [76] Repo, S., et al. A case study of a voltage rise problem due to a large amount of distributed generation on a weak distribution network. in *Power Tech Conference Proceedings, 2003 IEEE Bologna*. 2003.
- [77] Neagle, N.M. and D.R. Samson, Loss Reduction from Capacitors Installed on Primary Feeders. *Power Apparatus and Systems, Part III. Transactions of the American Institute of Electrical Engineers*, 1956. 75(3): p. 950-959.
- [78] Augugliaro, A., et al., Voltage regulation and power losses minimization in automated distribution networks by an evolutionary multiobjective approach. *Power Systems, IEEE Transactions on*, 2004. 19(3): p. 1516-1527.
- [79] Benitez-Rios, F.G., et al. Optimization of distributed generation penetration in distributed power electric systems. in *Power Engineering, Energy and Electrical Drives (POWERENG), 2011 International Conference on*. 2011.
- [80] Celli, G. and F. Pilo. MV network planning under uncertainties on distributed generation penetration. in *Power Engineering Society Summer Meeting, 2001*. 2001.
- [81] Kashem, M.A., et al. Distributed generation for minimization of power losses in distribution systems. in *Power Engineering Society General Meeting, 2006. IEEE*. 2006.
- [82] Mansour, M.O. and T.M. Abdel-Rahman, Non-Linear Var Optimization Using Decomposition And Coordination. *Power Apparatus and Systems, IEEE Transactions on*, 1984. PAS-103(2): p. 246-255.
- [83] Greatbanks, J.A., et al. On optimization for security and reliability of power systems with distributed generation. in *Power Tech Conference Proceedings, 2003 IEEE Bologna*. 2003.
- [84] Li, Y., D. Czarkowski, and F. de Leon, Optimal Distributed Voltage Regulation for Secondary Networks With DGs. *Smart Grid, IEEE Transactions on*, 2012. 3(2): p. 959-967.
- [85] Senjyu, T., et al., Optimal distribution voltage control and coordination with distributed generation. *Power Delivery, IEEE Transactions on*, 2008. 23(2): p. 1236-1242.
- [86] Salomonsson, D., L. Soder, and A. Sannino. An adaptive control system for a dc microgrid for data centers. in *Industry Applications Conference, 2007. 42nd IAS Annual Meeting. Conference Record of the 2007 IEEE*. 2007. IEEE.
- [87] Kiprakis, A. and A. Wallace. Maximising energy capture from distributed generators in weak networks. in *Generation, Transmission and Distribution, IEE Proceedings-*. 2004. IET.



- [88] Madureira, A.G. and J.A. Pecos Lopes, Coordinated voltage support in distribution networks with distributed generation and microgrids. *Renewable Power Generation, IET*, 2009. 3(4): p. 439-454.
- [89] Paserba, J.J., et al., Coordination of a distribution level continuously controlled compensation device with existing substation equipment for long term VAr management. *Power Delivery, IEEE Transactions on*, 1994. 9(2): p. 1034-1040.
- [90] Zhao, J., et al., joint optimization algorithm for network reconfiguration and reactive power control of wind farm in distribution system. *WSEAS transactions on circuits and systems*, 2009. 8(2): p. 268-279.
- [91] Corsi, S., et al., Coordination between the reactive power scheduling function and the hierarchical voltage control of the EHV ENEL system. *Power Systems, IEEE Transactions on*, 1995. 10(2): p. 686-694.
- [92] Turitsyn, K., et al. Distributed control of reactive power flow in a radial distribution circuit with high photovoltaic penetration. in *Power and Energy Society General Meeting, 2010 IEEE*. 2010.
- [93] Qureshi, M., et al., a survey of communication network paradigms for substation automation.
- [94] Engelken, L., A. Gay, and H. Tram, development of an information technology strategy and architecture for energy delivery utility mergers.
- [95] Roth, P.D., Communications architecture in modern distribution systems, in *CIRE20012001*.
- [96] Ochoa, L.F., C.J. Dent, and G.P. Harrison, Distribution Network Capacity Assessment: Variable DG and Active Networks. *Power Systems, IEEE Transactions on*, 2010. 25(1): p. 87-95.
- [97] Nguyen, P.H., J.M.A. Myrzik, and W.L. Kling. Coordination of voltage regulation in Active Networks. in *Transmission and Distribution Conference and Exposition, 2008. D. IEEE/PES*. 2008.
- [98] Siano, P., et al., Evaluating maximum wind energy exploitation in active distribution networks. *Generation, Transmission & Distribution, IET*, 2010. 4(5): p. 598-608.
- [99] Ochoa, L.F., A. Padilha-Feltrin, and G.P. Harrison, Time-series-based maximization of distributed wind power generation integration. *Energy Conversion, IEEE Transactions on*, 2008. 23(3): p. 968-974.
- [100] Willis, H.L., *Distribution Substations*, in *Power Distribution Planning Reference Book, Second Edition*. 2004, CRC Press.
- [101] Willis, H.L., *Feeder Layout, Switching, and Reliability*, in *Power Distribution Planning Reference Book, Second Edition*. 2004, CRC Press.
- [102] Willis, H.L., *Equipment Ratings, Loading, Lifetime, and Failure*, in *Power Distribution Planning Reference Book, Second Edition*. 2004, CRC Press.
- [103] Willis, H.L., *Service Level Layout and Planning*, in *Power Distribution Planning Reference Book, Second Edition*. 2004, CRC Press.
- [104] Burke, J., *power distribution engineering*. 1994: Marcel Dekker Inc.
- [105] Hossenlopp, L., *new solutions for the automation of large industrial distribution networks, in developments in power system protection2001*.
- [106] Mamo, X., et al., *distribution automation: the cornerstone for smart grid development strategy*, 2009.
- [107] Leung, L.C., S.K. Khator, and J. Ponce, optimal transformer allocation under single-contingency. *IEEE transactions on power systems*, 1996. 11(2): p. 1046-1051.
- [108] Willis, H.L., *Basic Line Segment and Transformer Sizing Economics*, in *Power Distribution Planning Reference Book, Second Edition*. 2004, CRC Press.

- [109] Jiang, D. and R. Baldick, Optimal electric distribution system switch reconfiguration and capacitor control. *Power Systems, IEEE Transactions on*, 1996. 11(2): p. 890-897.
- [110] Chowdhury, A.A. and D.O. Koval, radial feeder reconfiguration analysis, in *power distribution system reliability*. 2009, institute of electrical and electronics engineers, Inc. p. 416-427.
- [111] Gafni, E. and D. Bertsekas, Distributed Algorithms for Generating Loop-Free Routes in Networks with Frequently Changing Topology. *Communications, IEEE Transactions on*, 1981. 29(1): p. 11-18.
- [112] Tsai-Hsiang, C., et al., Feasibility study of upgrading primary feeders from radial and open-loop to normally closed-loop arrangement. *Power Systems, IEEE Transactions on*, 2004. 19(3): p. 1308-1316.
- [113] Brady, P., C. Dai, and Y. Baghzouz. Need to revise switched capacitor controls on feeders with distributed generation. in *Transmission and Distribution Conference and Exposition, 2003 IEEE PES*. 2003.
- [114] Carvalho, P.M.S. and L.A.F.M. Ferreira, Distribution quality of service and reliability optimal design: individual standards and regulation effectiveness. *Power Systems, IEEE Transactions on*, 2005. 20(4): p. 2086-2092.
- [115] Celli, G., M. Loddo, and F. Pilo, *Distribution Network Planning with Active Management*, in 6th World Energy System Conf2006: Torino, Italy.
- [116] Willis, H.L., *Choosing the Right Set of Line and Equipment Sizes*, in *Power Distribution Planning Reference Book, Second Edition*. 2004, CRC Press.
- [117] Willis, H.L., *Economics and Evaluation of Cost*, in *Power Distribution Planning Reference Book, Second Edition*. 2004, CRC Press.
- [118] Venkatesh, B., R. Ranjan, and H.B. Gooi, Optimal reconfiguration of radial distribution systems to maximize loadability. *Power Systems, IEEE Transactions on*, 2004. 19(1): p. 260-266.
- [119] Grainger, J.J. and S.H. Lee, Optimum Size and Location of Shunt Capacitors for Reduction of Losses on Distribution Feeders. *Power Apparatus and Systems, IEEE Transactions on*, 1981. PAS-100(3): p. 1105-1118.
- [120] Gozel, T., et al. Optimal placement and sizing of distributed generation on radial feeder with different static load models. 2005. IEEE.
- [121] Kim, T.E. and J.E. Kim. A method for determining the introduction limit of distributed generation system in distribution system. in *Power Engineering Society Summer Meeting, 2001*. 2001.
- [122] Hedman, K.W., et al., Optimal Transmission Switching&#x2014;Sensitivity Analysis and Extensions. *Power Systems, IEEE Transactions on*, 2008. 23(3): p. 1469-1479.
- [123] Quezada, V.H.M., J.R. Abbad, and T.G.S. Roman, Assessment of energy distribution losses for increasing penetration of distributed generation. *Power Systems, IEEE Transactions on*, 2006. 21(2): p. 533-540.
- [124] Shaheen, H.I., G.I. Rashed, and S.J. Cheng. Optimal location and parameters setting of UPFC based on GA and PSO for enhancing power system security under single contingencies. in *Power and Energy Society General Meeting - Conversion and Delivery of Electrical Energy in the 21st Century, 2008 IEEE*. 2008.
- [125] Caisheng, W. and M.H. Nehrir. Analytical approaches for optimal placement of distributed generation sources in power systems. in *Power Engineering Society General Meeting, 2005*. IEEE. 2005.
- [126] Dai, C. and Y. Baghzouz. On the voltage profile of distribution feeders with distributed generation. in *Power Engineering Society General Meeting, 2003, IEEE*. 2003.

- [127] Kashem, M.A. and G. Ledwich, Multiple Distributed Generators for Distribution Feeder Voltage Support. *Energy Conversion*, IEEE Transactions on, 2005. 20(3): p. 676-684.
- [128] Conti, S., et al., Integration of multiple PV units in urban power distribution systems. *Solar Energy*, 2003. 75(2): p. 87-94.
- [129] Baghzouz, Y. General rules for distributed generation-feeder interaction. 2006. IEEE.
- [130] Willis, H.L. Analytical methods and rules of thumb for modeling DG-distribution interaction. in *Power Engineering Society Summer Meeting*, 2000. IEEE. 2000.
- [131] Willis, H.L., Load Reach and Volt-VAR Engineering, in *Power Distribution Planning Reference Book*, Second Edition. 2004, CRC Press.
- [132] Hsiao-Dong, C., et al., Optimal capacitor placement, replacement and control in large-scale unbalanced distribution systems: modeling and a new formulation. *Power Systems*, IEEE Transactions on, 1995. 10(1): p. 356-362.
- [133] Willis, H.L., Planning and the T&D Planning Process, in *Power Distribution Planning Reference Book*, Second Edition. 2004, CRC Press.
- [134] Gelling, C.W. and R.J. Lordan, the power delivery system of the future. *the electricity journal*, 2003.
- [135] Bouford, J.D. and C.A. Warren, many states of distribution. *IEEE power & energy magazine*, 2007 (July/August 2007).
- [136] Koutroumpetis, G.N. and A.S. Safigianni. Optimum distributed generation penetration in a distribution network. in *PowerTech, 2009 IEEE Bucharest*. 2009.
- [137] Upadhyay, N. and A.K. Mishra. A method of determination of suitable location and capacity of DG units in a distribution system. in *Universities Power Engineering Conference (AUPEC), 2010 20th Australasian*. 2010.
- [138] Van Thong, V., J. Driesen, and R. Belmans, Interconnection of distributed generators and their influences on power system. *International Energy Journal*, 2005. 6(1).
- [139] Albadi, M.H. and E.F. El-Saadany, Demand response in electricity markets: An overview. 2007.
- [140] Goel, L., Q. Wu, and P. Wang, Reliability enhancement of a deregulated power system considering demand response. 2006.
- [141] Scott, N.C., D.J. Atkinson, and J.E. Morrell, Use of load control to regulate voltage on distribution networks with embedded generation. *Power Systems*, IEEE Transactions on, 2002. 17(2): p. 510-515.
- [142] Sridharan, K. and N.N. Schulz, outage management through AMR systems using an intelligent data filter *IEEE transaction on power delivery*, 2001. 16 (4): p. 669-675.
- [143] Gwang Won, K. and K.Y. Lee, Coordination control of ULTC transformer and STATCOM based on an artificial neural network. *Power Systems*, IEEE Transactions on, 2005. 20(2): p. 580-586.
- [144] Celli, G., et al. Distributed generation and intentional islanding: Effects on reliability in active networks. in *Electricity Distribution, 2005. CIRED 2005. 18th International Conference and Exhibition on*. 2005.
- [145] Liew, S.N. and G. Strbac, Maximising penetration of wind generation in existing distribution networks. *IEE proceedings online*, 2002.
- [146] Cook, R.F., Analysis of Capacitor Application as Affected by Load Cycle. *Power Apparatus and Systems*, Part III. Transactions of the American Institute of Electrical Engineers, 1959. 78(3): p. 950-956.
- [147] Lassila, J., et al., potential of power electronics in electricity distribution systems, in *CIRED seminar 2008: SmartGrid for distribution2008*.

- [148] Spees, K. and L.B. Lave, demand response and electricity market efficiency. the electricity journal, 2007. 20(3).
- [149] Kashem, M.A., V. Ganapathy, and G.B. Jasmon. network reconfiguration for load balancing in distribution networks. in IEE Proceedings for generation, transmission and distribution. 1999.
- [150] Baran, M.E. and F.F. Wu, network reconfiguration in distribution systems for loss reduction and load balancing. IEEE transactions on power delivery, 1989. 4(2): p. 1401-1407.
- [151] Sarfi, R.J., M.M.A. Salama, and A.Y. Chikhani, a survey of the state of the art in distribution system reconfiguration for system loss reduction. electric power system research, 1994. 31: p. 61-70.
- [152] Hedman, K.W., et al., optimal transmission switching with contingency analysis. IEEE transactions on power delivery, 2009. 24(3): p. 1577-1576.
- [153] Zhu, J., optimal reconfiguration of electrical distribution network, in optimization of power system operation. 2009, institute of electrical and electronics engineers. p. 503-543.
- [154] Staszkesky, D., D. Craig, and C. Befus, advanced feeder automation is here. IEEE power & energy magazine, 2005. sept/oct 2005.
- [155] Willis, H.L., Distribution System Reliability Analysis Methods, in Power Distribution Planning Reference Book, Second Edition. 2004, CRC Press.
- [156] Yang, Y., F. Lambert, and D. Divan, a survey on technologies for implimenting sensor networks for power delivery systems. 2007.
- [157] Sansawatt, T., L.F. Ochoa, and G.P. Harrison. Integrating distributed generation using decentralised voltage regulation. in Power and Energy Society General Meeting, 2010 IEEE. 2010.
- [158] Borenstein, S., M. Jaske, and A. Roseneld, dynamic pricing, advanced metering and demand response in electricity markets, 2002, university of california energy institute center for the study of energy markets. p. 103.
- [159] Dunn, R., Electric utility demand-side management 1999 Executive summary, 2002, energy information administration(EIA).
- [160] EPRI, the distribution system of the future, advanced distribution automation (ADA), EPRI electric power research institute.
- [161] Burke, R.B. and M.I. Henderson, incorporating demand resonse in operating reserve in New England. 2005.
- [162] Cramton, P., electricity market design: the good, the bad, and the ugly, in Hawaii International Conference on System Sciences2003.
- [163] DOE, Benefits of demand response in electricity markets and recommendations for achieving them: a report to the United States Congress Pursuant to section 1252 of the Energy Policy Act of 2005, 2006, U.S. Department of Energy.
- [164] Schisler, K. and K. Brief, The role of demand response in ancillary services markets. 2008: p. 3.
- [165] Hirst, E., reliability benefits of Price-reponsive demand. IEEE Power Engineering Review, 2002.
- [166] Hausmand, J.A., M. Kinnucan, and D. McFadden, A two-level electricity demand model: evaluation of the Connecticut time-of-day pricing test. 1979.
- [167] Caves, D., K. Eakin, and A. Faruqui, mitigating price spikes in wholesale markets through market-based pricing in retail markets. the electricity journal, 2000. 13(3): p. 13-23.
- [168] Hsiao, Y.T. and C.Y. Chien. multiobjective optimal feeder reconfiguration. in IEE Proceedings of generation, transmission, and distribution. 2001.

- [169] Ying-Yi, H. and H. Saw-Yu, Determination of network configuration considering multiobjective in distribution systems using genetic algorithms. *Power Systems, IEEE Transactions on*, 2005. 20(2): p. 1062-1069.
- [170] Begovic, M., D. Novosel, and M. Milisavljevic, trends in power system protection and control, in the 32nd Hawaii international conference on system sciences1999: Hawaii.
- [171] Sastry, M., integrated outage management system: an effective solution for power utilities to address customer grevances. *international journal of electronic customer relationship management*, 2007 1(1): p. 30-40.
- [172] Staszsky, D.M., use of virtual agents to effect intelligent distriubtion automation, in 2006 IEEE PES general meeting2006: Montreal, Quebec, Canada.
- [173] Roytelman, I., et al., multi-objective feeder reconfiguration distribution management system. *IEEE transactions on power systems*, 1996. 11(2): p. 661-667.
- [174] Wang, P., distribution network reconfiguration to prevent wires from icing, in IEEE PES general meeting2004: Denver, CO.
- [175] Singh, D. and K.S. Verma. Comparative analysis for penetration of distributed generation in power systems. in *Sustainable Energy Technologies*, 2008. ICSET 2008. IEEE International Conference on. 2008.
- [176] Miller, N., et al., Report on distributed generation penetration study. 2003: National Renewable Energy Laboratory.
- [177] Baran, M. and F.F. Wu, Optimal sizing of capacitors placed on a radial distribution system. *Power Delivery, IEEE Transactions on*, 1989. 4(1): p. 735-743.
- [178] Borkowska, B., Probabilistic Load Flow. *Power Apparatus and Systems, IEEE Transactions on*, 1974. PAS-93(3): p. 752-759.
- [179] Ross, D.W., et al., new methods for evaluating distribution automation and control (DAC) systems benefits. *IEEE transactions on power apparatus and systems*, 1981. PAS-100(6): p. 2978-2986.
- [180] Carvalho, P.M.S. and L.A.F.M. Ferreira, large-scale network optimization with evolutionary hybrid algorithms: ten years' experience with the electric power distribution industry, in *Computational Intelligence in Expensive Optimization Problems Adaptation, Learning, and Optimization*. 2010, SpringerLink. p. 325-343.
- [181] Jonnavithula, S. and R. Billinton, minimum cost analysis of feeder routing in distribution system planning. *IEEE transactions on power systems*, 1996. 11(4): p. 1935-1940.

